The biological role of viral tRNA-like molecules in a murine gammaherpesvirus infection

Anna Ruth Cliffe

October 2005

wellcome trust

Submitted for the degree of Doctor of Philosophy

The programme of research was carried out as part of a Wellcome Trust funded 4-year PhD entitled "The molecular and cellular basis of disease" at the Laboratory for Clinical and Molecular Virology, Royal (Dick) School of Veterinary Studies, University of Edinburgh, Summerhall, Edinburgh, UK.

Declaration

I declare that all work included in this thesis is my own except where otherwise stated. No part of this work has been, or will be, submitted for any other degree of professional qualification.

Anna Cliffe
2005

Laboratory for Clinical and Molecular Virology
University of Edinburgh
Summerhall
Edinburgh
EH9 1QH

Acknowledgements

I would like to thank my supervisors Professor Tony Nash and Dr Bernadette Dutia. Tony has given me so much inspiration throughout the project and his enthusiasm has been unwavering. Bernadette I can't thank enough; not only for her advice and technical assistance but also helping me through the ups and downs. A big thank you to Yvonne Ligertwood who has given me so much technical support, in particular her assistance in titrating numerous growth curves, usually in the sweltering heat. Ben Addams was an excellent honours student in the lab who helped in the construction of recombinant viruses, thank you. I would also like to thank the rest of the MHV-68/MDV group past and present for all creating a fantastic working environment. Also thanks to Lynda Wilson for her assistance with the confocal microscopy, Steve Mitchell for helping with the electron microscopy and Dr. Andy Cronshaw for his input in interpreting the mass-spec data.

A big thank you to my friends and family who have coped with my stresses over the last three years, especially my mum who has always been there to offer encouragement and Sarah who never failed to entertain and make me laugh, even when I'd reached the depths of despair. Also to my fellow PhD students, both past and present, who have provided both empathy and distraction. In particular a huge thank you to Clem for listening to my many rants and offering her unwavering support, or when all else failed, plying me with red wine. Finally, the support that Neil has given me over the last year has been tremendous, he's been there for me through the hardest period of my PhD, and I can't express how much I appreciate his help and encouragement.

Abstract

Members of the subfamily *Gammaherpesvirinae* commonly establish latency within lymphoid cells and are associated with lymphoproliferative disease. Gammaherpesviruses include the human pathogens Epstein-Barr virus and Kaposi's sarcoma-associated herpes virus. Due to the narrow host range of infection exhibited by these viruses and their limited productive growth *in vitro*, the events occurring during lytic replication and the establishment of latency are not well characterised. Murine gammaherpesvirus 68 (MHV-68) is able to undergo productive replication in a number of cell types *in vitro* and infects laboratory mice; consequently it provides an excellent model for study of gammaherpesvirus infection. MHV-68 encodes eight viral tRNA-like molecules (vtRNA1-8), which resemble cellular tRNAs in that they have a predicted cloverleaf-like secondary structure and are transcribed by RNA polymerase III. However unlike cellular tRNAs they are not amino-acylated and therefore do not function directly during protein synthesis. They are known to be expressed to high levels during both latency and lytic replication. However their role within infection is not known.

The aim of this project was to characterise the vtRNAs. The presence of the vtRNAs within purified, RNase treated viral stocks indicated their packaging within the MHV-68 virion. Although both viral and cellular mRNAs were also present, it appeared that the major RNA species packaged by MHV-68 were small RNA molecules, such as the vtRNAs. Incorporation of RNA molecules into the virion is not unique to MHV-68 as other herpesviruses have been found to package RNA, although the vtRNAs represent the only packaged small viral non-coding RNA molecules discovered so far. In addition, this is the first study to demonstrate the preferential incorporation of small RNA molecules by a herpesvirus. The mechanism by which the vtRNAs assemble into the virion is not clear. In situ hybridization demonstrated that within infected cells the vtRNAs localized to globular areas within the nucleus and were also found at high levels within the cytoplasm. Electrophoretic mobility shift assays performed using vtRNA1 and vtRNA4 indicated binding to protein complexes present within both the nucleus and cytoplasm of infected cells. Inhibition of vtRNA-protein binding by an anti-MHV-68 antibody indicated direct

interaction of the vtRNAs with viral protein(s). Hence it is likely that their incorporation is mediated through binding to viral protein(s) during virion assembly in either the nucleus or cytoplasm.

MHV-76 is a deletion mutant of MHV-68, which lacks all eight vtRNAs along with four other genes (M1-M4). The contribution of the vtRNAs to viral pathogenesis has been investigated by construction of recombinant MHV-76, which expressed vtRNAs1-5 under their natural promoters. The insertion of the vtRNAs into MHV-76 had no effect on the ability of the virus to replicate *in vitro*. In addition, the recombinant viruses displayed identical characteristics to MHV-76 following intranasal infection of BALB/c mice, demonstrated by the levels of lytic virus present within the lung and the levels of latent virus within the spleen. Therefore the role of the vtRNAs within infection remains to be determined and the recombinant viruses produced in this project will provide excellent tools to investigate their function further through both *in vitro* and *in vivo* analysis.

Contents

	Page
Title	i
Declaration	ii
Acknowledgments	iii
Abstract	iv
Contents	vi
List of Figures	xiii
List of Tables	xv
Abbreviations	xvi
Chapter One: Introduction	**1**
1.1. Herpesviruses	**2**
1.1.1. Classification	4
1.1.1. Alphaherpesviruses	4
1.1.2. Betaherpesviruses	4
1.1.3 Gammaherpesviruses	5
1.1.2. Herpesvirus structure	5
1.1.3. Herpesvirus genome	7
1.1.4. Herpesvirus life cycle	10
1.2. Gammaherpesviruses	**14**
1.2.1. Epstein-Barr virus	14
1.2.1.1. EBV latent infection	15
1.2.1.2. Disease associations	17
1.2.2. Kaposi's sarcoma-associated herpesvirus	21
1.2.2.1. KSHV molecular biology	22
1.2.2.2. KSHV disease associations	24
1.2.3. Herpesvirus saimiri	28
1.2.4. Gammaherpesviruses of veterinary importance	30
1.2.5. Animal models of gammaherpesvirus infection	31

1.3. Murine gammaherpesvirus-68 **34**
1.3.1. MHV-68 genome 35
1.3.2. MHV-68 virion composition 35
1.3.3. MHV-68 replication *in vitro* 38
1.3.4. MHV-68 primary infection *in vivo* 39
1.3.5. MHV-68 latency *in vivo* 41
1.3.6. MHV-76 and the left-hand end of MHV-68 44
1.4 Transfer RNA molecules **49**
1.4.1. tRNA structure 50
1.4.2. tRNA expression 52
1.4.3. tRNA function during viral infection 52
1.4.3.1. Plant virus tRNA-like structure 52
1.4.3.2. Cellular tRNA functions during retrovirus infection 54
1.5. Viral non-coding RNA molecules **56**
1.5.1. Alphaherpesvirus non-coding RNA molecules 56
1.5.2. Gammaherpesviruses non-coding RNA molecules 59
1.5.3. Adenovirus non-coding RNA molecules 63
1.5.4. Virally encoded miRNA 64
1.6. Project outline **65**

Chapter Two: Materials and methods **68**
2.1 Molecular cloning **69**
2.1.1. DNA digestion with restriction endonucleases 69
2.1.2. DNA Dephosphorylation 69
2.1.3. Ligation of DNA fragments 69
2.1.4. Transformation of One Shot TOP 10 Chemically competent bacteria 69
2.1.5. Preparation of glycerol stocks of transformants 70
2.1.6. Agarose gel electrophoresis 70
2.1.7. Isolation of DNA fragments from agarose gel using a Q1A Gel Extraction Kit (Qiagen) 70

2.2 DNA extraction **71**
2.2.1. Small scale extraction of plasmid DNA (miniprep) 71
2.2.2. Large scale preparation of plasmid DNA (midi and maxiprep) 71
2.2.3. Extraction of high-molecular weight viral DNA 72
2.2.4. Extraction of DNA from splenocytes 73
2.3 Southern analysis **74**
2.3.1. Digestion of high molecular weight DNA 74
2.3.2. Electrophoresis and transfer 74
2.3.3. Staining of molecular weight standards 75
2.3.4. Radiolabelling of DNA probes 75
2.3.5. Pre-hybridization and hybridization 76
2.3.6. Removal of radiolabeled probes from Southern blot membranes 76
2.4. Polymerase chain reaction **77**
2.4.1. Components of standard PCR reactions 77
2.4.2. PCR from crude lysates 77
2.4.3. Real-time PCR analysis 77
2.5. RNA extraction and manipulation **78**
2.5.1. RNA isolation using RNAwiz 78
2.5.2. Standard DNase treatment of RNA 79
2.5.3. DNAse treatment of pure viral RNA 79
2.5.4. Reverse transcription of RNA 80
2.5.5. RNA agarose gel electrophoresis 80
2.5.6. RNA electrophoresis using TBE-Urea gels 81
2.5.7. Radiolabelling of RNA using T4 RNA ligase 81
2.5.8. In Vitro Transcription of vtRNAs 82
2.6. Northern analysis **82**
2.6.1. Electrophoresis and blotting 83
2.6.2. Prehybridisation and hybridisation 83
2.6.3. Removal of radiolabeled probes from northern blot membranes 84
2.6.4. RNA dot-blotting 84

2.7 RNA *in situ* hybridization **85**
2.7.1. Generation of labelled RNA probe 85
2.7.2. Alkaline hydrolysis of labeled probe 86
2.7.3. Quantification of labeled RNA probe 86
2.7.4. Preparation of cytospins for RNA *in situ* hybridization 87
2.7.5. RNA *in situ* prehybridisation and hybridisation on cytospins 87
2.7.6. RNA *in situ* prehybridisation and hybridisation on tissue sections 87
2.7.7. Visualisation of probe using alkaline phosphatase 88
2.7.8. Visualisation of probe using Alexafluor488 88
2.8. Tissue culture techniques **89**
2.8.1. Maintenance of cell lines 89
2.8.2. Harvesting and counting cells 89
2.8.3. Preparation of cellular fractions 90
2.8.4. Transfection of cells by electroporation 90
2.8.5. Transfection of cells by Effectene 91
2.8.6. Generation of stably transfected cell lines 91
2.9 Virological methods **92**
2.9.1. Isolation of Single Plaques following Transfection 92
2.9.2. Purification of recombinant virus 93
2.9.3. Preparation of working viral stocks 93
2.9.4. Isolation of extracellular virus 94
2.9.5. Purification of virus by ultracentrifugation 94
2.9.6. RNase treatment of purified virus 95
2.9.7. Transmission electron microscopy 95
2.9.8. Treatment of cells with inhibitors of protein synthesis and viral DNA replication 96
2.9.9. Virus titration 96
2.9.10. One step/multistep growth curves 97
2.9.11. Infective centre assay 97
2.10. Protein techniques **98**
2.10.1. Electrophoretic-mobility shift assay (EMSA) 98
2.10.2. UV-crosslinking RNA-protein complexes 98

2.10.3. Isolation of protein from polyacrylamide gel 99
2.10.4. SDS-Page 99
2.10.5. Coomassie staining 99
2.10.6. Silver staining 100
2.10.7. Western Blotting 100
2.10.8. In-gel protein digestion for mass spectrometry 100
2.11. Statistical analysis **101**

Appendix 1 Cloning vectors used in this study 102
Appendix 2 Oligonucleotides used in this study 105
Appendix 3 Synthetic oligonucleotides used for *in vitro* transcription 108
Appendix 4 Stock solutions used in this study 109
Appendix 5 Commercial Suppliers 110

Chapter Three: The encapsidation of the vtRNAs **112**
3.1. Aims **113**
3.2. The timing of expression of the vtRNAs during lytic infection by RT-PCR **113**
3.3. RNA detection within purified virus preparations **115**
3.3.1. Intracellular virus purification and RNA detection 115
3.3.1.1. Purification of intracellular virus 115
3.3.1.2. Detection of the RNAs present by RT-PCR 116
3.3.2. Extracellular virus purification and RNA detection 119
3.3.2.1. Purification of extracellular virus 119
3.3.2.2. Nature of the RNA species present 122
3.3.2.3. Detection of the RNAs present by RT-PCR 127
3.4. Discussion **129**

Chapter Four: Characterizing the sub-cellular localization of the vtRNAs and potential interacting proteins **134**
4.1. Aims **135**

4.2. The localization of the vtRNAs during lytic and latent infection **136**
4.2.1. Dot-blot analysis on cellular extracts 136
4.2.2. In situ hybridisation 139
4.3. Potential vtRNA1 interacting proteins **140**
4.3.1. Electrophoretic mobility shift assays 140
4.3.2. Identification of protein complexes 144
4.4. Potential vtRNA4 interacting proteins **148**
4.4.1. Electrophoretic mobility shift assays 148
4.4.2. Identification of protein complexes 150
4.5. Discussion **153**

Chapter 5: Investigating the function of the vtRNAs during *in vitro* and *in vivo* infection **158**
5.1. Aims **159**
5.2. Construction of intRNA1-5 virus **159**
5.3. Construction of MHV-76intRNA1-5 revertant virus **160**
5.4. Southern analysis of the intRNA and intRNARev viruses **164**
5.5. Construction of WTTintRNA **169**
5.5.1. Cloning strategy 169
5.5.2. Purification of recombinant viruses 169
5.6. Construction of intRNA5 viruses **170**
5.7. Characterisation of MHV-76 insertion viruses *in vitro* **170**
5.7.1. vtRNA expression 170
5.7.2. Growth characteristics 174
5.8. Characterisation of MHV-76 insertion viruses *in vivo* **178**
5.8.1. Lytic replication in the lung 178
5.8.2. Acute latency within the spleen 178
5.8.3. Long term infection 187
5.9. Construction of a vtRNA expressing cell line **190**
5.10. Discussion **190**

Chapter six: Conclusion 198

References 206

List of figures

	Page
1.1 Herpesvirus virion	5
1.2 Herpesvirus genomic arrangements	8
1.3 KSHV, HVS and MHV-68 genomes	36
1.4 MHV-68 vtRNAs	48
1.5 tRNA secondary structure	51
1.6 HSV-1 latency associated transcripts	56
1.7 Viral non-coding RNA molecules	60
1.8 Structure and processing of miRNAs	66
3.1 vtRNA1 expression	114
3.2 MHV-68 purification strategy	117
3.3 Transmission EMs of sucrose gradient purified MHV-68	118
3.4 Sucrose cushion purified MHV-68 RT-PCR	120
3.5 Sucrose gradient purified MHV-68 RT-PCR	121
3.6 Transmission EM of extra-cellular MHV-68	123
3.7 RNA species within extra-cellular virus stocks	125
3.8 Northern blot on RNA from extra-cellular virus stocks	126
4.1 vtRNA subcellular localization	138
4.2 vtRNA in situ hybridization on cytospins	141
4.3 vtRNA1 EMSA	143
4.4 vtRNA1 EMSA in the presence of anti-MHV-68 antibody and late protein binding	145
4.5 Identification of vtRNA-protein complexes	147
4.6 vtRNA4 EMSA	151
4.7 Silver stain on vtRNA4-protein complex	152
5.1 intRNA construction	161
5.2 Plaque purification of intRNA(2)	162
5.3 intRNA(9) and intRNA(9)Rev Southern analysis	167
5.4 intRNA(9), intRNA(2) and intRNA(9)Rev Southern analysis	167
5.5 intRNA5 plaque purification	171
5.6 intRNA(9), intRNA(2) and intRNA(9)Rev RT-PCR	172

5.7 intRNA(9), intRNA(2) and intRNA(9)Rev northern analysis 173
5.8 intRNA(9), intRNA(2) and intRNA(9)Rev single-step growth curve in BHK-21 cells 175
5.9 intRNA(9), intRNA(2) and intRNA(9)Rev multi-step growth curve 176
5.10 intRNA(9), intRNA(2) and intRNA(9)Rev single-step growth curve in L929 cells 177
5.11 intRNA(9), intRNA(2) and intRNA(9)Rev lung titres 179
5.12 intRNA(9), intRNA(2) and intRNA(9)Rev infective centre assay 181
5.13 intRNA(9), intRNA(2) and intRNA(9)Rev d14 splenic viral load 182
5.14 In situ hybridization on intRNA(9) and intRNA(2) infected spleens 184
5.15 intRNA(9) and intRNA(2) vtRNA PCR 185
5.16 intRNA(9), intRNA(2) and intRNA(9)Rev whole spleen weights 186
5.17 Long term experiment 1: whole spleen weights d77 188
5.18 Long term experiment 1: infective centre assay d77 188
5.19 Long term experiment 2: whole spleen weights d70 and d120 189
5.20 vtRNA expression within stably transfected cell lines 191

List of tables

	Page
1.1 Human herpesvirus disease associations	3
1.2 EBV latent gene expression	16
1.3 MHV-68 virion proteins	37
3.1 Virus titres following sucrose gradient purification	117
3.2 RT-PCR on extracellular virus stock	128
4.1 MALDI-TOF analysis on proteins within vtRNA1-protein complex	149
5.1 Expected MHV-76, intRNA and intRNARev Southern blot hybridization patterns	166

Abbreviations

AIDS	Acquired immunedeficiency syndrome
AlHV	Alcelaphine herpesvirus
AP	Alkaline phosphatase
ATP	Adenosine triphosphate
BAC	Bacterial artificial chromosome
BART	*Bam*HI rightward transcripts
bp	Base pair
Bcl-2	B-cell lymphoma/leukaemia 2
BHK	Baby hamster kidney
BHV	Bovine herpesvirus
BL	Burkitt's lymphoma
BMV	Brome mosaic virus
BSA	Bovine serum albumin
CDK	Cyclin-dependent kinase
cDNA	Complementary DNA
CHX	Cyclohexamide
CNS	Central nervous system
CPE	Cytopathic effect
CTL	Cytotoxic T lymphocyte
CTP	Cytidine triphosphate
DMEM	Dulbecco's modified Eagle's medium
DNA	Deoxyribonucleic acid
ds	Double stranded
DTT	Dithiothreitol
E	Early
EBER	Epstein Barr virus-encoded small RNA
EBNA	Epstein Barr nuclear antigen
E. coli	*Escherichia coli*
EBV	Epstein Barr virus
EDTA	Ethylenediaminetetraacetic acid
EGTA	Ethyleneglycol-bis(β-aminoethyl)-N,N,N,N'tetraacetic acid

EHV	Equine herpesvirus
eIF	Eukaryotic initiation factor
EMSA	Electrophoretic mobility shift assay
FADD	Fas associated death domain
FCS	Foetal calf serum
FLICE	FADD-like interleukin 1β-converting enzyme
FLIP	FLICE inhibitory protein
GAPDH	Glyceraldehyde-3-phosphate dehydrogenase
GFP	Green fluorescent protein
gp	Glycoprotein
GTP	Guanine triphosphate
GPCR	G protein coupled receptor
HCl	Hydrochloric acid
HCMV	Human cytomegalovirus
HEPES	N'-[2-hydroxyethyl]piperazine-N'-[2-ethanesulphonic acid]
HHV	Human herpesvirus
HIV	Human immunodeficiency virus
HLA	Human leukocyte antigen
HSUR	Herpesvirus saimiri unique RNAs
HSV	Herpes simplex virus
HVS	Herpesvirus saimiri
ICAM	Intracellular adhesion molecule
ICP	Infected cell protein
Ig	Immunoglobulin
IE	Immediate early
IFN	Interferon
IL	Interleukin
IM	Infectious mononucleosis
IR	Inverted repeat
IRF	Interferon regulatory factor
IRES	Internal ribosome entry site
Kb	Kilobase

KS	Kaposi's sarcoma
KSHV	Kaposi's sarcoma associated herpesvirus
L	Late
LANA	Latency associated nuclear antigen
LAT	Latency associated transcript
LB	Luria-Bertani
LCV	Lymphocryptovirus
LHE	Left hand end
LMP	Latent membrane protein
MCD	Multicentric castleman's disease
MDV	Marek's disease virus
miRNA	Micro RNA
mRNA	Messenger RNA
MHC	Major histocompatibility complex
MHV	Murine herpesvirus
MOI	Multiplicity of infection
ND	Nuclear domain
NPC	Nasopharyngeal carcinoma
dNTP	deoxy nucleotide triphosphate
ORF	Open reading frame
OvHV	Ovine herpesvirus
PAA	Phosphonoacetic acid
PAGE	Polyacrylamide gel electrophoresis
PBS	Phosphate buffered saline
PCR	Polymerase chain reaction
PEL	Primary effusion lymphoma
PFU	Plaque forming units
P.I.	Post infection
PKR	Protein kinase R
PTLD	Post transplantation lymphoproliferative disease
pRB	Retinoblastoma protein
RDV	*Rhadinovirus*

RNA	Ribonucleic acid
RNAi	RNA interference
RPMI	Roswell park memorial institute
RPV	Rabbitpox virus
RT	Reverse transcriptase
RTA	Replication and transcription activator
SAP	SLAM associated protein
s.a.p	Shrimp alkaline phosphatase
SD	Standard deviation
SDS	Sodium dodecyl sulphate
siRNA	Small interfering RNA
SIV	Simian immunodeficiency virus
SLAM	Signalling lymphocyte activation marker
snRNP	Small nuclear riboprotein
ss	Single stranded
S/N	Supernatant
SPBS	Sterile phosphate buffered saline
SSC	Saline sodium citrate
STP	Simian transforming protein
TAE	Tris acetate EDTA
Taq	*Thermus aquaticus*
TBE	Tris borate EDTA
TE	Tris EDTA
TF	Transcription factor
TIP	Tyrosine kinase interacting protein
TLS	tRNA-like structure
TK	Thymidine kinase
TNF	Tumour necrosis factor
tRNA	Transfer RNA
TYMV	Turnip yellow mosaic virus
URNA	Unique RNA
UTP	Uracil triphosphate

UTR	Untranslated region
UV	Ultraviolet
v	Viral prefix
vtRNA	Viral tRNA-like molecule
v/v	Volumer per volume
VZV	Varicella zoster virus
w/v	Weight per volume
XLP	X-linked lymphoproliferative syndrome

Chapter 1: Introduction

1.1 Herpesviruses

1.2 Gammaherpesviruses

1.3 Murine gammaherpesvirus-68

1.4 Transfer RNA molecules

1.5 Viral non-coding RNA molecules

1.6 Project outline

1.1 Herpesviruses

Herpesviruses constitute a large family of at least 130 species of viruses, isolated from a variety of animal species as diverse as humans and oysters. They can be described as an evolutionarily old family of viruses that are well adapted for survival within their host species, so much so that many herpesviruses are only able to infect their natural host. Their apparent evolutionary success can be attributed to their ability to persist for the life-time of the host, rarely causing overt disease in immunocompetent individuals. However, in certain circumstances, such as infection of immunocompromised individuals or an alternative host species, serious illness can result. Most animal species can be infected by two or more distinct herpesviruses, for example there have been eight herpesviruses found to be associated with humans to date (Table 1).

Members of the *Herpesviridae* all share four significant properties:

1. They encode a large array of enzymes involved in nucleic acid metabolism (e.g. thymidine kinase), DNA synthesis (e.g. DNA polymerase) and protein processing (e.g. protein kinase).
2. The synthesis of viral DNA and capsid assembly occurs in the nucleus.
3. Production of infectious progeny invariably results in destruction of the host cell.
4. They have the capacity to maintain a latent infection within their natural hosts, expressing only a limited number of viral genes from a circularized genome. The exact cell type responsible for maintaining the latent infection varies between the different herpesviruses (Roizman and Pellet, 2001).

The ability to maintain a latent infection allows herpesviruses to persist for the life-time of the host. During latency the viral DNA circularizes to form an extra-chromosomal episome and gene expression becomes limited, to some extent facilitating the escape from the host immune response. Infectious progeny are produced through reactivation of the latent genomes, allowing transmission of the virus to a new host.

Subfamily	Genus	Virus	Disease associations
Alphaherpesvirinae	*Simplexvirus*	HSV-1	Cold sore, keratitis, ocular disease, encephalitis
		HSV-2	Genital lesions, encephalitis
	Varicellovirus	VZV	Chicken Pox, shingles Post herpetic neuralgia
Betaherpesvirinae	*Cytomegalovirus*	HCMV	Mononucleosis, congenital deformities, ocular disease
	Roseolovirus	HHV6	Liver dysfunction, Exanthema subitum (ES)
		HHV7	ES
Gammaherpesvirinae	*Lymphocryptovirus*	EBV	Infectious mononucleosis Burkitt's lymphoma, Hodgkin's disease, nasopharyngeal carcinoma, post-transplant lymphoproliferative disease
	Rhadinovirus	KSHV	Kaposi's sarcoma, primary effusion lymphoma, multicentric Castleman's disease

Table 1.1
Table of the known human herpesviruses and their clinical manifestations. Adapted from Fields Virology 4th edition (ed. Knipe and Howley)

1.1.1 Classification

Herpesviruses can be divided into three subfamilies: the *Alphaherpesvirinae*, the *Betaherpesvirinae*, and the *Gammaherpesvirinae.* Initial classification was based upon biological properties, including the host range of the viruses, the length of replication cycle, the ability of the virus to exhibit cell to cell spread in culture and the sites of latent infection. More recently however classification has been based on DNA sequence homology, similarities in genome sequence arrangement, and relatedness of viral proteins demonstrable by immunologic methods.

1.1.1.1 Alphaherpesviruses

The *Alphaherpesvirinae* contains the genera *Simplexvirus* [e.g. herpes simplex virus types 1 and 2, (HSV-1 and HSV-2)], *Varicellovirus* [e.g. varicella zoster virus (VZV)] and *Mardivirus* [e.g. Marek's disease virus (MDV)]. They represent a subfamily of herpesviruses with a capacity to establish latent infections mainly within sensory ganglia, with the exception of members of the *Mardivirus* genus which form a latent infection within T lymphocytes. They exhibit a variable host range and have a relatively short replication cycle with a rapid spread in culture, accompanied by efficient destruction of the host cell.

1.1.1.2 Betaherpesviruses

Members of the *Betaherpesvirinae* have restricted host range, and were initially characterized as exhibiting a long replication cycle and slow spread in culture, based upon the time taken for the virus to produce cytopathic effects. However, quantification of viral DNA load *in vivo* has shown a much more rapid replication cycle, with a doubling time of less than two days (Emery *et al*, 1999). Infected cells characteristically become enlarged, a process known as cytomegalia. Persistent infection occurs mainly within mononuclear cells (Mocarski and Courcelle, 2001), in addition to cells of the central nervous system, salivary glands and kidneys. The subfamily contains the genera *Cytomegalovirus* and *Roseolovirus.* Members of the *Cytomegalovirus* genus include human cytomegalovirus (HCMV) and its related

mouse counterpart, mouse cytomegalovirus (MCMV), and those of the *Roseolovirus* genus include human herpesviruses 6 and 7 (HHV-6 and HHV-7).

1.1.1.3 Gammaherpesviruses

The *Gammaherpesvirinae* constitute a sub-family with a very narrow host-range, in both the cell type and host species they are able to infect, with infection often being restricted to the family or order to which the natural host belongs. They show a varied ability to replicate *in vitro*, with only a small number of gammaherpesvirus species being able to undergo lytic replication in certain cell lines. Latent infection is maintained primarily but not exclusively within T- and B-lymphocytes. The subfamily contains the genera *Lymphocryptovirus* (e.g. EBV) and *Rhadinovirus* [e.g. Kaposi's sarcoma associated herpesvirus (KSHV), herpesvirus saimiri, (HVS) and murine gammaherpesvirus-68 (MHV-68)].

1.1.2 Herpesvirus Structure

The herpesvirus virion contains genetic information in the form of linear dsDNA found within an icosadeltahedral capsid approximately 100 to 110 nm in diameter composed of 162 capsomeres (Roizman and Pellet, 2001). The outer layer of the virion is composed of an envelope derived from patches of cellular membrane containing about a dozen viral proteins and glycoproteins (figure 1.1). The structure between the capsid and the envelope is known as the tegument, a complex, amorphous layer containing viral proteins; in the case of HSV-1, more than 15 tegument proteins have been identified (Mettenleiter, 2002). The tegument links the nucleocapsids to the envelope and maintains the integrity of the virion. The innermost layer of the tegument that is located adjacent to the nucleocapsid of HSV has been shown to exhibit icosahedral symmetry (Zhou *et al*, 1999), however recent evidence indicates that the innermost tegument of gammaherpesviruses is not icosahedral in structure but spherical (Dai *et al*, 2005). Herpesviruses range in size from 120 to nearly 300 nm in diameter, with the differences in size usually being due to variations within the size of the tegument.

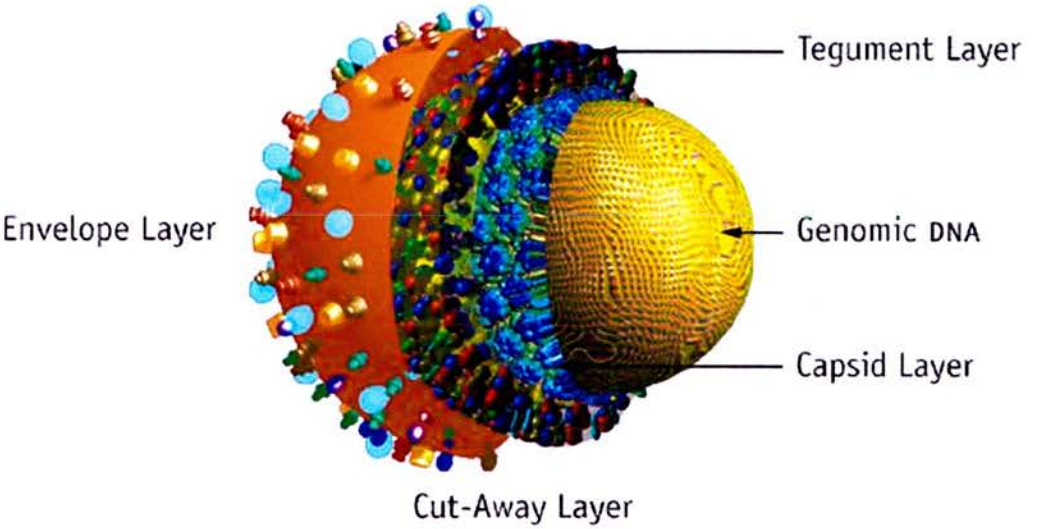

Figure 1.1
Schematic representation of a typical herpesvirus.
Taken from PRN Notebook; www.prn.org

1.1.3 Herpesvirus genome

The herpesvirus gemones range in size from approximately 120 to 250 Kbp and can be divided into six groups based on the presence and localization of repeat regions [figure 1.2 (Roizman and Pellet, 2001)]. They have been found to possess between 70 and 200 open reading frames (ORFs), however this is likely to be an under-estimation as the true complexity of the genomes becomes apparent. For example, alternatively spliced exons and translation frame-shifting result in the expression of different gene products from the same DNA sequence. ORFs can also be expressed which are entirely anti-sense to each other [e.g. HSV-1 $\gamma_1$34.5 and ORFs P and O (Lagunoff and Roizman, 1994)]. Gene overlaps in the same orientation are also common, resulting from promoter-regulatory sequences from 3' genes being located within the coding sequences of 5' ORFs. In addition, many herpesviruses express non-coding RNA molecules, such as the EBV encoded RNAs (EBERs), the latent associated transcripts (LATs) of HSV and the viral transfer RNA-like molecules (vtRNAs) of MHV-68. Furthermore, the recent discoveries of a number of microRNAs encoded by herpesviruses has resulted in an increase in the number of known herpesvirus non-coding RNA (Pfeffer *et al*, 2005a; Pfeffer *et al*, 2004), and it is possible that this number could increase further as the methods used for the detection of small RNA molecules become more sophisticated.

The majority of herpesvirus genes consist of a single ORF flanked by 5' and 3' nontranslated sequences of 30 to 300 bp and 10 to 30 bp respectively, a promoter sequence spanning 50-200 bp upstream of a TATA box and a 3' polyadenylation sequence. Transcription initiates from a site 20 to 25 bp downstream of the TATA box (Roizman and Pellet, 2001). For the majority of herpesvirus genes transcription is carried out by the host RNA polymerase II, with a few, such as the EBERs of EBV, transcribed by RNA polymerase III. A variety of viral genes have been found to be involved in both the up- and down-regulation of viral gene expression, for instance ICP4 of HSV-1 up-regulates the expression of an array of viral genes while also down-regulating its own expression (Roizman and Knipe, 2001). Most herpesvirus genes are not spliced, although every herpesvirus encodes a small number of spliced genes.

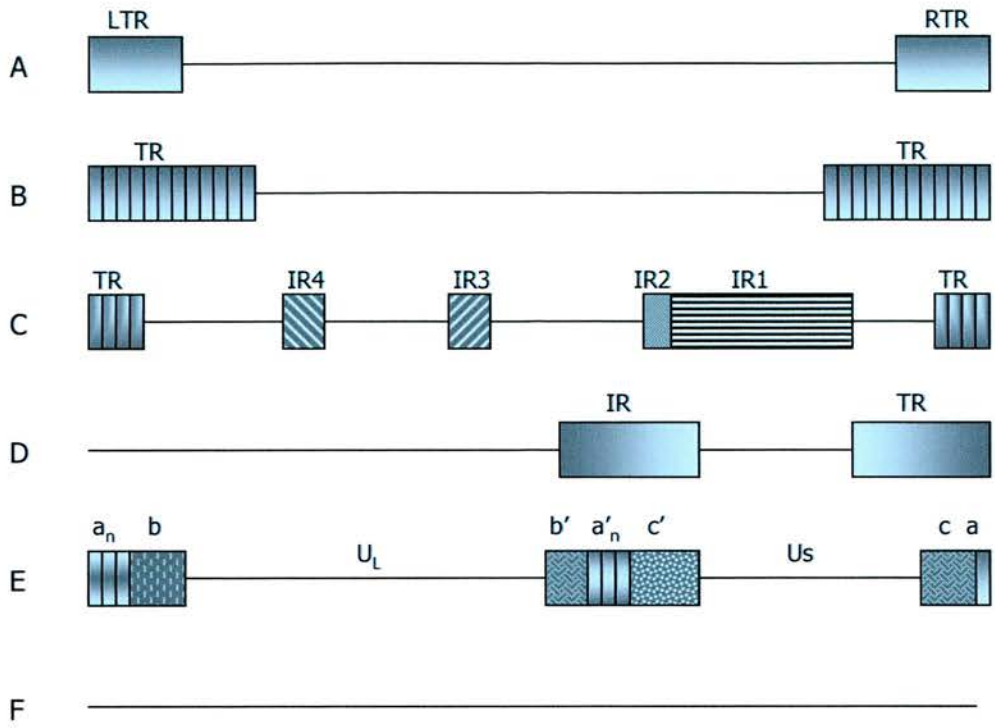

Figure 1.2
A schematic diagrammatic representation of the genome organisations for the different classes of herpesviruses. Members of group A (e.g. channel catfish herpesvirus) possess genomes containing left and right long terminal repeats (LTRs), where as group B herpesviruses have reiterated terminal repeat sequences (e.g. herpesvirus saimiri). Group C herpesviruses, such as EBV, have four internal repeat sequences within the unique region of the genome (IR1-IR4), in addition to reiterated terminal repeat sequences (TRs). In group D viruses (e.g. VZV), the single LTR is repeated in the reverse orientation within the unique region of the genome. Group E genomes contain one terminus with n copies of repeat sequences (a) next to a long repeat region (b). The opposite end of the genome has a single copy of a next to a repeat section (c). For group E herpesviruses (e.g. HSV and HCMV) the terminal ab and ca sequences are also found inverted within the unique region of the genome in the form of b'-a'_n-c', thus dividing the genome into unique long and unique short regions (U_L and U_s respectively), which are able to invert giving rise to four genomic isomers. No obvious repeat regions have been identified within group F genomes (e.g. tupaia herpesvirus).

Generally speaking, herpesviruses express two classes of protein; non-structural proteins necessary for viral DNA replication, and structural proteins that make up the virion framework. However, more than half of HSV-1 genes have been found to be nonessential for growth in culture, although they may not be dispensable for viral infection *in vivo* (Roizman and Pellet, 2001). Such genes have a variety of functions including creating a suitable environment for the replication and expression of viral DNA, evasion of the host immune response and establishment of the latent state.

There are 26 core genes which are conserved between the three families of herpesviruses, found within core gene blocks containing between 2 and 12 genes, in which the gene order and polarity is conserved in all herpesviruses (Roizman and Pellet, 2001). These include some of the virion structural proteins, along with proteins involved in gene regulation, nucleotide metabolism and DNA replication. Sequence similarities also exist at the sub-family level; for example the alphaherpesviruses encode proteins with homologies to VP16 and ICP4, which are not found in other herpesviruses (Roizman and Pellet, 2001). All herpesviruses encode genes homologous to cellular genes, with the gammaherpesviruses possessing the largest array of captured host genes; KSHV encodes 12 genes predicted to be of host origin (Choi *et al*, 2001).

Many herpesviruses genes have two or more distinct functions. The latency associated nuclear antigen (LANA-1) of KSHV has a variety of functions which allow the persistence of the virus within latently infected cells. By tethering the viral episome to cellular chromosomes it ensures equal segregation of virus into daughter cells during cell division (Ballestas *et al*, 1999). It also contributes to immortalization of the infected cell by targeting and inactivating the cellular proteins pRB and p53, (Friborg *et al*, 1999; Radkov *et al*, 2000) along with up-regulating the expression of the enzymatic subunit of telomerase (Knight *et al*, 2001). In order to down-regulate lytic-cycle gene expression LANA-1 is able to both decrease the expression of the lytic transactivator, Rta and antagonize its function (Lan *et al*, 2004), while also up-regulating the expression of the latency-associated genes (Renne *et al*, 2001). By

exhibiting a variety of functions it ensures persistence of the viral DNA within an immortalized cell and maintenance of the latent pattern of gene expression.

1.1.4 Herpesvirus Life cycle

Herpesvirus productive replication involves four key steps; 1) entry into the host cell, 2) viral gene expression, 3) viral DNA synthesis and 4) assembly and egress of the progeny virions. The replication cycle of HSV-1 is perhaps the best characterized of the herpesviruses, thus a description of herpesvirus replication is described as it occurs for HSV-1, although examples for other herpesviruses are also given.

Entry of herpesviruses into host cells can be broken down into three steps; an initial reversible attachment step, followed by irreversible co-receptor binding which in turn mediates fusion of the viral envelope with the plasma membrane. A number of cellular receptors are involved in this process, which in part explains the differences in cell and tissue tropism among the different herpesviruses. Initial attachment for the majority of herpesviruses occurs via binding to glycosaminoglycans (GAGs), for example the receptor for HSV attachment is known to be heparan sulphate which binds the viral gB and/or gC ligand (Roizman and Knipe, 2001). A notable exception is EBV, which instead binds complement receptor 2 (CR2, also known as CD21) on B lymphocytes via gp350 (Spear and Longnecker, 2003). Given that HSV is still able to infect cells devoid of GAGs, albeit with a diminished infectivity, the initial attachment most likely functions to concentrate virions at the cell surface but is not an absolute requirement for virus entry (Banfield *et al*, 1995).

In contrast, the interaction of HSV gD with several co-receptors is essential for cellular entry (reviewed in Spear, 2004), perhaps indicating that this step triggers the changes required for membrane fusion. gD is capable of binding to a number of cell surface receptors, which exhibit differential tissue distributions. These include herpesvirus entry mediator (HVEM, also known as HveA) (Montgomery *et al*, 1996), a member of the tumour necrosis factor receptor family, which is expressed in a variety of cell types included lymphocytes, epithelial cells and fibroblasts but not neurons. gD also interacts with members of the immunoglobulin superfamily,

namely nectin-1 and nectin-2 (Geraghty *et al*, 1998), which are expressed on cells of epithelial, fibroblastic, neuronal and haematopoietic origin. Within polarized epithelial cells they localize primarily to adherens junctions and may therefore be more important in cell to cell spread of the virus (Sakisaka *et al*, 2001), in addition to mediating infection of neurons (Simpson *et al*, 2005). Specific sites generated in heparin sulphate by 3-*0*-sulphotransferases, which are broadly distributed on a number of cell types, are capable of being bound by gD, although a role within infection of human cells has yet to be demonstrated (Shukla *et al*, 1999). In addition to allowing viruses to enter a variety of cell types, the differential expression of co-receptors may play a role in allowing viruses to exhibit different cellular tropisms during different stages of infection. This is perhaps best exemplified by work conducted on EBV, which is able to infect both epithelial and B cells. During B cell entry gp42 carries out a role analogous to HSV gD through binding HLA class II (Spear and Longnecker, 2003). The cellular receptor responsible for entry in epithelial cells has yet to be identified. Viruses lacking gp42 are unable to enter B cells but are still able to infect epithelial cells with equal efficiency (Wang *et al*, 1998). In B cells, gp42 is sequestered by HLA II, resulting in virions that are depleted in gp42 and are able to enter epithelial cells more efficiently than B-cells (Borza and Hutt-Fletcher, 2002).

Following co-receptor binding, viral entry then occurs by fusion of the virion envelope with the plasma membrane, a process which is unclear at the molecular level, although several virally encoded glycoproteins play a role; namely gB, and the gH-gL heterodimer, which are conserved in all three sub-families of Herpesviruses (Spear and Longnecker, 2003). It has been hypothesized that co-receptor binding by gD induces a rearrangement or conformational change in the viral proteins facilitating envelope fusion with the cellular membrane (Roizman and Knipe, 2001).

Following fusion with the cellular membrane, at least part of the tegument dissociates from the nucleocapsid. A number of tegument proteins, such as virus host shut-off protein (vhs), which modulate the cellular environment, remain in the cytoplasm, while others such as VP16, a protein involved in the regulation of viral

gene expression, are transported to the nucleus (Roizman and Knipe, 2001). The nucleocapsid is transported along microtubules to the nucleus, which it enters through the nuclear pores. Within the nucleus, viral DNA is released, circularizes and localizes in close proximity to nuclear domain-10 (ND-10) structures (Ishov and Maul, 1996).

HSV-1 infection facilitates the switch from cellular to viral gene expression by inhibition of host transcription, RNA splicing and transport, and protein synthesis. Viral gene expression takes place in a cascade fashion for all herpesviruses (Honess and Roizman, 1974), initiating with the immediate early (IE) or α-genes, which are classified as being expressed in the absence of *de novo* viral protein synthesis. In the case of HSV-1, the tegument protein VP16 plays an important role in enhancing the expression of the α-genes (Batterson and Roizman, 1983), which encode six proteins (ICP0, 4, 22, 27, 47 and $U_s1.5$). The products of α-genes typically function to regulate later gene expression as well as modification of the host cell. The second class of genes, the early (E) or β-genes, are classified based upon their dependence on viral protein synthesis but not DNA replication for their expression (Honess and Roizman, 1974). This can be attributed to their reliance on functional ICP4 for their expression (Roizman and Knipe, 2001). The β-genes encode proteins involved in DNA replication (e.g. ICP8) and nucleotide metabolism (e.g. thymidine kinase). The late (L) or γ-genes are expressed only in the presence of protein expression and viral DNA synthesis (Honess and Roizman, 1974). They can be further sub-divided into γ1- and γ2-genes (Roizman and Knipe, 2001). The γ1-, or leaky-late, genes are expressed relatively early following infection and are stimulated a few fold by viral DNA synthesis. The γ2- or true-late genes are not expressed in the absence of DNA replication. The γ-genes encode mainly structural components of the virion, including capsid proteins, which are translated in the cytoplasm and then imported into the nucleus where capsid assembly takes place.

Replication of viral DNA occurs following the expression of the β-genes. Several of the β proteins localise in prereplicative sites near ND-10 structures, where viral DNA synthesis initiates on the circular molecule (Maul *et al*, 1996), carried out by the viral

DNA polymerase and its accessory protein, a ssDNA binding protein (ICP8), a helicase primase complex of proteins and the origin binding protein. Initial replication proceeds in the theta replicative form, however this switches early in the replication cycle to a rolling-circle mechanism giving rise to concatemeric molecules (Roizman and Knipe, 2001). As DNA synthesis progresses, the progeny DNA molecules and replication complexes accumulate in the nucleus in globular structures known as replication compartments (Quinlan *et al*, 1984). It is within the replication compartments that the concatemeric DNA is cleaved and loaded into empty nucleocapsids.

The nucleocapsids exit the nucleus by budding through the inner nuclear membrane, from which they acquire a primary envelope distinct from that found on mature virions (Mettenleiter, 2002). Theories as to how final envelopment and budding of the virions from the host cell takes place have been widely disputed. One model suggests that virions retain their integrity, and traffic from the inner nuclear space to the Golgi in vesicles or within the lumen of the endoplasmic reticulum and viral proteins are subsequently modified during final maturation through the secretory pathway. However, the now widely accepted model involves fusion with the outer nuclear membrane or endoplasmic reticulum, resulting in loss of the primary envelope and translocation of the free nucleocapsids to the cytoplasm. The evidence supporting this model includes electron micrograms which demonstrate fusion of the primary envelope with the outer nuclear membrane (Granzow *et al*, 2001). In addition the composition of the envelope glycoproteins changes between primary envelopement within the nucleus and final release of the virus, for example the UL31 and UL34 are found within the primary envelope but not within extracellular enveloped virions (Skepper *et al*, 2001). Furthermore, tegumentation has been found to occur within the cytoplasm and not the nucleus, through an intricate network of protein-protein interactions resulting in the formation of both the inner and outer tegument (Mettenleiter, 2002). Following final envelopement mature virions are secreted from the cell via the vesicular route.

1.2 Gammaherpesviruses

1.2.1 Epstein-Barr virus

Epstein-Barr virus was initially discovered over 40 years ago within cells taken from Burkitt's lymphoma (BL), a childhood tumour common in sub-Saharan Africa with a geographical distribution suggestive of an infectious origin (Epstein *et al*, 1964). Thus, EBV represented the first candidate human tumour virus and has since been found to be associated with a number of malignancies. In addition to its presence within 96% of BL tumours, it is also associated with both lymphoid and epithelial tumours, such as Hodgkin's lymphoma and nasopharyngeal carcinoma. It represents an extremely promiscuous human virus, with over 90% of adults being seropositive (Magrath, 1990), reaching close to 100% in the developing world, wherein the majority of infections are acquired within the first three years of life. In contrast, in the developed world, 50% of individuals are sero-negative by the first decade consequently delaying primary infection until adolescence (Steven, 1996). This can result in a self limiting lymphoproliferative disease known as infectious mononucleosis. EBV has a very restricted host range, being able to persistently infect only humans, and is maintained as a latent infection within circulating B-lymphocytes. *In vitro* it is able to infect and transform resting B-lymphocytes, resulting in the formation of lymphoblastoid cell lines (Kieff and Rickinson, 2001).

EBV was the first herpesvirus to be cloned into *Escherichia coli*, enabling a comprehensive study of the viral genome (Arrand *et al*, 1981). It is classified as a group C herpesvirus, based upon the presence and localization of repeat sequences. The genome consists of 172kbp of unique DNA flanked by reiterated 0.5kbp terminal repeat sequences (Kieff and Rickinson, 2001). The unique region is divided by four reiterated 3kbp internal repeat sequences. Two EBV subtypes have been isolated, EBV-1 and EBV-2 (Kieff and Rickinson, 2001), which share extensive homology but differ in their regions encoding the EBNA antigens (EBNA LP, 2, 3A, 3B, 3C). The two subtypes exhibit differing geographical distributions and ability to immortalize lymphocytes, with EBV-1 having a greater ability to transform lymphocytes than EBV-2. However, no differences in disease association have been found.

1.2.1.1 EBV latent infection

EBV is capable of infecting primary human B-cells derived from peripheral blood, tonsils or foetal cord blood, leading to the formation of lymphoblastoid cells lines. B-lymphocytes at earlier stages of development, such as those derived from adult or foetal bone marrow can also be infected, albeit with a lesser efficiency (Kieff and Rickinson, 2001). Latent infection results in a restricted sub-set of viral gene expression which contributes to the maintenance of the viral episome and B-lymphocyte immortalisation. Various patterns of gene expression have been observed (table 1.2). During latent infection *in vitro* six viral nuclear antigens (EBNA-1, -2, -3A, -3B, -3C and -LP) as well as three membrane proteins (LMP-1, -2A and 2B), two EBV encoded RNAs (EBERs) and numerous spliced transcripts arising from the BamHI fragment (BARTs) family of transcripts are expressed, under the control of EBNA-2 (Ling *et al*, 1994). This pattern of gene expression is known as the latency III or growth program. Expression is initiated from one of two promoters, Cp and Wp, which function in a mutually exclusive fashion. Wp is utilized exclusively during initial infection, followed by a switch to Cp usage (Kieff and Rickinson, 2001).

The latency III expression program results in an activated phenotype, resembling that caused by antigenic stimulation, as demonstrated by the up-regulation of cell surface markers, such as CD23 and ICAM1 (Young and Rickinson, 2004). It can be hypothesised this functions to ensure growth transformation of the host cells and therefore amplify the numbers of latently infected B-lymphocytes. Consistent with this, the latency III phenotype can also be seen following the initial infection of naïve B-lymphocytes within the tonsils (Tierney *et al*, 1994) and during infectious mononucleosis (IM). However, during long-term infection the virus persists within long-lived memory B-lymphocytes within the peripheral blood. The exact mechanism by which the B-lymphocyte enters the memory population is still a subject of much debate. One hypothesis is that EBV directly infects pre-existing memory cells (Young and Rickinson, 2004). However, this still does not explain the need for EBV to drive proliferation and activation of naïve B-lymphocytes. A second hypothesis is that the EBV infected cells enter follicles where differentiation into

Latency program	Genes expressed	EBNA-1 Promoter	Example
Latency I/ Latency	EBNA-1 EBERs BARTs	Qp	Burkitt's lymphoma
Latency II/ Default	LMP1, LMP2, EBERs, BARTs	Qp	Hodgkin's disease
Latency III/ Growth	EBNA-1, 2, LP, 3A-C LMP1, LMP2, EBERs, BARTs	Cp/Wp	PTLD, Lymphoblastoid cell line

Table 1.2. EBV gene expression pattern during the different latency program including the promoter used to drive the expression of EBNA-1. Examples of disease states which exhibit the various gene expression patterns are shown, along with the latently infected lymphoblastoid cell line. Adapted from Kieff and Rickinson, 2001.

resting memory cells occurs through the process of the germinal centre reaction but with viral genes instead of antigen providing the signals required to drive differentiation (Babcock *et al*, 2000).

The differentiation of latently infected B-lymphocytes is accompanied by a change in the pattern of gene expression, initially to the latency II (or default) phenotype, as EBV-positive germinal centre tonsillar B-cells have been demonstrated to exhibit this pattern of gene expression (Babcock *et al*, 2000). In addition, EBV infected cells within Hodgkin's lymphoma resemble germinal centre B lymphocytes and also display the latency II pattern of gene expression (Staudt, 2000). At the molecular level, this occurs due to a switch in promoter usage from the Cp/Wp promoters to the Qp promoter, probably through host-cell mediated methylation of the Cp/Wp promoters (Schaefer *et al*, 1997). The pattern of gene expression during long term persistence of the virus following exit of the latently infected B lymphocytes from the tonsils and into the peripheral circulation is still a matter of debate. The latency I (or latency) phenotype was initially characterised *in vitro* within EBV-positive Burkitt's lymphoma B lymphocytes as expressing EBNA-1, the EBERs and the BARTS (Gregory *et al*, 1990). By exhibiting such a limited pattern of gene expression, the virus is able to escape cytotoxic T-cell (CTL) mediated attack as the only viral protein expressed, ENBA-1, contains internal alanine-glycine repeats which was identified as interfering with antigen processing (Mukherjee *et al*, 1998), although recent evidence suggests that EBNA-1 is accessible to the MHC class I pathway (Lee *et al*, 2004; Tellam *et al*, 2004). Within the long-lived circulating memory B-cell population *in vivo*, a variable pattern of gene expression has been detected with the majority of cells expressing only the EBERs and the BARTs, with occasional LMP2A expression and EBNA-1 expression during cell-division (Thorley-Lawson and Gross, 2004). Nonetheless, whatever the pattern of gene expression, it is clear that the virus is able to persist in a benign state within the memory B-cell population for the life-time of the host.

1.2.1.2 Disease Associations

Infectious virus can be found within the saliva of carriers, indicating a site of productive infection within the oral cavity. However, the actual cell type remains controversial, with one hypothesis being that infectious virus is released from B-lymphocytes (Niedobitek and Young, 1994), whereas an alternative hypothesis is that EBV undergoes a cycle of lytic replication within squamous epithelial cells (Sixbey *et al*, 1984). Transmission of the virus occurs through close oral contact (Yao *et al*, 1985) and primary infection is largely asymptomatic, however in certain instances it can result in infectious mononucleosis (IM). The nature of the predisposing factors for IM is not clear, however the age of acquisition is a determining feature, as there has been found to be a 30-50% risk factor for the development of IM when EBV is acquired during adolescence (Crawford, 2001). The reason for the age related disease association is not known, however it has been postulated to be related to the individual immune status or an increased viral dose. In addition, it is possible that there is a sexual route of infection, but it is unclear whether this is a contributing factor in the development of IM (Crawford, 2001). IM is thought to result from the direct infection of an inappropriate cell type, namely memory B-cells, resulting in the clonal expansion of this cell population (Thorley-Lawson, 2001). The resulting symptoms include fever, sore throat, enlarged and painful lymph glands, along with an accompanying severe and debilitating fatigue. The symptoms of IM have an immunopathogical basis, largely due to an increased number of circulating CD8 T-cells, dominated by the Vβ4 subtype.

In healthy individuals, the EBV infection is ultimately controlled by humoral and cell mediated responses, with CD8 T-cells playing an essential role. This is demonstrated by the fact that boys with a rare genetic abnormality known as X-linked lymphoproliferative (XLPS) disease are unable to control primary EBV infection, resulting in an often fatal hyper-acute IM-like syndrome. The mutated gene in XLPS, SAP (SLAM associated protein) is expressed on activated T-cells and NK cells, where it regulates signalling through the signalling lymphocyte activation molecule (SLAM) (Coffey *et al*, 1998). The mutated form seen in XLPS results in T cells

defective in lytic activity, resulting in a decreased ability to kill EBV-positive B lymphocytes (Dupre *et al*, 2005).

EBV is also associated with malignancies in the immunocompromised host, in particular those lacking a functional T-cell response. As a result of immunosuppressive therapy between 5 and 30% of transplant recipients develop post-transplantation lymphoproliferative disorder (PTLD) (Thompson and Kurzrock, 2004), a heterogeneous collection of disorders resulting from an expanded population of B-lymphocytes, which usually carry EBV. The known risk factors for PTLD include the degree of T-cell suppression and the EBV status of the recipient, with those undergoing primary infection at the time of immunosuppression being particularly susceptible (Crawford, 2001). In AIDS patients EBV is associated with a diverse spectrum of B-cell lymphomas (Rickinson and Kieff, 2001), along with being the causative agent of oral hairy leukoplasia (OHL), a benign lesion resulting from lytic replication of EBV in the superficial layers of the tongue epithelium (Greenspan *et al*, 1985).

EBV was initially isolated from endemic Burkitt's lymphoma, a neoplasm common in equatorial Africa and Papua New Guinea. (Epstein *et al*, 1964) Approximately 96% of cases are associated with EBV and the role of the virus in the BL has been demonstrated by studying the BL derived cell line, Akata; sub-clones which have lost EBV show decreased cell growth and will not induce tumours in mice (Shimizu *et al*, 1994). Given the geographical distribution of BL, it has been postulated that malaria acts as a cofactor. Various hypotheses have been put forward as to the role of malaria in BL; one being that continuous re-infection with malaria causing B-cell stimulation may contribute to an expanded number of EBV-infected, proliferating B cells (Thompson and Kurzrock, 2004). A second theory is that the immunosuppressive effects of malaria lead to decreased levels of EBV specific CTLs (Crawford, 2001). A hallmark of BL is a chromosomal translocation resulting in *c-myc* proto-oncogene translocation into the vicinity of the immunoglobulin loci leading to deregulated *c-myc* expression, resulting in continuous proliferation and inhibition of differentiation (Zech *et al*, 1976). The contribution EBV plays to BL is not clear, especially given

that the only viral genes expressed within BL derived cell lines *in vitro* are EBNA-1, the EBERs and BARTs. However, given that the EBV genome is maintained within BL cells it is clear that is does offer a growth advantage, perhaps by inhibiting apoptosis as both EBNA1 and the EBERs have been shown to be involved in the prevention of apoptosis (Kennedy *et al*, 2003; Komano *et al*, 1999).

Hodgkin's lymphoma (HL) accounts for 20% of all lymphomas in the Western World. EBV was first theorized to play a role in HL following the observation that IM is a risk factor (Thorley-Lawson and Gross, 2004). HL is typified by the large multinuclear Reed-Sternberg cells (RSC) along with Hodgkin's cells (known collectively as HRS). EBV can be detected within HRS cells in 50% of HL cases in developed countries, reaching almost 100% of cases in the developing world (Crawford, 2001). Despite comprising the malignant element of HL, HRS cells are vastly out numbered by mononuclear cells, which form the bulk of the tumour mass. As HRS cells contain hypermutated immunoglobulin genes it is believed they are formed from centrocytes which have traversed the germinal centre (Staudt, 2000). B-lymphocytes at this stage of differentiation are usually resting cells prone to apoptosis, however, expression of EBV gene products may provide the growth and survival signals promoting the transformation of these cells; LMP1 constitutively activates the CD40 signaling cascade leading to cellular proliferation (Lam and Sugden, 2003), whereas LMP2A mimics B-cell receptor signaling to maintain survival of the cells (Young and Rickinson, 2004). It can therefore be speculated that HL occurs following a mutation in a germinal centre B-cell during IM preventing its differentiation, thus resulting in the constitutive expression of LMP1 and LMP2A, which then provide the signals for enhanced tumour growth.

EBV has also been associated with malignancies of epithelial origin. Nasopharyngeal carcinoma (NPC) is a tumour of squamous epithelium of the post-nasal space, particular common in areas of South-East Asia and China, where it accounts for the commonest malignancy in men and second most common in women (Crawford, 2001). It can be divided into different forms based upon the differentiation status of the epithelial cells, with a clear link between EBV and the undifferentiated form.

Monoclonal EBV genomes can be found within the malignant epithelial cells, which show a restricted pattern of gene expression, comprising EBNA-1, LMP-1, LMP-2A and LMP-2B, along with the EBER and BART transcripts (Brooks *et al*, 1992). In addition, EBV is associated with approximately 10% of typical gastric adenocarcinomas (Thompson and Kurzrock, 2004). The mechanism by which EBV infects and transforms epithelial cells is not clear, although LMP-1 is believed to contribute to the malignant phenotype due to its ability to inhibit the differentiation of squamous epithelium *in vitro* and induction of a tumorigenic phenotype in animal models (Dawson *et al*, 1990; Nicholson *et al*, 1997).

It is evident that EBV infection and the role it plays in cellular transformation is extremely complex, especially given its varied pattern of gene expression in different B-cell populations. Despite being heavily studied, relatively little is known about initial events following infection, the establishment of latency and the switch to lytic infection, along with how it is able to contribute to malignant phenotypes. This is demonstrated by the continuing debate over the mechanism driving viral persistence, the contribution of EBV to cellular transformation and the role of squamous epithelium during both primary infection and virus transmission.

1.2.2 Kaposi's sarcoma-associated herpesvirus

Kaposi's sarcoma (KS) was initially described in 1872 by the Austrian-Hungarian dermatologist, Moritz Kaposi, as a rare idiopathic pigmentation of the skin (Kaposi, 1872). Following the outbreak of the AIDS epidemic there was increased interest in KS as it composed the major malignancy amongst AIDS patients, occurring in approximately 20% of male patients (Neipel and Fleckenstein, 1999). A virus similar to human herpesviruses was identified using representational difference analysis from an AIDS-KS skin lesion in 1993 (Chang *et al*, 1994). The new virus, named Kaposi's sarcoma-associated herpesvirus (KSHV, also known as HHV-8) was subsequently classified as the only human *Rhadinovirus* identified to date, genetically related to herpesvirus saimiri. It has since been linked to further malignancies, such as primary effusion lymphoma and Castleman's disease (Boshoff and Chang, 2001).

The distribution of KSHV infection is dependent upon geographical and behavioral risk factors. In the US it can be found in 0-10% of blood donors, whereas in Africa it has a sero-prevalence of over 50% (Chang and Moore, 2001). The mode of transmission of KSHV is not known. It can be found within both semen and saliva, and as homosexual men have a particular high infection rate (approaching 40% in some studies) it was hypothesized to have a sexual mode of transmission. In Africa, where sero- prevalence rates are higher, KSHV has an unknown non-sexual route of transmission, resulting in infection during childhood and adolescence (Chang and Moore, 2001).

1.2.2.1 KSHV Molecular Biology

The KSHV genome consists of a single long unique region of 145Kbp, flanked by a variable number of 801bp terminal repeat sequences. In common with other *Rhadinoviruses* the KSHV genome contains conserved gene blocks of structural and metabolic proteins common to all herpesviruses interspersed with non-conserved clusters of genes related to latency and host cell regulation (Chang and Moore, 2001). Like other *Rhadinoviruses*, KSHV encodes an array of cellular homologues, involved in sustaining and propagating the viral infection. These include cell cycle regulatory proteins (e.g. vCyclin), anti-apoptotic proteins (e.g. vBcl and vFLIP) and modulators of the host immune response [e.g. vIRF1 (Choi *et al*, 2001)]. Although many of these genes are unique to KSHV, they affect the same signaling pathways modulated by other herpesvirus proteins, in particular those from EBV (Moore and Chang, 1998).

Studying the gene expression pattern in KSHV infection is hampered by the lack of a cell line permissive for lytic replication. Latent virus can be propagated within primary effusion lymphoma (PEL) derived cell lines and subsequently reactivated using chemical treatment, such as phorbol esters. This allows the classification of genes into three classes (Sarid *et al*, 1998). The class I genes are not induced by chemical treatment and are therefore truly latent. They are composed of a cluster of three genes found at the right-hand end of the genome, translated from two transcripts; LT1 and LT2. LT1 encodes LANA-1, vCyclin and vFLIP, whereas in

LT2, the LANA-1 gene is spliced out resulting in a bicistronic transcript with translation of vFlip initiating from an internal ribosome entry site (Bieleski and Talbot, 2001; Talbot *et al*, 1999). LANA-1 is expressed in all latently infected cells and has a variety of functions (see section 1.1.3), including tethering the viral episome to cellular chromosomes. vCyclin and vFlip function to drive cell cycle progression and inhibit apoptosis (Choi *et al*, 2001). A further class I gene lying outside of this right-hand cluster is a B-cell specific latency gene, known as LANA-2, which is not expressed within KS lesions (Rivas *et al*, 2001). Class II transcripts are expressed at low levels in un-stimulated cells but are phorbol-inducible and are thus expressed during both lytic and latent infection (e.g. ORF K2). Class III transcripts are detectable only after phorbol treatment, and represent truly lytic genes. These include the most conserved herpesvirus genes involved in DNA replication and capsid assembly, along with a number of genes unique to KSHV (e.g. the polyadenylated nuclear RNA or PAN) (Chang and Moore, 2001).

Although PEL derived cell lines have proved useful for the study of KSHV gene expression, they do not entirely represent gene expression patterns *in vivo*. This is because the expression of certain genes, such as vCyclin and vFlip, are cell cycle dependent. Also, the activation of viral promoters using chemical treatment may result in the expression of genes not usually active during lytic replication (Chang and Moore, 2001). Furthermore, many KSHV genes exhibit tissue specific expression patterns, for example, although LANA-2 is classified as a class I gene, it is not found within latently infected spindle cells in KS lesions (Rivas *et al*, 2001), suggesting different patterns of latency similar to that exhibited by EBV. Latently infected cells within KS lesions, display a very limited gene expression pattern, with only LANA-1, vCyclin, vFlip and Kaposin expressed, whereas a substantial fraction of latently infected B-cells in Castleman's disease express a variety of proteins including LANA-1, vFLIP, vIRF-1, vIL-6, PF-8 SCIP, K8-1, K10, and K11 proteins. However it is not clear whether these represent an expanded pattern of latent gene expression or cells undergoing full lytic virus replication (Chang and Moore, 2001) and it has therefore not been unambiguously defined whether latently infected KSHV

cells display different patterns of gene expression akin to those exhibited within EBV-positive cells.

1.2.2.2 KSHV disease associations

Primary KSHV infection of immunocompetent individuals is usually asymptomatic, although in children primary infection may be associated with a febrile maculopapular skin rash (Plancoulaine *et al*, 2000), while a transient angiolymphoid hyperplasia was found to occur as part of a KSHV-seroconversion syndrome in an HIV-infected adult (Luppi *et al*, 2000). Asymptomatic carriers harbour the virus primarily in $CD19^+$ B-lymphocytes, although natural infection of endothelium, B cells, and possibly CD68+ monocyte-macrophage cells, prostate epithelia, and dorsal root sensory ganglion cells has been reported (Chang and Moore, 2001).

Kaposi's sarcoma is a tumour commonly found in the dermis but also occurring within internal organs, which presents as a brownish-purple lesion. Various independent findings have linked KSHV to the aetiological pathogenesis of KS (Boshoff and Weiss, 2001). KS can be divided into four epidemiological forms; classic KS, endemic KS, post-transplant or iatrogenic KS and HIV-associated KS, which are all associated with KSHV infection. Classic KS affects mainly elderly men of Mediterranean, eastern European, or Jewish heritage and generally presents as nodules on the lower extremities. Classic KS rarely metastasizes and patients survive for an average of 10–15 years before dying of an unrelated cause (Hengge *et al*, 2002). Endemic KS is found in sub-Sahara Africa, typically within immunocompetent individuals. It presents as a variety of different clinical manifestations, ranging from a benign nodular disease resembling classic KS to a more aggressive form which disseminates to the visceral organs and lymph nodes, and is found particularly in young children (Hengge *et al*, 2002). Post-transplant or iatrogenic KS occurs in patients following solid organ transplantation and in patients receiving immunosuppressive therapy, either as a result of primary KSHV infection or reactivation of latent virus. Although the course of disease may be rapidly progressive, withdrawal of immunosuppressive therapy usually results in spontaneous remission. HIV-associated KS is particularly aggressive, often arising

quickly over a period of a few days, initially forming macules and frequently evolving to papules and tumours. In the early days of the AIDS epidemic, 15% of all reported AIDS cases had KS as the primary AIDS defining illness. The overall risk of KS in AIDS patients was estimated to be more than 20,000-times greater than the general population and 300-times more than for other immunosuppressed patients (Beral *et al*, 1990). However, the introduction of HAART (highly active anti-retroviral therapy) in developed countries has resulted in HIV-associated KS occurring only sporadically, while in the developing world it remains a common disease.

Histologically, KS is a vascular tumour composed of a variety of cell types. It is characterised by the presence of proliferating spindle cells, which form irregular vascular channels, and are associated with an inflammatory infiltrate. It is the spindle cells that harbour KSHV in all forms of KS (Boshoff *et al*, 1995). The origin of spindle cells is not clear, as they possess endothelial markers (e.g. CD31) in addition to markers typical of macrophages and dendritic cells (e.g. factor XIIIa, CD14, and vascular cell adhesion molecule 1) (Huang *et al*, 1993; Nickoloff and Griffiths, 1989) Recently, spindle cells have been demonstrated to express vascular endothelial growth factor receptor (VEGFR)-3, usually expressed on lymphatic endothelium and neoangiogenic vessels, but not mature vascular endothelial cells, indicating that they are perhaps derived from endothelial precursor cells differentiated towards a lymphatic phenotype (Jussila *et al*, 1998). A matter of controversy is whether KS represents a polyclonal hyperplasia or monoclonal neoplasia. Spindle cells have been found that are both monoclonal and polyclonal in origin and despite constituting the major proliferating component of the tumour, they rarely exhibit a transformed phenotype (Salahuddin *et al*, 1988). Given the dependence upon cytokines for the growth of spindle cells *in vitro* (Ensoli *et al*, 1992), local cytokine production is believed to play a major role in the development of KS. Indeed, inflammatory cells present within KS, such as CD8 T-cells, monocytes-macrophages and dendritic cells, along with activated endothelium produce large amount of cytokines, angiogenic and chemotactic factors, such as IFN-γ, vascular endothelial growth factor (VEGF) and IL-8 (reviewed in Ensoli *et al*, 2000). These factors play a major role by triggering a

cascade of events resulting in the formation of a KS lesion, for example the differentiation and polyclonal proliferation of spindle cells, the recruitment of inflammatory cells and neoangiogenesis.

The role KSHV plays during KS tumorigensis is not fully understood. However, its importance within disease progression is highlighted by its presence within 90% of spindle cells in the advanced stages of all forms of KS (Boshoff and Weiss, 2001). The current model is that KSHV reactivates from latently infected B-cells following immunosuppression or as a result of local cytokine production. This leads to infection of endothelial precursor cells, perhaps arising as a consequence of neo-angiogenesis and neo-lymphangiogenesis also resulting from local cytokine release. KSHV infection of endothelial cells *in vitro* has been demonstrated to induce their differentiation to lymphatic endothelial cells and hence may influence the differentiation of spindle cells *in vivo* (Carroll *et al*, 2004). However local cytokine production also plays a key role in spindle cell differentiation given that only a few spindle cells harbour KSHV within early KS lesions. Nonetheless the presence of KSHV within the majority of spindle cells in more advanced lesions clearly indicates that latent infection offers a growth advantage (Boshoff and Weiss, 2001), perhaps resulting from the presence of latent gene products, such as LANA-1, vCyclin and vFlip. Spindle cells found within advanced cases of KS are often monoclonal and exhibit a transformed phenotype, most likely resulting from the long term expression of latency genes along with the deregulated expression of oncogenes (e.g. Bcl-2) and tumour suppressor genes (e.g. p53) (reviewed in Ensoli *et al*, 2001). Hence advanced KS can develop into a true clonal malignancy resulting from both latent infection with KSHV and local cytokine production.

KSHV is associated with a further malignancy seen predominantly in severely immuno-suppressed AIDS patients, known as body cavity-based primary effusion lymphoma (PEL). PEL presents as a malignant tumour confined to body-cavities, which lacks detectible mass or peripheral lymphadenopathy. Most PELs are thought to originate from post-germinal centre B-cells due to the presence of hypermutated immunoglobulin genes and markers of late stage B-cell differentiation, and are

considered to be clonal due to the presence of clonal immunoglobulin gene rearrangement and monoclonal KSHV terminal repeats (Verma and Robertson, 2003). PELs lack molecular defects usually associated with tumours of mature B-cells, such as activation of the proto-oncogenes c-*myc*, *bcl-2*, *bcl-6*, n-*ras* and k-*ras*, along with mutants in *p53*. PEL cells harbor KSHV genomes at very high copy numbers and are also regularly co-infected with EBV (Boshoff and Weiss, 2001). As described in section 1.2.2.1, KSHV genes expressed in PEL cells, namely vFLIP and vCyclin perhaps play a role in tumourigenesis by inhibiting apoptosis and driving cell cycle progression. In support of this a recent study identified vFLIP as being essential for the survival of PEL cells *in vitro* as down-regulation of vFLIP expression resulted in an increase in spontaneous apoptosis (Guasparri *et al*, 2004).

Multicentric Castleman's disease (MCD) is a lymphoproliferative disorder associated with KSHV. In MCD, the latently infected cell type, known as a plasmablast, belongs to the B-cell lineage (Du *et al*, 2001). Plasmablasts have an unusual phenotype as they exhibit a centroblastic morphology and yet do not harbour somatic mutations in their immunoglobulin genes. It is therefore thought that KSHV infects naïve B-cells and drives them to differentiate into plasmablasts without undergoing the germinal centre reaction. The IL-6 receptor is strongly expressed in the majority of KSHV-positive cells and a proportion of them also express a viral IL-6 homolog (vIL-6) (Oksenhendler *et al*, 2000). It is theorized that vIL-6 acts to drive both the differentiation of plasmablasts and development of lymphoproliferative lesions. MCD affects both HIV-positive and negative individuals. KHSV can be found in nearly 100% of HIV-associated cases (Cesarman *et al*, 1995) and unlike KS, MCD in HIV-positive patients does not often resolve in response to HAART and can progress to fatal lymphoma. KSHV is associated with MCD in 40-50% of HIV-negative patients, who have a worse prognosis than those who are KSHV-negative.

Although a large amount of knowledge has been amassed since the initial discovery of KSHV, little is known about the pathogenesis of KSHV *in vivo*. In particular the events occurring during primary infection, the sites of latency and the contribution of viral genes to the pathogenesis of disease are poorly understood.

1.2.3 Herpesvirus Saimiri

Herpesvirus saimiri (HVS) is the prototype Rhadinovirus, which is apathogenic within its natural host, the squirrel monkey (*Saimiri sciureus*); a South American dwelling New-World primate (Melendez *et al*, 1968). However, it results in T-cell lymphoma formation upon transmission to other new world primates, such as tamarins (*Sagius* spp), common marmosets (*Callithrix jacchus*) and spider monkeys (*Ateles geoffroyii*) (Fickenscher and Fleckenstein, 2001). *In vitro* HVS is able to transform both human and nonhuman cell T-cells to continuous growth in the absence of antigenic or mutagenic stimulation (reviewed in Tsygankov, 2005). Based upon pathogenic properties and sequence variability, HVS can be classified into three subgroups, A B and C (Medveczky *et al*, 1984). All subtypes cause lymphomas within tamarins; however subgroup C viruses exhibit the greatest oncogenicity within a variety of New World primates. Furthermore, they are the only subgroup capable of transforming human and rabbit T-lymphocytes *in vitro*, and inducing lymphoproliferative disease in Old World primates (Biesinger *et al*, 1992; Fickenscher and Fleckenstein, 2001). Subgroup B has the lowest oncogenic potential as demonstrated by their inability to cause T-cell lymphomas within the common marmoset.

The genome of HVS is composed of approximately 113 Kbp of unique DNA, flanked by a variable number of 1444bp terminal repeat fragments (Albrecht *et al*, 1992). It encodes 75 open reading frames, along with seven nontranslated small nuclear RNAs, known as herpesvirus saimiri U RNAs (HSURs). Its genome arrangement can be closely aligned with that of other *Rhadinoviruses* such as KSHV and the murine gammaherpesvirus, MHV-68. In common with other *Rhadinoviruses*, it contains numerous genes which show significant homology to cellular genes, such as a *vFlip* and *vCyclin*, the majority of which are dispensable for growth *in vitro* and tumour formation, indicating that they most likely play a role during persistence in their natural host (Fickenscher and Fleckenstein, 2001). All *Rhadinovirus* genomes contain unique left-hand regions and the oncogenic properties of HVS have been attributed to this region (Desrosiers *et al*, 1985). In agreement with this, the different transforming abilities of the three subgroups are related to sequence divergence

within the left hand region. In subgroups A and B, there is only one open reading frame within this region, known as simian transformation-associated protein (*stp*) A and B respectively, which possess limited sequence homology (Choi *et al*, 2000; Murthy *et al*, 1989). Two open reading frames can be found within the homologous region of subgroup C, known as *stp* C and *tip* (tyrosine kinase interacting protein), which are expressed as a bicistronic transcript. StpA and StpC are both oncoproteins that will transform fibroblasts *in vitro*, whereas StpB does not demonstrate transforming ability. Consistent with these results, StpA and StpC induce tumours in nude mice (Jung *et al*, 1991). The most convincing findings regarding the transforming properties of the Stp proteins ascribe their function to the association with tumor necrosis factor receptor-associated factors (TRAFs) and the subsequent activation of NF-κB (reviewed in Tsygankov, 2005). Although both StpC and Tip have been found to be required for cellular transformation by HVS subgroup C (Duboise *et al*, 1998), the exact function of Tip has not been elucidated, although it may be related to its ability to bind and become phosphorylated by Lck, a protein tyrosine kinase that is crucial to T-lymphocyte signaling and activation (Biesinger *et al*, 1995; Tsygankov, 2005).

Unlike EBV and KSHV, HVS has the ability to undergo lytic replication *in vitro*, facilitating both the study of productive replication and the generation of recombinant viruses. Given the tropism for T-cells and induction of T-cell lymphomas, it is not an ideal model for KSHV and EBV associated disease, however, it has proved useful for the study of oncogenesis *in vivo*. In addition, its ability to transform primary human T-lymphocytes *in vitro*, while maintaining many of their essential functions, facilitates the study of T-lymphocyte function (Mittrucker *et al*, 1993). Furthermore, HVS is able to infect a variety of human cells and persist at a high copy number in the form of non-integrated episomal DNA, allowing segregation to daughter cells during cell division. Due to its ability to provide sustained transgene expression over a long period of time, within both dividing and non-dividing cells (Frolova-Jones *et al*, 2000; Stevenson *et al*, 2000), HVS provides an excellent candidate as a gene therapy vector.

1.2.4 Gammaherpesvirus of Veterinary Importance

Malignant catarrhal fever (MCF) is a generally fatal lymphoproliferative disease of domestic cattle, deer and other farm animal species. It occurs as two different forms exhibiting differing geographical distributions; sheep-associated MCF, caused by ovine herpesvirus-2 (OvHV-2) which shows a world-wide distribution and wildebeest-associated MCF, caused by alcelaphine herpesvirus-1 (AlHV-1), which occurs only in Africa. Both OvHV-2 and AlHV-1 are non-pathogenic within their natural host species of sheep and wildebeest respectively, but cause disease following infection of an alternative host species. The manifestations of MCF include hyperplasia of the lymphoid organs and accumulation of T-lymphocytes within many tissues, accompanied by little or no viral replication. AlHV-1 can be grown in tissue culture, which has enabled its molecular characterization as a *Rhadinovirus*(Bridgen *et al*, 1989). OvHV-2 however can only be propagated within LCLs generated from animals affected by MCF, in a similar manner to EBV and therefore relative little is known about the genomic structure of OvHV-2. Cloning of the OvHV-2 genome as a cosmid library and subsequent sequencing reveals that although closely related to AlHV-1, it can be classified as a separate viral species (Rosbottom, 2003). However, little is known about the role of the viruses in disease pathogenesis.

Equine herpesvirus-2 and -5 have both been classified as gammaherpesviruses based on sequence analysis (Telford *et al*, 1993). The significance of EHV-2 as a pathogen of horses is not clear, although it has infection rates approaching 80% and has associations with a variety of clinical manifestations including respiratory disease and keratoconjunctivitis (Ruszczyk *et al*, 2004). No clear disease associations have been found for EHV-5, but as its prevalence within the UK approaches 25% in the adult horse population and therefore its possible role as an aetiological agent should not be neglected (Nordengrahn *et al*, 2002). A further virus with no known disease association is bovine herpesvirus-4 (BHV-4), classified as a gammaherpesvirus by partial sequence analysis, although it has been isolated from cattle with a variety of disease states (Lomonte *et al*, 1996). Recently, three porcine gammaherpesviruses have been identified, which are all lymphotropic. At least one of these viruses,

porcine lymphotropic herpesvirus 1, was found to be associated with PTLD in an immunosuppressed pig, which is of particular concern as pigs are potential candidates as donors for xenotransplantation to humans.

1.2.5 Animal models of gammaherpesvirus infection

The majority of the data regarding gammaherpesviruses infection have been amassed by studying viral-host interactions during long-term persistence and symptomatic disease, such as within PTLD and KS. However, this only allows information to be collected following the onset of disease and tells little about the factors preceding disease development. Studies of initial EBV infection have been limited to the study of infectious mononucleosis. However primary infection with gammaherpesviruses is largely asymptomatic. The narrow host range of the gammaherpesviruses has impeded studies into the early events following infection and the transmission to the diseased state. In order to try to understand these processes a suitable animal model of gammaherpesvirus infection is required, so as to understand not only the contribution of both viral and host factors to disease progression but also to investigate possible therapies and vaccination strategies.

Initial attempts were made to study gammaherpesvirus pathogenesis by inoculation of nonhuman primates with both EBV and KSHV. In the case of EBV, there is little evidence for infection following inoculation of old world primates, perhaps due to the presence of cross-reactive immunity from endogenous lymphocryptoviruses (LCV) or, as recent evidence suggests, as a result of species specific restriction for LCV-induced B-cell immortalization (Frank *et al*, 1976; Moghaddam *et al*, 1998). Various manifestations of EBV-related disease can be induced following infection of new world primates such as the cotton-top tamarin (*Sagunius oedipus*) and the common marmoset (*Callithrix jacchus*). EBV infection of the common marmoset, causes an infectious mononucleosis-like syndrome (Wedderburn *et al*, 1984), however, the extensive B-cell involvement seen within IM is not present in this model (Emini *et al*, 1986). Within the cotton-top tamarin, EBV causes an acute polyclonal proliferation of B-lymphocytes within all infected animals. However, animals that do not die from lymphoproliferative disease do not become persistently

or latently infected with EBV (Shope *et al*, 1973). Due to the resemblance to PTLD, in both the nature of the lymphoma and the EBV gene expression program (Young *et al*, 1989), EBV infection of the cotton-top tamarin has not only been used as a model for disease progression but also to study candidate vaccines (Epstein *et al*, 1985). However, numerous problems with this model make it an inaccurate analogy to EBV infection within its natural host; firstly the much more rapid disease progression, with tumour formation initiating at 14 to 21 days following infection; secondly the lack of persistent infection following disease recovery; and finally, the ability of EBV to cause lymphoproliferative disease in 100% of infected animals. In the case of KSHV, infection within both SIV positive and negative rhesus macaques has been investigated. However, inoculation resulted in a low level of infection in which no viral transcripts and accompanying pathologies were detected (Renne *et al*, 2004). Consequently this system is not a useful animal model for the study of human disease.

Therefore primate models using infection of simians with endogenous gammaherpesviruses have been explored. LCVs isolated from old world primates share a number of common features with EBV; they can immortalize B-cells from their natural host, they possess genomes that can be arranged collinearly and with a large degree of homogeneity (Wang *et al*, 2001). Although there appears to be a greater degree of heterogeneity between the latent proteins, the functional mechanisms of the majority of these genes are conserved. Hence, oral inoculation of rhesus macaques with an endogenous LCV results in a number of features analogous to EBV infection, such as lymphadenopathy, latent infection in the peripheral blood and virus persistence in oropharyngeal secretions (Moghaddam *et al*, 1997). The rhesus model can also be used to investigate the development of EBV related lymphomas within AIDS patients, as exemplified by the development of B-cell tumours containing latent LCV infection upon co-infection with SIV (Pingel *et al*, 1997).

A number of simian homologues of KSHV have been detected within old world primates, including rhesus macaques [e.g. rhesus rhadinovirus (RV2)], chimpanzees

[e.g. *Pan troglodytes* rhadinovirus-1 (PtRV1)] and baboons [*Papio anubis* rhadinovirus 2 (PanRV2)] (Desrosiers *et al*, 1997; Greensill *et al*, 2000; Whitby *et al*, 2003). Numerous studies have been undertaken to examine an association between these viruses and disease, often in the context of co-infection with HIV homologues. One model which shows some similarities to KSHV induced disease was achieved following co-infection of rhesus macaques with SIV and RV2, which occasionally resulted in a lymphoproliferative disease resembling MCD and an arteriopathy similar to vascular endothelial lesions seen in patients with KS (Mansfield *et al*, 1999). However, a reproducible system for the induction of KS or B-cell lymphomas in the rhesus macaque has not been achieved (Mansfield *et al*, 1999). Also, despite the large amount of sequence homology between the two genomes, RV2 lacks a number of genes unique to KSHV, namely K3, K5, K7 and K12 (Damania and Desrosiers, 2001).

Although nonhuman primate models show great promise for the study of gammaherpesvirus infections, they do have a number of drawbacks, such as a high expense, the requirement of high security measures and adherence to strict government regulations. Furthermore, the understanding of primate biology, including the immune response is not as advanced as in other animal species, and the development of transgenic animals is much more cumbersome. Therefore a murine model for gammaherpesvirus infections would be advantageous, especially given the availability of inbred colonies and numerous transgenic animals to allow investigations into the contribution of host factors to disease. Infection of severe combined immunodeficient (scid) mice has been used for the study of both KSHV and EBV infection. In the case of KSHV, inoculation into human foetal thymus and liver grafts in scid mice leads to the infection of $CD19^+$ B-lymphoctyes, mimicking KSHV infection of humans, although the lack of evident disease limits its use as an animal model for pathogenesis. (Dittmer *et al*, 1999). Scid mice have proved a useful model of EBV related post transplantation lymphoproliferative disease, by inoculation with peripheral blood mononuclear cells from EBV-seropositive individuals, facilitating the study of the mechanism of disease and potential therapies (Johannessen and Crawford, 1999). However, no reliable small animal model has

been developed for other EBV disease phenotypes. Murine gammaherpesvirus-68 (MHV-68) is able to cause both productive and latent infection within laboratory mice analogous to EBV infection (Sunil-Chandra *et al*, 1992a; Sunil-Chandra *et al*, 1992b). In addition, recombinant MHV-68 viruses can be easily produced *in vitro*, enabling the contribution of viral factors to infection to be examined. Such investigations have been carried out by both deletion of endogenous genes and insertion of foreign genes, such as those from KSHV (Douglas *et al*, 2004; Song *et al*, 2005). Hence, MHV-68 infection within laboratory mice can be used to investigate both the interactions between a gammaherpesvirus and its natural host, and for the study of gene function from alternative gammaherpesviruses, such as KSHV and EBV.

1.3 Murine Gammaherpesvirus-68

Murine gammaherpesvirus-68 (MHV-68, also known as murid herpesvirus 4) was initially isolated from the bank vole (*Clethrionomys glareolus*) in 1980 (Blaskovic *et al*, 1980). Ultrastructural examination of infected cells revealed typical herpesvirus morphological features, analogous to those of HSV-1 (Ciampor *et al*, 1981). In addition, passage in the brains of laboratory mice and growth characteristics *in vitro* suggested that it was an alphaherpesvirus (Svobodova *et al*, 1982a). However, certain characteristics *in vivo* were not consistent with those of alphaherpesviruses, such as the presence of MHV-68 within lung epithelium of new-borne mice, and its ability to cause severe pneumonia with widespread haematogenous viral spread (Blaskovic *et al*, 1984; Rajcani *et al*, 1985). Not surprisingly therefore, MHV-68 was officially classified as a gammaherpesvirus of the genus Rhadinovirus, based on sequence analysis (Efstathiou *et al*, 1990) and its ability to establish latent infection within B lymphocytes, macrophages, dendritic cells and epithelial cells further supports this classification (Flano *et al*, 2000; Sunil-Chandra *et al*, 1992b; Weck *et al*, 1999). Although initially isolated from the bank vole, MHV-68 has since been found to be endemic within the wood mouse population in the UK (Blasdell *et al*, 2003), and this is now believed to be the natural host species. Importantly MHV-68 is able to give rise to both lytic and latent infection within laboratory mice and is therefore an excellent small animal model in which to study the relationship between

a gammaherpesvirus and its host. MHV-68 also has the added advantage in that, unlike many gammaherpesviruses, it can lytically infect a variety of cell types *in vitro*, facilitating the study of the viral productive cycle in addition to the generation of recombinant viruses. This has been further simplified by the insertion of a bacterial artificial chromosome (BAC) sequence into the MHV-68 genome, allowing the manipulation of viral DNA within *E. coli* cells (Adler *et al*, 2000).

1.3.1 MHV-68 genome

The genome of MHV-68 is composed of a single unique region of 118kbp of DNA flanked by a variable number of 1.23Kbp terminal repeat region. The genome has been sequenced and the unique region has been found to have an approximate G+C content of 46%, whereas the terminal repeats are composed of 77.6% G+C, a similar content to KSHV and HVS, but significantly lower than EBV (Virgin *et al*, 1997). It encodes 73 open reading frames, along with eight viral tRNA-like molecules and nine predicted microRNAs (Bowden *et al*, 1997; Pfeffer *et al*, 2005b; Virgin *et al*, 1997). The genome consists of a number of conserved herpesvirus gene blocks and can be closely aligned with other Rhadinoviruses, such as KSHV and HVS (figure 1.3). In common with other Rhadinoviruses, MHV-68 possesses a number of genes that are homologous to cellular genes (Virgin *et al*, 1997), such as a vBcl-2, vCyclin-D and viral G-protein coupled receptor (vGPCR), which all appear to be dispensable for lytic growth *in vitro*, but play a variety of roles during *in vivo* replication and persistence (Gangappa *et al*, 2002; Song *et al*, 2005; van Dyk *et al*, 2000; Wakeling *et al*, 2001).

1.3.2 MHV-68 virion composition

The virion structure of MHV-68 is morphologically similar to other herpesviruses (Ciampor *et al*, 1981; Svobodova *et al*, 1982b) and predictably, the genome encodes genes homologous to capsid, tegument and glycoprotein genes from other herpesviruses (Virgin *et al*, 1997). Its ability to grow to high titre *in vitro*, unlike the human gammaherpesviruses, has enabled the identification of proteins associated with the MHV-68 virion (Bortz *et al*, 2003). These include homologues of capsid, tegument and envelope proteins encoded in other gammaherpesvirus genomes,

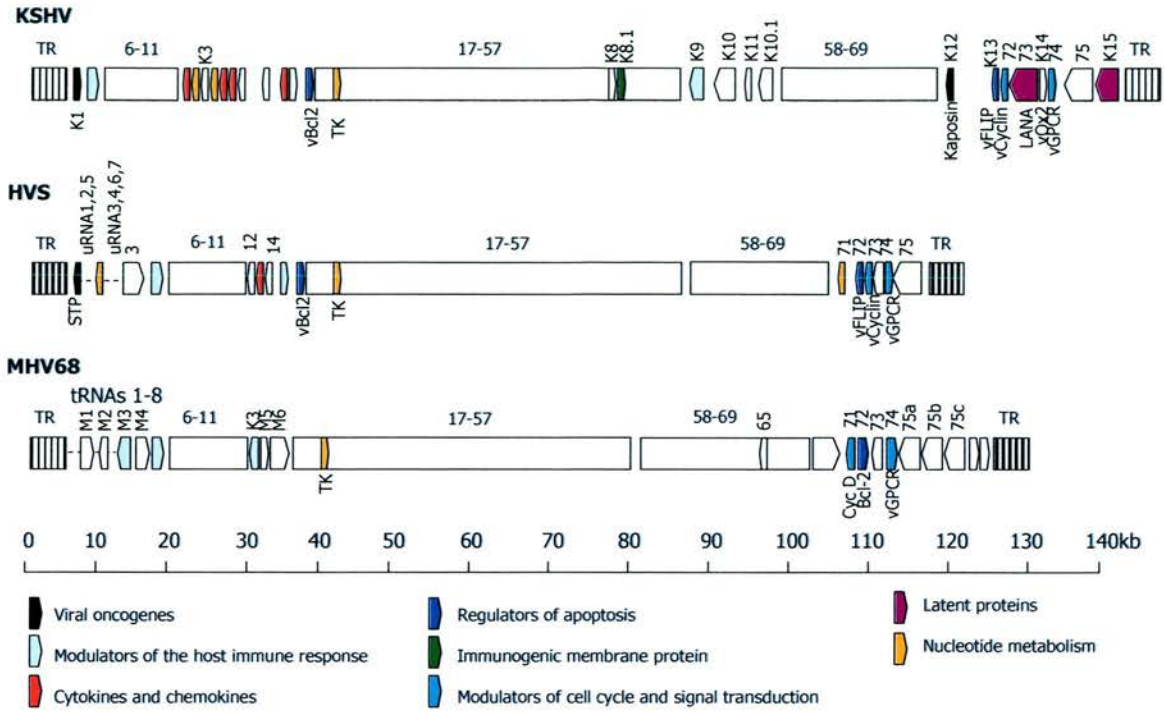

Figure 1.3 Diagrammatic representation of the MHV-68 genome aligned with the genomes of KSHV and HVS. Open boxes represent conserved gene blocks. Additional ORFs are depicted as arrows pointing in the direction of initiation of transcription. Abbreviations; TK, thymidine kinase; vFLIP, viral FLICE-like inhibitory protein; LANA, latency associated nuclear antigen; vGPCR, viral G-protein coupled receptor; STP, simian transformation-associated protein. Adapted from Nash *et al*, 2001.

Predicted location	Gene Product	Predicted function	Predicted Mass (kDa)	Reference
Capsid	ORF25	Major capsid protein	153.2	(Bortz *et al*, 2003)
Capsid	ORF62	Assembly/DNA maturation/Triplex-1	42.7	(Bortz *et al*, 2003)
Capsid	ORF26	Triplex-2	33.4	(Bortz *et al*, 2003)
Capsid	ORF65/M9	Small capsid protein	19.9	(Bortz *et al*, 2003)
Capsid	ORF29	DNA packaging	73.9	(Bortz *et al*, 2003)
Tegument	ORF75c	Tegument protein	145.7	(Bortz *et al*, 2003)
Tegument	ORF45	IRF7-binding homolog	22.4	(Bortz *et al*, 2003)
Tegument	ORF11	Unknown	48	(Boname *et al*, 2005)
Envelope	ORF8	gB/membrane fusion	96.6	(Bortz *et al*, 2003; Lopes *et al*, 2004)
Envelope	ORF22	gH/membrane fusion	82.9	(Bortz *et al*, 2003)
Envelope	M7	gp150/cell free spread	150	(Stewart *et al*, 1996) (de Lima *et al*, 2004)
Envelope	ORF27	gp48/cell-to-cell spread	48	(May *et al*, 2005b)
Envelope	ORF28	Unknown	8.5	(May *et al*, 2005a)
Unknown	ORF20	Fusion protein	28.3	(Bortz *et al*, 2003)
Unknown	ORF24	Unknown	82.9	(Bortz *et al*, 2003)
Unknown	ORF48	Unknown	37.9	(Bortz *et al*, 2003)
Unknown	ORF52	Unknown	14.8	(Bortz *et al*, 2003)

Table 1.3 Proteins associated with the MHV-68 virion. The predicted location of proteins within the virion and possible functions are shown.

present at levels comparable to other herpesviruses, along with a number of unique proteins. The virion associated proteins along with their predicted functions are listed in table 1.3. In addition, a number of cellular proteins are associated with the virion, such as annexin I and II, along with a cytoplasmic β-actin homolog. However a role for these proteins within the virion remains to be established.

1.3.3 MHV-68 replication *in vitro*

MHV-68 is able to replicate in a number of cell lines *in vitro*, including both epithelial and fibroblast cell lines. Recent advances in the generation of mutant viruses by the insertion of BAC sequence into the MHV-68 genome (Adler *et al*, 2000) have enabled the construction of replication deficient viruses for the study of genes essential for viral replication. In particular, two recent studies using signature-tagged transposon mutagenesis have identified a number of candidate genes involved in virus replication. The first study by Moorman et al, identified 16 ORFs essential for viral replication and a further six that when disrupted lead to decreased replication (Moorman *et al*, 2004). In a further study over 1150 MHV-68 mutants were generated, resulting in the identification of 41 candidate genes essential for growth *in vitro*, along with a further six that are required for efficient replication (Song *et al*, 2005). Both studies identified candidate genes essential for replication that are conserved between all families, such as those involved in viral entry (e.g. gH), DNA replication (e.g. ORF6) and tegument proteins (e.g. ORF65). In addition, genes found in other gammaherpesviruses (e.g. ORF 45, an IRF7 binding protein homologue/tegument protein) (Bortz *et al*, 2003; Jia *et al*, 2005b; Song *et al*, 2005) along with genes that are unique to MHV-68 (e.g. M8) have also been found to be essential for viral replication (Song *et al*, 2005).

The mechanism by which MHV-68 enters cells, including the cellular receptors used and corresponding viral ligands, is not fully understood and it appears to be a complex process involving a variety of molecules. Genes homologous to gB, gH and gL of HSV-1, which encode proteins involved in membrane fusion, are expressed by MHV-68. Although both gB and gH are essential for MHV-68 replication (Song *et al*, 2005), no functional role for these proteins has been established. Following viral

entry, the DNA translocates to the nucleus and like all herpesviruses, gene expression initiates in a cascade fashion (Ebrahimi *et al*, 2003) and viral gene expression can be detected as early as three hours following infection (Ahn *et al*, 2002). The lytic transactivator encoded by the *orf50* gene, Rta, is essential for the expression of viral genes, DNA replication and production of infectious virions (Wu *et al*, 2001), however, the mechanism responsible for Rta expression is not known, especially given that no homolog of HSV-1 VP16 has been identified in MHV-68. In addition to the expression of genes that are necessary for viral replication, a number of additional genes are expressed, such as vBcl-2, M3 and K3. Following DNA replication and virion assembly, MHV-68 either exits the cell to be released into the extra-cellular space, or directly infects adjacent cells. The exact mechanisms behind these two processes are not fully understood, although the viral glycoprotein gp48 is required for efficient cell-to-cell spread but not for the release of free virus, (May *et al*, 2005b), whereas the converse is true of gp150 (de Lima *et al*, 2004; Stewart *et al*, 2004). Intercellular spread is thought to be important within *in vivo* infection to facilitate escape from the host immune response, whereas the production of cell free virus is necessary for viral host-to-host transmission.

1.3.4 MHV-68 primary infection *in vivo*

Infection of laboratory mice with MHV-68 is usually carried out via the intranasal or intraperitoneal route, although gastric instillation has been shown to result in viral replication within intestinal epithelia and the establishment of latency within splenic B-lymphocytes (Peacock and Bost, 2000). Given that within the wood mouse MHV-68 is more often found within the respiratory tract than the spleen (Blasdell *et al*, 2003), the intranasal route is thought to more accurately mimic natural infection, and therefore a comprehensive review of viral infection via this route of inoculation will follow: Subsequent to intranasal infection, primary MHV-68 replication occurs predominantly within alveolar epithelial cells, although virus can also be detected within mononuclear cells during this phase (Sunil-Chandra *et al*, 1992a). Viral titres reach a peak at around five days following infection, which is typically accompanied by bronchiolitis and interstitial pneumonia. The large inflammatory infiltrate consists primarily of T-lymphocytes, monocytes and macrophages, (Sarawar *et al*, 2002),

with CD8 T-cells forming the major T-lymphocyte population. Hence, not surprisingly cytotoxic T-lymphocytes represent the major effector cell responsible for virus clearance from the lungs (Ehtisham *et al*, 1993), with neither γ-IFN, antibody nor CD4 lymphocytes playing a major role (Ehtisham *et al*, 1993; Sarawar *et al*, 1997; Usherwood *et al*, 1996b). Although virus cannot be detected by conventional plaque assay any later than ten days post-infection, the inflammatory infiltrate remains until the second week post-infection and focal accumulations of mononuclear cells can be seen as late as day 30 (Sunil-Chandra *et al*, 1992a).

The gene expression pattern within the lungs resembles that of lytic replication *in vitro*. (Martinez-Guzman *et al*, 2003). In addition to the expression of proteins required for viral replication, a number of proteins are expressed that are not necessary for lytic replication *in vitro*. These include a broad spectrum chemokine binding protein (M3), vBcl-2 and vGPCR. Interestingly, despite the large number of genes expressed, only four that are not required for lytic replication have been found to play a significant role during primary infection in the lung (Coleman *et al*, 2003; Song *et al*, 2005). Two of these genes are involved in nucleotide metabolism; thymidine kinase and dUTPase, which are required for the synthesis of dTMP and dUMP respectively. dTMP and dUMP are subsequently converted into dTTP, which is essential for DNA replication. Cellular thymidine kinase and dUTPase are only expressed within cycling cells and consequently herpesviruses encode viral homologues of these proteins in order to replicate their DNA within non-dividing cells. Therefore, the requirement of these enzymes during primary infection within the lung most likely reflects infection of fully differentiated epithelial cells that have exited the cell cycle. The roles of the two further proteins, ORF73 and ORF75a are not clear. ORF73 encodes a protein with 24.2% homology to KSHV LANA-1 (Virgin *et al*, 1997), which plays a variety of functions in during both lytic and latent replication (see section 1.1.3). At low levels of infection (1000pfu) a virus lacking ORF73 exhibited delayed replication kinetics (Moorman *et al*, 2003). However, at higher doses, the absence of ORF73 appears to have no effect on primary infection in the lung (Fowler *et al*, 2003; Moorman *et al*, 2003). The reason for an attenuated phenotype during lytic replication *in vivo* compared to *in vitro* for a virus with a

mutated ORF75a gene is not clear, particularly given that this encodes a tegument protein with unknown function (Song *et al*, 2005). In addition, a related virus, MHV-76, which lacks a portion of the left-hand sequence encompassing the M1-M4 genes along with eight viral tRNA-like molecules, is attenuated during primary infection within the lung (Macrae *et al*, 2001). However, no single gene has been found to be directly responsible for this phenotype (see section 1.3.6).

1.3.5 MHV-68 latency *in vivo*

From the lungs, MHV-68 enters the draining mediastinal lymph node (MLN), the site in which the initial infection of B-lymphocytes is believed to occur. A lymphadenopathy ensues resulting from a transient increase in the numbers of latently infected B-lymphocytes (Nash *et al*, 2001). At this stage, MHV-68 can also be detected within dendritic cells and macrophages, and it is the dendritic cell population that has been postulated to be responsible for carrying the virus from the lungs into the MLN (Nash *et al*, 2001). From the MLN, the virus traffics to the spleen and other lymphoid organs. In the absence of B-lymphocytes, MHV-68 can still be detected within the MLN; however there is little spread to other lymphoid organs, suggesting that B-cells play a major role in trafficking the virus from the MLN (Usherwood *et al*, 1996b). During the establishment of latency within the spleen, MHV-68 can be detected within germinal centre B-cells, macrophages and dendritic cells (Flano *et al*, 2000). The spleen undergoes splenomegaly between the second and third weeks due to a rapid expansion of latently infected germinal centre B cells. Following the peak of latency at day 14 post infection, the numbers of latently infected cells decline to levels at the limit of detection (Sunil-Chandra *et al*, 1992a), and long-term latency is preferentially maintained in both germinal centre B cells and memory B cells (Flano *et al*, 2002; Willer and Speck, 2003).

The mechanism by which MHV-68 gains access to the memory B-cell population is not clear, in particular, whether MHV-68 is able to drive the differentiation of B-cells into the memory phenotype, or if there is a bias for memory B-cell infection at later time points. During the establishment of latency, the rapid expansion of germinal centre B-cells is dependent on CD4+ T-cells, as demonstrated by the lack of

splenomegaly following depletion of this cell type (Ehtisham *et al*, 1993; Usherwood *et al*, 1996a). In addition, not only do the numbers of germinal centre B-cells increase, but so does the T-lymphocyte population, indicating that natural B- and T-cell interactions mediate the response (Usherwood *et al*, 1996a). Furthermore, the maintenance of MHV-68 latency is dependent on the development of memory B-cells, as demonstrated by the loss of latency in $CD40^{-/-}$ B-cells (Kim *et al*, 2003). It therefore appears likely that latency within memory B-cells results from the differentiation of latently infected germinal centre B-cells. However, the viral factors responsible for driving this differentiation are not known, especially given that MHV-68 does not encode homologs of LMP1 and LMP2A of EBV. Nevertheless it is clear that viral factors are required to drive B- and T-cell proliferation as a deletion mutant of MHV-68 lacking the unique left-hand end fails to cause splenomegaly (Macrae *et al*, 2001). Perhaps surprisingly, a further deletion mutant of MHV-68, lacking the M2 gene, was defective in its ability to cause an increase in the numbers of latently infected cells during the acute stage of latency but the overall increase in splenocytes numbers was unaffected (Macrae *et al*, 2003). This indicates that separate viral factors may contribute to the proliferation of latently infected B-lymphocytes and uninfected T-lymphocytes. In addition to the proliferation of B-lymphocytes and CD4+ T-cells, there is an increase in the number of circulating T-cells, dominated by the Vβ4+CD8+ subtype, resembling the rapid expansion of CD8+ cells seen in infectious mononucleosis (Tripp *et al*, 1997). Such a rapid expansion of CD8+ T-cells is suggestive of super-antigen driven proliferation, although cytokine production from CD4 T-cells clearly plays a role (Tripp *et al*, 1997). However, the viral factors responsible for the IM-like phenotype have not been characterized.

In addition to the lymphoid organs, latent MHV-68 infection can also be detected at other sites, including the blood, brain, kidney, liver and lung (Flano *et al*, 2003). In the natural host, the wood mouse, the lung represents the major site of latency (Blasdell *et al*, 2003). The establishment of latency within the lung of laboratory mice is not dependent upon re-seeding of virus via B-cells from the spleen, as demonstrated by viral persistence in both the presence and absence of B-cells

(Usherwood *et al*, 1996b). The cell type harboring the latent infection within the lung in wild-type mice is a matter of dispute; one study detects virus within epithelial cells using a co-staining in situ/immunocytochemistry approach (Stewart *et al*, 1998). However, a separate study using FACS sorting of lung cells reveals that during the initiation of latency, both epithelial and B-cells are latently infected, but during long-term latency MHV-68 is preferentially maintained within the B-cell population (Flano *et al*, 2003).

The mechanism responsible for switching from the lytic to the latent cycle of gene expression is not clear, although it appears that both viral factors, such as the shut-off of lytic cycle gene expression (May *et al*, 2004) and cellular factors, including increased NF-κB activity (Brown *et al*, 2003) are required. In common with all herpesviruses, MHV-68 exhibits a restricted pattern of gene expression during latency. Within the spleen, the transcripts expressed during the acute phase of latency include M1-M4, M8, ORF65, vBcl-2, K3, ORF73 and ORF74, along with vtRNAs1-8 (Bowden *et al*, 1997; Marques *et al*, 2003). However, the expression pattern appears to be cell type dependent, as M2 and ORF73 can not be detected in macrophages. In addition, dendritic cells have a much less restricted pattern of gene expression (Marques *et al*, 2003), although expression of lytic cycle transcripts, such as ORF50 and ORF6 within the non B-cell populations indicates that they may not represent true latently infected cells. In addition, a different pattern of gene expression appears to result following intraperitoneal infection, with M2, vBcl-2, ORF73 and ORF74 expressed within latently infected peritoneal cells and M2, M3 and ORF65 present within splenocytes at approximately 45 days post-infection, although the change in gene expression patterns over time has not been investigated in this model (Virgin *et al*, 1999). Whether MHV-68 exhibits differing gene expression patterns akin to EBV latency programs has not been addressed. However, it is possible given that numerous genes expressed during the early stages of latency are not present during long term infection, including vBcl-2, M2, M4 and ORF74 (Husain *et al*, 1999; Townsley *et al*, 2004; Wakeling *et al*, 2001). In addition, transcripts absent during long term persistence in the spleen, such as ORF74 and

vBcl-2, have been found at the same time points within the lung (Wakeling *et al*, 2001).

In common with other gammaherpesviruses, the latency associated genes of MHV-68 play a role in ensuring the maintenance of the viral episome within a long lived cell population. Although the precise roles of the latent genes have not been characterized, many have been found to be required for the efficient establishment of latency. These include a vBcl-2 (M11) with anti-apoptotic function (de Lima *et al*, 2005; Wakeling *et al*, 2001) and two genes which show homology to KSHV genes; the LANA-1 homolog; ORF73 (Fowler *et al*, 2003) and K3, which down regulates major histocompatibility complex (MHC) class I expression (Stevenson *et al*, 2002). The unique left-hand end of MHV-68, encompassing the M1 to M4 genes and eight vtRNAs is also required for the efficient establishment and reactivation from latency (see section 1.3.6).

1.3.6 MHV-76 and the left-hand end of MHV-68

MHV-76 was isolated at the same time as MHV-68, although from a different host species, the wood mouse (*Apodemus flavicollis*) and therefore proposed to represent a novel murid herpesvirus which perhaps possessed unique biological characteristics. However, fragment analysis of the entire genome, along with sequence analysis of the left-hand end, revealed that the genome of MHV-76 is essentially identical to that of MHV-68, except for a 9,538bp deletion within the left-hand end, encompassing the M1-M4 genes and all of the vtRNAs (Macrae *et al*, 2001; Virgin *et al*, 1997). Hence, it is apparent that MHV-76 represents either a naturally occurring or *in vitro* derived deletion mutant of MHV-68. In support of this, an independent *in vitro* deletion mutant was spontaneously generated which also lacked the same region of the genome (Clambey *et al*, 2002). During *in vitro* replication within a fibroblast cell line, MHV-76 exhibits identical replication kinetics to MHV-68. However, MHV-76 is attenuated during *in vivo* infection, as it exhibits a more rapid clearance from the lungs than MHV-68, with an accompanying increased inflammatory response. In addition, the expansion in latently infected B-cells within the spleen does not occur following MHV-76 infection, and the proliferation of uninfected CD4+ and CD8+ T-

cells is absent. However the exact function of the individual genes is not clear, although various studies using recombinant viruses have highlighted their potential roles within infection:

M1: The M1 ORF exhibits sequence homology to the *rabbitpox virus* (RPV) serine protease inhibitor (serpin) SPI-1, along with the M3 protein of MHV-68 (Bowden *et al*, 1997; Virgin *et al*, 1997). In RPV, SPI-1 determines host range and in addition, has been implicated in the regulation of apoptosis. However, although M1 and SPI-1 are homologous, it is unlikely that M1 exhibits a similar function given that it lacks the highly conserved hinge domain and reactive site loop present in SPI-1 and other inhibitory serpins (Clambey *et al*, 2000). The expression of M1 can be detected during lytic replication both *in vitro* and *in vivo* (Simas *et al*, 1999), and in macrophages, dendritic cells and B-cells in the spleen (Marques *et al*, 2003). Deletion of M1 from MHV-68 appears to have no effect during lytic infection within the lung, or in the capacity of the virus to establish latency, although the ability to reactivate from latency is increased, suggesting that M1 is able to suppress viral reactivation (Clambey *et al*, 2000). However, a conflicting study reported that deletion of M1 along with vtRNAs1-4 resulted in no difference in the ability of the virus to establish or reactivate from latency (Simas *et al*, 1998).

M2: M2 is unique to MHV-68, exhibiting no homology to known cellular or viral proteins (Virgin *et al*, 1997). It is highly expressed during lytic replication within the lung and the establishment of latency in the spleen (Husain *et al*, 1999). M2 contains an actively recognized CD8 T-cell epitope, constituting an important target for controlling the establishment of latency (Husain *et al*, 1999). A variety of studies using deletion mutants of MHV-68 have implicated M2 in either the establishment and/or reactivation from acute latency (Herskowitz *et al*, 2005; Jacoby *et al*, 2002; Macrae *et al*, 2003; Simas *et al*, 2004). However, this was not accompanied by a decrease in splenomegaly, suggesting that M2 has no effect on the proliferation of uninfected T-lymphocytes (Macrae *et al*, 2003). In particular, it has been suggested that M2 plays a role in facilitating the differentiation of latently infected B-cells into

the memory phenotype (Simas *et al*, 2004). However, the mechanism by which M2 functions has not been characterized.

M3: The M3 ORF encodes a secreted, broad spectrum chemokine binding protein, with no sequence similarity to known chemokine receptors (Parry *et al*, 2000; van Berkel *et al*, 1999). It possesses the capacity to bind all families of chemokines; C, CC, CXC and CX(3)C *in vitro*, resulting in a block in chemokine signaling (Parry *et al*, 2000; van Berkel *et al*, 2000). M3 is abundantly expressed during both productive and latent infection, with macrophages and dendritic cells constituting the most abundant source of M3 within the spleen (Marques *et al*, 2003). However, despite its abundant expression and ability to block chemokine activity both *in vitro* and *in vivo*, no clear effect of M3 upon the pathogenesis of MHV-68 has been established. In one study, deletion of the M3 ORF from MHV-68 had little effect on viral pathogenesis within either the lung or spleen, although it did have an effect on the modulation of the immune response following inter-cerebral inoculation (van Berkel *et al*, 2002). A conflicting study reported that deletion of M3 resulted in a decreased latent load in the spleen. In addition, this was found to be the result of CD8 T-cell mediated clearance of the virus from the spleen as depletion of CD8 T-cells reversed the phenotype (Bridgeman *et al*, 2001). However, the recombinant virus used in this study contained a LacZ gene expressed under the control of a CMV immediate early promoter. The insertion of this cassette into the left-hand end of the genome may have disrupted latency levels, perhaps resulting either from CD8 T-cell mediated immune response directed against LacZ, or alteration of the latency gene expression pattern due to a cis-mediated effect of the CMV promoter. Nevertheless, it seems unlikely that M3 plays no role in viral pathogenesis, and recent evidence suggests that the lack of M3 during infection of wood mice results in an increased inflammatory infiltrate within the lung composed largely of macrophages and T cells (D. Hughes, personal communication).

M4: M4 expression can be detected during lytic replication within the lung and the acute-phase of latency within the spleen, but not during long term persistence (Marques *et al*, 2003; Townsley *et al*, 2004). Insertion of M4 into the left-hand

region of MHV-76 results in elevated viral titers at early time points during productive infection in the lungs, demonstrating that M4 may subvert aspects of the innate immune response (Townsley *et al*, 2004). In addition, the insertion virus displayed an increased viral load in the spleen during the acute-phase of latency. However, akin to the M2 protein, insertion of the M4 gene into MHV-76 did not result in an increase in splenomegaly, once again demonstrating that independent factors contribute to the increase in latent load and lymphocyte proliferation. In keeping with its expression pattern, the insertion of M4 into MHV-76 did not affect the viral load during long-term persistence.

vtRNAs: MHV-68 encodes 8 vtRNAs, which appear to be unique to the virus. Based on sequence analysis, the vtRNAs are capable of forming a cloverleaf secondary structure (figure 1.4) (Bowden *et al*, 1997), in which the majority of invariant and semi-invariant bases typical of tRNAs are conserved (see section 1.4.1). However, they possess atypical anti-codon arms, which diverge in size and sequence from recorded tRNAs, hampering the assignment of amino acid specificity. In addition, each vtRNA shows little sequence similarity with known tRNAs sharing the same anti-codon, and importantly, the discriminator bases (nt73), which are known to be important for the recognition of aminoacyl-tRNA synthetase, are not conserved. It is therefore not surprising that at least four of the vtRNAs are not aminoacylated by cellular aminoacyl-tRNA synthetases. The vtRNAs each contain RNA polymerase III promoter elements and are transcribed monocistronically, although it appears that they may be processed from longer 3'-extended precursors (Pfeffer *et al*, 2005b). It is apparent that they are recognized and processed as tRNAs to some extent by the host cell, with the addition of 3' CCA termini (Bowden *et al*, 1997).

In vivo, the vtRNAs have been found to be expressed at high levels within the lung during both productive and latent infection. In addition, their expression can be detected during the acute-phase of latency and in long-term persistence within the spleen (Bowden *et al*, 1997). It is therefore likely that they play a role during both stages of infection, although their function has yet to be characterized. Deletion of

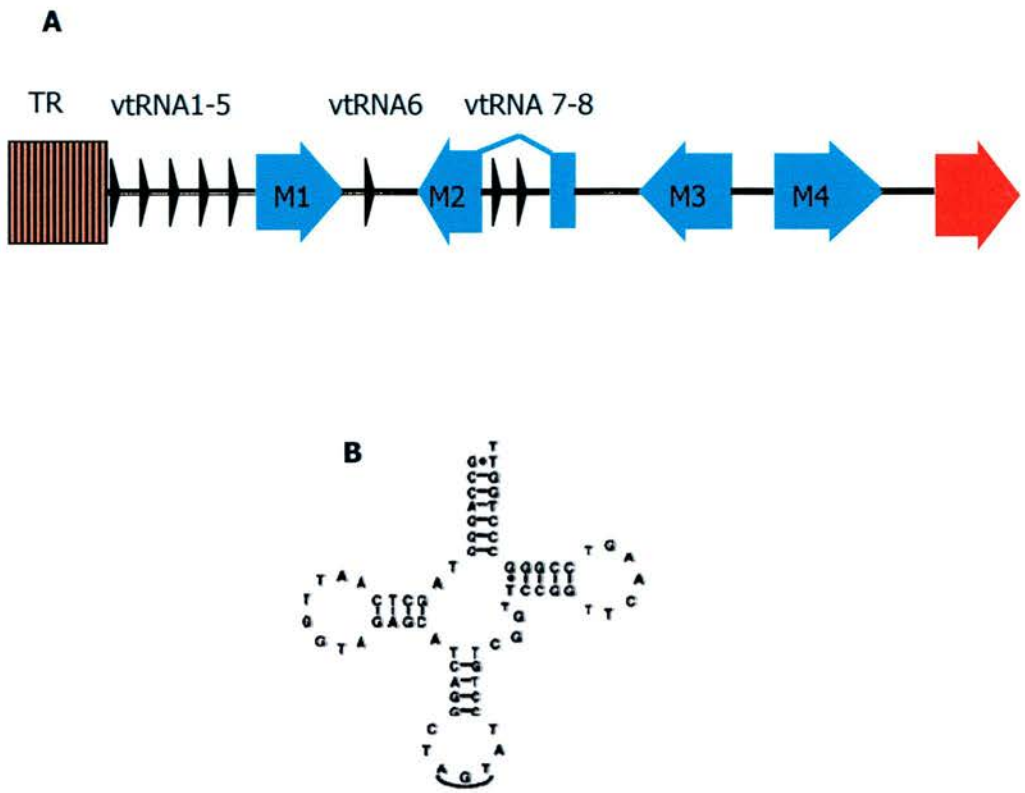

Figure 1.4 The vtRNAs of MHV-68. A) The location of the vtRNAs within the left-hand region of the genome, adapted from Bowden *et al*, 1997. B) Schematic representation of vtRNA5, taken from Bowden *et al*, 1997.

vtRNAs1-4, along with M1, did not affect the ability of the virus to replicate *in vitro* or to establish and reactivate from latency *in vivo* (Simas *et al*, 1998). However, as the virus still retained vtRNAs 5-8, it is likely that their function was not completely abolished, and given the similarity in structure it is likely that there is some redundancy in function between the vtRNAs. The role of the vtRNAs within primary infection in the lung has not yet been investigated.

miRNAs: Recently, nine predicted micro-RNAs (miRNAs) have been discovered within the left-hand region of the MHV-68 genome, two of which have been shown to be expressed during latent infection *in vitro* (Pfeffer *et al*, 2005b). The miRNAs are expressed from the vtRNA primary transcripts, which appear to be processed giving rise to both the vtRNAs and the miRNAs. The miRNAs of MHV-68 differ from cellular miRNAs; firstly due to their unusual expression by RNA polymerase III, and secondly due to the difference in hairpin length of the pre-miRNA molecules, which is much shorter than cellular pre-miRNAs. It is therefore probable that processing of the MHV-68 pre-miRNAs occurs via a different maturation pathway from that for cellular pre-miRNAs. The potential mRNA targets and hence the functional role of the viral miRNAs within infection is not known.

1.4 Transfer RNA molecules

Transfer RNA molecules (tRNA) are small RNA molecules, typically of 73-93 nucleotides in length, which possess a large amount of secondary structure. The majority of tRNAs have an amino acid attached to their 3' end, the identity of which is dependent upon the sequence of three nucleotides found within tRNA, known as the anticodon. tRNAs play a central role during protein synthesis; by recognition of the codon sequence found in mRNA molecules through complementary base-pairing with the anticodon, they allow amino acids to line up according to sequence of nucleotides in the mRNA. The functional role of tRNAs during protein synthesis is well known, and therefore will not be discussed in detail. However, tRNAs do exhibit additional functions during viral infections, and therefore a discussion of these, along with the basic structure and expression of tRNA will follow:

1.4.1 tRNA Structure

The nucleotide sequences of tRNA molecules form a predicted canonical cloverleaf secondary structure based upon intramolecular base-pairing. The classical model for tRNA structure is based upon three stems and loop regions, known as the D loop, anticodon loop and T loop, along with a variable region and acceptor stem (Holley *et al*, 1965). The acceptor stem contains a 3' C-C-A-OH sequence, added post-transcriptionally, which is the point of amino acid attachment (figure 1.5). Typically, the acceptor stem is composed of seven nucleotides, the T and anticodon stem of five, and the D stem of three or four. There is a greater variability in the size of the loops in comparison to the stems, with the T and anti-codon loops usually being composed of 7 nucleotides and the D loop containing a variable number of nucleotides (Dirheimer *et al*, 1995). However, as its name suggests, the greatest variation can be seen in the length of the variable region and tRNA molecules can be divided into two groups based upon the number of nucleotides within this region; class I tRNAs having short variable regions of 4 to 5 nucleotides in length and class II tRNAs having variable regions containing between 10 and 12 nucleotides (Dirheimer *et al*, 1995). However, caution must be applied when inferring tRNA secondary structure from DNA sequence analysis and in certain circumstances it is not possible to propose a secondary structure without isolation and structural determination of the tRNA molecules itself [e.g. Bovine mitochondrial tRNA(Ser)(UCN) (Yokogawa *et al*, 1991)]

Determination of the tertiary structure of tRNAs is extremely problematic as suitable crystals of tRNAs are required. Despite this, the three-dimensional structure of a number of tRNA molecules has been determined, largely using high resolution X-ray crystallography and nuclear magnetic resonance (Dirheimer *et al*, 1995). These studies have shown that despite a large variation in the primary sequence and secondary structure, tRNAs exhibit highly conserved three dimensional structures. Conserved nucleotides, known as the invariant and semi-invariant bases, form intramolecular interactions and facilitate folding into an L-shaped molecule, in which the anticodon is located at one end and the amino acid at the opposite end (Hou, 1993). This allows recognition by aminoacyl-tRNA synthetases, which add the

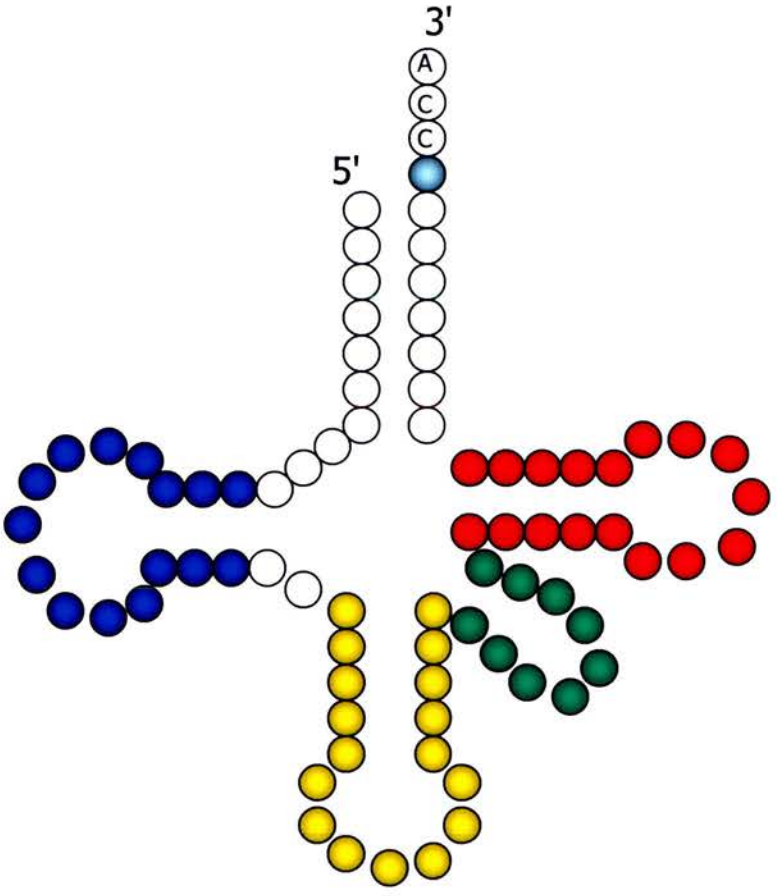

Figure 1.5. Typical two-dimensional cloverleaf structure of a tRNA molecule, showing the location of the D (blue), anticodon (yellow) and T (red) step and loops. The variable region (green) and discriminator nucleotide (pale blue) are also shown, along with the 3' CCA sequence.

correct amino acid onto the tRNA, via interactions with the anti-codon, the D-loop and the discriminator nucleotide, located at position 73 (Meinnel *et al*, 1995).

1.4.2 tRNA Expression

Unlike mRNAs, which are transcribed by RNA polymerase II, tRNAs are synthesized by RNA polymerase III. Transcription of tRNA initiates from transcription factor binding to two sequence stretches within the tRNA gene; box A (nucleotides 8-19) and box B (nucleotides 52-62), to which the transcription factors (TF) IIIB and IIIC bind respectively (Sprague, 1995). TF binding then allows RNA polymerase III to bind and transcription to take place. However, additional factors are involved in tRNA expression, many of which are shared with RNA polymerase II transcribed genes, including common transcription factors and promoter elements. In particular, the TATA-binding protein is essential for tRNA expression (Sprague, 1995). Both 5' and 3' flanking sequences are involved in the regulation of tRNA transcription. For example, individual members of the human $tRNA^{val}$ genes have been found to exhibit tissue specific expression patterns, resulting from sequence differences within the -51 and -17 boundary (Arnold and Gross, 1987). Furthermore, a number of viruses including HSV-1, adenovirus type 5 (Ad5) and hepatitis B virus up-regulate RNA polymerase III expressed genes (Berger and Folk, 1985; Gaynor *et al*, 1985; Wang *et al*, 1995). In the case of Ad5 the E1a gene increases the amount and activity of TFIIIC, resulting in the increased expression of both cellular tRNAs and a viral non-coding RNA molecule; VA1 (see section 1.5.5) (Berger and Folk, 1985). It can be postulated that viral up-regulation of tRNA expression results in an increased tRNA pool required for viral protein synthesis.

1.4.3 tRNA function during viral infection

1.4.3.1 Plant virus tRNA-like structures

A number of plant viruses possess tRNA-like domains within the 3' untranslated regions of their genomic RNA, including bromoviruses, tymoviruses and furo-like viruses. They exhibit varying aminoacylation abilities, which appear to be related to their degree of tRNA mimicry. They have been postulated to have a number of

functions, including the initiation of minus strand synthesis, regulation of protein translation, the provision of the viral telomere during replication and packaging of the genome into the virion (reviewed in (Florentz and Giege, 1995; Giege *et al*, 1998). The tRNA-like structure (TLS) found within the 3' region of the turnip yellow mosaic tymovirus (TYMV) and brome mosaic virus (BMV) have been the most intensively studied and therefore examples from research performed on these viruses will be given.

The TLS of TYMV closely resembles cellular tRNAs, in that it possesses a D, T and anticodon loop, exhibits the expected L-shaped architecture and is valylated by host aminoacyl-tRNA synthetase. However, in contrast to cellular tRNAs, the amino-acid acceptor stem contains a pseudoknot structure (Rietveld *et al*, 1983). In addition to recognition by cellular aminoacyl-tRNA synthetase, the TLS is also processed by CCA nucleotidyltransferase, resulting in the 3' addition of a CCA sequence, and has a high affinity for the translation initiation factor, eEF1A•GTP (Dreher, 1999). It is through the interaction with eEF1A•GTP that the TLS serves as a translational enhancer during protein synthesis, a function that is dependent upon aminoacylation (Matsuda and Dreher, 2004). In addition, the TLS acts as an amino acid donor during protein synthesis, with the incorporation of valine into the viral polyprotein, a function that is both cap- and Met-$tRNA_i^{Met}$-independent, suggesting a novel mechanism for internal initiation of mRNA translation (Barends *et al*, 2003).

In addition to acting as mRNAs, the genomes of positive strand RNA viruses also serve as templates for genome amplification, and the TLS of TYMV been found to function in a manner so as to direct the genomic RNA towards protein synthesis early in infection, and later to serve as a template for minus strand RNA synthesis. EF1A•GTP binding during protein synthesis has been found to prevent negative strand synthesis (Matsuda *et al*, 2004). It has therefore been hypothesised to be one mechanism by which the TLS delays RNA replication until late within infection when sufficient virally encoded RNA-dependent RNA-polymerase has been produced to compete with eEF1A•GTP for binding to the viral RNA. The TLS was initially believed to act as promoter directing minus strand synthesis, however

disruptions within the anti-codon, D- and T-loops had no effect upon minus strand synthesis (Singh and Dreher, 1998), indicating that the TLS does not serve as the origin of replication. This function has been mapped to the CCA sequence at the 3' terminus, although the TLS has been hypothesized to play a role in presenting the 3'-CCA sequence in an accessible conformation (Dreher, 1999).

The BMV genome is composed of three positive strand RNA molecules, which all possess 3' TLS sequences similar to those of TYMV. However, although the TLS of BMV is aminoacylated with the addition of tyrosine, it shows strong divergence from the canonical tRNA structure, and hence the location of the tyrosine identity elements is difficult to ascertain. In common with TYMV, the TLS of BMV appears to function to present the 3'-CCA in the necessary conformation required for minus strand synthesis, in addition to functioning as a translational enhancer (Barends *et al*, 2004). Furthermore, the TLS is thought to carry out a role analogous to that of the telomeres of chromosomal DNA (Rao *et al*, 1989), presumably by recruiting host CCA nucleotidyltransferase to maintain the intact termini. The TLS of BMV is also required for virion assembly, as demonstrated by the finding that in the absence of the TLS mature virions fail to form (Choi *et al*, 2002). However, mature virions can be assembled in the presence of either cellular tRNAs or the TLS in trans. In addition, host tRNAs can mediate the assembly of the virions both *in vitro* and within yeast cells (Cuillel *et al*, 1979; Krol *et al*, 1999), and hence both the tRNAs and TLS have been hypothesized to act as nucleating agents during capsid assembly, with the cellular tRNAs performing this function early in infection when the levels of viral components are low.

1.4.3.2 Cellular tRNA functions during retroviral infection

The retroviral life cycle involves conversion of single-stranded RNA genomes into double-stranded DNA for integration into the host genome. Retroviral DNA transcription is carried out by reverse transcriptase (RT); a multifunctional viral enzyme which acts as both an RNA-dependent DNA-polymerase and a ribonuclease H (RNaseH) to digest the RNA template following transcription (Baltimore, 1970; Goff, 2001). In order to provide the 3'-OH group required for RT-mediated DNA

polymerization, all retroviruses utilize host tRNAs to act as a primer (Marquet *et al*, 1995). The exact tRNAs used varies between the different retroviruses, with human-immunodeficiency virus type 1 (HIV-1) employing $tRNA^{Lys3}$ (Wakefield *et al*, 1995). The primer binding site on the viral genome is located approximately 200 nucleotides downstream from the 5'-end of the full-length RNA, and is complementary to the 18 nucleotide 3'-terminal of $tRNA^{Lys3}$ (reviewed by Gotte *et al*, 1999). The primer tRNA is annealed to the viral RNA upon infection of a new cell, so that cDNA synthesis takes place immediately following infection (Jiang *et al*, 1993). In order to achieve this, the tRNA is selectively packed into the virion, so that there is a higher percentage of the primer tRNA within the virion than in the cytoplasm. Given that the cognate aminoacyl-tRNA synthetase is also packaged via interactions with the virion protein Gag, it could be hypothesised that this allows incorporation of the correct tRNA (Cen *et al*, 2001). A further virion protein, Gag-Pol, interacts directly with the tRNA to stabilise the RNA/protein complex (Mak *et al*, 1994). In addition to functioning as primers for DNA minus strand synthesis, it has also been hypothesised that the tRNA, or additional small cellular RNA molecules, form a structural component of the virion, by acting as a scaffold during the assembly of Gag complexes (Muriaux *et al*, 2001; Wang and Aldovini, 2002).

1.5 Viral non-coding RNA molecules

1.5.1 Alphaherpesvirus non-coding RNA molecules

The latency associated transcripts (LATs) of HSV-1 are the only viral transcript detected within latently infected sensory ganglia (Spivack and Fraser, 1988; Wagner *et al*, 1988). The major LAT species is in the form of nonpolyadenylated stable 2kb intron (Farrell *et al*, 1991), spliced from a primary 8.3kb transcript, which can be further spliced to give rise to smaller 1.5kb and 1.4kb RNA molecules (Spivack *et al*, 1991). In addition to their presence during latent infection, the LATs are also expressed late during the lytic cycle, although the smaller 1.4kb and 1.5kb transcripts can not be detected at this stage of infection (Krause *et al*, 1990), indicating that the splicing pattern of the LATs is either tissue or life cycle specific. The sub-cellular localization pattern of the LATs also exhibits a tissue specific pattern; during latent

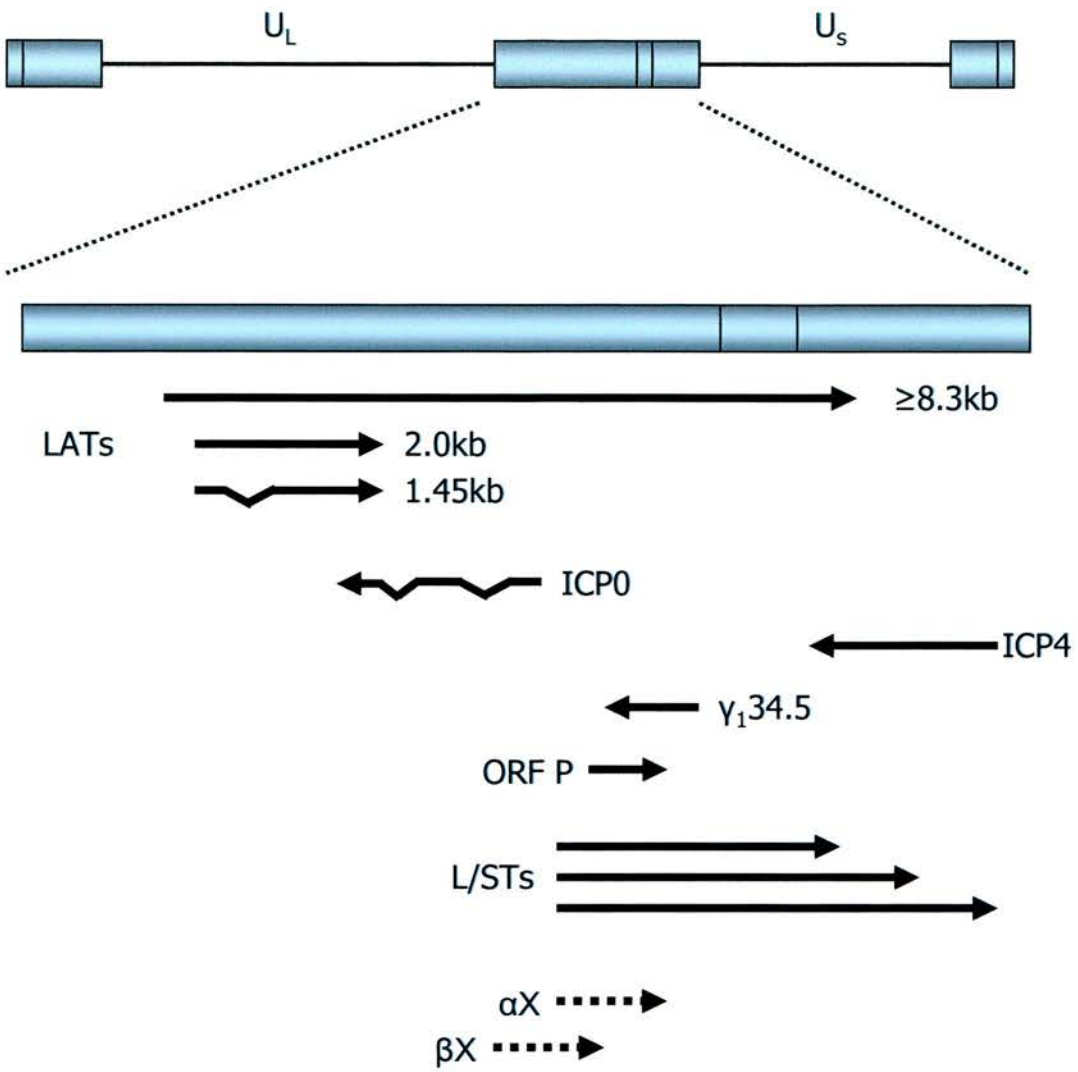

Figure 1.6 The localization of primary LAT transcript, along with the 2Kb and 1.45Kb introns within the HSV-1 genome. In addition, genes which are both anti-sense and co-linear to the LAT transcripts are shown. Adapted from Garber *et al*, 1997

infection they accumulate to high levels within the nuclei, but within lytically infected cells they localize predominantly within the cytoplasm (Nicosia *et al*, 1994). The location of the LATs within the genome of HSV-1 is shown in figure 1.6. The last 750bp of the 2kb intron is anti-sense to the lytic transactivator ICP0. In addition, the full length 8.3kb transcript is antisense to ICP4 and $\gamma_1$34.5 (Chou *et al*, 1990), and co-linear to ORF P (Lagunoff and Roizman, 1994), L/STs (Yeh and Schaffer, 1993) and αX and βX (Bohenzky *et al*, 1995). Therefore in order to the study the role of the LATs in infection, the introduction of mutations must not directly effect the expression of these overlapping ORFs. Despite this difficulty, a large number of LAT null viruses have been created by either deletion of sections of the LAT gene (Block *et al*, 1990; Leib *et al*, 1989; Thompson and Sawtell, 1997), deletion of promoter elements and transcription start site (Garber *et al*, 1997; Thompson and Sawtell, 1997) or disrupting LAT splicing (Kang *et al*, 2003). Characterisations of the various mutant viruses have revealed that the LATs function during the establishment of latency to increase the number of latently infected neurons (Kang *et al*, 2003; Thompson and Sawtell, 1997), but they appear to have no effect upon the viral DNA load within individual neurons (Leib *et al*, 1989; Thompson and Sawtell, 1997). In addition they have been found to be involved in facilitating the efficient reactivation from latency (Block *et al*, 1990; Drolet *et al*, 1999; Leib *et al*, 1989).

The exact mechanisms by which the LATs carry out their function are not clear. A LAT deletion virus showed increased productive-cycle gene expression within murine trigeminal ganglion neurons (Garber *et al*, 1997). In addition, expression of the 2kb LATs within a neuronal cell line resulted in down-regulation of ICP0 gene expression (Mador *et al*, 1998). This was initially postulated to be due to anti-sense repression of ICP0 expression; however this is unlikely to be the case as the 2kb LAT was later found to be unable to result in the anti-sense mediated repression of the ICP0 transcript (Burton *et al*, 2003). An alternative hypothesis is that the LATs somehow induce epigenetic changes resulting in the repression of productive cycle gene expression. Indeed, during latency, the promoters of lytic genes, such as DNA polymerase and TK, are associated with inactive or heterochromatin (Kubat *et al*, 2004). However, following infection with a LAT deletion mutant, lytic promoters

were more often associated with active or euchromatin, indicating that the LATs may promote the assembly of heterochromatin on productive cycle promoters (Wang, Q, Coen, D.M. and Knipe, D.M. in press). The LATs have also been found to block apoptosis both in the context of viral infection within latently infected neurons and in isolation following transfection into cells (Perng *et al*, 2000). The exact mechanism by which they do this is not clear; although it appears that they are able to block apoptosis induced by both the death receptor and mitochondrial apoptotic pathways (Henderson *et al*, 2002). By promoting neuronal survival during latency establishment, maintenance and reactivation the LATs would increase the numbers of latently infected cells in addition to preventing the premature death of neurons prior to the release of infectious virus.

As previously mentioned, the LATs are also present during productive infection where, in addition to the nucleus, they can also be detected within the cytoplasm. In the cytoplasm they associate with ribosomal proteins (Ahmed and Fraser, 2001), indicating that they carry out an additional function during lytic replication and therefore represent multifunctional non-coding RNA molecules.

The alphaherpesvirus of chickens, Marek's disease virus (MDV), expresses a number of LATs during latent infection of lymphocytes, which are encoded within the same region of the genome and are anti-sense to the MDV ICP4 gene. The LATs include two small, spliced RNAs of 0.9kb and 0.75kb, known as Marek's virus small RNAs (MSRs) as well as SARs and S RNAs (Cantello *et al*, 1994). The other RNAs include three highly spliced 3 co-terminal polyadenylated RNAs (McKie *et al*, 1995), a 2.7kb highly spliced polyadenylated RNA (Li *et al*, 1998) along with a 10kb unspliced RNA transcript that spans the entire region. The LATs can be detected within various lymphoblastoid cell lines and MDV lymphoma tissue. Although they can be detected during productive infection, it appears that their expression is down regulated during switch from latent to lytic infection (Cantello *et al*, 1997). During all stages of infection they localize predominantly within the nucleus, although no potential interacting proteins have been identified. The function of the MDV LATs during

infection is not clear, although one study suggests that they play a role in MDV-mediated tumour formation (Morgan *et al*, 2001).

1.5.2 Gammaherpesvirus non-coding RNA molecules

The best characterized non-coding RNA molecules of the Gammaherpesviruses are the EBV encoded small RNA molecules [EBERs (Lerner *et al*, 1981)]. In common with the vtRNAs of MHV-68, they are small, non-polyadenylated, un-capped RNA molecules, transcribed by the RNA polymerase III system. There are two EBER transcripts known as EBER I and EBER II of 162 and 172bp in length respectively, which both possess a stable secondary structure due to extensive intramolecular base-paring forming a number of short stem-loops (figure 1.7) (Glickman *et al*, 1988) Both EBERs can be detected at high levels during all latency programs, often reaching 10^7 copies per cell (Lerner *et al*, 1981) but they are absent from oral hairy leukoplakia, a mucocutaneous lesion that develops in patients infected with HIV that is composed of EBV lytically infected cells (Gilligan *et al*, 1990). In addition, EBER expression appears to be down-regulated following the initiation of lytic replication in vitro (Greifenegger *et al*, 1998), indicating that they are predominantly latently expressed. The EBERs reside mainly within the cell nucleus during mitosis, where they appear to become localized around chromosomes. However, during interphase they show a predominantly cytoplasmic pattern of staining, exhibiting a uniform distribution near to the nuclear membrane, although they do also exhibit a globular pattern of nuclear staining at this stage (Schwemmle *et al*, 1992).

The EBERs have been found to interact with a number of cellular proteins; within the nucleus they interact with La antigen, a protein that associates with the 3' ends of RNA polymerase III transcripts and protects them from exonuclease digestion (Wolin and Cedervall, 2002). Along with La protein, EBER-1 has been found to interact with an interferon (IFN) inducible, double stranded RNA dependent protein kinase [PKR (Clarke *et al*, 1991; Sharp *et al*, 1993)]. PKR is autophosphorylated in the presence of virus, a process mediated by double-stranded RNA, allowing it to phosphorylate and inactivate a protein synthesis initiation factor, eIF-2α and block translation. EBER-1 has been found to block both the autophosphorylation of PKR

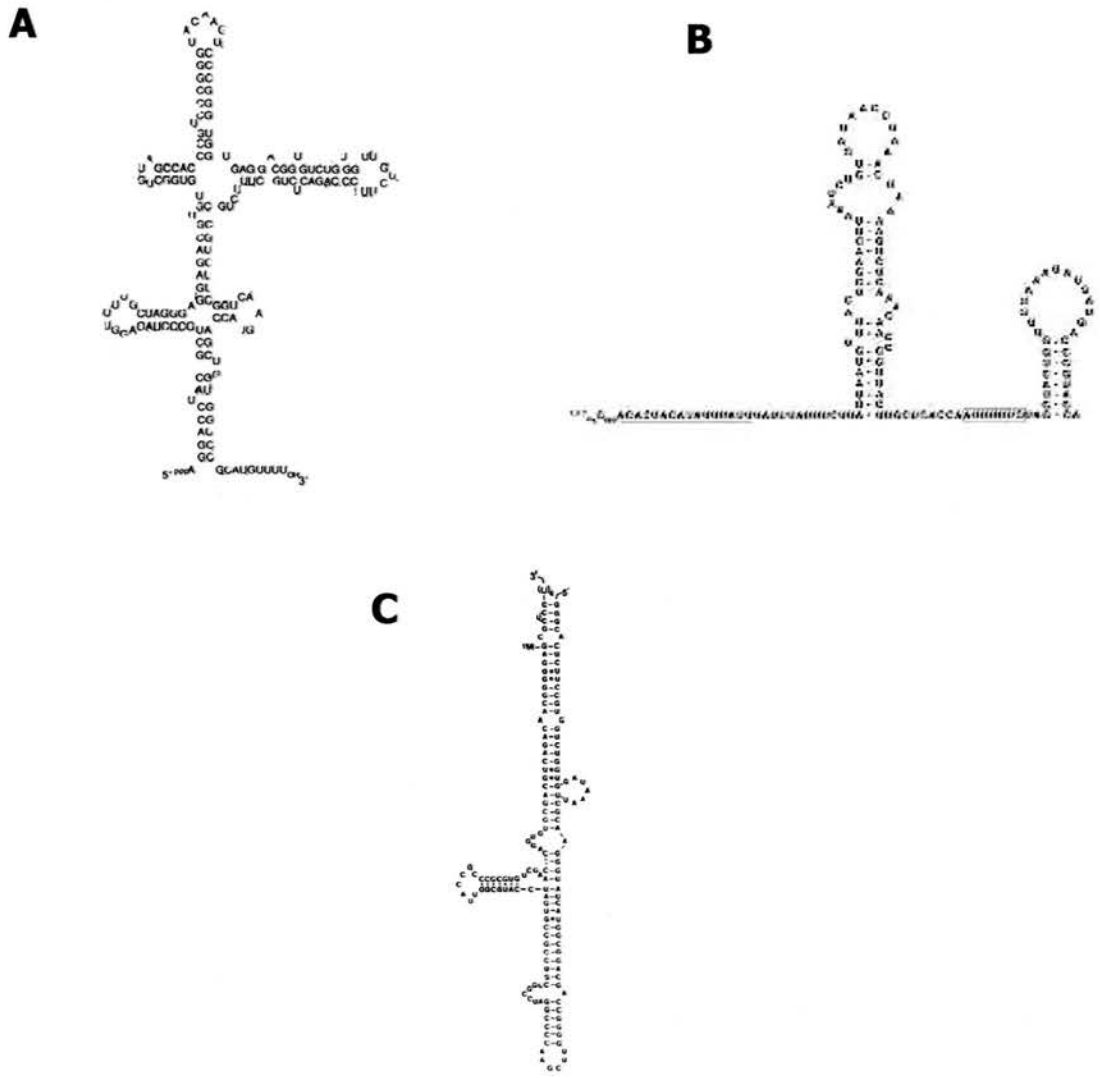

Figure 1.7 Diagrammatic representation of the predicted secondary structures of viral non-coding RNA molecules. (A) EBER-1 of EBV (taken from Glickman *et al*, 1988), (B) HSUR1 of HSV (taken from Lee and Steitz, 1990), (C) VAI of adenovirus (taken from Monstein and Philipson, 1981).

and the subsequent inactivation of eIF-2α. However, although EBER molecules are able prevent to the decrease in protein synthesis in response to dsRNA, they can also do so in a PKR independent manner (Laing *et al*, 2002), indicating that the EBERs possess addition mechanisms to regulate protein synthesis. The EBERs also associate with polyribosomes within the cytoplasm and have been found to interact with an abundant ribosomal protein, L22 (Toczyski and Steitz, 1991). The function of L22 is not clear, although it is involved in the 3;21 chromosomal translocation seen in some forms of acute myeloid leukaemia. In addition, L22 appears to interfere with the EBER-mediated regulation of protein synthesis resulting from both PKR-dependent and independent modes of action (Elia *et al*, 2004). It is therefore possible that L22 functions to sequester the EBERs and attenuate their effects upon the regulation of protein synthesis.

EBERs have also been found to confer clonability in soft agarose, resistance to apoptotic inducers and tumourigenicity in mice when expressed within an EBV negative Burkitt's lymphoma derived cell line (Komano *et al*, 1999). The exact mechanism by which EBERs are able to bring about this oncogenic phenotype is not known although it may be related to their ability to prevent PKR phosphorylation. They have also been found to induce interleukin-10 (IL-10) expression in a Burkitt's lymphoma derived cell-line (Kitagawa *et al*, 2000), which may act as an autocrine growth factor for the lymphoma, and *in vivo* may also be involved in suppressing a Th1 response. However, although they have also been found to greatly increase the frequency of colony formation when transfected into fibroblasts, they were not found to be tumorigenic in this context, and their oncogenic role within EBV infection therefore remains unresolved (Laing *et al*, 2002).

HVS genome contains seven viral U RNAs, known as HSURs, so called because their predicted secondary structure resembles that of cellular U RNAs (figure 1.7), which range in size from 75 to 143 nucleotides in length (Lee *et al*, 1988; Murthy *et al*, 1986). The HSURs are found within the unique left-hand region of the genome, which is essential for the transforming and oncogenic abilities of the virus but not viral replication. They are the most abundant gene produced within latently infected,

transformed T-cells, but despite this they are not required for transformation of cultured marmoset T cells by HVS (Ensser *et al*, 1999). Cellular U RNAs assemble into small nuclear ribonucleoproteins (snRNPs) and perform roles during mRNA maturation such as splicing and polyadenylation. HSURs share a number of common features with cellular U RNAs, in that they are transcribed by RNA polymerase II and acquire a trimethyl-guanosine cap (Lee *et al*, 1988). In addition they also associate with snRNPs, of the class Sm, the assembly of which is mediated by a cellular protein known as survival of motor neurons [SMN (Golembe *et al*, 2005)]. The HSURs have a higher affinity for SMN and can out-compete host U RNAs for assembly, although the functional significance of this during infection is not known.

The 5'-terminal sequences of HSUR1, HSUR2 and HSUR5 are highly conserved and possess AUUUA motifs occurring repeatedly. Similar AUUUA motifs, known as AU-rich elements (AREs), can be found with the 3'-untranslated regions of early response genes such as cytokines, lymphokines and proto-oncogenes and confer mRNAs instability. Given that the HSURs have been found to bind proteins involved in ARE mediated degradation (Myer *et al*, 1992), they have therefore been hypothesised to compete with cellular RNAs for factors involved in mRNA degradation and hence contribute to viral oncogenesis resulting from the altered expression of cytokines and proto-oncogenes. Indeed, cultured T cells transformed with HVS show altered expression of cytokines and other ARE-containing genes (De Carli *et al*, 1993; Medveczky and Medveczky, 1989). However, HSUR1 and HSUR2 appear to have little effect upon the levels of ARE-containing genes as measured by micro-array analysis within T cells *in vitro* (Cook et al, 2004). Nonetheless, HSUR1 and HSUR2 have been found to up-regulate the expression of genes associated with T-cell activation, such as the T-cell receptor β and γ chains (Cook *et al*, 2005), however the mechanism by which the HSURs achieve this is not clear.

KSHV expresses a polyadenylated nuclear RNA (PAN RNAs), an abundantly expressed RNA molecule, which is unlikely to encode protein (Sun *et al*, 1996). In addition, it does not associate with mature ribosomes or polysomes and is therefore believed to function as a non-coding RNA molecule. The PAN RNA differs from

other Herpesvirus non-coding RNAs in that it is expressed predominantly during viral lytic infection and not within latency, in addition to being polyadenylated. It shows a number of characteristics of some U RNAs in that it exhibits sequence homology to a stem-loop of U1 RNA and is composed of 33% uridine, a characteristic of some U RNAs. In addition, it co-localizes with Sm antigens in the nucleus. Although the PAN RNA has been hypothesized to play a role in gene silencing and splicing, its function within infection is not known.

1.5.3 Adenovirus non-coding RNA molecules

Various subtypes of Adenoviruses express one or two non-coding RNA molecules of approximately 160nt in length, known as VAI and VAII (figure 1.7) (Reich *et al*, 1966; Soderlund *et al*, 1976). They are transcribed by RNA polymerase III early within the infectious cycle, with the synthesis of VA1 increasing rapidly during the late stage of infection to become the most abundant RNA within the cytoplasm (Soderlund *et al*, 1976). In common with the herpesvirus non-coding RNA molecules, they have a stable secondary structure (Ma and Mathews, 1993). Deletion of VAI from the viral genome results in a decreased growth rate due to inefficient translation of viral mRNAs at late times within infection (Thimmappaya *et al*, 1982). The mechanism by which VAI enhances protein synthesis was later found to be dependent upon PKR activity (Clemens *et al*, 1994; Laing *et al*, 2002; Sharp *et al*, 1993). Adenoviruses produce large amounts of double-stranded RNA during their replication, and therefore have the potential to activate PKR, resulting in the subsequent phosphorylation of the translation initiation factor eIF2α leading to the inhibition of protein synthesis. In order to overcome this response, VAI is able to block PKR activity thereby preventing the phosphorylation of eIF-2α and allowing protein synthesis to proceed. Given that VAII has a limited ability to block PKR and mutant viruses that lack VAII grow as well as wild type in culture (Ma and Mathews, 1993; Thimmappaya *et al*, 1982), it is not thought to function in the same way as VAI. It has been found to bind dsRNA binding proteins, such as RNA helicase A, which is involved in transcriptional regulation, and NF90 (Liao *et al*, 1998). NF90 is a target for PKR phosphorylation and is able to both up and down-regulate regulate

protein synthesis (Reichman *et al*, 2002). However the significance of VAII-NF90 binding is not known.

In addition to its ability to stimulate protein synthesis in a PKR dependent manner, VA1 also has the potential to prevent the down-regulation in protein synthesis occurring as a result of RNA interference (RNAi). RNAi is a process resulting in the post-transcriptional gene silencing that relies upon short RNAs of approximately 21nt to target either the degradation or translational repression of specific mRNA (Storz, 2002). The short 21nt fragments are generated by the Dicer enzyme from two types of RNAs; small interfering RNAs (siRNAs), that can be processed from dsRNA or short-hairpin RNAs (shRNA), and microRNAs (miRNAs, see section 1.5.4). VA1 has been found to inhibit RNAi by interacting with two proteins known to bind RNA molecules during the RNAi response; Exportin 5 nuclear export factor and Dicer (Lu and Cullen, 2004). In this way VA1 is able to prevent both the nuclear export of shRNAs and pre-miRNAs in addition to preventing the generation of the target 21nt RNA fragment.

1.5.4 Virally encoded miRNA

MicroRNAs (miRNAs) were initially characterised as playing a role during the temporal control of larval development in *Caenorhabditis elegans* (Lee *et al*, 1993; Wightman *et al*, 1993). They have since been found to have a variety of functions within all metazoan eukaryotes, for instance within the fruit-fly they are involved in the regulation of cell proliferation, cell death and fat metabolism. They consist of a 22 nt duplex processed from a 60-70 nt stem-loop pre-miRNA (figure 1.8), which is initially processed from longer transcripts within the nucleus by the Drosha RNase III endonuclease (Bartel, 2004). The pre-miRNA is then transported to the cytoplasm, where it is further processed by Dicer into the mature miRNA. The miRNA can then associate with the RNA-induced silencing complex (RISC) resulting in the down regulation of gene expression, via one of two mechanisms; RNA cleavage or translational repression, with the latter occurring when there is an imperfect match between the miRNA and target mRNA (reviewed in Bartel, 2004). miRNAs are commonly expressed by RNA polymerase II, and can be encoded

within the 3' untranslated regions and introns of genes, in addition to specific chromosomal regions composed of tandem clusters of miRNA sequences.

Since the initial discovery of virally encoded miRNA within EBV (Pfeffer *et al*, 2004), they have been discovered in a number of other viral species, including other Gammaherpesviruses (KSHV and MHV-68) and Betaherpesviruses [HCMV (Pfeffer *et al*, 2005a)] in addition to simian virus 40 [SV40 (Sullivan *et al*, 2005)] and HIV-1 (Bennasser *et al*, 2004)]. In gammaherpesviruses, the miRNAs can be found within regions of the genome actively transcribed within latent infection and hence can be detected within latently infected cells. In contrast, the miRNAs of HCMV are spread across the viral genome and show a lytic cycle expression pattern. Potential targets for the viral miRNAs included cellular mRNAs, some of which are known to be down regulated during infection, for instance those of KSHV have been predicted to target B-cell specific genes that are known to be down-regulated at the mRNA level during KSHV latency (Cai *et al*, 2005). In addition, a number of viral miRNAs have been demonstrated which potentially target viral mRNAs, perhaps repressing viral replication, as is the case for miR-BART2 of EBV, which is capable of targeting the viral DNA polymerase mRNA for degradation (Pfeffer *et al*, 2004), along with miR-N367 of HIV-1, which can efficiently down-regulate viral transcription (Omoto and Fujii, 2005). In addition, the miRNA of SV40 specifically reduces the expression of viral T antigen resulting in decreased sensitivity to CD8+ T-cell killing (Sullivan *et al*, 2005). Hence, viral evolution has taken advantage of the miRNA pathway to regulate the expression of both viral and cellular genes during infection.

1.5 Project outline

The role of the vtRNAs within infection has not been extensively characterised and therefore it is currently unclear what biological function they fulfil. The aim of this study was to investigate the role of the vtRNAs within MHV-68 infection, firstly by examining their expression pattern and sub-cellular localization during *in vitro* infection. The second aim was to characterise the ability of the vtRNAs to bind proteins present within both infected and uninfected cells, given that it is likely that

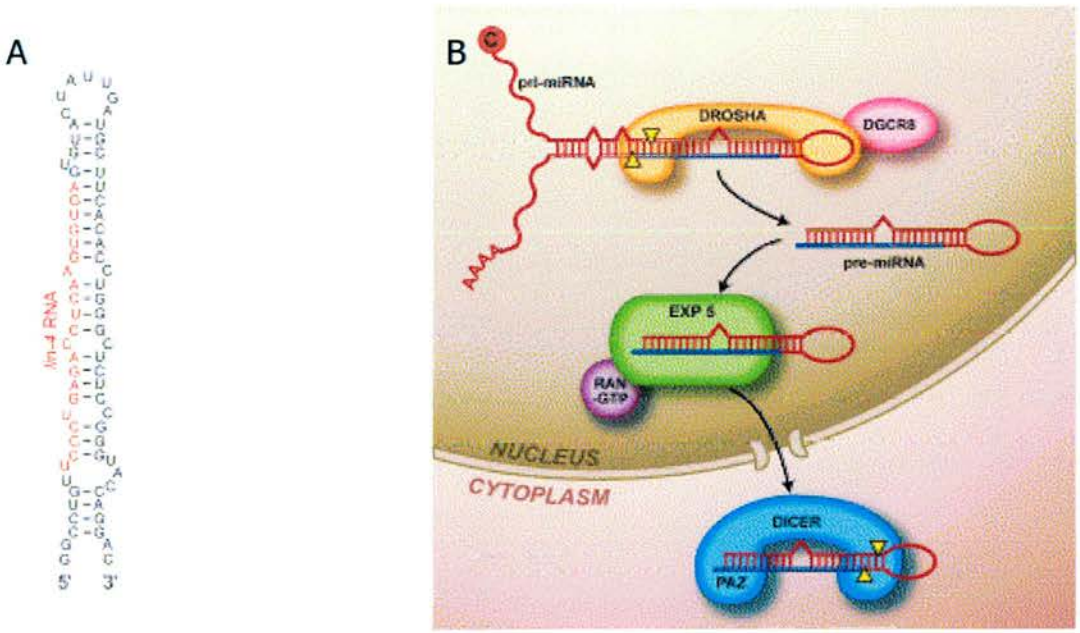

Figure 1.8. Structure and processing of miRNA molecules. A) Diagrammatic representation of a typical cellular miRNA (lin-4 RNA) showing the typical stem-loop structure (taken from Bartel, 2004). B) Schematic depiction of the processing and nuclear export of miRNAs. The long pri-miRNA transcripts are cleaved within the nucleus by the Drosha RNase III endonuclease, resulting in pre-miRNAs of approximately 60-70nt in length. The pre-miRNA is then exported into the cytoplasm via exportin 5 (EXP 5) prior to cleavage by Dicer into mature miRNAs (taken from Cullen, 2004).

their function is mediated via protein interactions. The final objective was to explore the contribution made by the vtRNAs to viral pathogenesis. This was achieved by insertion of the vtRNAs1-5 into the left-hand region of the MHV-76 genome. The behaviour of the recombinant virus was investigated during both *in vitro* and *in vivo* infection. By characterising the role of the vtRNAs within infection, it was hypothesised that this would give insight into the functions of other viral non-coding RNAs.

Chapter 2: Materials and methods

2.1 Molecular cloning

2.2 DNA extraction

2.3 Southern analysis

2.4 Polymerase chain reaction

2.5 RNA extraction and manipulation

2.6 Northern analysis

2.7 RNA *In Situ* Hybridization

2.8 Tissue culture techniques

2.9 Virological methods

2.10 Protein techniques

2.11 Statistical analysis

2.1 Molecular cloning

2.1.1 DNA digestion with restriction endonucleases

Restriction enzymes were purchased from either New England Biolabs or Invitrogen and used with the appropriate manufacturer's buffer. The reaction was set up in a total volume of 20-100µl, containing 10 units of enzyme per 1-10µg of DNA, ensuring that the concentration of restriction enzyme did not exceed 10% of the total reaction volume and incubated at a temperature recommended by the manufacturer (usually 37°C).

2.1.2 DNA Dephosphorylation

Dephosphorylation of the 5' phosphate groups of linearised DNA was carried out using Shrimp Alkaline Phosphatase (SAP, Invitrogen). Typically, 1 unit of SAP per 1µg DNA was added and incubated for 15 minutes at 37°C. Inactivation of SAP was carried out by heating to 65°C for 15 minutes.

2.1.3 Ligation of DNA fragments

For the ligation of cohesive ends, the insert DNA was incubated with digested plasmid DNA (at a ratio of 2:1), 1 Weiss unit of T4 DNA ligase (Invitrogen) and reaction buffer [25mM Tris pH7.6, 5mM $mgCl_2$, 5mM dithiothreitol, 25% (w/v) polyehthylene glycol 800 (Invitrogen)] for 5 minutes at room temperature. Aliquots of the reaction mixture were used to transform chemically competent cells by heat-shock.

2.1.4 Transformation of One Shot TOP 10 Chemically competent bacteria

Ligated DNA fragments (approximately 0.1-50µg) and 25µl of TOP 10 chemically competent bacterial (Invitrogen) were incubated on ice for 30 minutes. Transformation was carried out by heat-shocking at 42°C for 90 seconds followed by immediate transfer of the cells to ice. 250µl of SOC medium (Invitrogen) was then added, and the cells incubated at 37°C for 1 hour with horizontal shaking at 200rpm in an orbital shaker (Forma Scientific). Up to 200µl of cells were spread onto LB-

agar plates containing the appropriate selective antibiotic and incubated overnight at 37°C for colony formation. The plates were stored at 4°C for up to 6 weeks.

2.1.5 Preparation of glycerol stocks of transformants

For the preparation of glycerol stocks of transformed bacteria, 60% glycerol was added to 1.5mL of a log-phase bacterial culture. The culture was vortexed to allow uniform distribution of the glycerol prior to rapid freezing on dry ice. The culture was then transferred to -70°C for long-term storage. In order to recover the stored culture, the surface of the culture was scraped using a sterile pipette tip, streaked onto a LB-agar plate containing the appropriate selective antibiotic and incubated overnight at 37°C to allow colony formation.

2.1.6 Agarose gel electrophoresis

Electrophoresis of DNA was carried out in horizontal agarose (SeaKem®, Flowgen, UK) gels prepared in TAE buffer. The concentration of agarose (0.8-3.0%) was dependent on the size of DNA fragments to be separated. 0.5μg/ml (w/v) ethidium bromide was added to the gel whilst molten to allow visualisation of the DNA fragments. The appropriate volume of 10 x loading buffer [0.25% (w/v) orange G, 0.15% (w/v) Ficoll] was added to the DNA samples, which were loaded into the set gel. Samples were then electrophoresed at 60-90V in TAE buffer and visualised using UV a transilluminator (UVP).

2.1.7 Isolation of DNA fragments from agarose gel using a Q1A Gel Extraction Kit (Qiagen)

DNA fragments were excised from agarose gels using a clean, sharp scalpel blade under short-wave UV-light. Extraction of DNA was carried out using QIA Gel Extraction Kit (Qiagen) according to the manufacturer's instructions. 3 volumes of buffer QG was added to 1 volume of gel, assuming that 1mg of gel is equivalent to 1μl. The samples were incubated at 55°C for 10minutes with frequent vortexing to ensure complete melting of the gel. 1 volume of isopropanol was then added and thoroughly mixed by inversion. The entire mixture was then loaded onto a QIAquick

spin column and spun at > 15000 x *g* for 1 minute to bind the DNA, and then washed with 750µl of Buffer PE. To elute the DNA, either 50µl of elution buffer (10mM Tris-HCl, pH8.5) at 37°C or H_2O was added and the column centrifuged at > 15000 x g for one minute.

2.2 DNA extraction

2.2.1 Small scale extraction of plasmid DNA (miniprep)

Bacterial cultures were grown up from single isolated bacterial colonies picked from an LB-agar plate containing the appropriate selective antibiotic. The bacteria were incubated in 10mL LB-broth overnight at 37°C in an orbital shaker. The cultures were pelleted by centrifugation at 3000 x *g* for 5 minutes and the DNA extracted by alkaline lysis using QIAprep Miniprep (Qiagen) according the manufacturer's instructions. The bacterial pellet was resuspended in 250µl Buffer P1, to which 250µl Buffer P2 was then added and gently inverted ensure thorough mixing and lysis of the bacteria. 350µl Buffer N3 was added and the mixture immediately inverted repeatedly to avoid local precipitation of the DNA. The mixture was spun at approximately 17 900 x *g* for 10 minutes, and the entire supernatant loaded into a QIAprep Spin Column. The DNA was bound by centrifugation at >15 000 x *g* for 1 minute and subsequently washed with 750µl Buffer PE. To elute the DNA, either 50µl of elution buffer (10mM Tirs-HCl, pH8.5) at 55°C or H_2O was added and the column centrifuged at > 15000 x *g* for one minute.

2.2.2 Large scale preparation of plasmid DNA (midi and maxiprep)

Large scale preparation of plasmid DNA was carried out using an Endofree Plasmid Maxi Prep (QIAGEN) according to the manufacturer's instructions. Single colonies of transformed bacteria were picked from LB-plates containing the appropriate selective antibiotic, transferred to 10ml LB medium containing antibiotic and grown at 37°C for 8 hours in an orbital shaker to yield a starter culture. The starter culture was subsequently transferred to 100ml LB-medium containing the appropriate selective antibiotic and incubated overnight at 37°C in an orbital shaker. The bacterial cells were harvested by centrifugation at 6000 x *g* for 15 minutes at 4°C and

the pellet resuspended in 10ml Buffer P1. In order to lyse the bacterial cells, 10ml of Buffer P2 was then added and mixed by inverting prior to incubation for 5 minutes at room temperature. Succeeding this 10ml of chilled Buffer P3 was added to the lysed cells, which were subsequently mixed by inverting. The lysate was transferred to a QIAfilter Maxi Cartridge and incubated at room temperature for 10 minutes. To remove genomic DNA, proteins, cell debris and SDS, the lysate was filtered through the column. 2.5ml of Endotoxin removal buffer (Buffer ER) was then added and the mixture incubated on ice for 30 minutes. Equilibration of an anion-change column was achieved by addition of 10ml QBT buffer prior to addition of the filtered lysate. The column was washed successively with two 30ml aliquots of Buffer QC before elution of the bound DNA in 15 ml Buffer QN. The DNA was subsequently precipitated by the addition of 0.7 volumes isopropanol. Following thorough mixing, the DNA was pelleted by centrifugation at >15 000 x *g* for 30 minutes at 4°C, washed in 5ml of 70% ethanol and resuspended in 200µl TE buffer.

2.2.3 Extraction of high-molecular weight viral DNA

Initially 9 x 10^6 Baby Hamster Kidney cells BHK-21 cells were infected with virus at a multiplicity of 0.01 pfu/cell, as in section 2.9.3. The cells were incubated at 37°C/5% CO_2 until complete CPE was observed. The cells were subsequently harvested using a cell scraper (Nunc) and pooled into a 250ml polypropylene conical centrifuge flask. The cells were pelleted by centrifugation at 450 x *g* for 20 minutes and resuspended in 4ml ice-cold sterile PBS. Succeeding this, the cells were homogenised by 25 strokes of a dounce homogeniser on ice. The cell homogenate was transferred to a sterile plastic tube and spun at 2000 x *g* for 20 minutes at 4°C. The resulting virion containing supernatant was transferred to a fresh plastic tube and kept on ice. The pellet was resuspended in 1ml sterile PBS and re-homogenised and centrifuged as before. The supernatants were combined and layered onto a 20% (w/v) D-sorbitol cushion and pelleted by centrifugation at 141 000 x *g* for 1 hour and 20 minutes at 4°C (SW28 rotor, Beckman). The viral pellet was resuspended in 500µl 50mM Tris (pH8) followed by the addition of 5ml high molecular weight DNA extraction buffer (0.1M EDTA [pH 8], 0.5% [w/v] SDS, 0.2M Tris [pH 8] and 100µg/ml proteinase K) and incubated overnight at 53°C. The lysate was

subsequently transferred to a sterile 15ml polypropylene tube (Nunc). From this stage onwards only wide-bore pipette tips were utilized to prevent sheering of the high molecular weight DNA. An equal volume of phenol:chloroform:isoamyl alcohol (25:24:1) was added to the suspension and mixed for 30 minutes on a rotator. The resulting mixture was centrifuged at 450 x *g* for 5 minutes and the aqueous phase transferred to a fresh 15ml tube and the phenol:chloroform:isoamyl alcohol extraction repeated a further three times. To remove contaminating phenol, the sample was subject to two rounds of chloroform extraction. Following the final chloroform extraction the DNA was precipitated by addition of 0.3 volumes of 7.5M sodium acetate and 3 volumes 96% (v/v) ethanol. The DNA was subsequently pelleted by centrifugation at 8000 x *g* for 30 minutes at 4°C, washed twice with 70% (v/v) ethanol and resuspended in 500µl TE buffer. All viral DNA was stored at 4°C.

2.2.4 Extraction of DNA from splenocytes

DNA extraction from splenocytes was carried out using the DNeasy Tissue kit (QIAGEN, UK) according to the manufacturer's instructions. Approximately 1 x 10^7 splenocytes were pelleted by centrifugation at 300 x *g* for 5 minutes and resuspended in 180µl Buffer ATL. To this cell suspension 20µl Proteinase K (600mAU/ml) was added and the sample incubated overnight at 55°C with gentle agitation. Following complete digestion, 200µl Buffer AL was added and the suspension vortexed prior to incubation at 70°C for 10 minutes. 200µl ethanol was then added and the sample mixed thoroughly by vortexing before being loaded into a DNeasy Mini Spin Column. The DNA was bound to the column by centrifugation at >6000 x *g* for 1 minute, then washed with 500µl Buffer AW1 (6000 x *g*, 1 minute) and subsequently 500µl Buffer AW2 (20000 x *g*, 3 minutes). The DNA was eluted by addition of 200µl Buffer AE and incubated at room temperature for 1 minute prior to centrifugation at >6000 x *g*. The elution step was repeated and the DNA stored at 4°C.

2.3 Southern analysis

2.3.1 Digestion of high molecular weight DNA

Digestion of high molecular viral DNA differed from that of small DNA fragments, with respect to the reaction volume and incubation time. Reactions were set up in a final volume of 50µl, with 3µg DNA, ddH_2O and restriction endonuclease buffer and initially incubated for 1 hour at 4°C before the addition of enzyme. Once restriction enzyme was added (15 units), the reaction was gently stirred for 1-2 minutes on ice before incubation at the appropriate temperature (usually 37°C) for 30 minutes. Following this, a further 15 units of restriction enzyme was added to each reaction and gently stirred before incubation for 12 hours at the appropriate temperature.

2.3.2 Electrophoresis and transfer

Digested DNA samples (3µg) were run on a 0.8% agarose-TAE gel containing 0.5ug/ml ethidium bromide. The samples were dry-loaded onto the gel and initially run at 80V for 10 minutes in enough 1 x TAE buffer to touch the ends of the gel without complete immersion. The gel was then totally immersed in 1 x TAE buffer and electrophoresis continued at 60V for 6 hours. Once electrophoresis was complete, the gel was viewed under short wave UV light and photographed. The gel was then briefly rinsed in ddH_20 and immersed in 0.25N hydrochloric acid for 10 minutes. Succeeding this the gel was washed in excess denaturation solution (0.5MNaOH, 1M NaCl, 2 x 20 minutes) with constant agitation, then briefly washed with ddH_2O before immersion in neutralization buffer (0.5M Tris-HCl (pH7.5), 1.5M NaCl, 2 x 20 minutes) with gentle agitation. Transfer apparatus consisted of a large electrophoresis tank (Biorad, UK), partially filled with 10 x SSC. Two long strips of 3mm chromatography paper were trimmed the width of the gel and soaked in 10xSSC before being laid on the raised portion of the electrophoresis apparatus, with the ends of the chromatography paper submerged in 10 x SSC. The gel was placed face-down on the chromatography paper and all air bubbles removed. One sheet of uncharged nylon transfer membrane (Hybond N+, Amersham Biosciences, UK), was cut so that it measured 1mm less than the gel in both directions, and briefly soaked in ddH_20 prior to immersion in 10xSSC for 5 minutes to ensure uniform wetness before

assembly of the blot. The nylon membrane was placed onto the gel, followed by three sheets of chromatography paper (soaked in 4xSSC), cut to the size of the gel. Lastly a stack of paper towels were placed on top of the chromatography paper. A glass plate, with a weight positioned on top, was placed on top of the paper towels to provide uniform pressure, ensuring even transfer of the DNA to the nylon membrane. Parafilm (American National Can, Chicago, USA) was placed round the edges of the gel to prevent direct transfer of 10xSSC to the stack of paper towels. Blotting was allowed to proceed for a maximum of 24 hours at room temperature. Following transfer, the nylon membrane was removed from the apparatus and the DNA cross-linked to the membrane with a Stratalinker 2400 (Stratagene, UK). The membrane was wrapped in saran wrap and stored at -70°C until hybridization.

2.3.3 Staining of molecular weight standards

Following transfer and UV-crosslinkage, the lane containing the molecular weight standards was excised from the membrane and immersed in 1M acetic acid for 10 minutes at room temperature. The acetic acid solution was then decanted and replaced with a methylene blue stain [0.2% (w/v) methylene blue, 0.4M acetic acid, 0.4M sodium acetate]. After 10 minutes incubation in staining solution, the nylon strip was rinsed, with agitation, in dH_2O until the DNA standards were visible.

2.3.4 Radiolabelling of DNA probes

Southern blots were probed with radiolabeled dsDNA probes specific for either the vtRNAs 1-4, derived from an *Eco*RI and *Hind*III digest of pEH1.4 (Bowden *et al*, 1997), or the *Hind*IIIG fragment of MHV-76, corresponding to nucleotides 11099-16237. In order to produce radiolabeled dsDNA probes, the Ready-to-go^{TM} DNA labelling kit was used (Amersham Biosciences, UK). Initially, 50ng of DNA was denatured by heating to 100°C for 2 minutes and made up to a total of 45µl with TE buffer. The denatured DNA was added to the Ready-to-go DNA labelling beads; to which 50µCi of ^{32}P-dCTP was subsequently added once the bead had fully dissolved. The labelling reaction was then allowed to proceed for 25 minutes at 37°C. Unincorporated nucleotides were removed by Micro-Bio-Spin Chromatography

(BioRad, UK) columns. Briefly, the columns were initially spun at 1000 x g to remove the packing buffer (10mM Tris, pH7.4). Subsequently the labelled probe was added to the column and spun at 1000 x *g* for 4 minutes. The flow through from this elution (containing the radiolabeled DNA probe) was retained. The purified radiolabeled probe was denatured by incubation at 100°C for 2 minutes.

2.3.5 Pre-hybridization and hybridization

Pre-hybridization and hybridization of the membrane was carried out using ULTRAhyb™ Ultrasensitive Hybridization Buffer (Ambion, UK). The ULTRAhyb™ was initially warmed to 68°C to remove any precipitated material. A volume of 6-10ml was used depending on the size of the membrane, and prehybridization carried out for 30 minutes at 42°C with constant rotation. The same aliquot of Ultrahyb was used for hybridization, to which half of the total volume (usually 20µl) of radiolabeled DNA probe was added. Hybridization was allowed to proceed at 42°C overnight with constant rotation. Membranes were initially washed twice with 2 x SSC, 0.1% SDS (w/v) for 5 minutes at 42°C, followed by two washes with 0.1 x SSC, 0.1% (w/v) SDS for 15 minutes at 55°C. For detection of the radiolabeled probe, the membrane was wrapped in saran wrap and placed in a cassette and exposed to Hyperfilm ECL (Amersham, UK) for up to 24 hours.

2.3.6 Removal of radiolabeled probes from Southern blot membranes

Bound radiolabelled dsDNA probes were stripped from the nylon membrane by immersion of the membrane in boiling 0.1% (w/v) SDS until the solution cooled to room temperature. The membrane was subsequently washed with 2 x SSC for 15 minutes. Stripped membranes were exposed to X-ray film for 24 hours to assess for complete removal of the probe.

2.4 Polymerase chain reaction

2.4.1 Components of standard PCR reactions

PCR reactions were carried out using *Taq* polymerase (Invitrogen, UK). The concentration of $MgCl_2$ varied from 1.5-5mM depending on the primers used. A typical reaction mix also consisted of 100ng of template DNA, PCR reaction buffer (20mM Tris [pH 8.4], 50mM KCl, Invitrogen, UK), 100μM of each dATP, dCTP, dGTP and dTTP, 50pmol of each primer (MWG-Biotech, Germany) and 5U of *Taq* DNA polymerase. All PCR primers were purchased from MWG-Biotech, and are shown in Appendix 2 along with their optimum annealing temperatures. PCR reactions were carried out in an Omnigene thermal cycler (Thermohybaid). A modified hot-start method was routinely used to increase the specificity of the amplification. Briefly, the reaction mix was overlaid with mineral oil (Sigma, UK) and heated to 94°C for 3 minutes. Reactions were then held at 80°C before the addition of *Taq* DNA polymerase. A typical PCR reaction program consisted of an initial denaturing step (94°C, 45 seconds), an annealing step of variable temperature dependent upon the primers in use, and an elongation step (72°C, 1 minute). Following 35-40 cycles, reactions were incubated at 72°C for 7 minutes before cooling to room temperature.

2.4.2 PCR from crude lysates

A modified PCR method was occasionally used for amplification of viral DNA from crude cellular lysates. In this instance, reactions were set up in a similar manner as the standard PCR protocol, except proteinase K (Sigma, UK) was added to the reaction mixture, to a final concentration of 0.4μg/μl. Reactions were overlaid with mineral oil (Sigma, UK) and incubated at 65°C for 15 minutes, followed by 95°C for 5 minutes to inactivate the proteinase K. The modified hot-start method was then employed as described for the standard PCR protocol.

2.4.3 Real-time PCR analysis

Real-time PCR analysis to quantify the viral genome load was performed on a Rotorgene (Corbett Research, UK). Following DNA extraction a portion of the

ORF50 gene was amplified and the levels of dsDNA product determined using the intercalating dye SYBR green. In addition, a portion of the cellular β-actin gene was also amplified in order to normalise the levels of DNA present within the individual samples. Reactions contained 100ng DNA, PCR reaction buffer [50mM Tris-HCl, 10mM KCl, 5mM $(NH_4)_2SO_4$, 20mM $MgCl_2$, pH8.8), 50pmol of each primer (MWG-Biotech, Germany), 40μM each of dATP, dCTP, dGTP and dTTP, 0.7μl SYBR green and 0.15U FastStart™ Taq DNA polymerase (Roche), in a total reaction volume of 20μl. In all reactions, an initial denaturation step was carried out by incubation at 95°C for 10 minutes. 40 cycles of amplification were carried out, which consisted of denaturation at 95°C for 15 seconds, annealing at 62°C for 20 seconds and extension at 72°C for 20 seconds. The amplification efficiencies of the samples were compared to a standard curve, generated from the serial dilution of either cloned template (ORF50) or a PCR amplified fragment of the gene (β-actin) and amplified in parallel. In the case of OFR50 amplification, standards were spiked with 10ng mouse tail tip DNA. The genome copy number was calculated from the cycle number at which the SYBR green signal crossed a set threshold on the standard curve, known as the Ct value. All products were evaluated by melting analysis to determine the specificity of individual reactions.

2.5 RNA extraction and manipulation

2.5.1 RNA isolation using RNAwiz

Total RNA was isolated from both cells and virus using RNAwiz™ (Ambion). The material from which RNA was to be isolated was initially resuspended in an appropriate volume of RNAwiz™; in the case of *in vitro* infection of cells, 2 x 10^6 C127 cells were used and the RNA extracted in 1ml of RNAwiz, for purified virus 1ml of RNAwiz was used per 250μl of RNase treated virus. For adherent cells, the cells were initially washed with 5 ml sterile PBS and the cells harvested directly in RNAwiz. On occasion, the cells were not adherent and were thus pelleted by centrifugation at 300 x *g*, washed in sterile PBS prior to addition of RNAwiz. The samples were homogenized by vigorous pipetting and at this point were stored at -80°C until the RNA extracted. Once the samples had completely defrosted, they

were incubated at room temperature for 5 minutes to ensure complete dissociation of the nucleoproteins from nucleic acids. 0.2 starting volumes of chloroform was subsequently added and the homogenate mixed by vortexing for 20 seconds prior to incubation at room temperature for 10 minutes. The samples were centrifuged at 10 000 x *g* at 4°C for 15 minutes and the aqueous phase transferred to a fresh 2ml eppendorf tube (Axygene, UK). 0.5 starting volumes of H_2O and 1 starting volume of isopropanol were then added, mixed well and incubated at room temperature for 10 minutes. The RNA was recovered by centrifugation at 10 000 x *g* for 15 minutes at 4°C. The resulting supernatant was discarded and the pellet washed in 1 starting volume of chilled 75% ethanol by vortexing. The RNA was subsequently pelleted by centrifugation at 10 000 x *g* for 5 minutes. The supernatant was then discarded, the RNA pellet air dried for 10 minutes and resuspended in 30µl RNAse free ddH_2O. RNA was stored at -70°C.

2.5.2 Standard DNase treatment of RNA

Contaminating DNA was removed from RNA samples by recombinant DNase I using DNA-*free*™ (Ambion, UK). 5ug of RNA was treated with 4 units DNase I in a total reaction volume of 13µl containing DNase I buffer (10mMTris-HCl pH7.5, 25mM $MgCl_2$, 5mM $CaCl_2$, Ambion, UK). The reaction was allowed to proceed at 37°C for 30 minutes before the addition of 1.3µl of DNase inactivation reagent (Ambion, UK) and the samples incubated at room temperature for 2 minutes. The inactivation reagent was pelleted by brief centrifugation. An aliquot of 5µl RNA was removed for RT-PCR analysis.

2.5.3 DNAse treatment of pure viral RNA

In order to DNase treat RNA isolated directly from virions, a modified protocol was employed. 5µl of RNA was initially DNase treated as for the standard method. However, following inactivation of the DNAse, the RNA was transferred into a fresh 0.5ml microfuge tube and the RNA incubated at 95°C for 3 minutes, prior to the addition of DNase I buffer and 4 units DNase I. The reaction was allowed to proceed for 1 hour at 37°C before the addition of 1.3µl of DNase inactivation reagent (Ambion, UK) and the samples incubated at room temperature for 2 minutes. The

inactivation reagent was pelleted by brief centrifugation. An aliquot of 5µl RNA was removed for RT-PCR analysis.

2.5.4 Reverse transcription of RNA

The generation of cDNA from DNased RNA was carried out using Superscript™ II (Invitrogen). Initially, approximately 2µg of RNA was incubated with 100µM of each dATP, dTTP, dCTP and dGTP, and 200ng of random primers (Amersham) in a total volume of 12µl and incubated at 65°C for 5 minutes. The mixture was subsequently chilled on ice and spun down briefly. To this, 4µl first strand buffer (250mM Tris-HCl [pH8.3], 375mM KCl, 15mM $MgCl_2$, Invitrogen), 2µl 0.1M dithiothreitol and 40U RNaseOUT (Invitrogen) were added and gently mixed prior to incubation at room temperature for 10 minutes, followed by incubation at 42°C for 2 minutes. 200U Superscript™ II was added to the mixture and incubated at 42°C 50 minutes before terminating the reaction by heating to 70°C for 15 minutes. For RT-PCR 2µl of cDNA was then used per PCR reaction.

2.5.5 RNA agarose gel electrophoresis

RNA samples were run on a denaturing agarose gel. In most instances, 10µg of total RNA was used per lane and was initially diluted to a 20µl final volume with RNAse-free ddH_2O. 5µl of loading buffer (per 10ml: 16µl saturated aqueous bromophenol blue, 80µl 0.5M EDTA [pH 8], 720µl 37% (w/v) formaldehyde, 2ml 100% glycerol, 3.084ml formamide, 4ml 10× MOPS buffer [200mM MOPS, 50mM sodium acetate, 10mM EDTA, NaOH to pH 7], 100µl dH_2O) was added to each sample and incubated at 65°C for 5 minutes. Following this, the RNA samples were immediately chilled on ice. Molten agarose [(200ml, 1.2% (w/v)] was cooled to 65°C before the addition of 3.6ml of 37% formaldehyde and 2µl 10mg/µl ethidium bromide (Sigma, UK). The gel was subsequently set and run at 30V for 30 minutes with re-circulating running buffer [per litre: 100ml 10× MOPS buffer, 20ml 37% (w/v) formaldehyde, 880ml RNAse-free dH_2O] prior to sample loading. Samples were then loaded into the gel, and electrophoresed at 20V for 8-12 hours. 5µg of an RNA molecular weight

marker (0.24-9.5kb RNA ladder, Invitrogen, UK) was loaded alongside RNA samples as a reference.

2.5.6 RNA electrophoresis using TBE-Urea gels

In order to resolve labelled RNA molecules between 10 and 150 nucleotides in length, RNA was run on NOVEX™ TBE-urea 10% polyacrylamide gel (Invitrogen). NOVEX™ RNA sample buffer was added and the samples denatured by heating to 95°C for 3 minutes. Decade Markers™ (Ambion) were also labelled and run alongside RNA samples as a reference. The markers were radiolabeled with [γ-^{32}P] ATP by incubation with 10μCi [γ-^{32}P] ATP for 1 hour at 37°C. They were subsequently cleaved by addition of 2μl cleavage reagent and 8μl RNAse-free dd$H_2$0, and incubation at room temperature for 5 minutes. An aliquot of 4μl was loaded onto the gel. RNA samples were run in 0.5 x TBE for 1 hour at 180V.

2.5.7 Radiolabelling of RNA using T4 RNA ligase

RNA isolated from virions was radiolabeled with [^{32}P] cytidine 3', 5'-bisphosphate (pCp) using T4 RNA ligase (New England Biolabs). 10μl of RNA was incubated with T4 reaction buffer (50mM Tris-HCl, 10mM $MgCl_2$, 1mM ATP, 10mM DTT, pH7.8), 10% (v/v) DMSO, 20U SUPERase-In™ RNase inhibitor (Ambion, UK), 250μCi [^{32}P] pCp and 20 units T4 RNA ligase for 30 minutes at 37°C. Unincorporated nucleotides were removed with Micro-Bio-Spin Chromatography columns. Briefly, the columns were initially spun at 1000 x *g* to remove the packing buffer (10mM Tris, pH7.4). Subsequently the labelled probe was added to the column and spun at 1000 x *g* for 4 minutes. The flow through from this elution (containing the radiolabeled RNA probe) was retained. The samples were run on either a 1% (w/v) agarose gel containing 6.7% (v/v) formaldehyde made up in 1 x MOPS buffer or a pre-poured NOVEX™ TBE-urea 10% polyacrylamide gel. In the case of RNA resolved by electrophoresis on an agarose gel, 5μg of an RNA molecular weight marker (0.24-9.5kb RNA ladder, Invitrogen, UK) was also radiolabeled as above and loaded alongside RNA samples as a reference. All gels were fixed in 10% acetic acid/20%methanol for 20 minutes, and agarose gels dried

for 2 hours at 80°C. For detection of the radiolabeled RNA, the gels were wrapped in saran wrap and placed in a cassette and exposed to Hyperfilm ECL (Amersham) for up to 6 days.

2.5.8 In Vitro Transcription of vtRNAs

vtRNAs were transcribed in vitro using T7-MEGAshortscript™ (Ambion). The DNA templates consisted of annealed synthetic oligonucleotides encoding a T7 promoter and the vtRNA containing a 5'CCA sequence (see Appendix 3). In the case of vtRNA1 a partially single stranded template was utilized, which contained double stranded sequences only within the T7 promoter, whereas the entire vtRNA4 template was double-stranded. The DNA template was incubated with 2µl 10 x transcription buffer, 0.5µl of each ATP, GTP and UTP, 10pmole DNA template, 2µl T7 MEGAshortscript™ enzyme mix and either 0.5µl CTP or 40µCi ^{32}P-CTP. In vitro transcription was allowed to proceed for 2 hours at 37°C prior to digestion of the DNA template by addition of 2U DNase I (Ambion) and incubation at 37°C for 10 minutes. Micro-Bio-Spin Chromatography (BioRad, UK) columns were used to remove unincorporated nucleotides. Briefly, the columns were initially spun at 1000 x g to remove the packing buffer (10mM Tris-HCl, pH7.4), which was then replace with 10mM Tris-HCl, pH8 by adding 500µl buffer to the column, spinning at 1000 x g for 1 minute and disposing of the flow through. This was repeated a further three times. Subsequently the vtRNA was added to the column and spun at 1000 x g for 4 minutes. The flow through from this elution (containing the vtRNA) was retained. The vtRNAs were then folded by heating to 80°C for 90 seconds, followed by cooling to room temperate. $MgCl_2$ was added to a final concentration of 20mM and the vtRNA placed on ice.

2.6 Northern analysis

2.6.1 Electrophoresis and blotting

10µg of total RNA was run on a denaturing agarose gel (1%) at 20V for 12 hours. The gel was then briefly visualised under short-wave UV light, prior to rinsing with ddH_2O. The gel was subsequently washed in 5 gel volumes of 0.01N NaOH/3M

NaCl for 20 minutes and the RNA immediately blotted onto a nylon membrane (Hybond N+, Amersham Biosciences, UK). Transfer was carried as for Southern blotting with the following modifications; transfer occurred in the presence of 20 x SSC and the filter paper was pre-wetted in 10 x SSC. Following transfer, the membrane was soaked in 6 x SSC for 5 minutes with gentle agitation. The RNA was cross-linked to the membrane with a Stratalinker 1200 (Stratagene UK) and stored at -80°C until hybridization.

An alternative approach was taken in order to transfer RNA that had been run on NOVEX™ TBE-urea 10% polyacrylamide gel (section 2.5.6). Following electrophoresis, RNA was immediately electrophoretically transferred to a Zetaprobe™ membrane (Biorad) at 200mA for 1 hour in 0.25 x TBE, using a semidry blotter (Amcos). The RNA RNA was cross-linked to the membrane with a Stratalinker 1200 (Stratagene UK) and stored at -80°C until hybridization.

2.6.2 Prehybridisation and hybridisation

Northern blots were hybridised with dsDNA probes, generated as described for Southern hybridisation. Pre-hybridisation and hybridisation was performed at 42°C with Ultrahyb (Ambion, UK). For Northern analysis, half the total volume of the radiolabeled probe (usually 20µl) was used for overnight hybridisation. Membranes were washed at 42°C twice for 5 minutes in 2 × SSC, 0.1% (w/v) SDS followed by two washes for 15 minutes each in a 0.1 × SSC, 0.1% (w/v) SDS at 65°C. The membrane was exposed to X-ray film as described above.

An alternative approach was also taken to detect small RNAs of less than 150 nucleotides in length. Labelled RNA probes were produced by incorporation of ^{32}P CTP using the mirVana™ miRNA probe construction kit (Ambion). Briefly, 2µl oligonucleotides (100µM) encoding the T7 promoter and the appropriate probe containing an 8 base sequence complementary to the 3' end of the T7 promoter sequence (see appendix 3), were mixed with 6µl of DNA hybridization buffer and subsequently annealed by heating to 70°C for 5 minutes followed by incubating at

room temperature for 5 minutes. A double stranded template was then generated by addition of 2µl 10 x Klenow reaction buffer, 2µl dNTP mixture and 2µl Exo-Klenow, and made up to a total volume of 20µl. The mixture was incubated at 37°C for 30 minutes. *In vitro* transcription was then carried out by taking 1µl of the dsDNA template and adding 2µl of 10 x transcription buffer, 0.5nM ATP, GTP and UTP, 25µCi ^{32}P CTP and 2µl T7 RNA polymerase. The mixture was incubated at 37°C for 30 minutes, following which the DNA template was removed by incubating with 1µl DNase I for 10 minutes at 37°C. Unincorporated nucleotides were removed as described in section 2.3.4 and 10µl used for overnight hybridisation as described for dsDNA probes.

2.6.3 Removal of radiolabeled probes from Northern blot membranes

Double-stranded DNA probes were removed from Northern blots as described for the removal of radiolabeled probes from Southern blots.

2.6.4 RNA Dot-Blotting

Cellular extracts were prepared from C127 cells infected with MHV-68 and S11 cells (section 2.9.3). The volume of cell extract was normalised to the volume of the extract of nuclear pellet so that an equivalent volume of cell extract was dotted onto the membrane. 10µl of the extract of nuclear pellet and equivalent volumes of nucleoplasm and nuclear membrane fractions, and volume of cytoplamsic fraction equivalent to 5µl of the extract of nuclear pellet were DNase treated by incubation with 2 units DNase I (Ambion, UK) and 2.5µl DNase I buffer (10mMTris-HCl pH7.5, 25mM $MgCl_2$, 5mM $CaCl_2$, Ambion, UK) in a total volume of 25µl, and incubated at 37°C for 1 hour. 1.3µl of inactivation reagent was subsequently added and the mixture incubated for 2 minutes at room temperature. The DNase treated samples were then dotted onto a nylon membrane (Hybond N+, Amersham Biosciences, UK) and air dried before cross-linking onto the membrane using the auto-crosslink programme on a Stratalinker 1200 (Stratagene UK). Hybridization as

described for Northern blotting. Quantification of the dots was carried out using Labworks 4TM (Ultra-Violet Products).

2.7 RNA *In Situ* Hybridization

2.7.1 Generation of labelled RNA probe

In situ hybridization was carried out using digoxygenin labeled anti-sense probes derived from pEH1.4, a plasmid consisting of nucleotides 106 to 1517 encompassing vtRNA1-4, cloned into pBlue Script (a gift from Dr. S. Efstathiou). The plasmid was initially digested with *Hin*dIII. Following digestion an equal volume of phenol:chloroform was added and the mixture thoroughly vortexed followed by centrifugation at 10 000 x *g* for 10 minutes. The aqueous phase was transferred to a fresh 1.5ml microfuge tube and contaminating phenol was removed by addition of 1 volume chloroform. The mixture was again thoroughly vortexed and spun at 10 000 x g for 10 minutes and the aqueous phase transferred to a fresh 1.5ml microfuge tube. The DNA was subsequently precipitated by addition of 2.5 volumes 99.5% (v/v) ethanol (VWR, UK) and 0.1 volumes 3M NaOAc (pH5.5). The DNA was resuspended in 30ul TE buffer and a 1µl sample run on a 0.8% agarose gel to ensure complete cleavage of the plasmid.

The digoxygenin labeled riboprobe was *in vitro* transcribed by T7 RNA polymerase using the DIG RNA labelling kit (Roche). Transcription was carried out in a total reaction volume of 20µl containing 1µg template DNA, 2µl 10 x T7 transcription buffer (400mM Tris-HCl pH 8, 60mM $MgCl_2$, 100mM dithioltreitol, 20mM spermidine), 1mM of each ATP, CTP and GTP, 0.65mM UTP, 0.35mM Biotin-16-UTP (Roche) and 40 units T7 RNA polymerase. The reaction was incubated at 37°C for 2 hours before termination by the addition of 2µl 0.2M EDTA (pH8). The RNA was subsequently precipitated by the addition of 1µl yeast tRNA (1mg/ml), 2.5 volumes of cold 99.5% ethanol and 0.1 volumes of 3M NaOAc (pH5.5) and incubated on dry ice for 1 hour. The RNA was pelleted by spinning at 10 000 x g for 30 minutes at 4°C and the supernatant removed before washing the pellet in 70%

ethanol. The RNA pellet was air dried and resuspended in 45µl RNase free H_2O (Sigma, UK).

2.7.2 Alkaline hydrolysis of labeled probe

In order to digest the digoxygenin labeled RNA probe to a length of approximately 170 nucleotides, alkaline hydrolysis was carried. The optimum time for hydrolysis was calculated using the following equation; $t = L_0\text{-}L_f / (K \times L_0 \times L_f)$, in which t=time, L_0=initial fragment length, L_f=final fragment length and K=0.11. Therefore, the optimum hydrolysis time required to digest the probe generated by *in vitro* transcription of EH1.4 was 47 minutes. Alkaline hydrolysis was carried out by addition of 5µl 0.4M $NaHCO_3$, 0.6M Na_2CO_3, pH 6.2 to the labeled probe. The reaction incubated at 60°C for the required length of time, before being neutralized by the addition of 5µl 3M NaOAc pH4.6. The digested probe was ethanol precipitated and resuspended into 50µl RNase free H_2O (Sigma, UK).

2.7.3 Quantification of labeled RNA probe

Digoxygenin labelled RNA probe was serially diluted in RNase free ddH_2O (Sigma, UK) from 1/10 to 1/100000. 5µl diluted probe was dotted onto 0.22µm nitrocellulose membrane (Micron Separations, USA), and air dried before cross-linking using the auto-crosslink function on a Stratalinker 1200 (Stratagene UK). The membrane was subsequently washed in buffer I (0.1M maleic acid, 0.15M NaCl, pH7.5, 3 x 5 mins) prior to blocking with buffer II (buffer I containing 0.1% normal sheep serum), for 30 minutes with constant agitation. After removal of buffer II the membrane was incubated for 1 hour with anti-digoxygenin-alkaline phosphatase antibody (Roche, Germany), diluted 1/5000 in buffer II. The membrane was subsequently washed with buffer I containing 0.3% (v/v) tween-20 (3 x 15 minutes), followed by buffer III (0.1M Tris-HCl, 0.1M NaCl, 50mM $MgCl_2$, pH9.5, 1 x 5 minutes). Detection of alkaline phosphatase was then carried out by incubation with 5-bromo-4-chloro-3-indolyl phosphate/nitroblue tetrazolium (BCIP/NBT, Sigma, UK). The colour intensity was compared to that of a dilution series of control DIG-labeled neo anti-sense RNA (Roche, Germany), ranging from 10µg/ml to 0.1ng/ml.

2.7.4 Preparation of cytospins for RNA *in situ* hybridization

C127 cells were infected with MHV-68 or MHV-76 at a multiplicity of infection of 5 pfu/cell, for various time points ranging from one to 24 hours. The cells were subsequently trypsinized, fixed in 10ml of PLP [2% (w/v) paraformaldehyde, lysine, periodate fixative) for 10mins and resuspended in PBS to a concentration of $1x10^5$. 200µl of cell suspension was pelleted onto Superfrost Plus slides (VWR) at 1000rpm for 5mins. The slides were post-fixed in PLP for 15mins and rinsed in PBS for 5 minutes and immediately processed for in situ hybridization.

2.7.5 RNA *in situ* prehybridisation and hybridisation on cytospins

The slides were initially washed three times in PBS for 10 minutes, followed by permeabilisation in 0.5% triton x-100 in PBS for 10 minutes at 4°C. Subsequently the slides were rinsed in PBS (3 x 10 minutes) followed by 2 x SSC (5 minutes). 200ng/ml of labeled probe was diluted in hybridisation buffer [50% (v/v) formamide, 5 x salts (0.05M EDTA, 0.05M PIPES, 0.6M NaCl, pH6.8) 0.1 x SDS, 5 x Denhardts, 0.25mg/ml salmon sperm DNA (sigma), 0.25mg/ml yeast tRNA (sigma), 20U/ml heparin and 5mg/ml dextran sulphate] and heated to 95°C for 2 minutes. DTT was added to 10mM and 60µl of solution added to each slide. Slides were covered in parafilm to prevent evaporation of the hybridization buffer and incubated at 55°C overnight. Slides were subsequently immersed in 4 x SCC and the parafilm removed. Unbound probe was removed by washing with 2 x SSC (2 x 15 minutes, 37°C), followed by 1 x SSC (2 x 15 minutes, 37°C) and finally 0.2 x SSC (2 x 15 minutes, 55°C).

2.7.6 RNA *in situ* prehybridisation and hybridisation on tissue sections

RNA in situ hybridization was also carried out on formalin fixed, paraffin embedded tissue sections, of 5-7µl thickness. In order to remove the paraffin wax, the sections were incubated in xylene, twice for 5 minutes, following which they were rehydrated through descending concentrations of ethanol and finally distilled water. The sections were then equilibrated in PBS for 5 minutes and then treated with 0.1% (w/v)

protease IV (Sigma) for five minutes at room temperature. The sections were subsequently washed in PBS and dehydrated by incubation (2 x 5 minutes) in 100% ethanol containing 0.03M ammonium acetate. The sections were then air-dried prior to addition of 100µl prehybridization buffer [50% (v/v) formamide, 5 x Denharts, 5 x salts (0.05M EDTA, 0.05M PIPES, 0.6M NaCl, pH6.8), 0.25mg/ml salmon sperm DNA (sigma), 0.25mg/ml yeast tRNA (sigma), 20U/ml heparin and 0.01% SDS]. The salmon sperm DNA was denatured by heating to 100°C for 2 minutes before being added to the prehybridization buffer. The sections were then incubated at 55°C for at least an hour, following which the prehybridization buffer was removed and hybridization carried out using labelled probe as described in section 2.7.7.

2.7.7 Visualisation of probe using alkaline phosphatase

Detection of the digoxygenin labelled probes was carried out using an anti-digoxygenin alkaline phosphatase conjugated antibody (Roche, Germany). Sections were initially blocked in 2% normal sheep serum in PBS for 2 hours at room temperature, and excess liquid removed. Anti-digoxygenin (0.5U/ml) in 2% normal sheep serum/PBS was subsequently added to the sections and incubated overnight at room-temperature. Excess antibody was removed by washing three times in PBS for 15 minutes. Alkaline phosphatase was detected using 5-bromo-4-chloro-3-indolyl phosphate/nitroblue tetrazolium (BCIP/NBT) and the sections counterstained with Nuclear Fast Red (Vector Laboratories, UK), prior to processing in 100% ethanol (2 x 5 minutes) and xylene (2 x 3 minutes). The slides were mounted in Vectamount permanent mounting media (VectorLabs, UK).

2.7.8 Visualisation of probe using Alexafluor488

Fluorescence detection of the digoxygenin labelled probe was carried out using a primary anti-digoxygenin antibody made in sheep (Roche, Germany), followed by a secondary biotinylated anti-sheep antibody, made in rabbit (Vector Labs, UK), and streptavidin-alexafluor 488 (Molecular Probes, USA). Briefly, the slides were blocked in 2% normal rabbit serum (NRS) in Tris-buffered saline (TBS) for 1 hour at room temperature. The primary antibody was used at a concentration of 0.4ng/µl in 2% NRS/TBS and incubated at room temperature for 1 hour 30 minutes, followed by

three 15 minutes washes in TBS. The secondary antibody was subsequently added at a concentration of 10ng/μl in 2% NRS/TBS for 1 hour 30 minutes and washed as above in TBS followed by incubation for 1 hour with streptavidin/alexafluor 488 in 2% NRS/TBS. Following three washes in TBS, the slides were processed in 100% ethanol (2 x 5 minutes) and xylene (2 x 3 minutes). The slides were mounted in VECTASHIELD™ mounting media for fluorescence with propidium iodide (Vector Labs, UK).

2.8 Tissue culture techniques

2.8.1 Maintenance of cell lines

All cell lines were cultured in sterile plastic-ware (Nunc, UK) and incubated at 37°C with humidified 5% CO_2. Baby Hamster Kidney fibroblast cells (BHK-21) were cultured in Glasgow's Modified Eagles Medium, supplemented with 10% (v/v) tryptose phosphate broth (Invitrogen, UK), 10% (v/v) new-born calf serum (NBCS, Invitrogen, UK), 2mM L-glutamine (VWR, UK) 100U/ml penicillin (VWR, UK) and 100U/ml streptomycin (VWR, UK). Murine C127 cells, of epithelial fibroblastic origin, were maintained in Dulbecco's Modified Eagles Medium supplemented with 10% (v/v) foetal calf serum (Invitrogen, UK), 2mM L-glutamine (VWR BDH), 100U/ml penicillin (Merck BDH) and 100U/ml streptomycin (Merck BDH). S11 cells cultured in Roswell Park Memorial Institute (RPMI, Invitrogen, UK) medium supplemented with 10% (v/v) foetal calf serum (Invitroegn, UK), 2mM L-glutamine (Invitrogen, UK), 100U/ml penicillin (Invitrogen, UK), 100U/ml streptomycin (Invitrogen, UK) and 50μM 2-mercaptoethanol.

2.8.2 Harvesting and counting cells

Adherent cell lines were maintained in sub-confluent growth, and were removed from tissue-culture flasks by trypsinisation. Growth medium was decanted before brief washing of the cell monolayer in 0.02% (w/v) versene. The monolayer was then incubated with 0.25% (w/v) trypsin (Invitrogen, UK) until the cells detached by moderate agitation. Trypsin was inactivated by the addition of an equal volume of fresh growth medium prior to centrifugation at 450 × *g* for 5 minutes at room

temperature. The resulting cell pellet was re-suspended in the desired volume of fresh growth medium. An aliquot was then diluted 1:1 with 0.1% trypan blue (w/v). The number of unstained cells was determined to calculate the viable cell count, before re-seeding of the cells in fresh cell culture flasks.

2.8.3 Preparation of cellular fractions

Cellular fractions were prepared from both MHV-68 and mock infected C127 cells, along with S11 cells. Cells were infected as described in section 2.8.3 and resuspended into 1ml sterile PBS prior to cooling on ice for 5 minutes and spun at 150 x g for 5 minutes. The cells were subsequently resuspended in ice-cold EBKL buffer [25 mM HEPES, pH 7.6, 5 mM $MgCl_2$, 1.5 mM KCl, 2 mM DTT, 0.1% NP-40 9 (v/v) and 0.5mM mammalian protease inhibitors (Sigma, UK), which were added immediately prior to use] and lysed on ice by 20 strokes in a dounce homogenizer. The cytoplasmic and nuclear extracts were separated by centrifugation at 600 x g for 5 minutes at 4°C and the supernatant containing the cytoplasmic fraction transferred to a fresh microfuge tube. The nuclei were then washed in 1ml EBMK buffer [25 mM HEPES, pH 7.6, 5 mM $MgCl_2$, 1.5 mM KCl, 75 mM NaCl, 175 mM sucrose, 2 mM DTT and 0.5mM mammalian protease inhibitors (Sigma, UK), which were added immediately prior to use], spun at 150 x *g* and then washed in EBMK buffer containing 0.5% (v/v) NP-40. Following centrifugation, the supernatant containing the outer nuclear membrane was removed and the nuclei incubated in EBKL buffer for 10 minutes and subsequently gently lysed by the drop-wise addition of KCl to a final concentration of 0.2M. The lysed nuclei were spun at 10 000 x *g* for 10 minutes at 4°C, and the supernatant containing the nucleoplasm removed. The pellet containing chromatin, nuclear membranes and nucleoli was sonicated in EBMK buffer for 15 minutes in a bath sonicator, and then the debris was pelleted by centrifugation at 10 000 x *g* for 10 minutes at 4°C. All fractions were stored at -80°C.

2.8.4 Transfection of cells by electroporation

BHK-21 cells were grown to 60-70% confluency before trypsinisation and re-suspension to a final concentration of 2.5×10^6 cells/ml in supplemented Glasgow's medium. 800µl of this cell suspension was added to an electroporation cuvette (Equibio, UK), prior to the addition of 10µg vector DNA and 5µg viral DNA. The mixture was gently pipetted before the cells were electroporated with an Easyject electroporator (Equibio, UK). A double pulse was used and the conditions were as follows: 1st pulse, 600V, 25µF, 99mΩ; 0.1 second delay; 2nd pulse, 250V, 1050µF, 99mΩ. Following electroporation, the cell suspension was mixed briefly with a Pasteur pipette before transfer to 10ml of pre-warmed supplemented Glasgow's medium. The cuvette was subsequently washed with an aliquot of medium to remove any remaining transfected cells. The transfected cells were then seeded into 96-well microtiter plates, or 6-well plates, depending on the application.

2.8.5 Transfection of cells by Effectene

BHK cells were transfected with plasmid DNA using Effectene Transfection reagent (Qiagen). Cells were seeded (typically $4x10^5$ cells/well in a 6 well plate) the day before transfection to reach approximately 70% confluence. 1µg DNA per well was made up to 150µl total volume with buffer EC (DNA condensation buffer). Following addition of 8µl Enhancer, the mixture was vortexed briefly and incubated at room temperature for 5 minutes. 25µl of Effectene reagent were then added to the DNA mix and vortexed for 10 seconds. The samples were incubated at room temperature for 10 minutes. During incubation the cells to be transfected were washed in SPBS and 4ml fresh medium was added. 1ml medium was added to the Effectene-DNA complexes, mixed by pipetting and added to the cells drop-wise. Cells were then incubated at 37°C, in the presence of 5% CO_2.

2.8.6 Generation of stably transfected cell lines

C127 cells were transfected with the expression vector pLXSN encoding the vtRNAs1-5 or empty plasmid. Following transfection, the cells were incubated at 37°C for 3 days, before being exposed to the selection agent (G418 sulphate,

500μg/ml, Gibco). The concentration required to select cells carrying the neomycin resistance gene was previously derived. The cells were passaged for one week, following which they were harvested by trypsinization and counted. Approximately 5 cells were added to a well of a 96 well microtiter plate and the volume of medium was adjusted to 200μl by addition of a 1:1 ratio mixture of fresh medium and preconditioned medium produced by culturing C127 cells for 24 hours. A serial two-fold dilution series was then generated in adjacent wells. The cells were then incubated at 37°C for eight hours and the wells examined for the presence of single cells. Those containing single cells were grown to confluency and then subjected to two further rounds of limiting dilution subcloning.

2.9 Virological methods

2.9.1 Isolation of Single Plaques following Transfection

For isolating single plaques following transfection the transfected cells were seeded at different dilutions into 96-well microtiter plates. Assuming a 50% survival rate, the transfected cells were added to varying concentrations of untransfected BHK-21 cells, such that transfected cells were diluted 1:2, 1:5, 1:10 and 1:20 in a background of untransfected BHK-21 cells with a total of 1×10^4 cells added per well. This permitted efficient isolation of single plaques within a single well of a microtiter plate. Wells containing single plaques were scraped with a Gilson pipette to detach adherent cells from the microtiter plate. The resulting cell suspension was thoroughly mixed by pipetting, before transfer of half the suspension to a cryovial for storage at -80°C. The remaining cell suspension was pelleted by centrifugation at $2000 \times g$ for 7 minutes and the resulting supernatant decanted. The cell pellet was washed with 500μl 20mM Tris (pH 8), 1mM EDTA before a further centrifugation step at $2000 \times g$ for 7 minutes. The supernatant was discarded and the cell pellet re-suspended in 50μl 20mM Tris (pH 8), 1mM EDTA. The cell suspension was then subject to one freeze thaw cycle to disrupt cell membranes before overnight incubation at 56°C in the presence of 0.4μg/μl proteinase K (Sigma, UK). Proteinase K was inactivated by incubation of the sample at 90°C for 15 minutes. 10μl of this crude DNA preparation was used per PCR reaction.

2.9.2 Purification of recombinant virus

Two approaches were taken to purify the recombinant viruses. Firstly using a limiting dilution assay as follows: an aliquot of frozen plaque pick was added to a sub-confluent BHK-21 cell monolayer within one well of a 96-well microtiter plate. The volume of medium was adjusted to 200µl, and mixed by pipetting. A serial two-fold dilution series was then generated in adjacent wells, with each well in the dilution series also containing a sub-confluent BHK-21 cell monolayer. The plates were then incubated at 37°C with 5% CO_2 for five days. Following this incubation, wells were examined for the presence of viral plaques. Any wells containing single plaques were harvested and processed for PCR analysis as described in section 2.9.1. An alternative method involved seeding 6-well plates with BKH-21 cells, which were infected with various dilutions of frozen plaque picks (from 1/1000 to 1/1,000,000), in a final volume of 5ml. The 6-well plates were then incubated overnight at 37°C with 5% CO_2. After 24 hours, the medium was removed with a Pasteur pipette and the adherent cells were over-layed with 1% agarose. The agarose was produced by addition of 10ml supplemented Glasgow's medium to 10ml of 2% PBS-agarose (Seaplaque, Flowgen, UK). After 3 days incubation at 37°C with 5% CO_2, plaques were viewed microscopically, and the plaque (and overlaying agar plug) removed with a pasteur pipette containing a small volume of medium. The resulting plaque picks were immediately subjected to three freeze-thaw cycles prior to a further round of purification using the limiting dilution approach described above. Wells containing single viral plaques were harvested and subjected to DNA extraction and PCR analysis as above.

2.9.3 Preparation of working viral stocks

Viral stocks were produced in BHK-21 cells. BHK-21 cells were harvested and counted as described. Cells were subsequently re-suspended in growth medium at a concentration of 1×10^7 cells/ml, and infected with virus at an MOI of 0.001. The cells were incubated at 37°C for 1.5 hours with shaking to enhance infection. The resulting cell suspension was transferred to Tc175 flasks at a seeding density of 3×10^6 cells per flask. Infected monolayers were generally incubated for 5-6 days, or

until they reached 100% CPE. Once complete CPE was observed, the cells were removed from the flasks with a cell scraper (Nunc) and the cell suspension centrifuged at 2000 × *g* for 20 minutes. The cell pellet was re-suspended in a minimal volume of sterile PBS before homogenisation with 40 strokes of a chilled Dounce homogeniser. The homogenate was then transferred to a glass universal tube and sonicated in a sonicating water-bath for 15 minutes at 4°C. Following centrifugation (2000 × *g* for 20 minutes at 4°C), the supernatant was transferred to a fresh sterile universal tube and held on ice. The cell pellet was re-suspended in 1ml of sterile PBS, re-homogenised, and centrifuged at 2000 × *g* for 20 minutes at 4°C. The supernatants were pooled and stored in aliquots at -70°C.

2.9.4 Isolation of extracellular virus

In order to isolate extracellular MHV-68 and MHV-76, virus was grown in murine embryonic fibroblasts (MEFs) derived from a type I $IFN^{-/-}$ mouse. The cell line was immortalised by stable transfection with the SV40 T antigen, and designated αβ SV1 MEFs. Cells were infected at an MOI of 0.001 pfu/cell as in section 2.9.3 incubated for 5-6 days, or until complete CPE was evident. Once complete CPE was observed, the cells were removed from the flasks with a cell scraper (Nunc) and the cell suspension centrifuged at 2000 × *g* for 20 minutes. The resulting supernatant was centrifuged at 20,000 x *g* for 2 hours at 4°C in order to pellet the virus. Extracellular virus was further purified by ultracentrifugation at 141 000 x *g* for 1 hour and 20 minutes at 4°C (SW28 rotor, Beckman) through a 20% (w/v) D-sorbitol cushion and the pellet resuspended in the appropriate buffer depending on the application.

2.9.5 Purification of virus by ultracentrifugation

Cell associated MHV-68 and MHV-76 was purified by ultracentrifugation. Virus was produced from BHK-21 cells and extracted as in section 2.8.3. The crude viral stock was layered onto a 20% (w/v) sucrose cushion and spun at 141,000 x *g* for 1 hour and 20 minutes at 4°C (SW28 rotor, Beckmann). The pellet was resuspended in 1ml RNase ONE buffer (100mM NaCl, 50mM Tris-HCl, 10mM $MgCl_2$, 1mM dithiothreitol, pH7.9) for treatment with RNase ONE, or 5ml of sterile PBS if

ultracentrifugation through a sucrose gradient was undertaken. The viral stock was further purified by banding on a discontinuous sucrose gradient consisting of 55%, 30% and 10% sucrose layered in descending order. The viral stock was layered onto the top of the gradient and banded by ultracentrifugation at 141,000 x g for 18 hours at 4°C, following which a viral band was clearly visible. The band was removed and sterile PBS added to a total volume of 20ml, and the purified virus was concentrated by ultracentrifugation at 141,000 x *g* for 1 hour and 20 minutes, and resuspended in 1ml RNase ONE buffer. Purified virus was stored at -80°C.

2.9.6 RNase treatment of purified virus

Contaminating RNA within pure viral stocks was digested using RNase ONE (New England BioLabs and Ambion). 750µl purified virus in RNase ONE buffer (100mM NaCl, 50mM Tris-HCl, 10mM $MgCl_2$, 1mM dithiothreitol, pH7.9) was treated with 700units of RNase ONE for 5 hours at 37°C.

2.9.7 Transmission electron microscopy

Processing for transmission electron microscopy was carried out by the University of Edinburgh, college of medicine and veterinary medicine electron microscope unit. Briefly viruses were centrifuged and fixed in 3% (w/v) glutaraldehyde in 0.1M sodium cacodylate buffer for 2 hours. The virus pellets were then washed in 3x10 minute changes of 0.1M sodium cacodylate buffer to remove residual glutaraldehyde. They were then post-fixed in 1% (w/v) Osmium tetroxide in 0.1M Sodium cacodylate buffer for 45 minutes followed by 3x10 minute washes in 0.1M Sodium cacodylate to remove residual osmium tetroxide. The virus pellets were subsequently dehydrated in 50%, 70%, 90%, 100% acetone changes for 10 minutes each, prior to embedding in Araldite resin. Ultrathin sections, 60nm thick were taken, stained in uranyl acetate and Lead Citrate then viewed in a Philips CM12 transmission electron microscope (FEI UK Ltd, Cambridge, England). Areas of interest were photographed on Kodak 4489 electron image film.

2.9.8 Treatment of cells with inhibitors of protein synthesis and viral DNA replication

In order to produce cellular extracts of MHV-68 infected cells were treated with an inhibitor of protein synthesis cycloheximide (CHX) or a herpesviral DNA polymerase inhibitor, phosphonoacetic acid (PAA). Cells were treated with 100μg/ml of either CHX or PAA for 1 hour prior to viral infection. For viral infection, 1×10^7 cells were infected at an MOI of 5 with shaking for 1.5 hours in the presence of the appropriate inhibitor. Following this, the cells were seeded into Tc175 tissue culture flasks (Nunc) and fresh medium containing either CHX or PAA was added. The cells were then incubated at 37°C for 8 hours before trypsinisation and subsequent extraction of cellular extracts.

2.9.9 Virus titration

For the titration of infectious virus within tissues, tissues were homogenised in a minimal volume of medium (1.8ml) before subjection to one freeze-thaw cycle (-80°C) to disrupt cellular membranes. The frozen homogenate was thawed on ice before centrifugation at 2000 × *g* for 5 minutes at 4°C to clarify the homogenate. Subsequently, 440μl of supernatant was transferred into 3.96ml of fresh growth medium and mixed thoroughly to produce a 1:10 dilution. This process was repeated to generate a serial ten-fold dilution series. To each dilution, 2×10^6 BHK-21 cells were added (in 0.2ml of medium) and shaken at 250rpm for 1 hour at 37°C. 2ml of each dilution was added to a 60mm Petri dish, to which 3ml of growth medium had been dispensed. Each dilution was plated in duplicate. For each experiment, mock-infected BHK-21 cells were plated out as negative controls. The plates were incubated for four days at 37°C in the presence of 5% CO_2. Following incubation, plates were fixed with 10% (w/v) neutral-buffered formaldehyde before staining with 0.1% (w/v) toluidine blue. Plaques were scored microscopically, and the titre determined by the following calculation: viral titre = (plaque count × dilution)/2. For determining the titre of viral stocks, a similar procedure was undertaken, except that a 44μl aliquot of viral stock was added to 4ml of medium, from which a serial ten-fold dilution series was created.

2.9.10 One step/multistep growth curves

Single-step and multi-step growth *in vitro* was analysed by infecting either BHK-21 cells or L929 cells in suspension for 90 minutes at a multiplicity of infection (MOI) of 5 (single-step growth) or 0.05 (multi-step growth). Cells were pelleted by centrifugation at 450 × *g* for 5 minutes and re-suspended in fresh complete Glasgow's medium four times to remove unbound virus before the seeding of 1×10^6 cells (multi-step) or 2×10^6 cells (one-step) into each well of a 24-well plate. At specific times post-infection, the plates were removed from the incubator and stored at -70°C, prior to harvesting. The cells were harvested by repeated pipetting with a Gilson pipette, subject to three freeze-thaw cycles, and infectious virus was determined by plaque assay as described. All infections were performed in duplicate, with each infection titrated in duplicate.

2.9.11 Infective centre assay

The infective centre assay was used to determine the frequency of *ex vivo* reactivation from latently infected splenocytes. Upon organ harvesting, spleens were stored in 5ml of RPMI medium supplemented with 10% foetal calf serum, 2mM L-glutamine, 100U/ml penicillin, 100U/ml streptomycin and 50μM 2-mercaptoethanol. Spleen cells were isolated from the spleen casing with a scalpel blade, producing a single-cell suspension in 5ml of RPMI. The cell suspension was transferred to a pre-rinsed 20ml universal tube and was centrifuged at 450 × *g* for 5 minutes at 4°C. The supernatant was decanted and the pellet was re-suspended in the remaining liquid. Erythrocytes were lysed by the addition of 1ml of sterile ddH_2O to the cell suspension, and equilibrium was restored by the addition of 9ml of sterile PBS. Following thorough mixing, cell debris was allowed to settle before transfer of the splenocyte suspension to a fresh pre-rinsed universal tube. The sample was then ceintrifuged at 450 × *g* for 5 minutes at 4°C. The supernatant was discarded and the cell pellet re-suspended in 5ml of supplemented RPMI. The viable cell count of the suspension was determined, and 10-fold dilutions of splenocytes were added with 1×10^6 BHK cells (in 5ml RPMI medium) to 60mm Petri dishes (Nunc). Each dilution was plated in duplicate. The contents of the plates were thoroughly mixed before

incubation at 37°C with 5% CO_2 for 5 days. Plates were fixed and counted as described for the titration of infectious virus.

2.10 Protein techniques

2.10.1 Electrophoretic-mobility shift assay (EMSA)

Electrophoretic mobility shift assays were carried out using radiolabeled vtRNAs prepared as described in section 2.5.8. They were incubated with cellular extracts as follows: 25,000cpm RNA were incubated with ~5μg cellular extracts and 0.05μg poly(dI-dT) in a total volume of 20μl binding buffer (20mM HEPES/KOH pH 7.5; 50mM KCl; 10mM $MgCl_2$, 0.1% (v/v) NP40; 5% (v/v) glycerol). For competition reactions, between 2.5ng and 10ng of the appropriate unlabelled vtRNA, yeast tRNA or 18S ribosomal RNA was added to the reaction. Following 20 minutes incubation at room temperature the samples were loaded onto a 5% (w/v) polyacrylamide gel containing 0.5x TBE. The gel was run in 0.5x TBE for 1 hour at 30mA and transferred to a cassette for exposure to Hyperfilm ECL (Amersham) at -80°C.

2.10.2 UV-crosslinking RNA-protein complexes

The polyacrylamide fragment containing the RNA-protein complex was excised and placed on a glass slide on ice. RNA-protein complexes were crosslinked by incubation under UV light of 254nm, held at a distance of 4mm away from the samples for 17 minutes. The gel sections were then transferred to a 1.5ml microfuge tube and immersed in 2.5mg/ml of RNase A in native gel buffer (50 mM Tris 50 mM Glycine) and incubated at 37°C for 30 minutes in order to digest uncrosslinked RNA. Excess buffer was then removed and incubation continued at room temperature for a further 30 minutes. 50μl of 2 x loading buffer was subsequently added and the samples mixed overnight at room temperature. The samples were heated to 100°C for 5 minutes prior to SDS polyacrylamide electrophoresis as described in section 2.10.4. The gel was subsequently dried at 80°C for 2 hours placed in a cassette and exposed to Hyperfilm ECL (Amersham) at -80°C for up to 6 days.

2.10.3 Isolation of protein from polyacrylamide gel

EMSAs were carried out using unlabelled vtRNAs in order to isolate the RNA-protein complexes. The binding reaction was carried out as described in section 2.10.1 but on a larger scale, i.e. 1ml total volume. A radiolabeled reaction was used as a marker. Unlabelled complexes were excised at positions indicated by the labeled complexes. Proteins were eluted from the gel by overnight incubation in 4mL protein elution buffer [50mM Tris pH 7.9; 0.1mM EDTA, 5mM DTT; 150mM NaCl; 0.1% (v/v) SDS] at 4°C on a rotator. Proteins were subsequently concentrated using VIVASPIN 10,000 columns (Vivascience) by centrifugation at 5,000 x g at 4°C for 30 minutes. Concentrated samples were stored at -20°C.

2.10.4 SDS-Page

Proteins were separated by SDS-PAGE following UV crosslinking to labeled RNA, or prior to direct staining or Western blotting. Protein samples were made up to a total volume of 20µl with 5x loading buffer (20% (v/v) glycerol; 2% (v/v) SDS; 0.125mM Tris pH 6.8; 0.4% (w/v) bromophenol blue; 5% β-mercaptoethanol). Samples were boiled for 5 minutes before loading onto the gel (resolving gel: 10% acrylamide/bisacrylamide; 0.375M Tris pH 8.8; 0.1% (v/v) SDS; 0.1% (w/v) ammonium persulphate (APS); 0.01% (v/v) TEMED. Stacking gel: 3.4% (w/v) acrylamide/bisacrylamide; 140mM Tris pH 6.8; 0.1% (w/v) SDS; 0.05% (w/v) APS; 0.01% (v/v) TEMED). Gels were run at 200mA each in running buffer (25mM Tris; 192mM glycine; 0.1% (v/v) SDS).

2.10.5 Coomassie staining

Gels were incubated in Coomassie stain (0.25% (w/v) Coomassie Blue R250; 40% (v/v) methanol; 7% (v/v) acetic acid) with shaking for at least 1 hour. After a brief rinse with de-stain (50% (v/v) methanol; 10% (v/v) acetic acid) gels were incubated in de-stain until bands were clear.

2.10.6 Silver staining

Gels were fixed in 45% (v/v) ethanol, 35% (v/v) glacial acetic acid for 20 minutes followed by a 10 minute wash in 10% (v/v) ethanol, and subsequently washed three times in ddH_20, prior to incubation in Farmers reagent reducer [0.3% (w/v) sodium thiosulphate; 0.15% (w/v) potassium ferricyanide; 0.05% (w/v) sodium carbonate) for 1 minute. Following three further washes in ddH_20, gels were incubated in 0.1% (w/v) $AgNO_3$ for 30 minutes and then briefly rinsed in ddH_2O. Gels were developed in 2.5% (w/v) Na_2CO_3, 0.05% (v/v) formaldehyde until bands were of the desired intensity and fixed in 30% (v/v) methanol, 10% (v/v) prior to drying for 2 hours at 80°C.

2.10.7 Western Blotting

Proteins were transferred to nitrocellulose membrane using a semidry blotter (Amcos), at 0.8mA/cm^2 (i.e. typically at 60mA for a 48cm^2 gel) in transfer buffer (25mM Tris-HCl, 150mM glycine, 10% (v/v) methanol, pH 8.3)) for 1 hour. The membrane was then washed twice in distilled water and incubated in blocking buffer [3% (w/v) nonfat dry milk (Marvell^{TM}) in TBS] for 1 hour with constant agitation. The primary antibody anti-MHV-68 antibody was diluted 1/200 in blocking buffer and incubated with the membrane for 2 hours at room temperate with constant agitation. Following two washes in distilled water, incubation was carried out with alkaline phosphatase conjugated secondary antibody diluted 1/2000 in blocking buffer, for 20 minutes at room temperature with constant agitation. The membrane was subsequently washed for 10 minutes in TBS and then 10 minutes in TBS-0.05% Tween 20. A NBT/BCIP tablet (Sigma) was dissolved into 10mL water and poured onto the membrane. Once the bands had reached the desired intensity the membrane was rinsed with distilled water and allowed to dry.

2.10.8 In-gel protein digestion for mass spectrometry

Protein extracts were run on 12% SDS-PAGE gels and incubated overnight in 5-10 gel volumes SYPRO ruby (Molecular Probes). The gel was then washed in four changes of ddH_20 over a two hour time period and visualized using a UV

transilluminator (UVP). Protein bands were excised and transferred to a clean Eppendorf tube. Tryptic digestion was carried out by the Edinburgh Protein Interaction Centre (EPIC). Briefly, gel slices were incubated in for 2x30mins in 200mM NH_4HCO_3 (ABC) in 50% acetonitrile (ACN) at 30°C to remove SDS. The proteins were subsequently reduced by incubation in20mM DTT, 200mM ABC, 50% CAN for 1h at 30°C, followed by three washes in 200mM ABC, 50% ACN. The gel slices were then incubated in 50mM iodoacetamide (IAA), 200mM ABC, 50% ACN at room temperate in the dark for 20min, prior to three washes in 20mM ABC, 50% ACN. The gel slices were subsequently cut into 2mm x 1mm pieces and centrifuged at 10 000 x *g* for 2mins. They were then immersed in ACN until the bands turned white, following which the ACN was decanted and the gel sliced dried. Tryptic digestion was carried by addition of 12.5 ng/µl trypsin in ABC and initially incubated at 4°C until the gel swelled, following by incubated at 32°C for 16-24 hours. MALDI-TOF mass spectrometry then was carried out using a Voyager DE STR MALDI-TOF mass spectrometer (Applied Biosystems) and the masses submitted to the MS-fit search engine in order to identify the proteins present.

2.11 Statistical analysis

All statistical analysis was carried out using SPSS (SPSS Inc, USA). Viral titre, real-time PCR and dot-blot analysis data were assessed for statistical significance using the non-parametric Mann-Whitney test.

Appendix 1. Cloning vectors used in this study

A

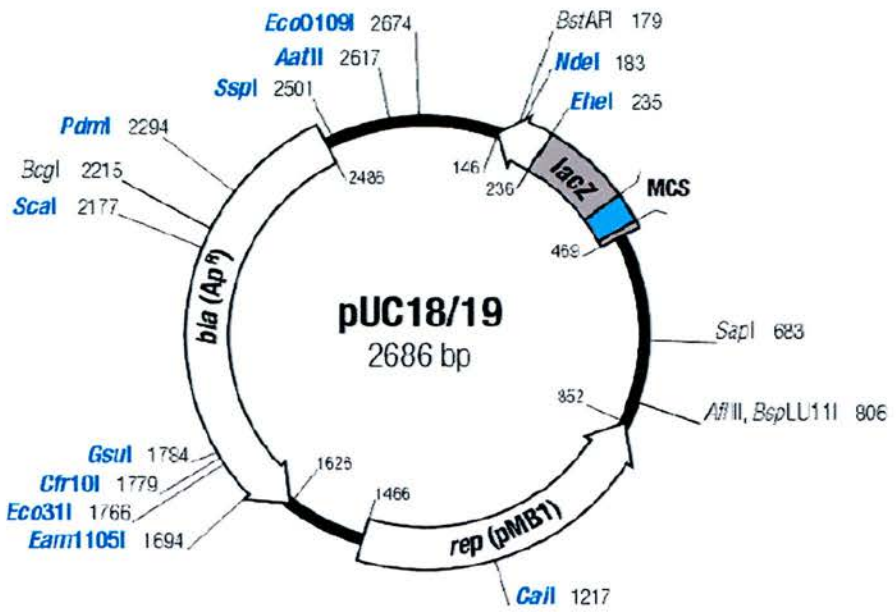

B

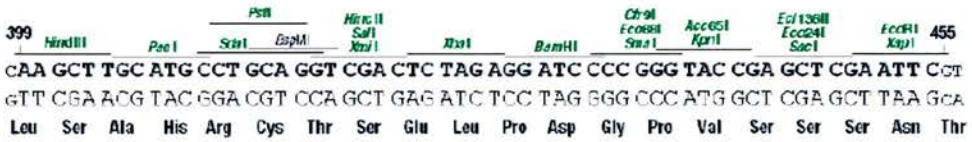

Vector pUC18. Vector pUC18 (A) and its polylinker region (B) are shown.

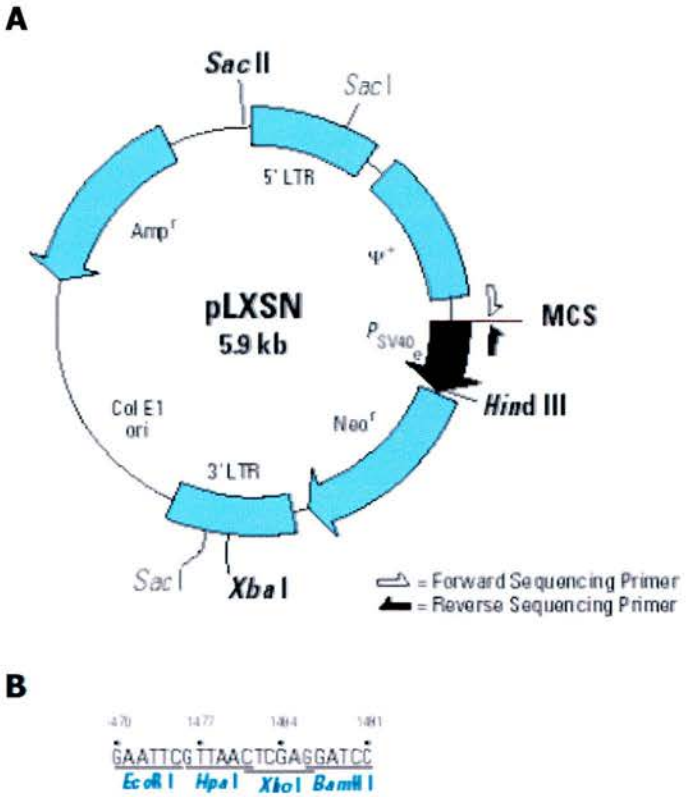

Vector pLXSN Vector pLXSN (A) and its polylinker region (B) are shown

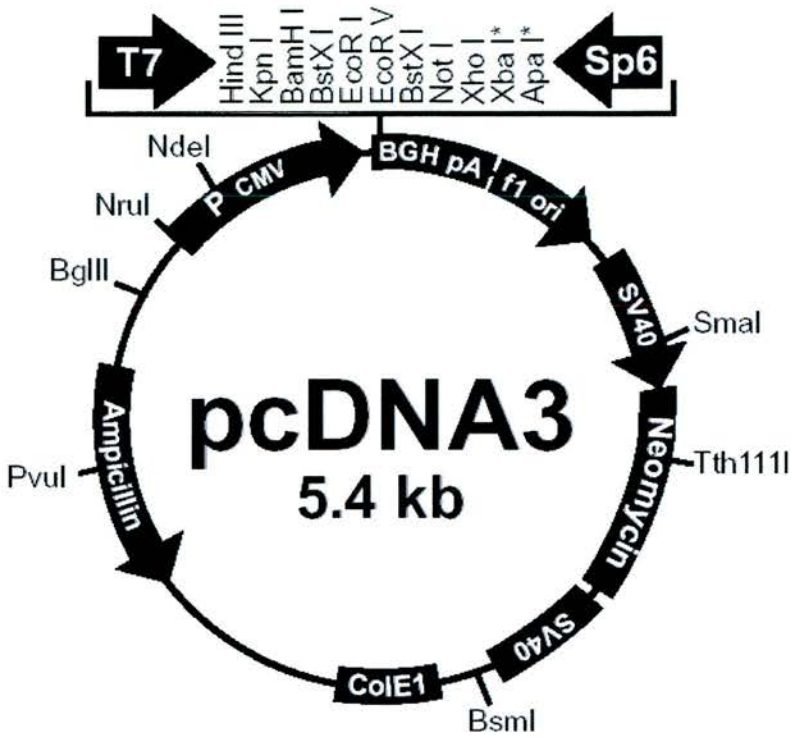
T7
Hind III
Kpn I
BamH I
BstX I
EcoR I
EcoR V
BstX I
Not I
Xho I
Xba I*
Apa I*
Sp6
NdeI
P CMV
BGH pA
f1 ori
SV40
SmaI
NruI
BglII
pcDNA3
5.4 kb
Ampicillin
PvuI
Neomycin
Tth111I
SV40
ColE1
BsmI

Appendix 2. Oligonucleotides used in this study

Sense (S) Antisense (A)	Primer Pair	Anneal Temp	Amplified region
vtRNA1-S	5'- TAGAGCAACAGGTCACCG ATC-3'	56°C	MHV-68 vtRNA1 Nt 146-215 70bp product
vtRNA1-A	5'- TAGAGCAACAGGTCAC C GATC-3'		
vtRNA2-S	5'- GGTAGAGCAGCGGTTCCT-3'	56°C	MHV-68 vtRNA2 Nt 505-573 69pb product
vtRNA2-A	5'- ACTCCCCCTCTCAACCA-3'		
vtRNA3-S	5'-TGGCAGGCCAACATA-3'	55°C	MHV-68 vtRNA3 Nt 918-980 63pb product
vtRNA3-A	5'-CGTGCTCCTCGATGGTCA-3'		
vtRNA4-S	5'-GCGGCAGGCTCATC-3'	56°C	MHV-68 vtRNA4 Nt 1205-1266 62bp product
vtRNA4-A	5'-ATCTCAACTCTGCGTCGG-3'		
vtRNA5-S	5'-TAGAGCATCAGGCTAGTA-3'	51°C	MHV-68 vtRNA4 Nt 1607-1669 63bp product
vtRNA5-A	5'-CTCCACCTTTAACCAG-3'		
vtRNA6-S	5'-GCGTAGCTCAATTGT-3'	53°C	MHV-68 vtRNA6 Nt 3608-3771 92bp fragment
vtRNA6-A	5'-GGCCACTCAACAGAC-3'		
vtRNA7-S	5'-GAGCGGCAGACACCA-3'	58°C	MHV-68 vtRNA7 Nt 4967-5034 68bp fragment
vtRNA7-A	5'-TAGCTGGCCAGGACT-3'		
vtRNA8-S	5'-CCCATCCTGTTGGTT-3'	51°C	MHV-68 vtRNA8 Nt 5418-5471 54bp fragment
vtRNA8-A	5'-CGCGGGTAGCTAGTC-3'		
EH14E-S	5'-CTCTAAAGCTCTCTTATG ACG-3'	55°C	MHV-68 Nt 1255-1605 351bp fragment
EH14F-A	5'-GGGTACATAAGCGGCTGT GC-3'		

Sense (S) Antisense (A)	Primer Pair	Anneal Temp	Amplified region
tRNAforBam-S	*Bam*HI 5'-GC*GGATCC*GCTTTTTGT GCTGGTGC-3'	53°C	MHV-68 vtRNAs1-5 Nt 112-1695 1583bp fragment
tRNARev-A	5'-GCGGATCCATGCATCAGTA ATCTTA*GGTACCG*-3' *Bam*HI		
tRNAfor2-S	Sal*I* *5'*-ACG*CGTCGA*CGCAGCGCAC CGCTTATG-3'	55°C	MHV-68 vtRNA5 Nt 1477-1695 218bp fragment
tRNARev-A	5'-GCGGATCCATGCATCAGTA ATCTTA*GGTACCG*-3' *Bam*HI		
M3-S	5'-TAACAGGCAGATTGCCATT CCC-3'	55°C	MHV-68 M3 Nt 6560-6946 386bp fragment
M3-A	5'-TGGCACTCAAACTTGGTTG TGG-3'		
ORF65-S	5'-CAGGGAGCATCAAGTGTC CC-3'	55°C	MHV-68 ORF65 Nt 94068-94240 172bp fragment
ORF65-A	5'-GTCAGACATAGACCCTGG ATCAG-3'		
M11-S	5'-TTAGAAGGCACTATGACA GC-3'	57°C	MHV-68 M11 Nt 103560-103779 219bp product
M11-A	5'-TGTGTCATGCAATCGTCC A-3'		
DNApol-S	5'-GTCAATTCAAGGGGAAG CG -3'	55°C	MHV-68 DNA Pol Nt 19743-20220 477bp product
DNApol-A	5'-CAGGGAAAACAACAGC TTGGAG -3'		
ORF50-S	5'-GGCACATTTGCTGCAGAAC CCAG-3'	62°C	MHV-68 RTA Nt 68486-68841 355bp fragment
ORF50-A	5'-GAACGGCGCCTGTGTACTC AAAGG-3'		
TR-S	5'-GTTTTGGCCCTCAGCAGG GTC-3'	56°C	MHV-76 Left-end Nt 119382-9786 315bp product
M4B-A	5'-CGCGGAATTCGGTTCTAG AAAGTCATAAATCTC-3'		
Act-S	5'-TTGTATGGTGGGAATGGGG TCA-3'	57°C	Murine β-actin 514bp product
Act-A	5'-TTTGATGTCACGCACGATT TC-3'		

Sense (S) Antisense (A)	Primer Pair	Anneal Temp	Amplified region
ActIN-S	5'-CGTTGACATCCGTAAAGA CC-3'	62°C	Murine β-actin 202bp product
ActIN-A	5'-CTGGAAGGTGGACAGT GA-3'		
ActOUT-S	5'-GTACTCCTGTTGCTGAT CC-3'	62°C	Murine β-actin 272bp product
ActOUT-A	5'-GTACTCCTGCTTGCTGAT CC-3'		
GAPDH-S	5'-TGGATATTGTTGCCATCAAT GACC-3'	58°C	Murine GAPDH 380bp product
GAPDH-A	5'-GATGGCATGGACTGTGGT CATG-3'		

Appendix 3. Synthetic oligonucleotides used for *in vitro* transcription

T7 Promoter

5'-AATTTAATACGACTCACTATA-3'

tRNA1 reverse

5'-TGGGACCAGAGCTCGGACTTGAACCGAGAACCAGGATCGGTGACCTG
TTGCTCTACCAATTGAGCTACTCTGGCCCTATATAGTGAGTCGTATTAAA
TT-3'

tRNA4 forward

5'-GATCCTAATACGACTCACTATAGGGTCGGGGTAGCTCAATTGGTAGCG
CGGCAGGCTCATCCCCTGCAGGTTCTCGGTTCACCGGGTCCCGACGCCA-
3'

tRNA4 reverse

5'-TGGCTCGGGACCCGGGATTGAACCGAGAACCTGCAGGGGATGAGCC
TGCCGCTCTACCAATTGAGCTACCCCGACCCTATAGGTCGTATTA-3'

tRNA1 Northern probe

5'-GCCAGAGTAGCTCAATTGGTCCTGTCT-3'

For all oligonucleotides, the T7 promoter is shown in red and the 3' CCA coding sequence in blue.

Appendix 4. Stock solutions used in this study

TE buffer	10mM Tris-HCl (pH8.0) 1mM EDTA
TAE buffer	0.04M Tris-acetate 1mM EDTA
TBE buffer	0.44M Tris-borate 0.44M Boric acid 12mM EDTA
Luria-Bertani (LB) medium	1% (w/v) tryptone 0.5% (w/v) yeast extract 1% (w/v) NaCl
LB agar	1 x LB broth, 1.5% (w/v) bacto-agar
SOC media	1 x LB broth, 20mM glucose 20mM $MgCl_2$
Phosphate-buffered saline (PBS)	150mM, 2.5mM KCl 10mM Na_2HPO_4, 1mMKH_2PO_4 (pH7.4)
20 x SSC	3M NaCl, 300mM sodium citrate (pH7)
50 x Denhardt's buffer	1% (w/v) Ficoll 400 1% (w/v) Polyvinylpyrrolidone 1% (w/v) Bovine serum albumin fraction V

Appendix 5. Commercial Suppliers

Ambion Inc., Ambion (Europe) Ltd., Ermine Business Park, Spitfire Close, Huntingdon, Cambridgeshire, PE29 6XY, UK. www.ambion.com

Amersham Biosciences UK Ltd., Amersham Place, Little Chalfont, Buckinghamshire, HP7 9NA, UK. www.amershambiosciences.com

Bio-Rad Laboratories Ltd., Bio-Rad House, Maylands Avenue, Hemel Hempstead, Hertfordshire, HP2 7TD, UK. www.bio-rad.com

Corbett Research, Unit 296 Cambridge Science Park, Milton Road, Cambridge, CB4 0WD, UK www.corbettresearch.com

Equibio, Action Court, Ashford Road, Middlesex, TW15 1XB, UK. www.equibio.com

Flowgen, Findel House, Excelsior Road, Ashby Park, Ashby de la Zouch, Leicestershire, LE65 1NG, UK. www.flowgen.co.uk

Invitrogen Ltd., 3 Fountain Drive, Inchinnan Business Park, Paisley, PA4 9RF, UK. www.invitrogen.com

Millipore, 80 Ashby Road, Bedford, Massachusetts, USA. www.millipore.com

MWG Biotech (UK) Ltd., Mill Court, Featherstone Road, Wolverton Mill South,Milton Keynes, MK12 5RD, UK. www.mwgbiotech.com

Nalgenunc International, 75 Panorama Creek Drive, Rochester, NY, 14625, USA. www.nalgenunc.com

New England Biolabs (UK) Ltd., 73 Knowl Piece, Wilbury Way, Hitchin, Hertfordshire, SG4 0TY, UK. www.neb.com

Promega UK Ltd., Delta House, Chilworth Research Centre, Southampton, SO16 7NS, UK. www.promega.com

Roche Diagnostics Ltd., Bell Lane, Lewes, East Sussex, BN7 1LG, UK. www.roche.com

QIAGEN Ltd., Boundary Court, Gatwick Road, Crawley, West Sussex, RH10 9AX, UK. www.qiagen.com

Sigma-Aldrich Company Ltd., Dorset, UK. www.sigmaaldrich.com

Stratagene Europe, Gebouw California, Hogehilweg 15, 1101 CB Amsterdam, Zuidoost, The Netherlands. www.stratagene.com

Thermohybaid, Action Court, Ashford Road, Ashford, Middlesex, TW15 1XB, UK. www.thermohybaid.com

UVP Ultraviolet Products Ltd., Unit 1, Trinity Hall Farm Estate, Nuffield Road, Cambridge CB4 1TG. www.uvp.com

Vector Laboratories, , Accent Park, Bakewell Road, Orton Southgate, Peterborough, PE2 6XS, www.vectorlabs.com

Vivascience AG Feodor-Lynen-Straße 21, 30625 Hannover, Germany, www.vivascience.com

VWR International Ltd. Merck House Poole BH15 1TD, www.vwr.com

Chapter 3: The encapsidation of the vtRNAs

3.1 Aims

3.2 The timing of expression of the vtRNAs during lytic infection by RT-PCR

3.3 RNA detection within purified virus preparations

3.4 Discussion

3.1 Aims

Herpesviruses gene expression takes place in a cascade fashion, which is related to the function of the gene products (see section 1.1.4). Expression of the vtRNAs has been previously classified as immediate early based upon their expression in the presence of cyclohexamide and phosphoacetic acid (PAA), yet their exact timing of expression has not previously been fully investigated. The initial objective of this study was therefore to characterise the expression pattern of the vtRNAs during lytic infection. However, a preliminary investigation indicated that the vtRNAs were present within the viral stock used for the experiment and hence either contaminated the stock or formed part of the virus particle. Consequently purified virus stocks were produced using different preparation methods to determine firstly whether the vtRNAs are packaged within the virion and secondly whether additional RNA species are packaged.

3.2 The timing of expression of the vtRNAs during lytic infection by RT-PCR

Determination of the exact timing of expression of the vtRNAs was carried out following *in vitro* infection of the mouse epithelial C127 cell line. Cells were infected with MHV-68 produced by growing the virus within BHK-21 cells. In BHK-21 cells, MHV-68 virions remain cell associated and hence, in order to release the virus, the infected cells were lysed by dounce homogenization and the nuclei removed by centrifugation. The resulting virus stock was titrated on BHK-21 cells. C127 cells were then infected with MHV-68 at an MOI of 5 pfu/cell for various times, from 30 minutes to 24 hours post-infection, following which the RNA was extracted from the cells. The integrity of the RNA was checked by electrophoresis on a 1% agarose gel (data not shown) and its concentration was quantified by spectrophometry. The RNA was then DNase treated to remove any contaminating DNA and RT-PCR was carried out, using primers specific for vtRNA1 (Ebrahimi *et al*, 2003). Electrophoresis of the PCR products was carried out on a 3% agarose gel. As figure 3.1 shows, vtRNA1 was present at all time points following infection, from 30 minutes to 24 hours post-infection. No PCR product was present when the reverse

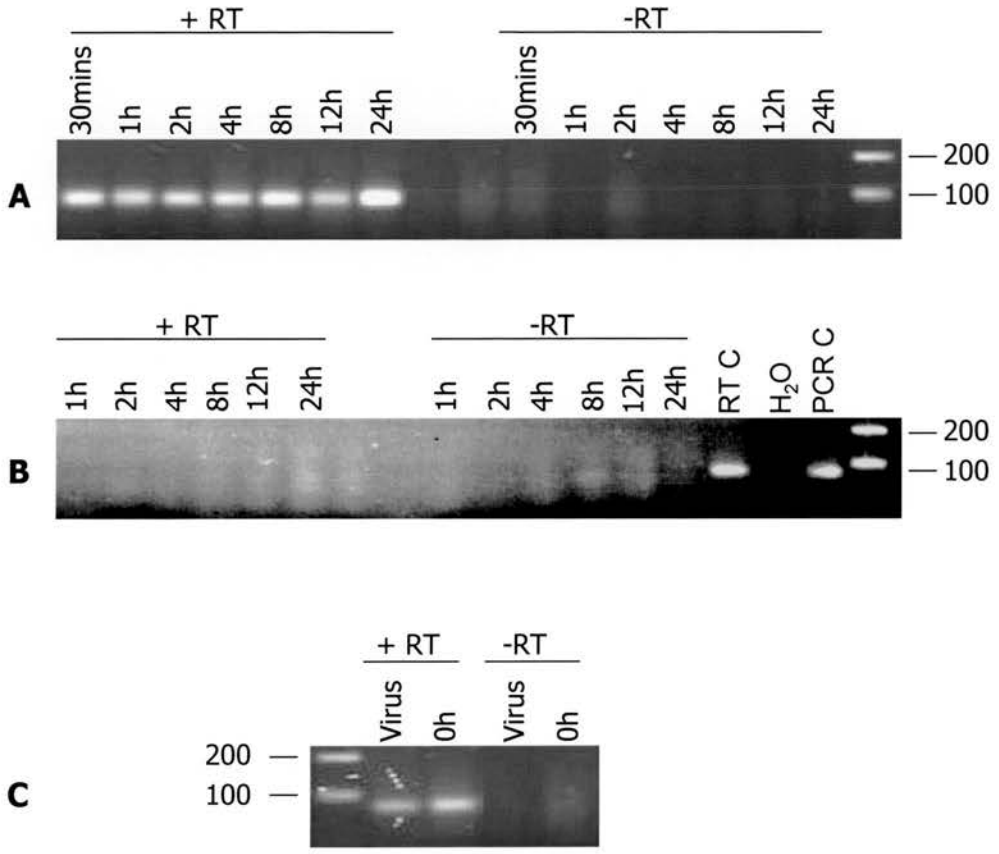

Figure 3.1 The expression of vtRNA1 within C127 cells infected with either MHV-68 (A and C) or MHV-76 (B) prepared from the cytoplasmic fraction of infected BHK-21 cells. C127 cells were infected at a MOI of 5 PFU/cell for various time points, as indicated, and the RNA extracted for RT-PCR analysis (A). In addition, RNA was isolated from the MHV-68 viral stock used in the experiment and immediately following infection of C127 cells (C). The PCR was carried out using vtRNA1 specific primers and the products run on a 3% TAE-agarose gel. The size of molecular weight markers in bp are shown. Abbreviations; RT reverse transcription; C, positive control; PCR C, PCR positive control.

transcriptase step was not included in the reaction, indicating that no contaminating vtRNA DNA was present. No PCR product was detected following infection with MHV-76 or mock infected cells.

Previous characterisation of the transcriptome profile of MHV-68 within C127 cells failed to detect immediate early gene expression by micro-array analysis prior to 8 hours post-infection (Ebrahimi *et al*, 2003). Therefore the presence of the vtRNAs as early as 30 minutes following infection is surprising, especially given that in this time period the virus needs to bind to and enter the cells and the DNA be transported to the nucleus in order for transcription to take place. Although it is possible that expression could have taken place by this time, it is perhaps more likely that the vtRNAs were already present within the viral stock used for the infection. In order to investigate whether this was the case, C127 cells were infected with MHV-68 and RNA extracted immediately. In addition RNA was extracted from the viral stock. Once again, the RNA was DNase treated and RT-PCR carried out for vtRNA1. A PCR product of the correct size was present immediately following infection and in the virus stock. No product was visible in the absence of the reverse transcriptase, thus indicating that all DNA had been digested prior to the reverse transcription step. The presence of vtRNA1 within both the virus stock and immediately following infection indicates that it is either a contaminant of the virus stock or encapsidated within the virus particle. Given that the virus stock used for the infections was produced from a crude cellular lysate of infected BHK-21 cell, it is possible that the vtRNAs could contaminate the stock, especially given the high levels of vtRNAs present within the cytoplasm (see section 4.2).

3.3 RNA detection within purified virus preparations

3.3.1 Intracellular virus purification and RNA detection

3.3.1.1 Purification of intracellular virus

In order to investigate whether the vtRNAs either contaminated the virus stock used in section 3.2 or if they are present within the virus particle, the virus stock was purified to remove any contaminating cytoplasmic RNA. MHV-68 was grown in

BHK-21 cells until a cytopathic effect (CPE) could be seen, after which the cells were lysed and the nuclei removed by centrifugation. The resulting virus preparation was purified by ultracentrifugation on a 20% sucrose cushion (figure 3.2) and treated with RNase ONE to remove any contaminating RNA. The resulting virus stock was titrated on BHK-21, and found to have a titre of $3x10^9$ pfu/ml.

To further purify the virus stock, the sucrose cushion virus preparation was then ultracentrifuged through a 5-55% sucrose gradient, following which an obvious, opaque virus band was present (designated the virus band) which was removed. In addition the band immediately above the virus band (the upper band) and the lower band, which also included the pellet, were also removed. The bands were then concentrated by ultracentrifugation and treated with RNase ONE to remove any contaminating RNA. It is clear that banding of the virus on a sucrose gradient results in a loss of 99% of the virus titre (table 3.1), most likely due to the osmotic stress created as the virions enter higher sucrose concentrations. Transmission electron micrographs taken of negatively stained sucrose gradient purified virions revealed the presence of both fully formed, enveloped virions, in addition what appeared to be empty nucleocapsids. Despite purification through a sucrose gradient, contaminating debris, most likely as a result of homogenization of the infected cells or osmotic lysis of the virus, appeared to co-purify with the virus particles (figure 3.3).

3.3.1.2 Detection of the RNAs present by RT-PCR

To determine whether the vtRNAs were present within the virus particles, the virions were treated with RNaseONE to digest any remaining RNA exterior to the particles, then lysed by addition of RNAwiz (Ambion), which also inactivated the RNaseONE, and the RNA subsequently extracted. This was initially carried out on the sucrose cushion purified viral stocks. The RNA was then treated with either RNaseONE or mock treated and re-precipitated, followed by DNase treatment. In order to remove all contaminating viral DNA, the RNA was DNase treated twice, with a denaturation step (95°C for 3 minutes) prior to the second treatment. RT-PCR was carried out for vtRNA1 and the PCR product run on a 3% agarose gel (figure 3.4). vtRNA1 appeared to be present by RT-PCR analysis within this purified virus stock.

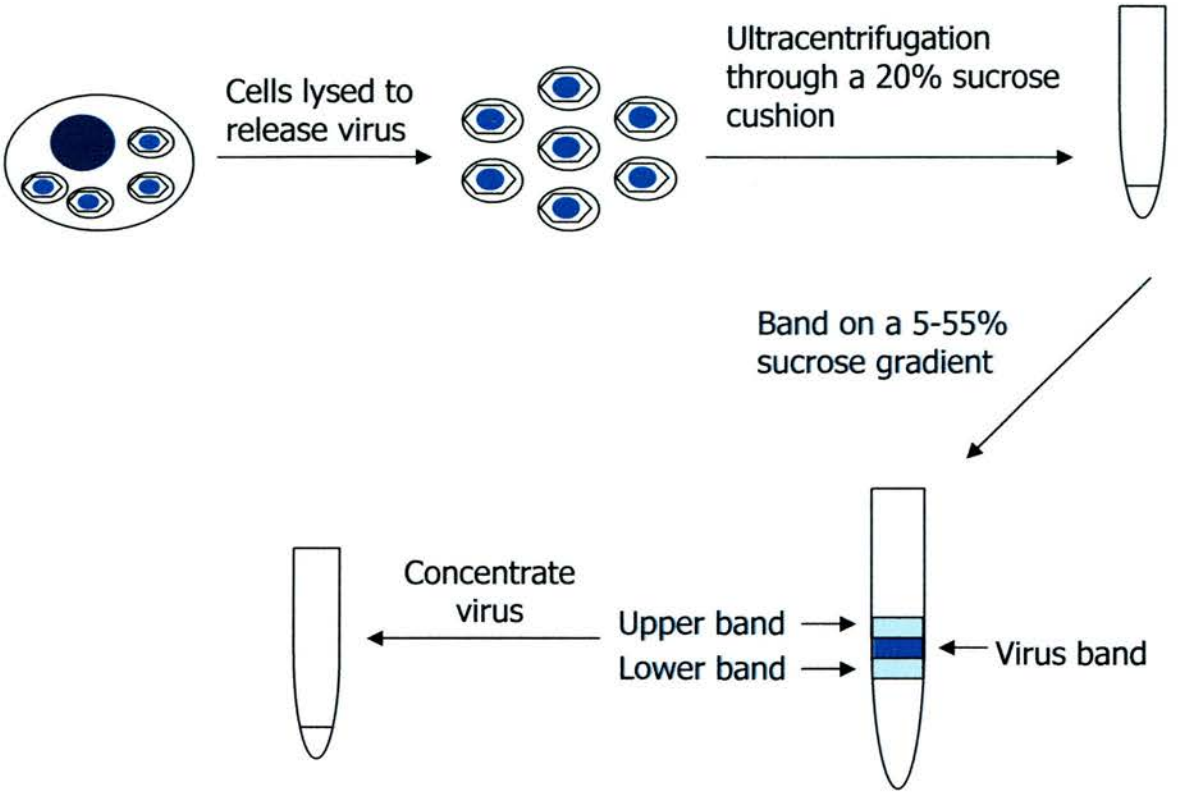

Figure 3.2 Purification strategy for MHV-68 grown within BHK-21 cells. Virus was initially isolated from the cytoplasm of BHK-21 cells. The cytoplasmic extract was purified by ultracentrifugation through a 20% sucrose cushion, followed by a further ultracentrifugation step through a 5-55% sucrose gradient, resulting the in appearance of an obvious virus containing band. This band, along with the upper and lower bands were removed and concentrated by ultracentrifugation.

Virus band	Titre (PFU/ml)
Sucrose cushion	$3x10^9$
Virus band	3×10^7
Upper band	9.5×10^5
Lower band	9.25×10^6

Table 3.1 Viral titres of virus purified as in figure 3.2.

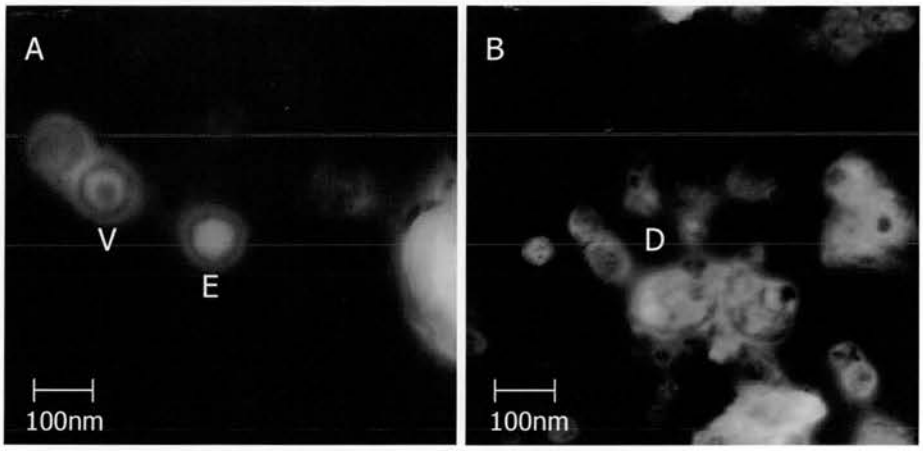

Figure 3.3 Transmission electron micrograph of MHV-68 virions grown within BHK-21 and purified on a 10-55% sucrose gradient. Virions were negatively stained with uranyl acetate and lead citrate. Two different fields of view (A and B) are shown. In A, both virus (V) and empty capsids (E) can be seen, whereas in B, a large amount of either virus or cellular debris (D) is present.

Following treatment with the RNase, no PCR product was visible, indicating that RNaseONE is able to digest vtRNA1. In addition, PCR amplification was not a result of contaminating genomic DNA, as no band was present when the reverse transcriptase was absent from the reaction. PCRs were also carried out on the cDNA for the remaining vtRNAs, which were all found to be positive. In addition, the presence of highly expressed viral and cellular mRNAs was also investigated. M3, the most abundantly expressed mRNA within infected cells at the time of infection was also found within the purified viral stock, as were the cellular mRNAs, GAPDH and β-actin, indicating that the virus preparation still contained contaminating cytoplasmic material or that mRNA molecules were also encapsidated within the virus particles.

The same procedure was carried out on all three bands of the sucrose gradient purified virions. Following RT-PCR for vtRNA1, a band of the correct size was present for the higher titre virus and lower bands (figure 3.5). A faint product was also visible following RT-PCR on the RNA isolated from the upper-band virions. However, no viral or cellular mRNA molecules, such as M3 or β-actin, could be detected in any of the bands by RT-PCR. Although the sucrose gradient purified virus stock appeared to be cleaner than that purified through a sucrose cushion, as judged by the removal of the mRNA molecules, electron-micrographs of the virus preparations revealed that they still contained cellular debris (figure 3.3). In addition, a 2 log decrease in viral titre during the purification step resulted in a lower RNA yield and hence it is not clear whether the mRNAs could not be detected due to their levels falling below the limit of detection, or as a result of further purification of the virions. In addition, the loss in viral titre hampered any further experimentation into the exact nature of the RNA species present within the viral preparations and hence a different method for the production of high titre, purified virus stocks was employed.

3.3.2 Extracellular virus purification and RNA detection

3.3.2.1 Purification of extracellular virus

A simpler way to produce viral stocks free from contaminating cytoplasmic material is to purify virus which is released from infected cells into the supernatant, as no

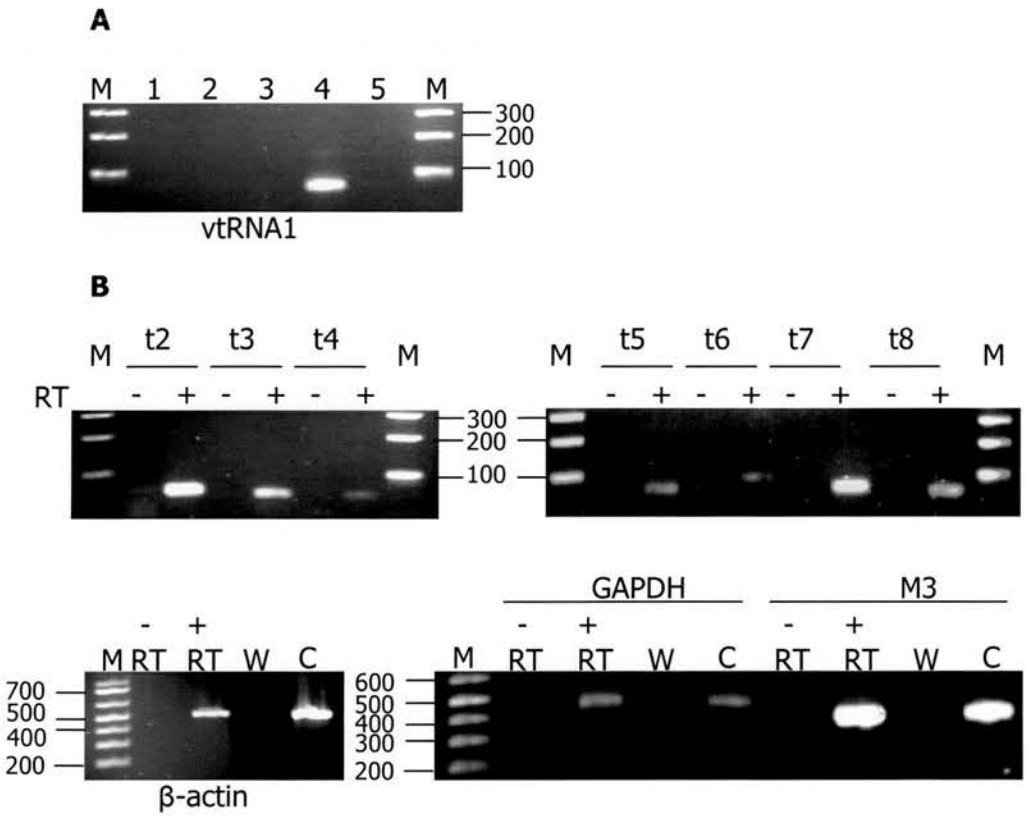

Figure 3.4 RT-PCR on RNA extracted from MHV-68 virions grown in BHK-21 cells and purified through a sucrose cushion. A; for vtRNA1; 1, RNA treated with RNaseONE –RT; 2, RNA treated with RNaseONE +RT; 3, RNA –RT; 4, RNA +RT; 5, ddH_20. B; RT-PCR for the remaining vtRNAs (t2-t8), β-actin, GAPDH and M3. PCR products were analysed on 1-3% TAE-agarose gels. The size of molecular weight markers (M) in bp are shown. Abbreviations; W, ddH_20; C, positive control; RT, reverse transcription.

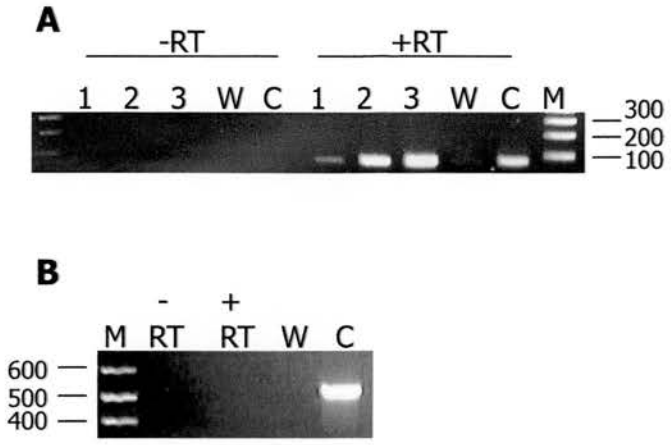

Figure 3.5 RT-PCR on RNA extracted from MHV-68 grown in BHK-21 and purified through a sucrose gradient. RT-PCR was carried out for vtRNA1 (A) and β-actin (B) on virus taken from the upper band (1), lower band (2), virus band (3), ddH_20 (W) and a positive control (C). In B, RNA was extracted from the virus taken from the virus band. PCR products were analysed on 1% TAE-agarose gels. The size of molecular weight markers in bp are shown.

homogenization of the infected cells is required. However, BHK-21 cells produce very low levels of extra-cellular virus. Therefore, in order to produce highly purified, high titre virus preparations, both MHV-68 and MHV-76 were grown within type I interferon receptor deficient $(IFNR)^{-/-}$ murine embryonic fibroblasts (MEFs), which produce high levels of extracellular virus (*J. Stewart*, personal communication). This allows much easier purification of the viral stock as large amounts of contaminating cytoplasmic material are absent. Following CPE the supernatant was removed and centrifuged to concentrate the extracellular virions. The concentrated preparation was then purified by ultracentrifugation through a 20% sucrose cushion followed by treatment with RNase ONE to remove any remaining extra-viral RNA molecules. Both the MHV-68 and MHV-76 viral stocks were titrated on BHK-21 cells, and were found to contain $5x10^{10}$ PFU and $1.25x10^{10}$ PFU respectively. Transmission electron microscopy of the resulting virus stock indicated that it contained high levels of enveloped virions and relatively little contaminating debris (figure 3.6). In addition, a mock preparation was produced following the same protocol.

3.3.2.2 Nature of the RNA species present

The size of RNA molecules present within both MHV-68 and MHV-76 was investigated. Although MHV-76 lacks the vtRNA molecules it was included in the experiments in order to determine whether additional RNA species are present within the purified virus preparations in the absence of the vtRNAs. Hence, both MHV-68 and MHV-76 were grown within type I $IFNR^{-/-}$ MEFs and purified as in section 3.3.2.1, followed by lysis of the virions and RNA extraction. The total RNA was then end-labelled using T4 RNA ligase and [^{32}P] pCp. An RNA ladder was also labelled in the same way. Any unincorporated nucleotides were removed and the samples run overnight on a 1% denaturing agarose gel. The gel was then dried down and exposed to photographic film. As can be seen in figure 3.7, the RNA molecules detected by T4 RNA ligase labelling within both the MHV-68 and MHV-76 pure viral preparations are less than 240 nucleotides in length. No other RNA species could be detected using this method. Hence it appears that both MHV-76 and MHV-68 preferentially package small RNA molecules, although the exact nature of those present in MHV-76 is not clear. The absence of any RNA species in the mock

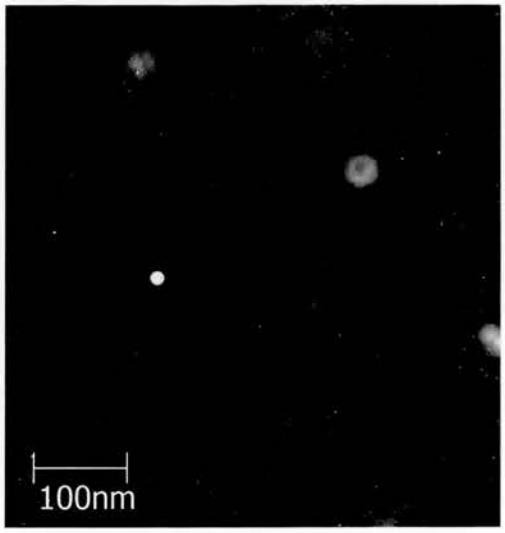

Figure 3.6 Transmission electron micrograph of MHV-68 virions grown in type I IFNR$^{-/-}$ MEFs and purified through a 20% sucrose cushion. Virions were negatively stained with uranyl acetate and lead citrate.

infected preparation indicates protection of the RNA within the virions and not contamination from cellular RNA molecules.

In order to determine the exact size of the RNA species present, the experiment was repeated but this time the labelled RNA run on a 10% polyacrylamide/urea gel, which separates RNA molecules of between 10 nucleotides and 150 nucleotides in length. The RNA samples were run alongside a labelled RNA ladder, containing molecules that range in size from 10 nucleotides to 150 nucleotides. The major RNA species extracted from both MHV-68 and MHV-76 viral preparations were approximately 70 nucleotides in length (figure 3.7) therefore indicating that in the absence of the vtRNA (i.e. in MHV-76), the virus is able to package RNA molecules of the same size. Minor bands of around 120 and 150 nucleotides were also present within both the viral preparations. Once again, no labelled RNA could be detected within the mock infected preparation.

In order to determine that the small polynucleotides present within MHV-68 represent the vtRNAs, Northern blot analysis was carried out. RNA was extracted from both MHV-76 and MHV-68 and run on a 10% polyacrylamide/8M urea gel and electrophoretically transferred to a Zetaprobe^{TM} membrane (Biorad). Hybridization was carried out using an *in vitro* transcribed ^{32}P CTP labelled probe specific for the fist 20 nucleotides of vtRNA1. As figure 3.8 shows, two RNA species of approximately 70 and 90 nucleotides in length were detected. No hybridization was detected to MHV-76 RNA. The 70 nucleotide fragment corresponds to fully processed vtRNA, however the nature of the longer transcript is not clear, although it is possible that it represents RNA that has been semi-processed from the longer primary transcript.

Therefore it is clear that the 70 nucleotide band seen following total RNA labelling contains the vtRNAs. However, it is not clear whether additional RNA molecules of the same size, such as cellular tRNAs are also present. Although it is possible, given the size of the RNA molecules present, that the small encapsidated species present

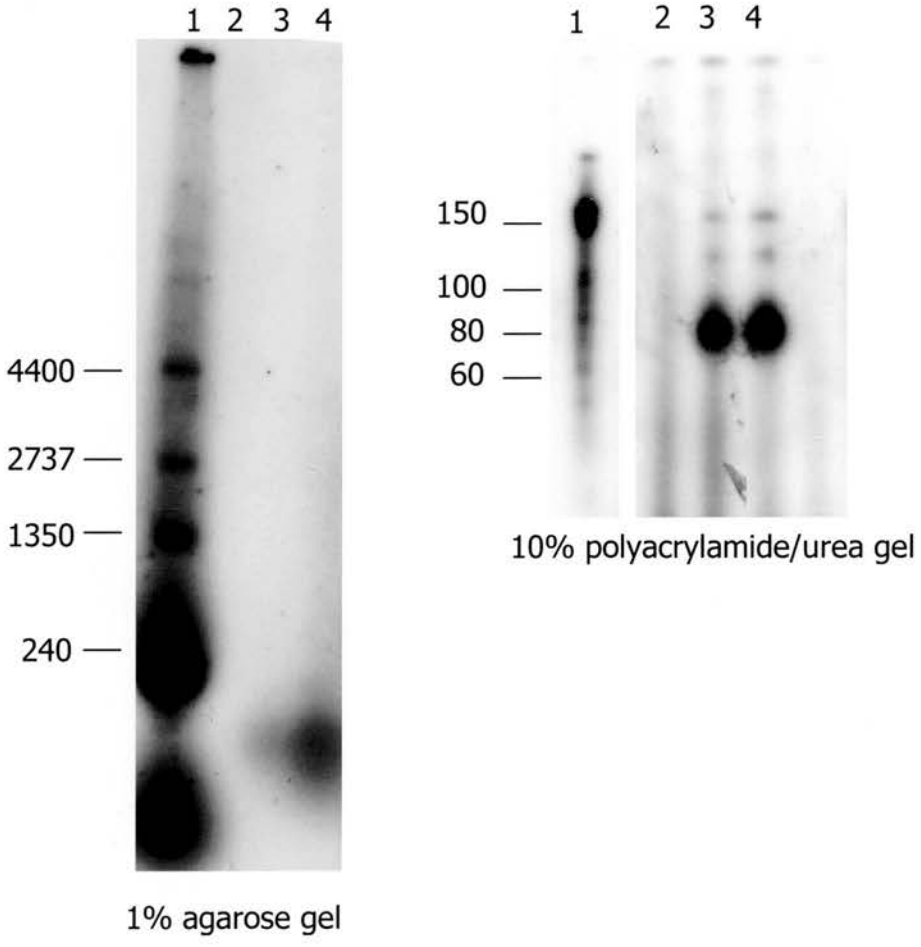

Figure 3.7 Analysis of the RNA species present within purified virus stocks, grown in type I IFNR$^{-/-}$ MEFs. RNA was isolated from a mock infected preparation (lane 2), extracellular or MHV-76 (lane 3) or MHV-68 (lane 4) virions, radiolabelled with ^{32}P-CTP and ran on either an agarose or polyacrylamide/urea gel. The size in nucleotides of radiolabelled RNA markers are also shown (lane 1).

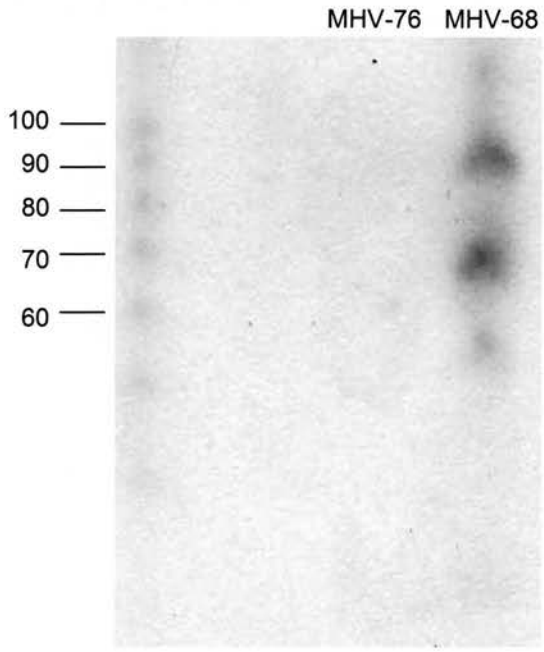

Figure 3.8 Northern-blot analysis of the RNA species present within purified virus stocks, grown in type I IFNR$^{-/-}$ MEFs. RNA was isolated from either MHV-76 or MHV-68 and run a 10% polyacrylamide/urea gel. Hybridization was carried out using a ^{32}P CTP labelled RNA probe specific for the first 20 nucleotides of vtRNA1.The size of molecular weight markers is shown in nucleotides on the left.

within MHV-76 represent cellular tRNAs, their identity has not been unequivocally defined. Given that the vtRNAs are not aminoacylated, it can be assumed that any amino-acylated RNA molecules packaged within the virus particles represent cellular tRNA molecules. In order to assess what proportion of RNA molecules present within both MHV-68 and MHV-76 are aminoacylated, RNA was extracted from virions under acidic conditions and radiolabeled. An aliquot of RNA was then de-acetylated by increasing the pH. Given that acetylated and de-acetylated tRNAs exhibit differing migrations on acidic polyacrylamide/urea gels, it would be possible to establish the proportion of acetylated RNA present. However, this approach was not successful, most likely due to the inability of the T4 RNA ligase to work at the acidic conditions required to maintain the aminoacylated state of the tRNAs.

3.3.2.3 Detection of the RNAs present by RT-PCR

In order to determine the specific RNA species present within MHV-68 and MHV-76 viral particles, RT-PCR was carried out on the RNA extracted from the extra-cellular virions. The RNA samples were DNase treated twice, with a denaturation step prior to the second treatment to ensure that all contaminating genomic DNA was removed, and reverse transcribed to generate cDNA. PCR reactions were carried out on the cDNA using primers specific for all eight vtRNAs, cellular (GAPDH and β-actin) and viral mRNA molecules. M3 and M9 mRNAs are present at high levels at the late times of infection when the virus particles are maturing. M11 and DNA polymerase (ORF9), although expressed, are present at much lower levels (Ebrahimi *et al*, 2003). The results of the PCR are summarised in table 3.2. All the vtRNAs were found to be present within the MHV-68 viral preparation, except vtRNA7. Although this PCR was repeated a number of times and a positive control included in the reaction, vtRNA7 was never detected. As predicted, none of the vtRNAs were present within either a MHV-76 or mock infected preparation. The viral mRNA M3 could be detected within MHV-68, but once again not in MHV-76, which is as expected given that it lacks the M3 gene. Additional viral mRNAs could be detected within both MHV-68 and MHV-76, including M9, and surprisingly given their apparent low level of expression M11 and DNA polymerase mRNAs were also found to be encapsidated. The detection of cellular mRNAs within the viral stocks

	MHV-68	MHV-76	Mock
vtRNA1	+	-	-
vtRNA2	+	-	-
vtRNA3	+	-	-
vtRNA4	+	-	-
vtRNA5	+	-	-
vtRNA6	+	-	-
vtRNA7	-	-	-
vtRNA8	+	-	-
M3	+	-	-
M9	+	+	-
M11	+	+	-
DNA pol	+	+	-
Beta-Actin	+	+	-
GAPDH	+	-	-

Table 3.2 RNA species present within a pure MHV-78, MHV-76 and a mock infected preparation grown within type I IFNR-/- MEFs, as determined by RT-PCR.

appeared to vary, with both GAPDH and β-actin being present within the MHV-68 preparation. However, GAPDH mRNA could not be detected by RT-PCR within the MHV-76 preparation. No cellular RNA molecules could be detected by RT-PCR within the mock infected preparation. Hence it is apparent that the presence of RNA molecules within the virus preparations is due to their protection within the virion and not a result of contamination from cellular RNA.

3.4 Discussion

It is apparent from these results that the vtRNAs are packaged within the MHV-68 virion particle, as determined by their presence within different viral preparations produced from both intracellular and extracellular virions. Extensive treatment of the virions with a nuclease to digest RNA exterior to the virus particles prior to RNA isolation makes it unlikely that the results are due to contaminating RNA. It is possible that homogenization of infected cells results in the production of membranous vesicles which may also contain vtRNAs, however the presence of the vtRNAs within extracellular virions which did not contain homogenized cellular material argues against this. RT-PCR analysis on virion RNA samples demonstrated that along with the vtRNAs, both viral and cellular mRNA molecules are also present within the MHV-68 virion. However, mRNAs can only be detected within intracellular and extracellular viral preparations purified through a sucrose cushion but not those banded on a sucrose gradient. Sucrose gradient purification resulted in a significant loss of viral titre, most likely due to the osmotic lysis of the virions within high concentration sucrose. The inability to detect mRNA by RT-PCR within this viral preparation is most likely a consequence of the reduction in the level of RNA extracted, and not due to further purification of the virions. This is supported by the presence of mRNAs within the higher titre extracellular viral preparation, which upon electron microscopy appeared to contain less contaminating cellular debris.

Although mRNA molecules are present within the MHV-68 particle, the vtRNAs appear to be present with a greater abundance, given that they are the only RNA species that can be detected by RT-PCR analysis on lower titre viral stocks. In

addition, direct labelling of the total RNA present within the virion indicated that the major encapsidated RNA species are small RNA molecules of approximately 70 nucleotides in length, whereas no longer length transcripts were visible. Although it is possible that the mRNA detected represents degradation products, these would have to be of at least 300 nucleotides in length to be detected by the PCR assay used. Although the vtRNAs represent the most abundant virion RNA species identified in this study, the exact amount of vtRNAs present within the virus particles has not been investigated. In order to calculate the copy number, the efficiency of the RNA extraction would have to be known. RNA is extracted from virions using a phenol/guanidine thiocyanate approach, instead of using commercially available RNA extraction columns, due to the fact that these usually exclude small RNA molecules. Hence it is difficult to ensure total recovery of the RNA from the purified virions, especially when working with such small quantities.

Interestingly, a deletion mutant of MHV-68 which lacks the vtRNAs (MHV-76) also appears to encapsidate small RNA molecules of the same size. Given that the most abundant RNA species within cells of approximately 70 nucleotides in length are tRNAs, it is likely that the encapsidated RNA species within MHV-76 are cellular tRNAs. This raises the question of whether MHV-68 also encapsidates cellular tRNAs along with the vtRNAs but unfortunately it was not possible to ascertain whether cellular tRNAs were indeed present within both the MHV-76 and MHV-68 virions.

Cellular and viral mRNA have previously been found to be packaged within the HCMV and HSV virions (Bresnahan and Shenk, 2000; Greijer *et al*, 2000; Sciortino *et al*, 2001). In addition a recent study by Bechtel *et al* demonstrated that along with 10 viral mRNA molecules, the non-coding PAN RNA is encapsidated by KSHV (Bechtel *et al*, 2005). However, this is the first demonstration of the selective packaging of small RNA molecules by a herpesvirus. All previous studies were based upon the detection of specific transcripts by RT-PCR, northern blotting and micro-array analysis, but not the total RNA present and hence it is not clear whether the high level of encapsidation of small RNA is unique to MHV-68.

A matter of controversy is the mechanism by which RNA is incorporated within herpesvirus particles. In the case of HCMV it has been demonstrated that viral and cellular RNAs are packaged in proportion to the relative quantities present within infected cells at the time of virion assembly (Terhune *et al*, 2004). Work done on HSV-1 indicates that the packaged viral RNA does not correspond to the most abundantly expressed transcripts present within infected cells, however the cellular transcripts incorporated were representative of the most abundant cellular mRNAs (Sciortino *et al*, 2001). In the case of KSHV, the majority of RNA species packaged are present at very high levels at the time of virion assembly, although by contrast a single incorporated transcript encoding ORF17 appears to be preferentially packaged above more abundantly expressed unincorporated transcripts (Bechtel *et al*, 2005). Whether the specific RNA incorporated by MHV-68 is related to the relative abundance within the cell at the time of virion assembly is not clear. A superficial analysis of the RNA species present indicates that the very highly expressed vtRNAs are the most abundant viral RNA within the virion. However, the M11 transcript is one of the least abundantly expressed genes within infected cells (Ebrahimi *et al*, 2003) and yet this is also present within the virion. Therefore a comprehensive study of the relative levels of all RNA species compared to those within infected cells needs to be undertaken to establish whether RNA is incorporated by MHV-68 in relation to the expression levels within cells late within infection.

A second theory is that mRNA is selectively packaged, perhaps through binding to viral proteins, in a way analogous to that of genomic RNA packaging by RNA viruses. However the basis of this selectivity remains unclear, especially as no *cis*-mediated packaging elements have been identified within herpesvirus packaged RNA. In addition, they appear not to be selected based upon their kinetic class as the RNA extracted from MHV-68 represents immediate early (vtRNAs), early (M3 and DNA polymerase) and late (M9) transcripts (Ebrahimi *et al*, 2003). It is possible that there is a structural or size basis for selection given that the most abundant viral RNA species within the MHV-68 are the highly structured vtRNAs.

The key issue that arises from this data is the possible function of encapsidated RNA, and in particular the vtRNAs. In the case of mRNA it can be hypothesized that their immediate translation within the cell results in the formation of a cellular environment more conducive to viral infection. In fact it has been shown that a number of virion mRNAs delivered into the cell are translated (Bechtel *et al*, 2005). The expression of the broad spectrum chemokine binding protein encoded by M3 (Parry *et al*, 2000; van Berkel *et al*, 2000) may be required at early time points following infection *in vivo* to subvert the immune response. In addition, M11 encodes vBcl-2 which blocks apoptosis (Roy *et al*, 2000; Wang *et al*, 1999) and may be required to function early within infection to subvert the apoptosis response. It is less clear what function DNA polymerase may have at very early time points following infection, unless it plays additional roles during infection aside from the replication of viral DNA. However, given that the vtRNAs do not encode protein, they are not delivered into the host cell to allow immediate translation. However, it is possible that whatever role the vtRNAs play during infection it is beneficial for the virus to deliver the vtRNAs immediately upon infection of the host cell. Further investigations into the functional roles of the vtRNAs within infection are required to determine whether this is likely to be the case. However this does not explain the apparent encapsidation of small RNA molecules by MHV-76, although it is possible that in the absence of the vtRNAs the virus still maintains the mechanism response for vtRNA packaging and cellular tRNAs are incorporated in their place, effectively by mistake.

A further hypothesis is that the packaged RNA has a structural role, either acting as a scaffold during virion assembly or maintaining the integrity of the virion. tRNAs of both viral and cellular origin have been proposed to act as nucleating agents during the assemble of the plant virus, brome mosaic virus (Choi *et al*, 2002). In retroviruses, the viral genome is important for virion assembly, however in its absence, this role can be fulfilled by nonspecifically incorporating cellular RNA (Muriaux *et al*, 2001; Wang and Aldovini, 2002). In addition to functioning during the assembly of retrovirus particles, RNA has also be found to be an integral part of the structure of retrovirus particles demonstrated by the disruption of the particle in

the presence of both an RNase and detergent but not detergent alone (Muriaux *et al*, 2001). Unfortunately the contribution of RNA to maintaining the integrity of MHV-68 virion could not be answered in this study as treatment with detergent results in stripping away the outer part of the viral tegument. If RNA, and in particular low molecular weight RNA, is important in virion assembly and structure, this would explain the incorporation of cellular tRNAs within the MHV-76 virion. It could be argued that if tRNAs are required for either assembly of the virus particle or maintaining its integrity then it may be advantageous for the virus to express large amounts of tRNA molecules, in the form of the vtRNAs. In order to determine whether the vtRNAs do indeed play a structural role within the virion, it is important to deduce the exact location of the vtRNAs within the virus particle. This could be achieved through electron-microscopy *in situ* hybridization or removal of the tegument from the virion by nonionic detergents and deoxycholate (Gibson and Roizman, 1972) and investigating whether they are found within the tegument or nucleocapsids. In addition, the identification of possible interacting proteins both within the virion and infected cells would help determine the possible functions of encapsidate vtRNAs and their method of incorporation.

Chapter 4: Characterizing the sub-cellular localization of the vtRNAs and potential interacting proteins

4.1. Aims

4.2 The localization of the vtRNAs during lytic and latent infection

4.3 Potential vtRNA1 interacting proteins

4.4 Potential vtRNA4 interacting proteins

4.5 Discussion

4.1 Aims

In order to shed light on the function of the vtRNAs, it is necessary to investigate their sub-cellular localization pattern and potential interacting proteins. Non-coding RNAs are able to bind a variety of proteins and exhibit differing localization patterns that can be related to their function. For instance, certain non-coding RNAs are found predominately within the nucleus. These include the small U RNAs that assemble into small ribonucleoprotein particles (snRNPs) to function predominantly in RNA splicing, although they have also been associated with transcription initiation (Kwek *et al*, 2002), transcription elongation (Yang *et al*, 2001) and telomere maintenance (Seto *et al*, 1999). The HSURs of HVS resemble cellular small U RNAs and are therefore thought to function in a similar manner. This is further confirmed by their nuclear localization and ability to assemble into snRNPs. They have been found to up-regulate the expression of host genes linked to T-cell activation (Cook *et al*, 2005). Although the mechanism by which they achieve this is unknown it is likely to be related to their assembly into snRNPs. The LATs of HSV-1 also localize predominantly to the nucleus, although they can be found in the cytoplasm during lytic infection indicating that their function is dependent upon the cell-type and/or replication cycle (Ahmed and Fraser, 2001).

miRNAs can be found within both the nucleus and cytoplasm. In the nucleus they are able to regulate transcription by mediating chromatin remodeling (Mourelatos *et al*, 2002; Volpe *et al*, 2002). In the cytoplasm they regulate translation by either stimulating mRNA degradation or causing translational repression (Bartel, 2004). Both these functions of miRNAs are mediated by their interactions with Dicer. Other non-coding RNAs found in the cytoplasm include VAI and the EBERs (Jimenez-Garcia *et al*, 1993; Schwemmle *et al*, 1992), which both prevent the dsRNA stimulated decrease in protein synthesis (Laing *et al*, 2002). VAI is able to do this by binding PKR and preventing its activation (Ghadge *et al*, 1991). In addition it has been found to bind the nuclear export protein Exportin 5 along with Dicer to inhibit RNA silencing (Lu and Cullen, 2004). The mechanism by which the EBERs function has not been fully characterised, although they are able to bind PKR and prevent its activation (Clarke *et al*, 1991). In addition their cytoplasmic localization pattern

suggests that they operate at the level of translational control (Schwemmle *et al*, 1992).

A common theme of non-coding RNAs is their ability to regulate protein synthesis, through a variety of mechanisms. It can therefore be hypothesized that the vtRNAs also function in such a manner, especially given their resemblance to cellular tRNAs. Investigating whether they have a predominantly nuclear or cytoplasmic localization will shed some light on whether this would occur at the level of transcription and RNA processing (i.e. within the nucleus) or translational control (i.e. in the cytoplasm). In addition, although they have been shown to resemble tRNAs, it is not known to what extent they share the same processing pathways and mechanisms of action. tRNAs are transcribed and processed within discrete nuclear regions prior to export to the cytoplasm (Thompson *et al*, 2003). Therefore investigating whether they exhibit the same localization pattern will help to determine whether they exhibit certain characteristics of cellular tRNAs.

Furthermore, it is apparent from the results in chapter 3 that the vtRNAs are packaged within the MHV-68 virion. However, what it not clear is the mechanism by which they are incorporated into the maturing virus particle. Virion proteins have been identified in both HSV-1 and HCMV that are capable of binding packaged RNA (Sciortino *et al*, 2002; Terhune *et al*, 2004). Therefore investigating the sub-cellular localization pattern of the vtRNAs and identifying putative vtRNA binding proteins may help in the understanding of how the vtRNAs are packaged within the virion, where within the virus particle they can be found and the possible functions of packaged vtRNAs.

4.2 The localization of the vtRNAs during lytic and latent infection

4.2.1 Dot-blot analysis on cellular extracts

The localization pattern of the vtRNAs was initially investigated by examining their relative distribution within different cellular fractions; cytoplasm, nuclear membrane, nucleoplasm and the extract of the nuclear pellet which contains the nucleolar

material. The localization of the vtRNAs was investigated *in vitro* during both productive infection of the C127 mouse cell line and the latently infected B-lymphocyte, S11 cell line. The relative levels of vtRNAs within the various extracts was measured by dot-blot analysis using a probe specific for nucleotides 106-1517 of MHV-68 and hence the vtRNAs1-4 (Bowden *et al*, 1997).

C127 cells were infected at a multiplicity of infection of 5pfu/cell for 18 hours. Cellular extracts were produced from both cell types as described in section 2.8.3. DNase I treatment was then carried out in order to remove any DNA found within the extracts. Due to the difference in volume between the cellular extracts, the volumes were normalized with respect to the total volume of the smallest extract; the extract of nuclear pellet. In the case of the nuclear membrane, nucleoplasm and the extract of nuclear pellet, volumes equivalent to 10µl of extract of nuclear pellet were spotted onto a nylon membrane for dot-blot analysis. However, due to the much larger volume of the cytoplasmic fraction, a volume equivalent to only 5µl of extract of nuclear pellet was spotted onto the membrane. Hybridization was subsequently carried out using the *Eco*RI/*Hin*dIII digested fragment of pEH1.4 (Bowden *et al*, 1997), which detects the vtRNAs1-4. Following autoradiography, the intensity of the dots, and hence the relative levels of the vtRNAs present within each dot, was analysed using the Labworks 4^{TM} program, taking into account the fact that the relative volume of the cytoplasmic fraction was half that of the other factions.

It appeared that during both lytic and latent infection, the highest proportion of the vtRNAs was present within the cytoplasm (64% and 57% respectively, figure 4.1). In both the lytically and latently infected cells, the vtRNAs could also be detected within the three other fractions. The fraction containing the second highest levels of the vtRNAs was the nucleoplasm (18% in lytic infection, 19% in latent infection), followed by the nuclear membrane (13% in lytic infection, 11% in latent infection), with the vtRNAs showing their lowest abundance within the extract of the nuclear pellet (8% during lytic infection, 9% in latent infection). In addition, there was no significant difference ($p>0.05$ Mann-Whitney test) in the relative levels of the vtRNAs during lytic and latent infection in the any of the extracts.

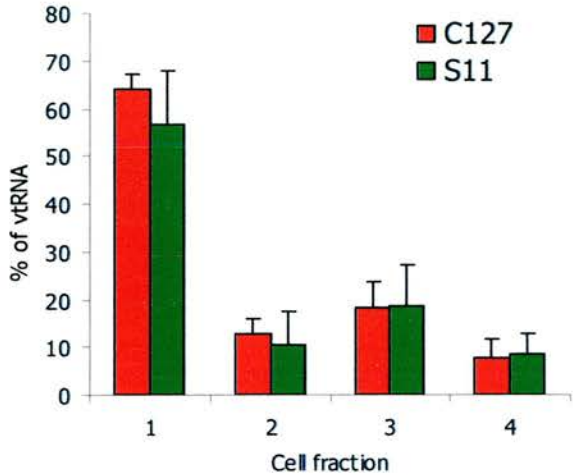

Figure 4.1 Dot blot analysis of the relative sub-cellular localization of the vtRNAs, performed on either C127 cells infected at an MOI of 5 PFU/cell for 18 hours or S11 cells. Cellular fractions were produced containing the cytoplasm (1), nuclear membrane (2), nucleoplasm (3) and extract of the nuclear pellet, containing the chromatin, nucleolar material and nuclear membranes (4). Hybridization was carried out using a probe specific for vtRNAs1-4 (pEH1.4, nt 106 to 1517). Quantification was carried out using Labworks 4™ software. Data shown represent the means and standard deviations of two separate experiments.

4.2.2 In situ hybridisation

In order to examine the localization pattern of the vtRNAs in more detail, *in situ* hybridisation was carried out using an anti-sense probe corresponding to nucleotides 106-1517 of MHV-68, which recognises the vtRNAs 1-4. This was derived from a *Hin*dIII digestion of pEH1.4. The digoxygenin (DIG) labelled probe was produced by *in vitro* transcription using T7 RNA polymerase and the size of the resulting RNA checked by electrophoresis on a 1% agarose gel. The probe was then digested to a length of 170bp by alkaline hydrolysis. The concentration of labelled probe present was estimated by dot-blot analysis and compared to a control probe of known concentration (data not shown).

In order to investigate the localisation of the vtRNAs during infection, cytospins were produced from C127 cells infected with MHV-68 for 18 hours at an MOI of 5pfu/cell. Detection of the dig-labelled probe was initially carried out using an anti-dig/alkaline phosphatase conjugated antibody and 5-bromo-4-chloro-3-indolyl phosphate/nitroblue tetrazolium (BCIP/NBT). As figure 4.2A shows, a positive signal could be seen within cells infected with MHV-68 but not within mock infected cells. In the majority of the infected cells the vtRNAs appear to localize to discrete areas of the nucleus. The specificity of probes used for in situ hybridization is often demonstrated by using a sense probe as a negative control. However, in this instance a sense probe was not used as a negative control, as this was often found to result in a positive signal, although of a lower intensity than the anti-sense probe (data not shown). This is perhaps due to the fact that the vtRNAs have regions which are complementary, and hence the sense probe may be able to undergo a certain amount of base-pairing with the vtRNAs. Instead, to establish that the hybridization was specific for the vtRNAs, a recombinant MHV-76 virus known as intRNA(9) was utilized, which expresses the vtRNAs1-5 from the left-hand end of the genome (see section 5.3). In situ hybridization was carried out following infection with both intRNA(9) and MHV-76. intRNA(9) infection gave a staining pattern within cells identical to that seen within MHV-68. No staining could be seen in cells infected with MHV-76. Given that the only difference between MHV-76 and intRNA is the

presence of the vtRNAs, this indicates that the probe hybridizes specifically to the vtRNAs.

In order to investigate in greater detail the exact localization pattern of the vtRNAs, fluorescent *in situ* hybridization was carried out. This allows the sections to be viewed using confocal microscopy and hence gives a greater resolution. In order to do this, the dig-labeled probe was detected using a primary antibody, followed by a secondary biotin-conjugated antibody and streptavidin/alexafluor 488. C127 cells were once again infected at a MOI of 5 pfu/cell, but this time for various times from 1 hour to 24 hours As figure 4.2 shows, the vtRNAs can first be detected by in situ hybridisation at 3 hours p.i., where they localize to specific areas within the nucleus, forming between one and three large dots. At later time-points (from 12 hours onwards), their nuclear distribution pattern changes, as the numbers of vtRNA containing areas increase and they exhibit a more globular distribution pattern. By 12 hours p.i. they are also present at high levels within the cytoplasm. This is in agreement with the data on the dot blot analysis on the cellular factions. In order to investigate the localization of the vtRNAs during latent infection, in situ hybridisation was carried out on the latently infected S11 B-cell line. Once again the vtRNAs localize mainly within the cytoplasm, but unlike during lytic infection, their localization is much more globular and they appear to be peri-nuclear. To determine that the probe is binding to the vtRNAs and not DNA, the cytospins were treated with both RNase A and DNase ONE prior to hybridisation. Pre-treatment with the DNase did not affect the staining pattern; however treatment of the slides with the RNase resulted in loss of the signal, indicating that the probe is specific for RNA and not DNA.

4.3 Potential vtRNA1 interacting proteins

4.3.1 Electrophoretic mobility shift assays

Electrophoretic mobility shift assays (EMSAs) are a method of detecting nucleic acid–protein interactions. Radiolabelled RNA is mixed with protein extracts and then electrophoresed through a non-denaturing polyacrylamide gel. Any RNA–protein

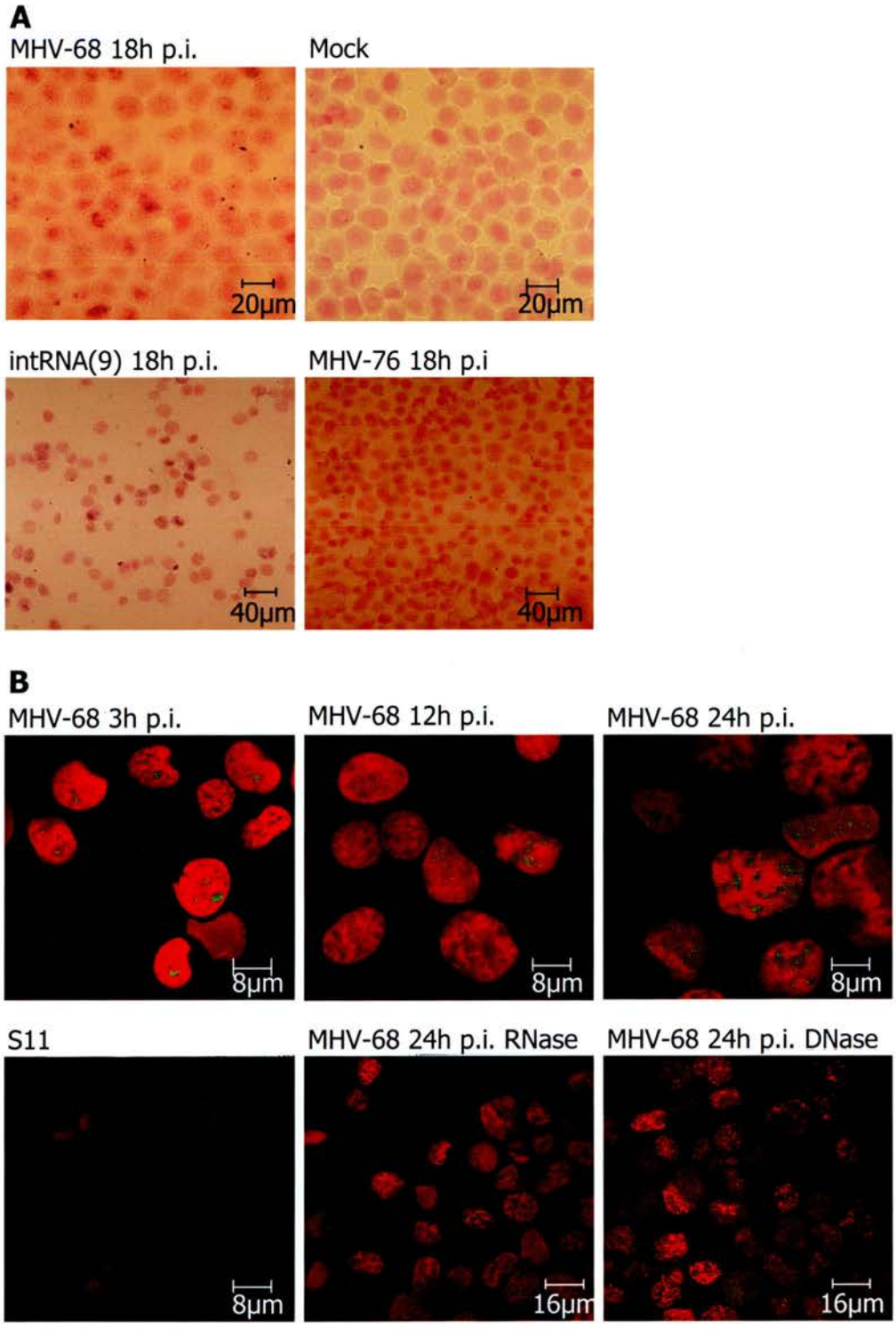

Figure 4.2 In situ hybridization for vtRNAs1-4 performed on either C127 cells infected at an MOI of 5 PFU/cell as indicated or S11 cells. Detection of the digoxygenin (dig) labelled probe was carried out using either anti-dig-AP (A) and BCIP/NBT, or a secondary antibody-biotin conjugate and streptavidin-alexafluor 488 (B). Sections were counterstained in nuclear fast red (A) or propidium iodide (B).

complexes that are formed run with a slower mobility through the gel in comparison with non-complexed RNA, and can therefore be visualized following exposure of the gel to radioactive film.

The DNA template used for *in vitro* transcription of vtRNA1 was produced by annealing synthetic DNA oligomers, resulting in a double stranded T7 RNA polymerase promoter and single stranded vtRNA1 coding sequence containing the 3' CCA sequence, which is added to the vtRNA post-transcriptionally *in vivo* (see appendix 3). Following *in vitro* transcription of radiolabeled vtRNA1 the template DNA was digested by DNase ONE and unincorporated nucleotides removed by passage through a size exclusion chromatography column. The resulting radiolabeled RNA was refolded as described in section 2.5.8 Additional RNA species were also generated by *in vitro* transcription; unlabelled or cold vtRNA1 and human 18S ribosomal RNA.

The protein extracts used in the reactions were produced from C127 cells, which were either mock infected or infected with MHV-68 at an MOI of 5pfu/cell for 18 hours. Cytoplasmic and nuclear extracts were produced from the cells, as described in section 2.8.3. Radiolabeled vtRNA1 was mixed with protein and incubated for 20 minutes at room temperature. The reactions were then run on a 5% polyacrylamide gel and exposed to photographic film. Two RNA-protein complexes could be visualised following incubation with protein extracts from both the nucleus and cytoplasm of infected cells, however no complexes were present following incubation with cellular extracts taken from uninfected cells (figure 4.3) indicating that vtRNA1 is capable of interacting with proteins or protein complexes present only within infected cells. The specificity of the interaction was investigated by carrying out the binding reaction in the presence of excess homologous and non-homologous competitor RNA. Formation of the complexes was inhibited by the presence of excess unlabelled vtRNA1, but not equivalent concentrations of 18S RNA or yeast tRNA. Hence the interaction is specific for the vtRNA1.

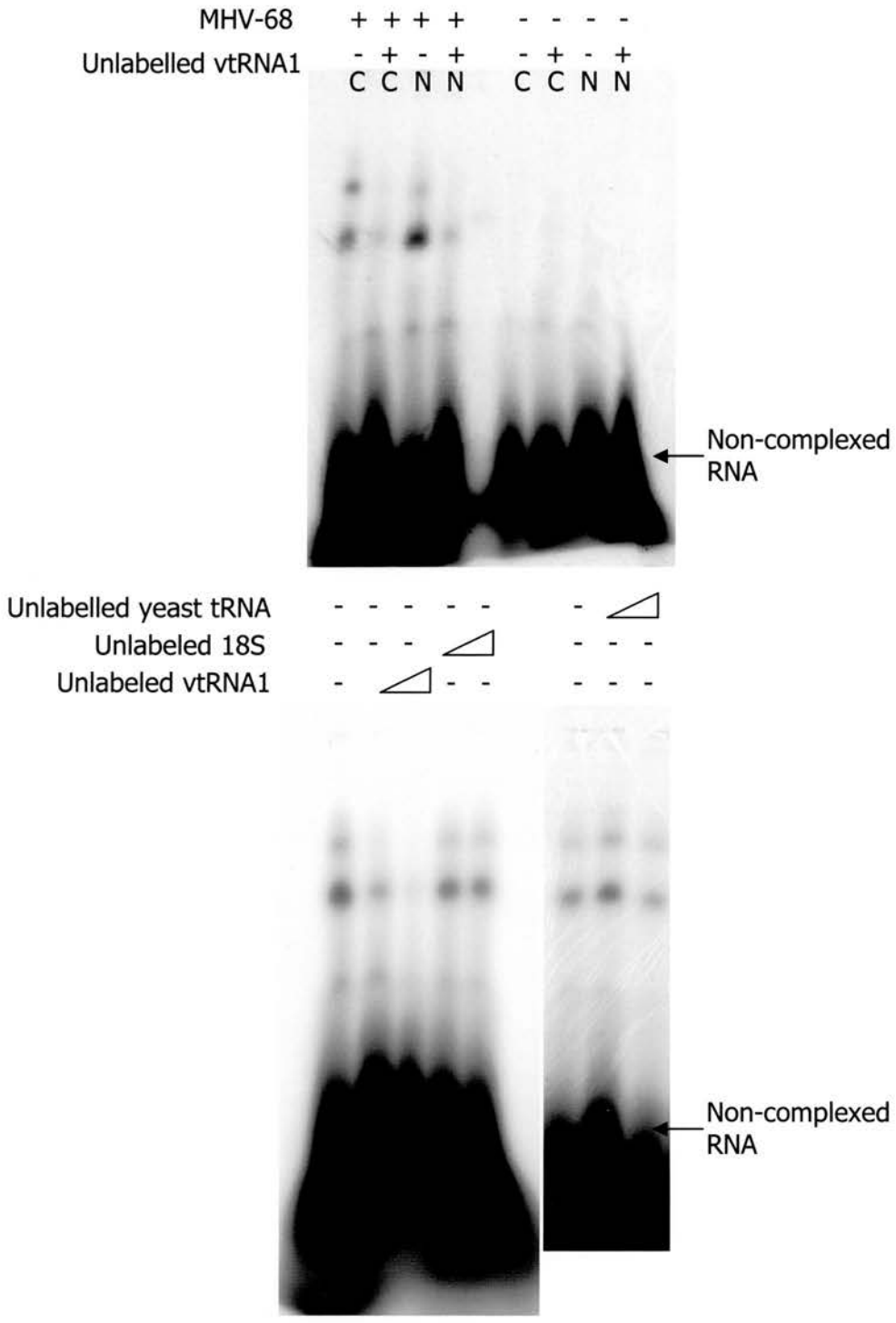

Figure 4.3 Electophoretic mobility shift assays using radiolabeled vtRNA1 and cellular extracts of C127 cells infected with either MHV-68 at an MOI of 5 pfu/cell or mock infected. The assays were carried out using both cytoplasmic (C) and nuclear (N) extracts. Increasing concentrations of unlabelled vtRNA1, 18S RNA and yeast tRNA (2.5ng; also shown as +, and 10ng) were also including in the reactions, represented as open triangles. The RNA/protein complexes were analysed on a 5% TBE-polyacrylamide gel.

The identification of proteins present with the RNA-protein complex is possible by addition of a specific antibody to the reaction mixture, resulting in either super-shifting of the band due to the formation of a higher molecular weight complex or loss of the complex as RNA-protein binding is inhibited. Reactions were therefore carried out using radiolabeled vtRNA1 and cytoplasmic extracts taken from MHV-68 infected C127 cells, in the presence of equivalent concentrations of a polyclonal anti-MHV-68 antibody produced in rabbits or normal rabbit serum (figure 4.4A). Incubation in the presence of the anti-MHV-68 antibody resulted in the loss of the two protein complexes following electrophoresis. A faint band of a higher molecular weight was also visible. Incubation in the presence of normal rabbit serum had no effect upon the assay. It therefore appears that the interaction is blocked by the addition of the anti-MHV-68 antibody and therefore the vtRNA1 interacts directly with viral protein(s).

In order to characterise further the viral protein(s) capable of binding to vtRNA1, the expression class of the protein was investigated. Treatment of cells with cyclohexamide (CHX) and phosphonoacetic acid (PAA) prior to virus infection blocks protein synthesis and DNA replication respectively. Protein extracts were produced from MHV-68 infected C127 cells which were either untreated or pre-treated with CHX or PAA. EMSAs were carried out by incubation of labelled vtRNA1 with the cellular extracts. As figure 4.4B shows, protein complexes were present following incubation with both nuclear and cytoplasmic extracts from untreated cells, but not from those treated with CHX or PAA. vtRNA1 therefore binds viral protein(s) expressed following the onset of viral DNA replication.

4.3.2 Identification of protein complexes

Geck *et al* have previously described a method to UV cross-link RNA-protein complexes excised from polyacrylamide gels, by subjecting gel slices containing the complexes to UV light, enabling the cross-linked RNA-protein complex to be electrophoresed on a denaturing SDS-polyacrylamide gel (Geck *et al*, 1994). This allows the size of proteins which directly interact with RNA within a complex to be determined. EMSAs were therefore carried out using cytoplasmic extracts produced

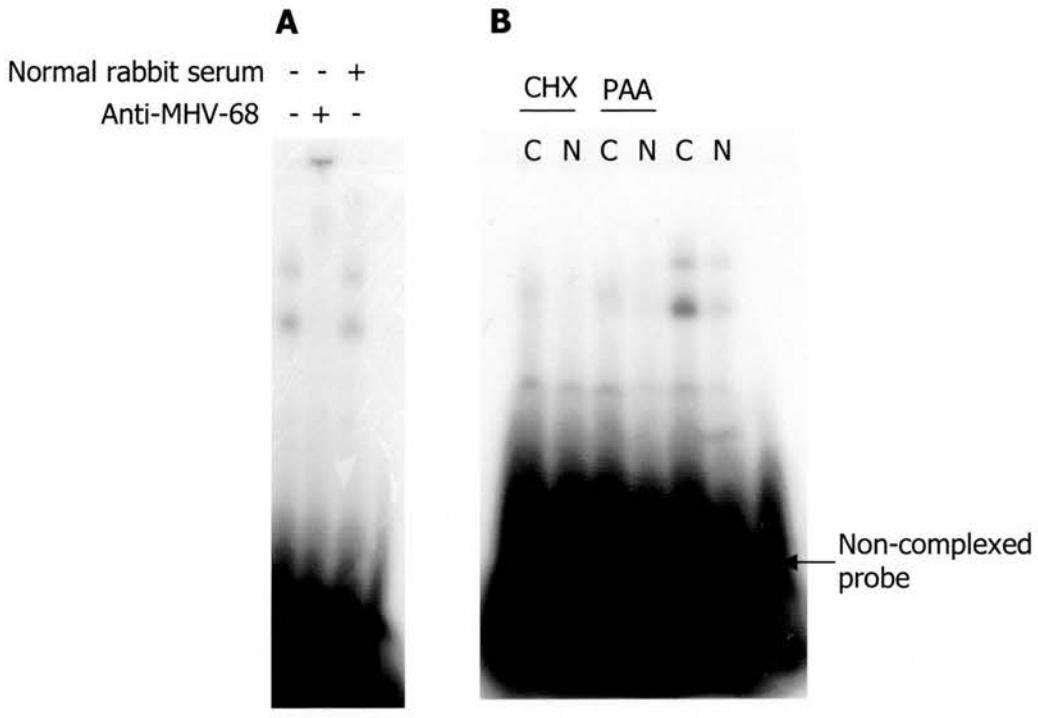

Figure 4.4 Electrophoretic mobility shift assays using radiolabelled vtRNA1 and cellular extracts from MHV-68 infected C127 cells, in the presence of equivalent concentrations anti-MHV-68 polyclonal antibody or normal rabbit serum (A). Assays were also carried out using either nuclear (N) or cytoplasmic extracts (C) from MHV-68 infected untreated cells or cells pre-treated with either cyclohexamide (CHX) or phosphonoacetic acid (PAA) to block protein synthesis and DNA replication respectively. The RNA/protein complexes were analysed on a 5% TBE-polyacrylamide gel.

from MHV-68 infected C127 cells. The locations of RNA-protein complexes were determined following autoradiography, the two bands excised and UV crosslinked at a wavelength of 254nm, for 17 minutes. The gel slices were then treated with a nuclease to digest any RNA not cross-linked to protein. The gel slices were subsequently run on a 12% SDS polyacrylamide gel. Following this procedure, bands were only visible following crosslinking of protein complex 2 but not complex 1, perhaps because the RNA-protein interactions within complex 1 are less stable or due to there being less protein or vtRNA1 present. The two RNA-protein complexes were of approximately 38 and 55KDa in size (figure 4.5B).

Elution of proteins from RNA-protein complexes following EMSAs has been previously described (Heaton *et al*, 2001; Ranish and Hahn, 1991). This technique was therefore used to try to identify proteins present within the two vtRNA1-protein complexes. *In vitro* transcription of cold vtRNA1 was carried out on a larger scale and refolded as previously described. Binding reaction were carried out using labelled vtRNA1, in addition to a larger scale cold reaction with cytoplasmic extract produced from MHV-68 infected C127 cells. Using the labelled complexes as a guide the corresponding sections of the gel, where the unlabelled reactions were run, were excised and proteins eluted. The eluted proteins were concentrated using spin columns and run on a 12% SDS-PAGE gel, which was then subjected to silver staining (figure 4.5C). Within complex 1 many protein bands were visible, ranging from approximately 40KDa to 170kDa. A major band of 48kDa was clearly visible. Only 4 bands were visible within complex 2, of approximately 48kDa, 60kDa, 70kDa and 100kDa respectively. As for complex 1, the major band present within complex 2 was of approximately 48kDa. In order to try and identify proteins present within complexes 1 and 2, the extracts were once again run on a 12% SDS PAGE gel and subjected to SYPRO ruby staining. However, the only bands that could be visualized following SYPRO ruby staining were the higher molecular weight bands along with a band of 50kDa. The individual bands were excised from the gel and subjected to MALDI-TOFF mass spectrometry (carried out by the Edinburgh Protein Interaction Centre). The proteins present are shown in table 4.1. Most of the proteins represent house keeping genes present at high levels within cells. Given that there is

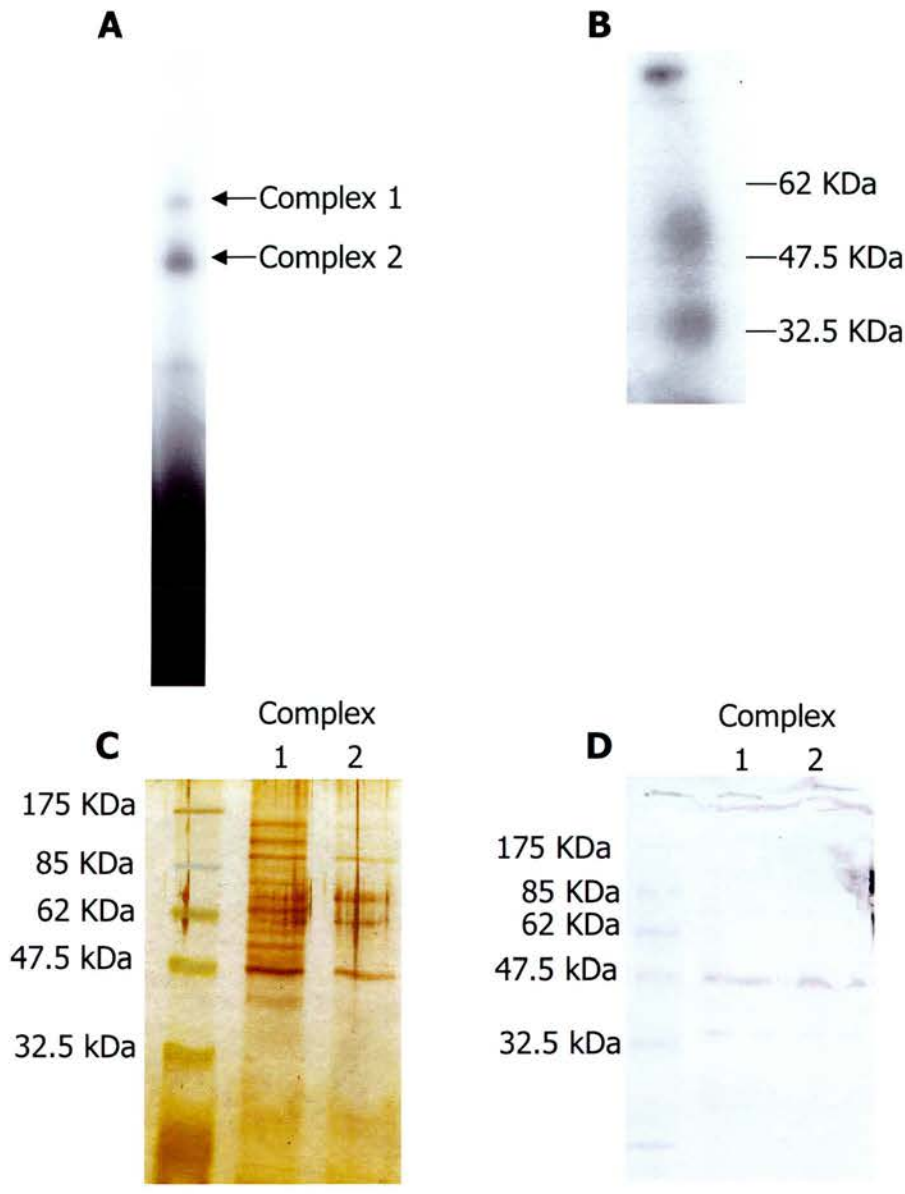

Figure 4.5 Identification of the protein complexes in band 1 and band 2. The designation of the two bands is shown in a typical EMSA in A. Both radiolabelled vtRNA1/protein complexes were excised from the gel, UV crosslinked and run on an 12% polyacrylamide/SDS gel. Bands were only visible following cross linking of complex 2 (B). The proteins from each complex were eluted and run on 12% polyacrylamide/SDS gels and either silver-stained (C) or Western blotted using a polyclonal anti-MHV-68 antibody (D). The molecular weight of protein markers are shown.

no obvious function of these proteins within the vtRNA-protein complex, they are perhaps most likely contaminants of the complex. However, one protein was identified as mouse jmjdla protein, a mouse protein of unknown function that contains a jmjC domain, thought to be involved in chromatin organisation by modulating heterochromatisation (Balciunas and Ronne, 2000).

The protein complexes eluted from the EMSA were also subjected to Western blot analysis, using an anti-MHV-68 polyclonal antibody (figure 4.5D). In both complexes bands of approximately 38kDa and 48kDa could be visualised, which were not present within a control blot performed on uninfected cytoplasmic extract. Taking together both the UV-crosslinkage results and experiments on the eluted proteins, it appears that the complexes contain at least two proteins capable of binding directly to vtRNA1, of approximately 38kDa and 55kDa in size and two viral proteins of approximately 38kDa and 48kDa. Further work is required to determine whether the 38kDa protein capable of directly binding vtRNA1 represents a viral protein. In addition, the complexes appear to contain a number of other proteins, at least some of which are very abundant cellular proteins, such as actin, which may not be part of the complex and are perhaps contaminants of the experiment.

4.4 Potential vtRNA4 interacting proteins

4.4.1 Electrophoretic mobility shift assays

In order to identify proteins capable of interacting with a second vtRNA, EMSAs were carried out using vtRNA4. The vtRNA was *in vitro* transcribed from annealed synthetic DNA oligomers consisting of the vtRNA sequence, the T7 RNA polymerase promoter and a 3' CCA sequence. However, unlike the template used for the *in vitro* transcription of vtRNA1 which was partially single-stranded, the one used for vtRNA4 was entirely double-stranded. Assays were carried out by incubation of labelled vtRNA4 with cellular extracts taken from both uninfected and MHV-68 infected C127 cells (figure 4.6A). The cellular fractions used in the assay consisted of the cytoplasm, nuclear membrane, nucleoplasm and extract of the

Band	Protein	MW (kDa)	Percentage mass tolerance (ppm)	% Masses Matched
1	Jmjdla	147	100	13%
1	Proplyl endopeptidase	81	50	12%
1	m-calpain	79	50	11%
1	Extracellular signal-related kinase 7	61	50	11%
2	Heat-shock protein 90-β	83	50	37%
2	B-actin	42	50	7%

Table 4.1 Proteins identified by mass spectrometry within vtRNA1-protein complexes in bands 1 and 2. The proteins from each complex were eluted, run on 12% polyacrylamide/SDS gels and stained with SYPRO-ruby. Visible bands were excised and subjected to MALD-TOFF mass spectrometry. Proteins present were identified using MS-FIT, using a percentage mass tolerance of either 50 or 100 parts per million (ppm). The molecular weight and the percentage peptide coverage of the identified protein are shown.

nuclear pellet, which contains the chromatin, nucleolar material and nuclear membranes. RNA-protein complexes were clearly visible following incubation with the cellular fractions taken from MHV-68 infected C127 cells, which resembled the two RNA-protein complexes formed when vtRNA1 was used in the reaction. In addition, RNA-protein complexes exhibiting different migrations were present following incubation with both the nuclear membrane fraction and nucleoplasm produced from uninfected C127 cells.

The specificity of the interaction of vtRNA4 with proteins present within uninfected C127 cells was investigated by incubating with increasing concentrations (2.5ng and 10ng) of unlabelled vtRNA4, along with equivalent concentrations of *in vitro* transcribed 18S RNA and yeast tRNA (figure 4.6B). The formation of the RNA-protein complexes was out-competed by excess unlabeled vtRNA4 (10ng) but not by equivalent concentrations of 18S RNA and yeast tRNA and hence the vtRNA-protein interaction is specific.

4.4.2 Identification of protein complexes

The proteins present within the vtRNA4-protein complex were eluted from the polyacrylamide gel as previously described for vtRNA1. Using labelled vtRNA4 as a guide the corresponding sections of the gel the unlabelled RNA-protein complexes were excised and the proteins eluted. Following concentration, the eluted protein was electrophoresed on a 12% SDS-PAGE gel and subjected to silver staining (figure 4.7). A number of proteins were present within the complex, ranging from approximately 33kDa to 170kDa. Major protein bands were present of approximately 33kDa, 47kDa, 60kDa, 80kDa and 90kDa. However, insufficient quantities of proteins were extracted for SYPRO ruby staining and therefore could not be analysed by mass spectrometry. Therefore the identity of the cellular protein(s) capable of interacting with vtRNA4 remains to de determined.

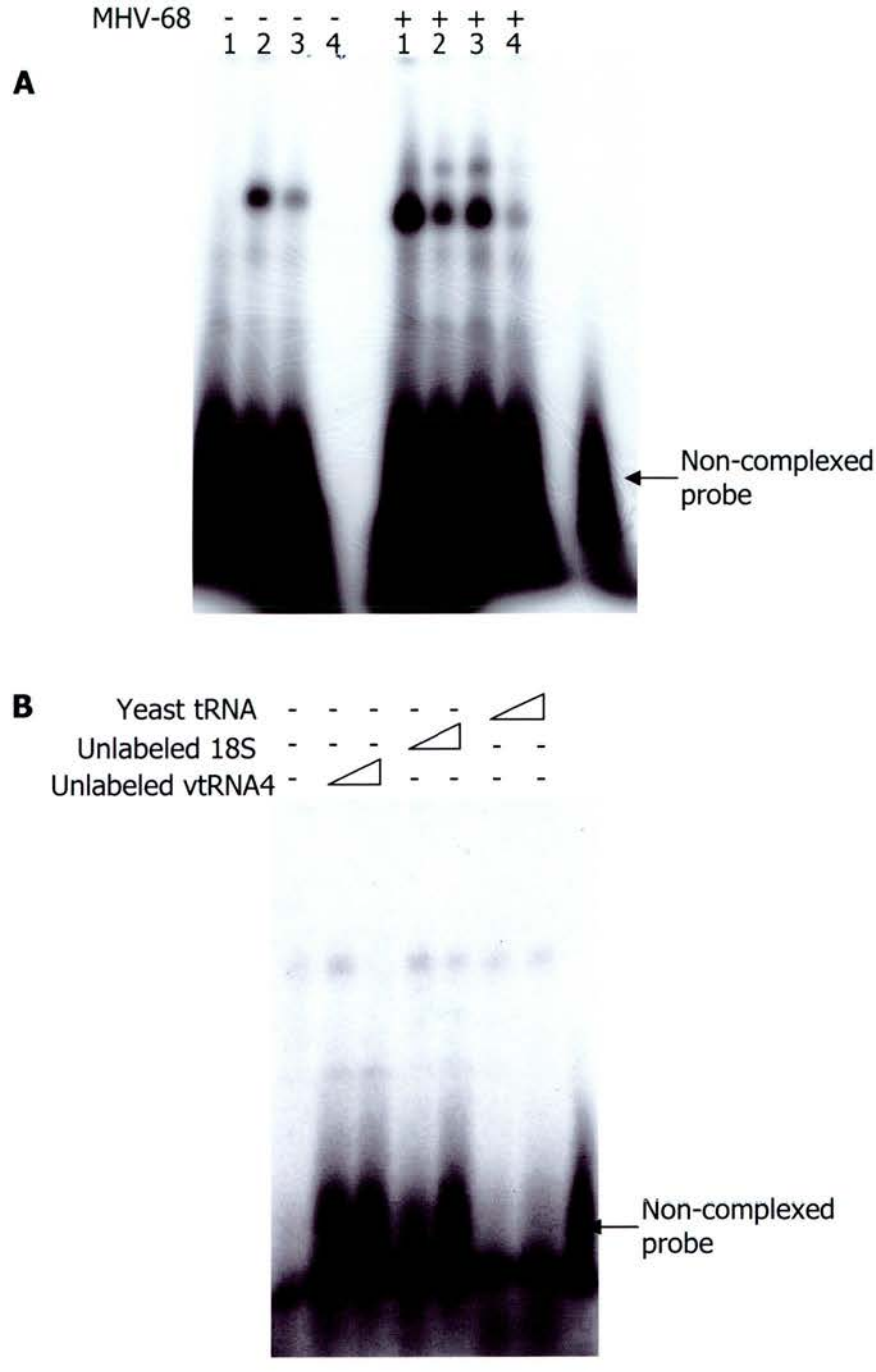

Figure 4.6 Electrophoretic mobility shift assays using vtRNA4 and cellular extracts from infected and uninfected C127 cells. Cellular fractions composed of cytoplasm (1), outer nuclear membrane (2), nucleoplasm (3) and the extract of nuclear pellet, which contains chromatin, nuclear membranes and nucleolar material (4) were used in the assay (A). The specificity of vtRNA4 binding to proteins within the nucleoplasm of uninfected cells was investigated by carrying out the assay the presence of increasing concentrations (2.5ng and 10ng) of unlabelled vtRNA 4, 18S RNA and yeast tRNA, shown as open triangles (B). The RNA/protein complexes were analysed on a 5% TBE-polyacrylamide gel.

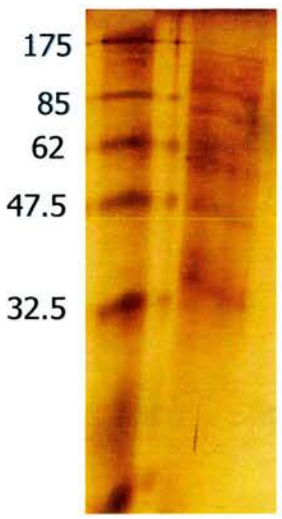

Figure 4.7 Identification of the protein complexes present within the vtRNA4-protein complex, as identified by electophoretic mobility shift assay. The proteins present within the vtRNA4-protein complex, formed by incubating vtRNA4 with nucleoplasm from uninfected cells, were eluted and run on 12% polyacrylamide/SDS gels and silver-stained. The molecular weight of protein markers are shown.

4.5 Discussion

In this study, the sub-cellular localization of the vtRNAs and potential interacting proteins have been investigated. It is clear from chapter 3 that the vtRNAs are packaged within the MHV-68 virion and are released into the cell immediately following infection. However they could not be detected by *in situ* hybridization within the cytoplasm of infected cells immediately following infection. This is perhaps because they were below the limit of detection of the assay at this stage. The localization could first be seen at three hours post-infection within isolated areas of the nucleus. This is reminiscent of the localization pattern of newly transcribed cellular tRNAs (Thompson *et al*, 2003) and therefore although the identity of these areas has not been investigated, it could be speculated that this reflected transcription and early processing within the nucleolus. By 24 hours post-infection they showed a globular pattern of nuclear staining. Given that at late time points in infection viral RNA synthesis is closely linked to DNA replication, it can be hypothesized that this globular distribution pattern reflects vtRNA synthesis occurring within replication compartments. However, further investigations such as co-staining for viral DNA replication proteins are required to determine if this is the case. At this time, the vtRNAs were found at high levels within the cytoplasm as demonstrated by both *in situ* hybridization and dot-blot analysis. This was also the case for latently infected cells, although minor differences could be seen by *in situ* hybridization in the cytoplasmic distribution between productively and latently infected cells; in the former the vtRNAs appeared to be spread throughout the entire cytoplasm, whereas in the latter they appeared to localize to the peri-nuclear region. It is possible that the more diffuse distribution pattern observed within lytically infected cells is a result of packaging of the vtRNAs within newly formed virions in the cytoplasm. However, it may also indicate that the vtRNAs function differently within the two different cell types.

As mentioned in section 4.1, non-coding RNAs display differing localization patterns which can be related to their function. If one function of the vtRNAs is the regulation of protein synthesis, their abundance within the cytoplasm suggests that this occurs at the level of translation. Such a localization pattern is similar to that seen for both

VAI of adenovirus and the EBERs of EBV, which have both been found to regulate translation within the cytoplasm. Therefore it is possible that the vtRNAs carry out a similar role. In order to further characterise the function of the vtRNAs in the cytoplasm it is necessary to identify cytoplasmic proteins with which they interact. In this study EMSAs were carried out to determine whether the vtRNA1 and vtRNA4 are capable of interacting with proteins. EMSAs have an advantage over other techniques in that the proteins extracted are in their native conformation. In addition, the vtRNAs could be radiolabeled in such a way as to minimise any disruption to their secondary structure and without adding elements to either their 3' or 5' ends that might interfere with protein binding. It is clear from the EMSA data that at least one vtRNA (vtRNA4) is capable of specifically interacting with cellular protein(s). Unfortunately it was not possible to discover the nature of these proteins within the course of this study. Further work is required to determine the identity of the vtRNA4 binding protein(s), perhaps utilizing the conditions optimized in this study to either scale up the binding reaction to try to extract larger amounts of vtRNA-binding protein, or trying alterative techniques such as immobilizing the vtRNAs and pulling down proteins that bind.

Although it was not possible to identify proteins from uninfected cells capable of interacting with the vtRNAs, one protein was identified from the eluted vtRNA1-protein complex present within infected cells as Jmjdla, a mouse protein of unknown function that contains a jmjC domain, which is thought to be involved in chromatin organisation by modulating heterochromatisation (Balciunas and Ronne, 2000). Chromatin remodelling plays an important role in the regulation of gene expression during both lytic and latent herpesvirus infection (reviewed in Efstathiou and Preston, 2005). In addition, recent data suggest LATs of HSV-1 play a role in regulating lytic cycle gene expression during latency by promoting the assembly of heterochromatin on productive cycle promoters (Wang, Q, Coen, D.M. and Knipe, D.M. in press). If this represents a generic feature of herpesvirus non-coding RNAs, it is possible that the vtRNAs are able to form a complex with proteins involved in chromatin remodelling. Given that they can be found in the nucleus in areas that resemble replication compartments, the vtRNAs could potentially operate at the level

of transcription to regulate the expression of viral genes. However, it is also possible that this protein was a contaminant of the reactions and further work is required to determine whether the vtRNAs form complexes with proteins containing jmjC domains to play a role in the regulation of gene expression.

It is clear that in order to localize within the cytoplasm, the vtRNAs must be exported across the nuclear membrane, and this is reflected by their presence within the nuclear membrane containing cellular fraction. However, the mechanism by which they are able to do this is not clear. Two proteins have been found to be involved in the translocation of cellular tRNAs across the nuclear membrane; exportin-t and exportin-5 (Gwizdek *et al*, 2004; Lund and Dahlberg, 1998). Both proteins employ proof-reading mechanisms to ensure that only mature tRNAs are exported to the cytoplasm, as exportin-t requires the addition of 3' CCA sequences to tRNA molecules, whereas exportin-5 mediates the export of amino-acylated tRNA molecules. As the vtRNAs do possess post-transcriptionally added 3' CCA sequences, it could be predicted that the vtRNAs are exported from the cytoplasm via exportin-t. However, exportin-5 also facilitates the export of pre-miRNAs and other viral non-coding RNAs such as VAI of adenovirus (reviewed in Rodriguez *et al*, 2004), and it is therefore possible that this protein may be responsible for the translocation of the vtRNAs, either in their mature form or as longer full length transcripts, which also contain predicted miRNA sequences. Investigations into the exact nature of the vtRNA transcripts within the different cellular fractions would indicate whether they are processed within the nucleus prior to export or within the cytoplasm and therefore which export pathway they are likely to utilize. It is also possible that they are exported by a third pathway which is dependent upon viral and not cellular proteins.

The vtRNAs represent the major viral RNA species incorporated into the MHV-68 virion. However, the function of the encapsidated vtRNAs is not understood. Understanding the mechanism by which they are incorporated may give an indication of the function of packaged RNA. Virion assembly is a complex process involving DNA packaging, capsid assembly, peri-nuclear transport and virion tegumentation

and envelopment (Roizman and Knipe, 2001). The formation of the virion begins in the cytoplasm, with the assembly of the nucleocapsids. Immature capsids then move into the nucleus, where the viral genomes are loaded into the empty capsids within particular loci in the nucleus known as replication compartments. The nucleocapsids then leave the nucleus after obtaining a tegument layer that is required for passage through the inner nuclear membrane; however, the composition of this initial tegument varies from that of the mature tegument. Final tegumentation takes place within the cytoplasm through a network of protein-protein interactions, the complexity of which is only just being understood.

The localization pattern of the vtRNAs gives some insight into the mechanism by which they are packaged. At late times within infection when virion assembly is taking place, the vtRNAs could be found within both the nucleus and cytoplasm. In the nucleus they exhibited a globular distribution pattern, which possibly reflects ongoing transcription within replication compartments where capsid assembly takes place. It is possible that the presence of the vtRNAs at the sites of capsid formation results in their incorporation and subsequent translocation across the inner-nuclear membrane within the nucleocapsids. However given that the major incorporated RNA species within the virion were found to be of approximately 70 nucleotides in length, it appears that the fully processed and not the immature vtRNA transcripts are selectively incorporated, thus arguing against their immediate packaging following transcription.

Given the abundant cytoplasmic distribution pattern late within infection, it is possible that the vtRNAs assemble in the cytoplasm to form part of the tegument layer. Based on a number of observations, packaged RNA in other herpesviruses has been hypothesized to be present within the tegument. Firstly, the encapsidated RNA of HCMV was found to localize predominantly within the cytoplasm and not the nucleus (Terhune *et al*, 2004). Secondly, tegument proteins from both HSV and HCMV have been shown to be capable of binding RNA species that are packaged within the virion (Sciortino *et al*, 2002; Terhune *et al*, 2004). It is therefore useful to identify viral proteins capable of interacting with the vtRNAs in order to determine

the mechanism by which they are packaged. EMSAs demonstrated the interactions of both vtRNA1 and vtRNA4 with protein complexes present solely within infected cells indicated binding to viral proteins and this was confirmed by the ability of an anti-MHV-68 polyclonal antibody to block the interaction.

Despite the clear interaction of the vtRNAs with viral protein(s), the identity of the viral protein could not be determined in this study. The majority of late proteins expressed by MHV-68 represent structural proteins (Ebrahimi *et al*, 2003), and therefore the observation that the vtRNA bound viral protein(s) expressed following the onset of viral DNA replication suggested binding to a viral structural protein. UV-crosslinking of the vtRNA-protein complexes indicated direct binding to proteins of approximately 38kDa and 55kDa, whereas Western-blotting of the protein complexes identified viral proteins of 38kDa and 47kDa in size. Virion proteins of similar sizes include the ORF45 tegument protein (48kDa) and ORF48 (37.9kDa). ORF45 has been implicated in transcriptional activation (Jia *et al*, 2005); however the functional significance of this is unclear. The function of ORF48 is unknown and sequence analysis using BLAST failed to detect any known functional domains within either protein.

Additional methods were attempted to try to identify the vtRNA-binding proteins. North-western blotting is another technique used to identify RNA-protein interactions, in which proteins are electrophoretically separated in denaturing gels, blotted onto a nylon membrane, re-natured and then reacted with a labelled riboprobe. This was attempted using proteins extracted from MHV-68 virions. No interactions between the proteins and the vtRNAs could be identified, however this does not mean that vtRNAs do not interact within virion proteins as it is possible that the proteins did not re-nature correctly. Hence further investigations are required to determine the identity of the vtRNA-binding proteins in order to gain an understanding into how the vtRNAs are incorporated into the virion and the potential functions of the vtRNAs.

Chapter 5: Investigating the function of the vtRNAs during *in vitro* and *in vivo* infection

5.1. Aims

5.2. Construction of intRNA1-5 virus

5.3. Construction of MHV-76intRNA1-5 revertant virus

5.4. Southern analysis of the intRNA and intRNARev viruses

5.5. Construction of WTTintRNA

5.6. Construction of intRNA5 viruses

5.7. Characterisation of MHV-76 insertion viruses *in vitro*

5.8. Characterisation of MHV-76 insertion viruses *in vivo*

5.9. Construction of a vtRNA expressing cell line

5.10. Discussion

5.1 Aims

The role of the vtRNAs within infection has not been extensively characterised and therefore it is currently unclear what biological function they fulfil. Deletion of vtRNAs1-4 along with M1 from MHV-68 resulted in no difference from wild type virus during either *in vitro* replication or in the ability of the virus to establish a latent infection (Simas *et al*, 1998). However, it is possible that the individual vtRNAs have overlapping functions and thus deletion of just four vtRNAs would not completely abrogate their function. Within the MHV-68 genome the vtRNAs are found interspersed amongst the M1 and M2 genes (figure 1.4), making deletion of all eight vtRNAs particularly problematic. Hence, MHV-76 has been utilized for the study of the vtRNAs within infection by construction of recombinant knock-in viruses containing the vtRNAs. Given that MHV-76 is a deletion mutant of MHV-68, the left hand genes can be inserted into MHV-76 in a position equivalent to that in MHV-68 without disrupting genes required for viral replication or the establishment and reactivation from latency. This approach has been used successfully in our laboratory to assess the role of the M4 gene within infection (Townsley *et al*, 2004).

5.2 Construction of intRNA1-5 virus

In order to investigate the contribution of the vtRNAs within infection, a knock in virus of MHV-76 had previously been produced (T. Heckel, Y. Ligertwood and B.M. Dutia) by insertion of vtRNAs1-5 into the left-hand end of MHV-76 (intRNA). The recombination cassette used to generate intRNA (pL2a5) consists of the vtRNA1-5 genes flanked by MHV-68 derived sequences common to both MHV-68 and MHV-76: partial M4 and ORF4 gene sequences (bp 9540-10914) and a 1213bp terminal repeat fragment derived from a *Pst*I digestion of the terminal repeat, which cuts at nt11870 (fig 5.1). Given that each terminal repeat corresponds to nt118237-11940, the terminal repeat region present within the recombination cassette contains 463 nucleotides of 5' sequence downstream of 840 nucleotides of 3' sequence (figure 5.1). The resulting recombinant virus had been purified by serial dilution plaque purification (see section 2.9.2) and was found to be free from contaminating wild-

type MHV-76 by Southern blot analysis. The resulting virus will be referred to as intRNA(9). A further independent clone was produced using the same recombination cassette. The L2a5 plasmid was partially digested to yield a 4.3kb fragment containing vtRNAs and homologous MHV-76 sequences, to prevent the incorporation of plasmid DNA into MHV-76 during construction of intRNA1-5. BHK-21 cells were co-transfected by electroporation and wells containing single plaques isolated as described in section 2.9.1. Viral DNA was then extracted and PCR undertaken for the presence of the vtRNA fragment using the tRNAfor2 and tRNArev primers (see appendix 2).

Selections of plaque picks were then purified away from MHV-76 using both the limiting dilution assay and agarose overlay methods (see section 2.9.2). Using the limiting dilution approach, DNA could be extracted from the individual plaques and PCR carried out, firstly to detect the vtRNAs, and secondly using the M4B/TR primer pair to amplify a section of DNA from the terminal repeats to the residual M4 sequence present within MHV-76, thus allowing the detection of contaminating parental virus. Due to the small volume produced when plaques were picked under an agarose overlay, DNA could not be extracted for PCR analysis and therefore all plaques picked under an agarose overlay were immediately subjected to a cycle of limiting dilution plaque purification, following which the DNA could be extracted. Following two rounds of limiting dilution plaque purification and one agarose overlay, the viral stock was found to be free from contaminating MHV-76 (figure 5.2). A further three rounds of limiting dilution plaque purification was carried out to ensure any remaining MHV-76 that was below the level of detection for the PCR assay was removed and a homogenous viral stock produced. The resulting virus will be referred to as intRNA(2).

5.3 Construction of MHV-76intRNA1-5 revertant virus

In order to confirm that any observed phenotype with the intRNA viruses is the result of vtRNA expression and not due to unwanted mutations in other areas of the genome, a revertant virus was produced by restoration of the intRNA(9) genome to

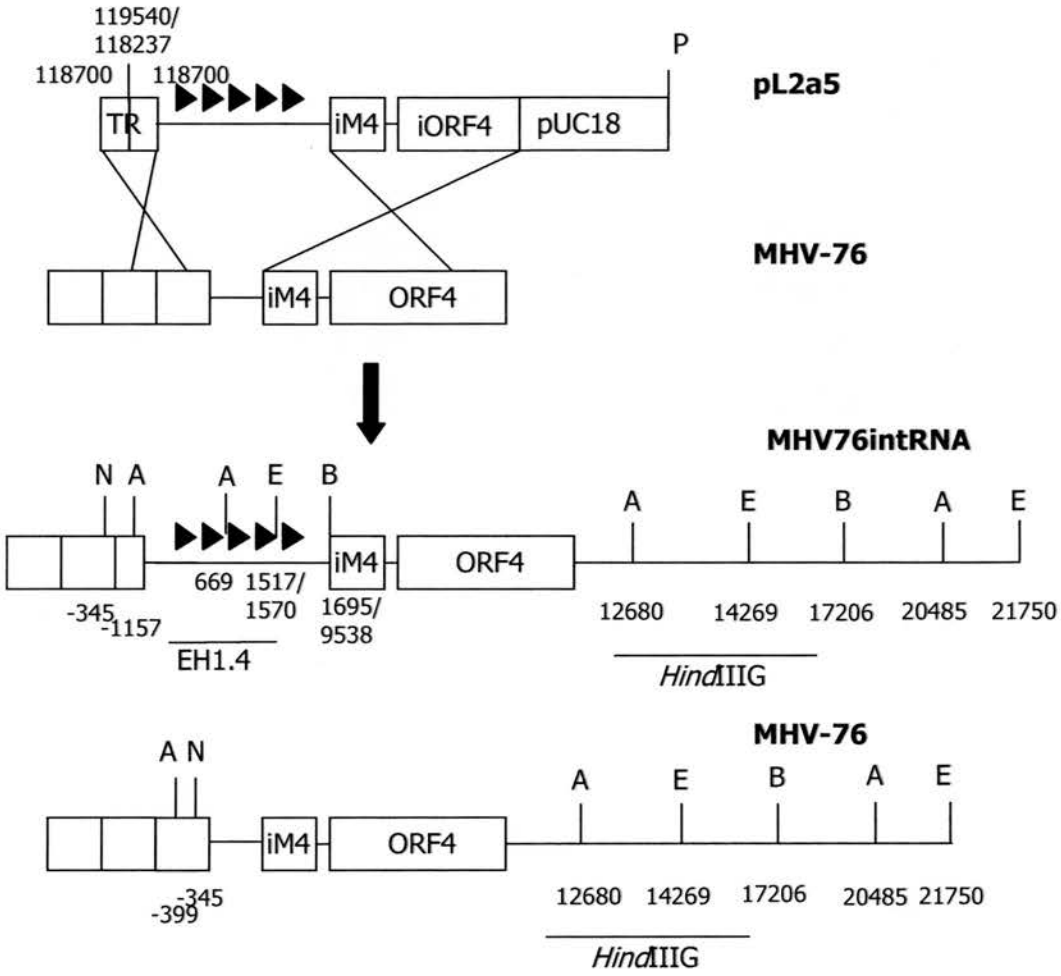

Figure 5.1 Schematic diagram demonstrating the construction of the intRNA viruses by homologous recombination between MHV-76 DNA and L2a5 plasmid. The L2a5 plasmid consists of vtRNA1-5 (shown as filled triangles), along with the *Psf*I fragment of the terminal repeats and partial M4 and ORF sequences. Approximately 24kb of the left-hand region of MHV-76 is shown, along with the restriction endonuclease cutting sites for *Bam*HI (B), *Eco*RI (E), *Psf*I (P), *Apa*I (A) and NotI (N). The location of the probes *Hind*IIIG and EH1.4, used for Southern analysis are indicated.

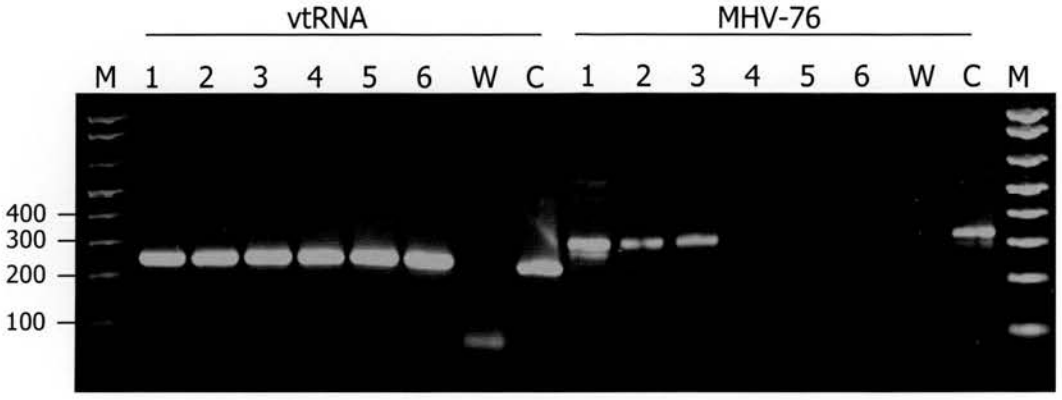

Figure 5.2 Screening plaque picks for intRNA1-5 and MHV-76. Single plaques were picked following transfection (1) or successive rounds of serial dilution plaque purifications (2-6). PCR analysis was carried out on the extracted DNA using primers which amplify the vtRNAs or wild-type MHV-76. Gel electrophoresis of the PCR products was carried out through a 1% TAE-agarose gel. The size of molecular weight marker in bp is shown on the left. Abbreviations; M, 1Kb-plus markers; W, negative control (ddH_2O); C, positive control.

that of MHV-76. This was initially attempted using the L1a5 plasmid, from which L2a5 was derived and hence contains the 1.2kb *Pst*I fragment of the terminal repeats and 1.4 kb of sequence homologous to the left-hand end of MHV-76. The MHV-76 fragment was removed from the plasmid by digestion with *Hind*III and *Eco*RI, and gel purified. BHK-21 cells were co-transfected by electroporation with the DNA fragment and intRNA(9) DNA, and single plaques isolated. The DNA was extracted and PCR carried out using the M4B/TR primer pair to detect wild-type MHV-76. However, this procedure was repeated three times with 64 plaques screened each time and all found to be negative for MHV-76. In order to control for the presence of viral DNA, PCRs were also carried out for both DNA polymerase and the vtRNAs, which were all positive (data not shown).

It was possible that the MHV-76 PCR reaction was not sensitive enough to detect any revertant DNA within a mixed population of intRNA(9) virus and revertant virus. An alternative approach was therefore taken, by utilizing a multiplex PCR, using both the DNA polymerase primers along with EH14E and EH14F primers, which amplify a region containing the vtRNAs (see appendix 2) within the same reaction to generate two distinct products of 477bp and 351bp respectively. This would show the relative abundance of viral DNA present containing the vtRNAs and therefore indicate whether revertant virus was present within a plaque. The assay was optimized so that the vtRNA and DNA polymerase products were amplified with equal efficiency within the same reaction, using intRNA(9) DNA as a control. In order to detect the relative abundance of the two DNA sequences, it was necessary that the reaction did not reach saturation and therefore a limited number of cycles were performed. However, using this approach, all plaques contained an equal amount of both DNA polymerase and vtRNA DNA, indicating that no revertant virus was present (data not shown).

Due to the fact that no positive plaques could be detected using L1a5 co-transfection, a cosmid was used instead. Cosmid M1 (cM1) is a previously published cosmid corresponding to nt115165-26842 of MHV-76 encompassing part of ORF75a, M12, 13 and 14 from the right hand end of MHV-76, a full terminal repeat and ORFs 4-11,

K3, M5 and the first 288bp of M6 from the left-hand end (Macrae *et al*, 2001). Co-transfection of cM1 with intRNA(9) DNA into BHK-21 resulted in the formation of 12 plaques positive for revertant virus when screened by PCR for MHV-76 and using the multiplex approach as described above.

After two rounds of plaque purification using an agarose over lay and 4 rounds using a limiting dilution approach, one transfection clone (48) was found to be free from contaminating intRNA(9). To ensure that a homogenous viral stock was present that was free from any small amounts of intRNA(9) virus that was below the level of detection of the PCR assay, a further three rounds of limiting dilution plaque purification were carried out. The resulting virus will be referred at as intRNA(9)Rev.

5.4 Southern analysis of the intRNA and intRNARev viruses

Viral DNA was extracted from MHV-76, both intRNA viruses and intRNA(9)Rev grown within BHK-21 cells as described in section 2.2.3. Southern analysis was performed on the viral DNA to determine whether the fragments had inserted correctly into the genome and to ensure that the revertant virus was identical to MHV-76. Restriction endonuclease digestions were carried out using either *Bam*HI or *Eco*RI and *Not*I. An additional Southern analysis was carried out following construction of intRNA(2) by digestion with *Bam*HI and *Apa*I. The cut sites for these enzymes are shown in figure 5.1 and the size of expected fragments in table 5.1. In order to check whether the vtRNAs had been correctly inserted into the left-hand end of MHV-76, hybridization was carried out using the *Eco*RI/*Hin*dIII digested fragment of pEH1.4 (Bowden *et al*, 1997), which detects the vtRNAs1-4. Hybridization to *Eco*RI/*Not*I digested DNA revealed a major band of 2.2kb, along with a fainter, minor band of 1.87kb (figure 5.3). Sequence analysis revealed that the 5' end of the genomes of the intRNA viruses contained the 463bp sequence corresponding to nt118237-118700 (depicted in figure 5.1), as a result of homologous recombination of MHV-76 DNA with the L2a5 recombination cassette, which contains the *Pst*I fragment of the terminal repeats. During viral replication, an oligoclonal population of viral DNA is produced containing variable numbers of

terminal repeat sequences. Hence the 2.2kb band corresponds to the size of the expected band following digestion with *Not*I within the terminal repeats, whereas the smaller 1.86kb band corresponds to linearised DNA containing only a single 463 nucleotide fragment of terminal repeat sequence. In keeping with this, digestion with *Bam*HI, which cuts at 1695 and therefore downstream of the vtRNAs (figure 5.1) but does not cut within the terminal repeat region, yielded a fragment of 2.1kb in length corresponding to the linearised viral DNA containing 463 nucleotides of terminal repeat sequence. The bands of 3.3kb and above correspond to linearised viral DNA with successive numbers of terminal repeats present. There appear to be minor differences in the *Bam*HI digestion pattern between the two intRNA viruses indicating that there may be small abnormalities in the terminal repeats of intRNA(2) (figure 5.4). However, Southern blotting carried out on *Apa*I digested DNA yielded bands of the correct size, once again indicating correct insertion of the vtRNAs into both recombinant virus clones.

In order to determine whether the vtRNAs had inserted correctly into the genome with respect to upstream sequences, hybridization was also carried out with a labelled fragment of MHV-68 (*Hind*IIIG fragment, nt 11099-16237), firstly on *Eco*RI/*Not*I and *Bam*HI digested DNA (figure 5.3) and then following the construction of intRNA(2), on *Apa*I and *Bam*HI digested DNA (figure 5.4). This resulted in fragments of the correct size as predicted by sequence analysis, verifying that the vtRNAs had inserted correctly into the left-hand region of MHV-76.

Southern analysis carried out on the revertant virus digested with *Bam*HI, *Not*I/*Eco*RI or *Apa*I yielded bands of the expected size based upon sequence analysis (table 5.1, figure 5.3, figure 5.4), which were identical to those seen following Southern analysis on MHV-76. Extra bands were present following *Eco*RI/*Not*I digestion (figure 5.3), although these most likely resulted from undigested DNA and not due to changes in the genome structure as further Southern analysis on the revertant virus yielded a band of the correct size (figure 5.4). In addition, no hybridization could be seen using the probe specific for the vtRNAs, indicating they

Digest	MHV-76	MHV-76intRNA	intRNArev
NotI/EcoRI	5.1, 4.85	2.2, 1.87* 7.5, 4.9	11.37
BamHI	8.9 +1.2 ladder.	2.1,+1.2 ladder, 7.7	8.9 +1.2 ladder.
ApaI	7.8, 3.5	0.984, 0.964, 7.8, 3.2	3.5, 7.8Kb

Table 5.1 The fragment sizes (in Kb) produced following restriction endonuclease digest of viral DNA. Those indicated in red correspond to fragments detected with the *Hind*IIIG probe, whereas those in red are detected using EH1.4. * denoted a minor band due to the presence of a small number of viral genomes possessing only a partial terminal repeat sequence (see text).

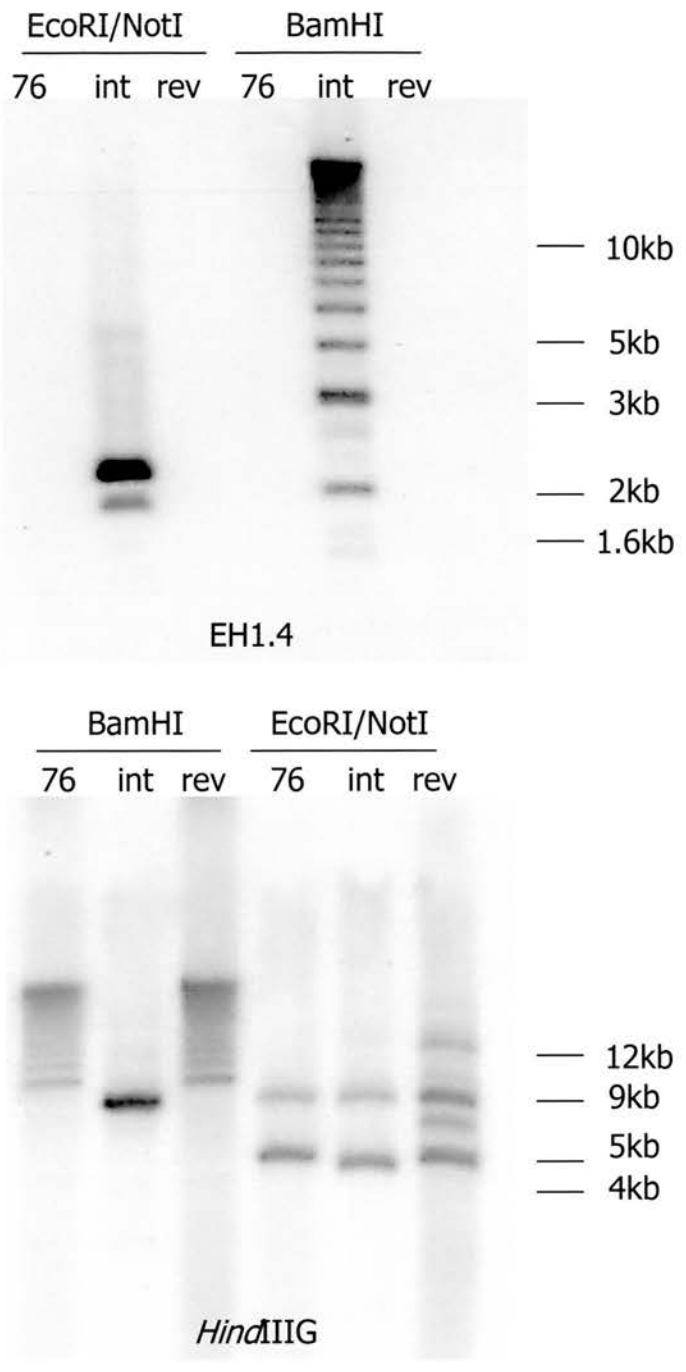

Figure 5.3 Southern analysis of mutant viruses. DNA from MHV-76 (76), intRNA9 (int) and intRNA9rev (Rev) was digested with either *Bam*HI or *Not*I and *Eco*RI. Hybridization was carried out using probes specific for either vtRNAs1-4 (EH1.4, nt 106-1517) or a probe generated from the *Hind*IIIG fragment of the MHV-68 genome (nt 11099-16237). Probes used are indicated below the appropriate autogradiograph. The sizes of the molecular weight markers are shown to the right of the autoradiographs.

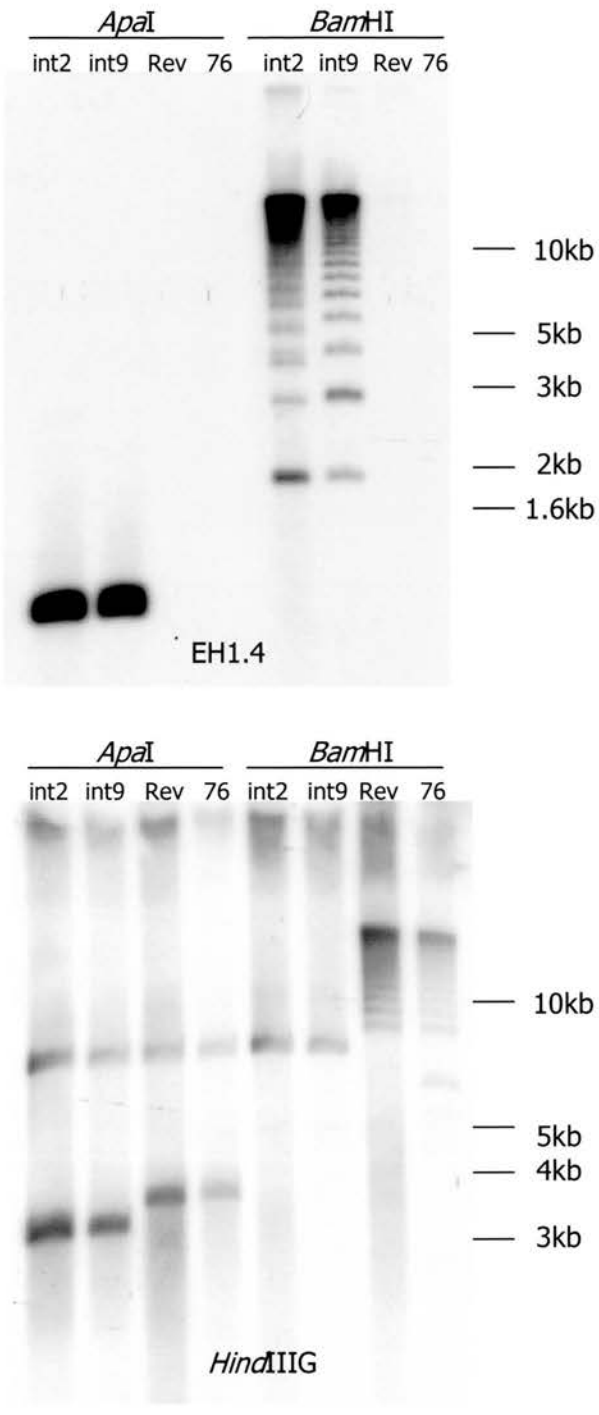

Figure 5.4 Southern analysis of mutant viruses. DNA from MHV-76 (76), intRNA(2), intRNA(9) and intRNA(9)Rev was digested with either *Bam*HI or *Apa*I. Hybridization was carried out using probes specific for either vtRNAs1-4 (EH1.4, nt 106-1517) or a probe generated from the *Hind*IIIG fragment of the MHV-68 genome (nt 11099-16237). Probes used are indicated below the appropriate autogradiograph. The sizes of the molecular weight markers are shown to the right of the autoradiographs.

had been successfully removed from the revertant virus and it had been fully purified so that no contaminating intRNA(9) virus was present in the stock.

5.5 Construction of WTTintRNA

5.5.1 Cloning strategy

Due to the presence of a small population of viral DNA molecules which possessed only half a terminal repeat at the 5' end of the genome, the production of further mutant viruses which would have wild-type terminal repeats (designated WTTintRNA) was attempted. The recombination cassette used for the generation of WTTintRNA was produced using a previously constructed plasmid, pBS-76LHE, which is composed of a 3kb fragment of MHV-76 (nt 9539-12569) cloned into the BamHI/EcoRI sites of pBS. vtRNAs1-5 were amplified from the MHV-68 genome with PfuTurbo DNA polymerase (Stratagene, UK) using the tRNAforNotI and tRNArev primers, which yielded a PCR product of 1.7kb containing vtRNAs1-5. The primers used generated upstream *Bam*HI and downstream *Not*I restriction sites to allow directional cloning. Following gel purification and digestion with the appropriate restriction endonucleases, the insert was directionally cloned into pBS-76LHE. Correct insertion of the vtRNAs was confirmed by restriction digest.

For creation of WTTintRNA, pBS-76LHE/vtRNA1-5 was partially digested with *Eco*R1/*Not*I to yield a 4.7kb band containing the vtRNAs and downstream 3kb fragment homologous to MHV-76. This was performed to prevent undesirable recombination events that may incorporate plasmid DNA into MHV-76 during the formation of WTTintRNA. BHK-21 cells were co-transfected with the excised DNA and MHV-76 DNA and single plaques isolated from wells of a 96 well microtitre plate. PCR analysis was carried out on the viral DNA and 5 plaques (designated 1-5) were found to be positive for the vtRNAs.

5.5.2 Purification of recombinant viruses

Purification of WTTintRNA was attempted for all five viral stocks using the limiting dilution approach. After one round of purification, clones 1-3 were still positive for

the vtRNAs by PCR. After two rounds, only clones 1 and 3 contained the vtRNAs. After four rounds of purification, the presence of the vtRNAs could not be detected by PCR within any of the plaque picks. To ensure that viral DNA was present, PCR was also undertaken for MHV-76 and all plaques were found to be positive. Hence it appeared that the WTTintRNA virus could not be maintained, perhaps because the insert sequence was not stable and further recombination events had taken place to revert the virus back to parental MHV-76, or because they were attenuated for *in vitro* growth. Hence it was decided that the WTTintRNA viruses could not be produced in this study.

5.6. Construction of intRNA5 viruses

In addition, mutant viruses were also constructed by insertion of vtRNA5 into the left-hand end of MHV-76 in order to establish whether a single vtRNA plays a role within infection. The recombination cassette had been previously generated by Ben Addams, and consisted of a DNA fragment from MHV-68 (nt1477-1695) inserted between the terminal repeat and residual M4/ORF4 fragments of pL1a5. Co-transfection with MHV-76 DNA was also carried out by Ben Addams and five plaques were found to be positive for vtRNA5. However, after six rounds of limiting dilution plaque purification and two agarose over-lays, although a number of plaques were positive for vtRNA5, all plaques were also positive for MHV-76 (figure 5.5). As the mutant virus could not be purified away from MHV-76 it was decided that it could not be used to determine the role of vtRNA5 within infection.

5.7 Characterisation of MHV-76 insertion viruses *in vitro*

5.7.1 vtRNA expression

As vtRNA knock-in recombinant MHV-76 viruses could not be produced that possessed wild-type terminal repeat sequences, it was decided that the original intRNA viruses would be used to characterize the role of the vtRNAs within infection. In order to ensure that all five vtRNAs were expressed from the intRNA1-5 viruses, C127 cells were infected at an MOI of 5 pfu/cell for 18 hours and the RNA extracted. RT-PCR analysis was carried out using primers specific for all five

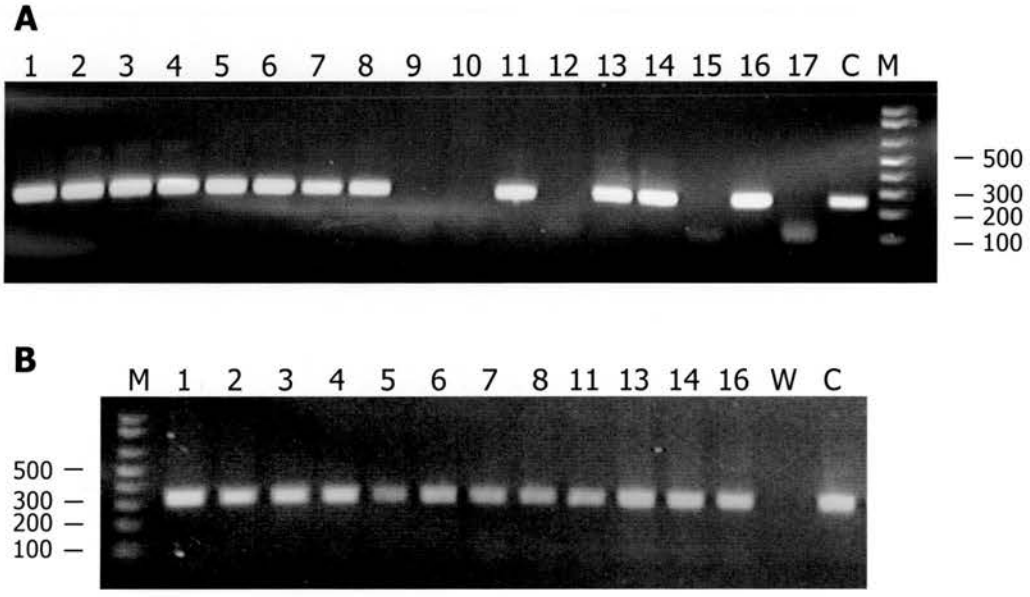

Figure 5.5 Screening plaque picks for intRNA5. Single viral plaques were harvested following transfection. Following six rounds of serial dilution plaque purification along with two rounds of single plaque selection using an agarose overlay, single plaque isolates were analysed for the presence of the vtRNA5 (A) and all vtRNA5 positive plaques for MHV-76 (B). Single plaque isolates are denoted numerically (1-17). In addition both negative control (ddH_2O, W) and positive control (C) PCR reactions were carried out. PCR products were analysed on a 1% TAE-agarose gel. The sizes of molecular weight markers (M) in bp are shown.

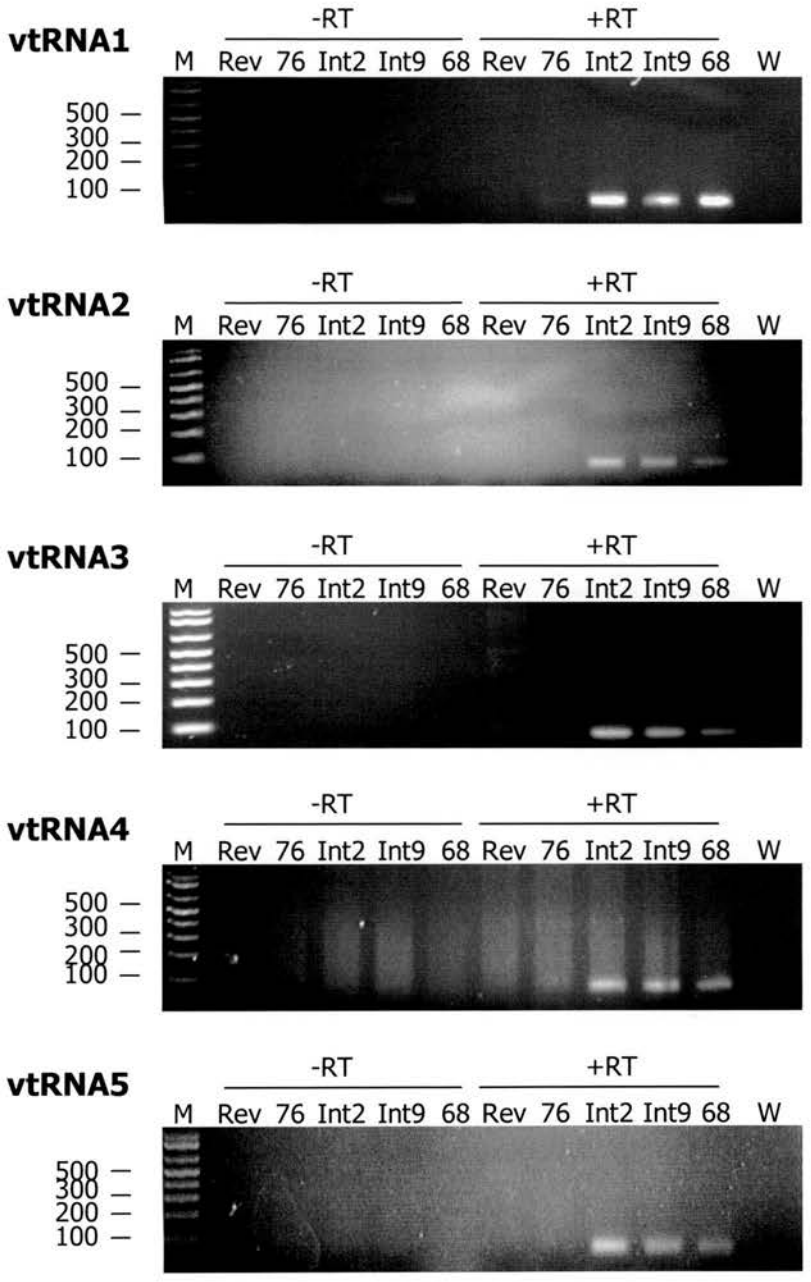

Figure 5.6 The expression of the vtRNAs1-5 from MHV-68, MHV-76, intRNA(2), intRNA(9) and intRNA(9)Rev. RNA was extracted from C127 cells were infected at an MOI of 5 pfu/cell for 18 hours. RNA was DNAase treated and RT-PCR carried out for the vtRNAs1-5 (+RT). Control reactions in the absence of reverse transcriptase (-RT) were also carried out, along with negative control PCR reactions (ddH_2O, W). PCR products were analysed on 3% TAE-agarose gels. The sizes of molecular weight markers (M) in bp are shown.

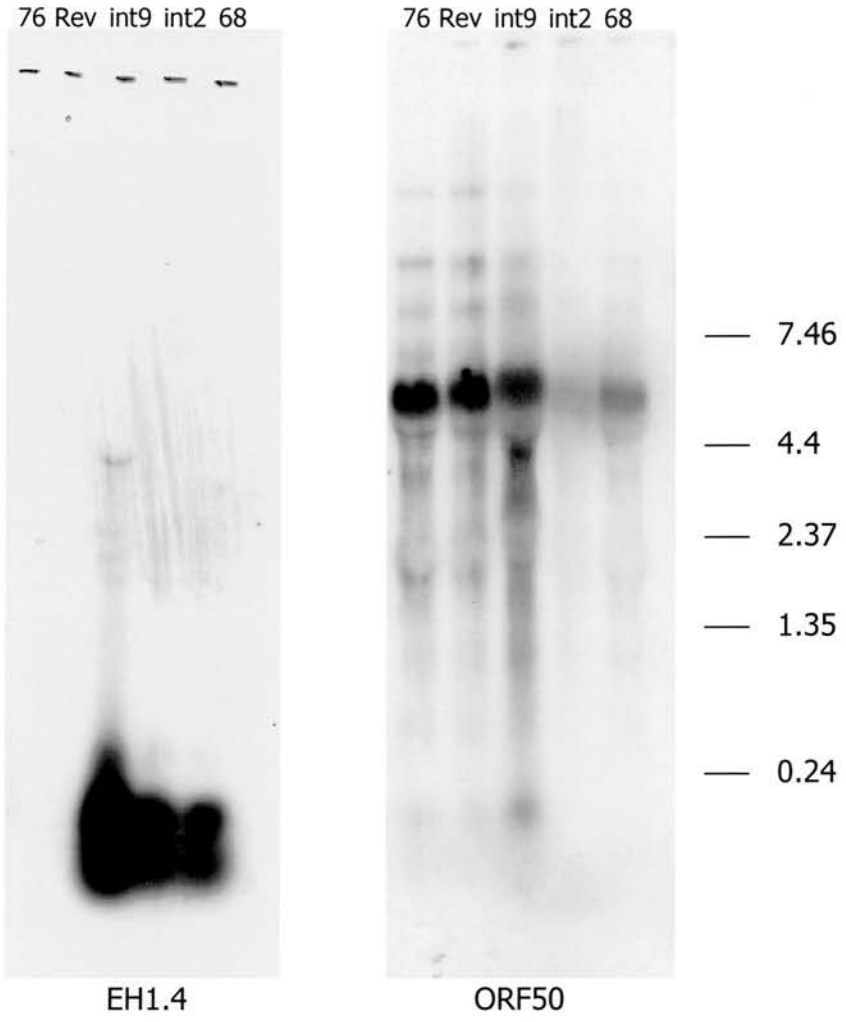

Figure 5.7 Northern analysis of vtRNA1-4 transcription by MHV-76, MHV-68, intRNA(9), intRNA(2) and intRNA(9)Rev. RNA was extracted from C127 cells infected at an MOI of 5 pfu/cell for 18 hours. Hybridization was carried out using a probe specific for vtRNAs1-4 (EH1.4, nt 106-1517) or a probe spanning the ORF50 region (nt68483-68838). The sizes of the molecular weight markers, in Kb are shown to the right of the autoradiographs.

vtRNAs, which were all found to be expressed (figure 5.6). The level of expression was also verified and compared to that of MHV-68 by northern blot analysis (figure 5.7). Hybridization was carried out using a probe specific to vtRNAs1-4 (EH1.4), along with an ORF50 probe, which was used to control for the amount of RNA present. Hybridization with the probe specific for the vtRNAs yielded bands of the correct size (less than 240nt in length). Although there appeared to be greater expression of the vtRNAs from intRNA(9), once this is normalised to the amount of RNA present, as indicated by hybridization of the ORF50 probes, it was clear that the approximate level of expression for the intRNA viruses was comparable to that of MHV-68. As expected, no vtRNA expression could be detected within MHV-76 and intRNA(9)Rev infected cells.

5.7.2 Growth characteristics

In order to assess the growth kinetics of the vtRNA1-5 expressing viruses in comparison to MHV-76 and MHV-68, both single step and multistep growth analysis were carried out. Single step growth curves were carried out within BHK-21 cells, to assess a single replication cycle. Cells were infected at an MOI of 5pfu/cell and duplicate samples taken at time points from 0h to 72h p.i. Samples were titrated on BHK-21 cells and the final viral titre at each time point was calculated. It was apparent that both the recombinant viruses, along with the revertant virus, replicated with identical kinetics to MHV-76 and MHV-68 (figure 5.8). Multistep growth curve analysis was also carried out within BHK-21 cells, by infection at an MOI of 0.05, and duplicate samples taken at time points from 0h to 144h p.i. The resulting growth curve can be seen in figure 5.9. The data indicate that the recombinant viruses replicate with identical kinetics to wild-type viruses and therefore the expression of the vtRNAs within MHV-76 has no effect upon the cell-to-cell spread of the virus. In addition, this indicates that any abnormalities within the terminal repeats of intRNA(2), as detected by Southern blotting (figure 5.4), had no deleterious effect on the ability of the virus to replicate *in vitro*.

Due to the fact that BHK-21 cells are a hamster cell line, it is possible that any effect that the vtRNAs might have upon replication may not be effective within BHK-21

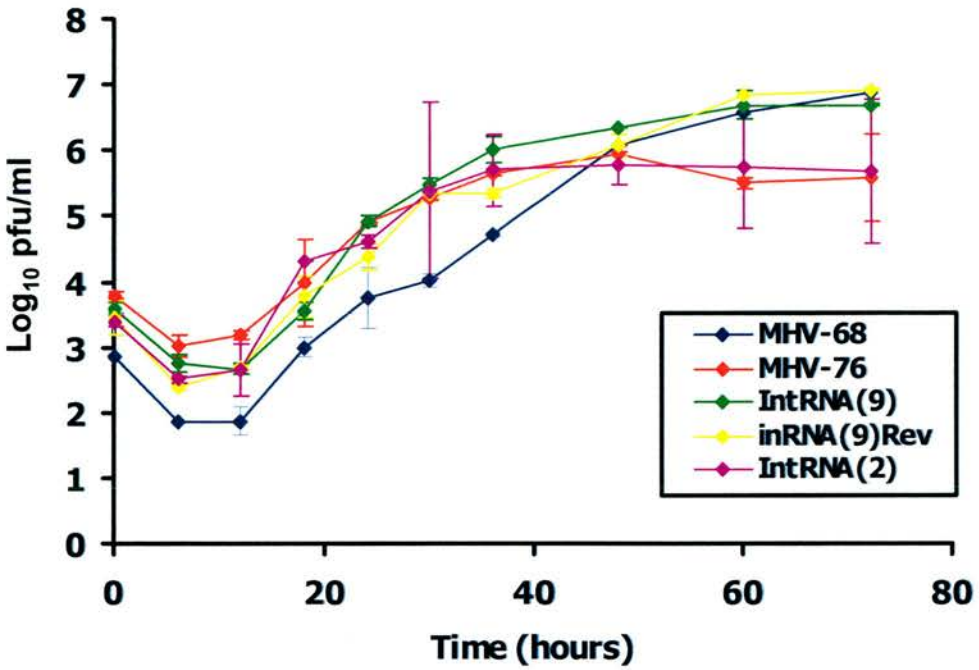

Figure 5.8 Single step replication of MHV-68, MHV-79, intRNA(9), intRNA(2) and intRNA(9)Rev in BHK-21 cells in vitro, using an MOI of 5 pfu/cell. Values represent two independent experiments, with each sample titrated in duplicate. Data points represent the virus titre $\log_{10}$ ± standard deviation. The time in hours represents the time post-infection.

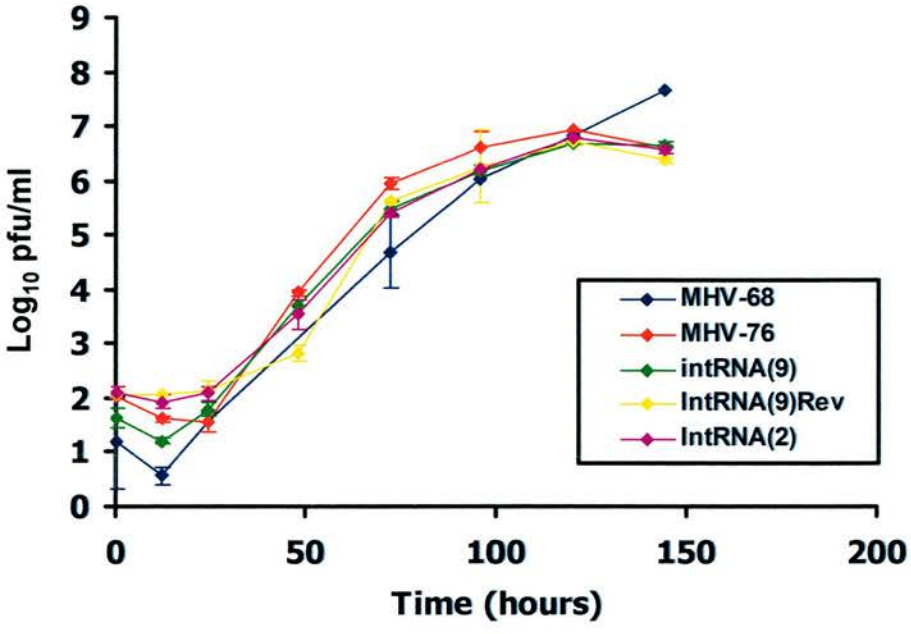

Figure 5.9 Multi-step replication of MHV-68, MHV-79, intRNA(9), intRNA(2) and intRNA(9)Rev in BHK-21 cells in vitro, using an MOI of 0.05 pfu/cell. Values represent two independent experiments, with each sample titrated in duplicate. Data points represent the virus titre $\log_{10}$ ± standard deviation. The time in hours represents the time post-infection.

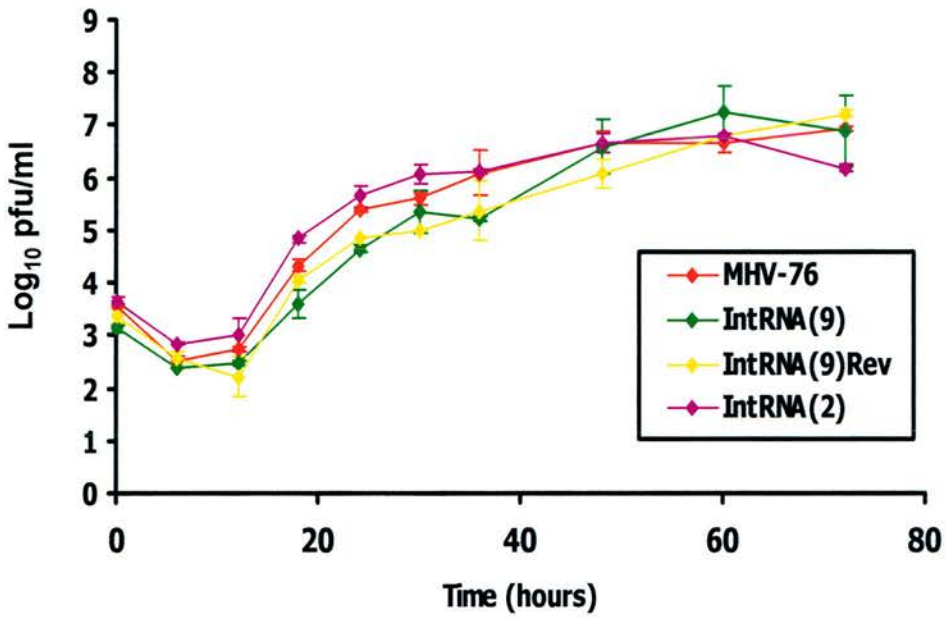

Figure 5.10 Single step replication of MHV-68, MHV-79, intRNA(9), intRNA(2) and intRNA(9)Rev in L929 cells in vitro, using an MOI of 5 pfu/cell. Values represent two independent experiments, with each sample titrated in duplicate. Data points represent the virus titre $\log_{10}$ ± standard deviation. The time in hours represents the time post-infection.

cells. Therefore, a single-step growth curve was also carried out with the mouse L929 fibroblast cell line. Samples were once again taken in duplicate and titrated on BHK-21 cells. As figure 5.10 shows, expression of the vtRNAs within MHV-76 did not affect the replication kinetics of the virus within L929 cells.

5.8 Characterisation of MHV-76 insertion viruses *in vivo*

5.8.1 Lytic replication in the lung

In order to investigate the contribution of the vtRNAs to the pathogenesis of MHV-68, 200 3-4 week old female BALB/c mice were infected intranasally with $4x10^5$ pfu of either MHV-68, MHV-76, intRNA(2), intRNA(9) and intRNA(9)Rev, with four mice infected with each virus per time point. Lungs were harvested at 2, 4, 6, 8 and 10 days p.i. and assessed for productive infection as by plaque assay described in section 2.9.9. All titrations were performed in duplicate. At 2 days p.i. there was a significant increase in the level of the mutant viruses compared to MHV-76 ($p<0.05$, Mann Whitney test) (figure 5.11). However, there was no difference between the levels of either intRNA(2) or intRNA(9) compared to the revertant virus. At such an early time point it is likely that levels of productive infection within the lung is particularly sensitive to small variations in the viral inoculum. By four days post-infection there is no significant difference between any of the viruses ($p>0.05$, Mann Whitney test). However, by 6 days p.i. there is significantly less productive infection within mice infected with MHV-76 compared to MHV-68, which is in agreement with previous findings (Macrae *et al*, 2001). At this time-point there is no difference between the two intRNA viruses and the revertant compared to MHV-76. At 8 days p.i. productive infection can only be detected with 2/4 mice infected with MHV-68, but not in any other the other mice.

5.8.2 Acute latency within the spleen

Acute latency is this period following infection with MHV-68 up to day 40 when there is a rapid increase in the number of latently infected splenocytes. At this time a variety of genes are expressed which are not detected during long term latent

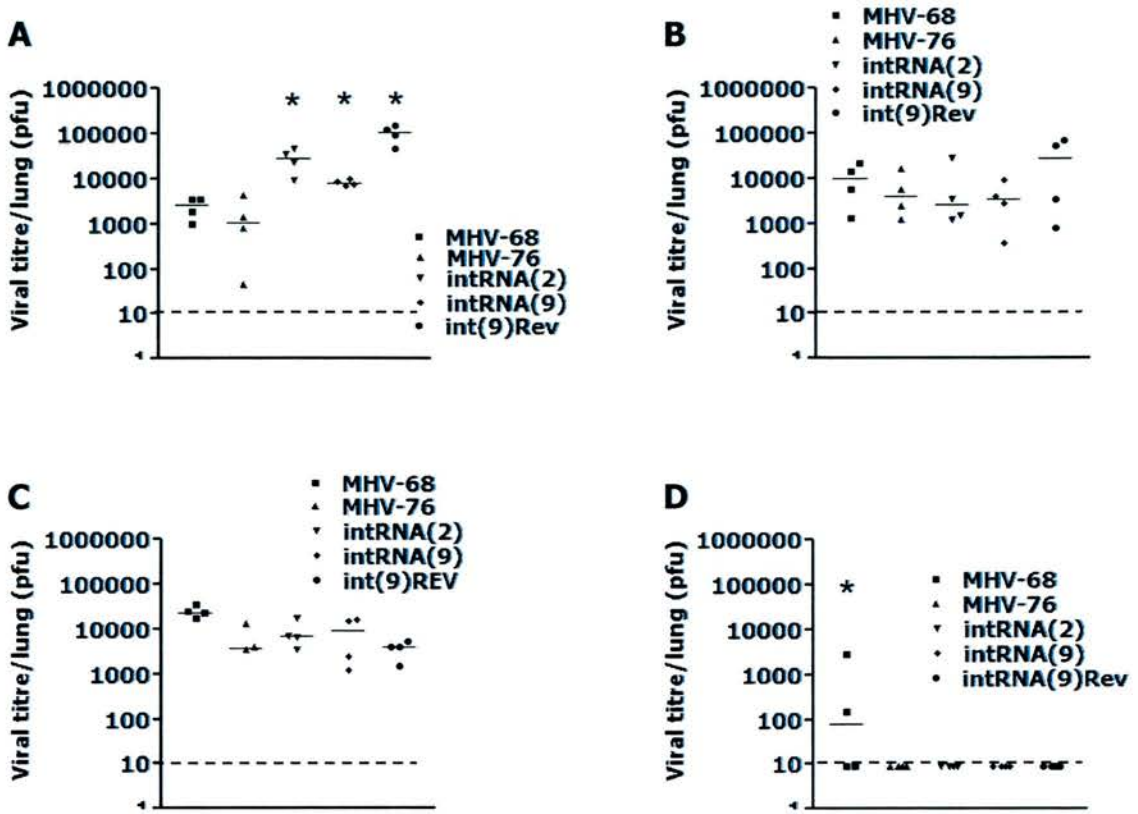

Figure 5.11 Viral titres in the lungs of BALB/c mice infected intranasally with 4 x 10^5 pfu of either MHV-68, MHV-76, intRNA(2), intRNA(9) or intRNA(9)Rev. Lungs were harvested at day 2 (A), day 4 (B), day 6 (C) and day 8 (D) post-infection. Data shown are compiled from one experiment using four mice per time point, with each titration carried out in duplicate. Each data points represents the viral titres from individual mice, with the mean viral titres displayed as a solid line. The dashed line represents the limit of detection of the assay (10pfu). Viruses which have mean viral titres that vary significantly ($p \leq 0.05$ in a Mann Whitney test) are indicated by *.

infection (see section 1.3.5). The viral load following intra-nasal infection during this period was measured by *ex vivo* reactivation (infective centre) assay, real-time PCR and *in situ* hybridization for the vtRNAs. In addition, the extent of splenomegaly was assessed by measurement of whole spleen weight.

The results of the *ex vivo* reactivation assay are shown in figure 5.12. In mice infected with MHV-68, infective centres could be detected from day 7 onwards, with a peak of latency, reaching 1500 infective centres/10^7 splenocytes between days 10 and 14 p.i. In contrast, mice infected with MHV-76 showed a markedly reduced level of infective centres, at least 10 fold less than MHV-68 during the peak of latency at day 10. This is in agreement with previous findings (Macrae *et al*, 2001). Furthermore, latency levels appeared to decrease from day 10 onwards. Both of the intRNA viruses and the revertant showed infective centre levels that were not significantly different to those seen with MHV-76 at all time points ($p>0.05$, Mann Whitney test).

Ex vivo reactivation takes into account both the level of latent load within the spleen and the ability of the virus to reactivate from latency. In order to measure the viral latent load in isolation, real-time PCR analysis was carried out on DNA extracted from splenocytes. The levels of viral DNA were measured by amplification of ORF50, and normalised to the levels of cellular DNA present as determined by amplification using primers specific for β-actin. Latent load was measured at day 14 pi. As figure 5.13 shows, there is significantly higher latent viral load within mice infected with MHV-68 than MHV-76 and both recombinant viruses. There was no significant difference between the latent loads of the recombinant viruses compared with either MHV-76 or intRNA(9)Rev. Therefore both recombinant viruses were able to establish and reactive from latency in a manner indistinguishable from the parental wild type virus.

In situ hybridization was also carried out to further clarify the results of the real-time assay in determining that the intRNA viruses establish latency at much lower levels than MHV-68. In addition, the vtRNAs are used to visualise latent infection with

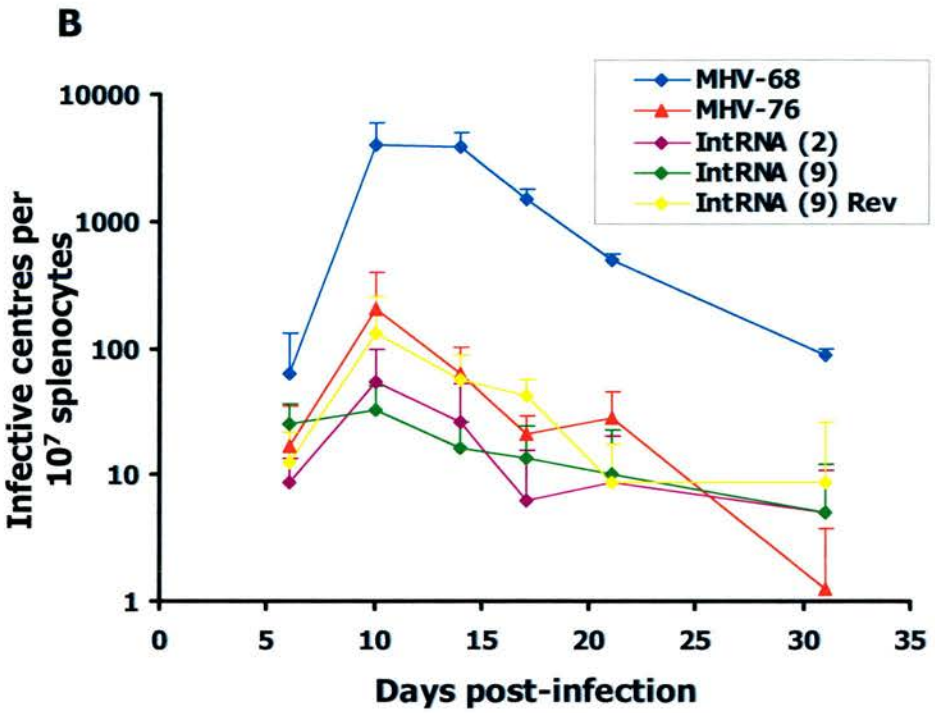

Figure 5.12 Latent virus in the spleens of BALB/c mice infected intranasally with 4 x 10^5 pfu of either MHV-68, MHV-76, intRNA(2), intRNA(9) or intRNA(9)Rev, as determined by ex vivo reactivation assay (infective centre assay). Data points represent the mean number of infective centres per 1 x 10^7 splenocytes for four mice ± the standard deviation.

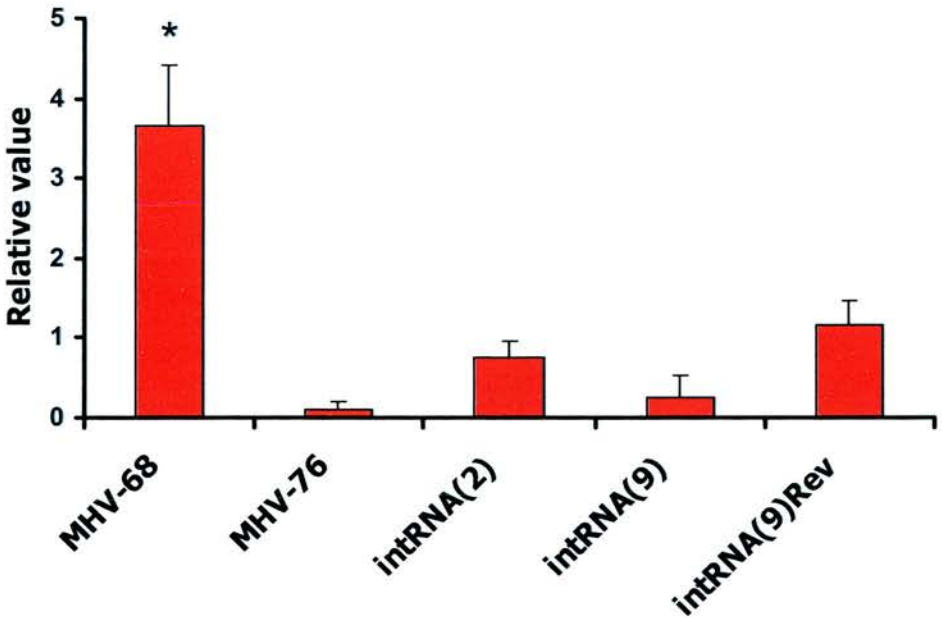

Figure 5.13 Determination of the viral latent load in splenocytes of BALB/c mice infected intranasally with 4 x 10^5 pfu of either MHV-68, MHV-76, intRNA(2), intRNA(9) or intRNA(9)Rev. Total DNA was extracted from splenocytes at 14 days post-infection and quantitative PCR carried out using a Rotorgene (Corbett Research). The levels of viral DNA were quantified by amplification of a region of the ORF50 gene and normalized to the levels of cellular DNA as determined by the amplification of a region of the β-actin gene. The mean and standard deviation of four mice per group are shown. Viruses which have mean viral latent load that vary significantly ($p \leq 0.05$ in a Mann Whitney test) are indicated by *.

MHV-68. However, the absence of the vtRNAs from MHV-76 has meant that the behaviour of MHV-76 within the spleen has not been fully characterized. Hence in situ hybridization against the intRNA viruses will give an indication of how MHV-76 behaves. Sections were taken from spleens 14 days post-infected, and processed for in situ hybridization using EH1.4, which recognizes the vtRNAs1-4. Within MHV-68 infected mice, a high level of vtRNA expression could be detected within the splenic germinal centres (figure 5.14). However, in all four mice infected with either intRNA(9) or intRNA(2) no staining could be detected. There were two possible reasons for the lack of staining; firstly due to the expression of the vtRNAs within these mice being below the level of detection or secondly as a result of the genomes reverting back to that of the parental MHV-76 virus.

In order to determine whether the genomes of the intRNA viruses had reverted, PCR analysis were carried out on DNA extracted from spleens at 14 days post-infection. A portion of the vtRNA region of the genome was amplified using the tRNAfor2 and tRNArev primers, which indicated that DNA sequences encoding the vtRNAs were present within the spleens of mice infected with both intRNA viruses (figure 5.15). The apparent lower levels of vtRNA DNA in spleens infected with the intRNA viruses is most likely a result of the decreased viral load within these mice. vtRNA encoding DNA could not be detected within one mouse infected with intRNA(9), and it is not clear whether this is due to the lack of the vtRNAs or because the amount of DNA present is below the limit of detection of the assay. PCRs were also attempted for parental MHV-76 DNA within these mice, using the M4B/TR primer pair, however, this failed to amplify DNA sequences taken from MHV-76 infected mice and therefore could not be used to determine whether a proportion of the intRNA viruses had reverted back to wild-type. Unfortunately RNA was not extracted at the time of organ harvesting and therefore the presence of the vtRNAs within infected spleens could not be analysed.

Although it was apparent that the insertion of vtRNAs 1-5 into MHV-76 had no effect upon the ability of the virus to establish latency, it was still possible that they could play a role in the splenomegaly seen following infection with MHV-68.

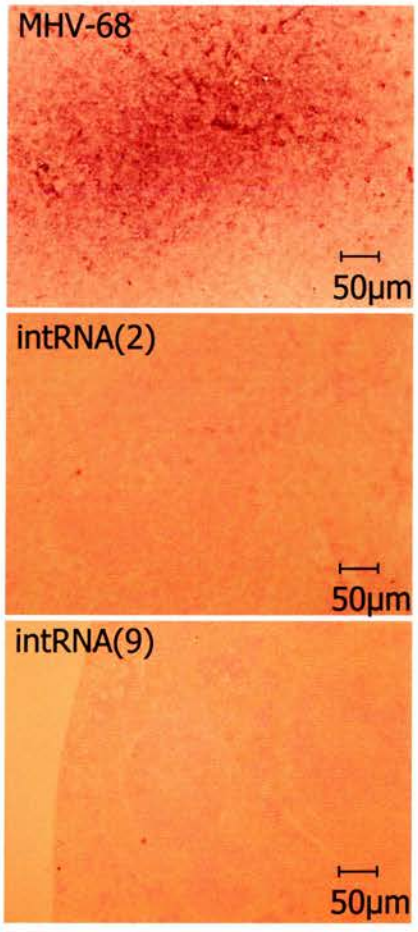

Figure 5.14 In situ hybridization to detect the vtRNAs during latent infection. BALB/c mice were infected intranasally with 4 x 10^5 PFU of either MHV-68, intRNA(2) or intRNA(9). Spleens were removed at 14 days p.i. and fixed in paraformaldehyde prior to wax embedding and sectioning. Hybridization was carried out using a probe specific for the vtRNAs1-4 (EH1.4, nt 106-1517). Sections were counter-stained with nuclear fast red and viewed using a an Olympus BX51 microscope.

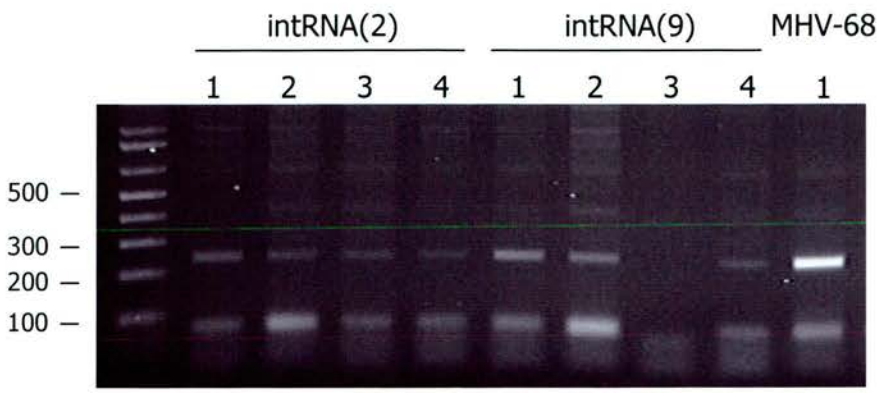

Figure 5.15 PCR on DNA extracted from spleens of BALB/c mice infected intranasally with 4 x 10^5 pfu of either intRNA(2), intRNA(9) or MHV-68. Total DNA was extracted from splenocytes at 14 days post-infected and PCR carried out to detect the presence of the vtRNAs within the viral genomes, using the tRNAfor2 and tRNArev primers, which give a PCR product of 218bp. Each lane represents DNA extracted from individual mice (numbered 1-4). PCR products were analysed on a 2% TAE-agarose gel. The sizes of molecular weight markers (M) in bp are shown.

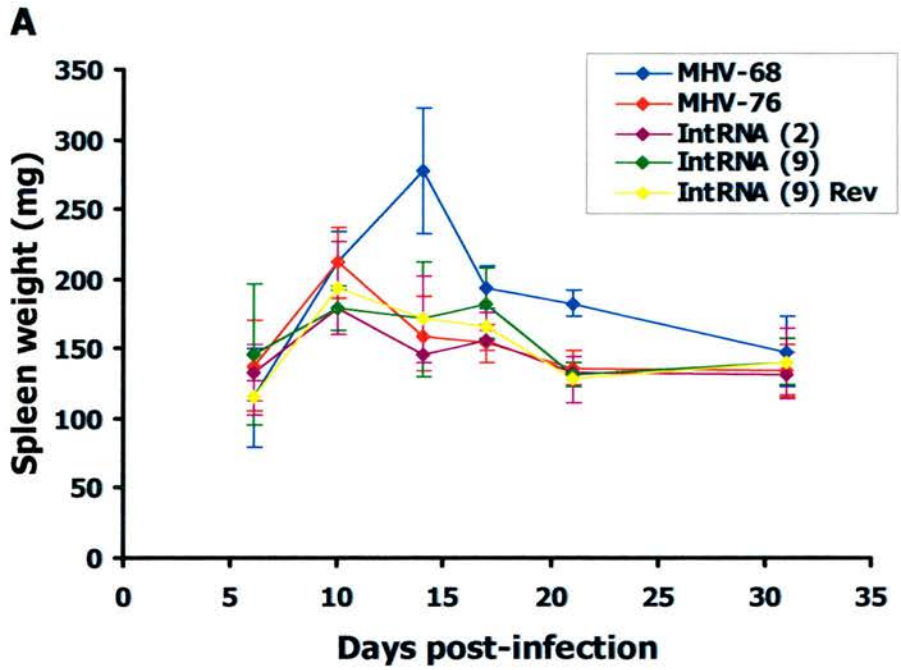

Figure 5.16 Whole spleen weights of BALB/c mice infected intranasally with 4 x 10^5 PFU of either MHV-68, MHV-76, intRNA(2), intRNA(9) or intRNA(9)Rev. Data points represent the mean spleen weight of four mice ± the standard deviation.

However, the degree of splenomegaly, as assessed by whole spleen weight, did not significant vary from MHV-76 for both intRNA viruses ($p>0.05$, Mann Whitney test). As expected, infection with MHV-68 did result in splenomegaly (figure 5.16).

5.8.3 Long term infection

During the maintenance of long-term latency with MHV-68, the gene expression pattern changes. Many genes expressed during the acute stage of latency, such as M3, M4, vGPCR and M11 are no longer expressed. At this stage, the vtRNAs are one of the few genes that are expressed and hence it is possible that they play a role in the maintenance of long term latency. Spleens were harvested at 77 days post-infection and assessed for the degree of splenomegaly, as measured by whole spleen weight, and the levels of latent virus by infective centre assay. 1/4 mice infected with intRNA(4) and 1/5 with intRNA(9) showed an increase in spleen weight to approximately three times the weight of the other spleens (figure 5.17). However, this was not accompanied by an increase in the levels of latent virus present within the spleens (figure 5.18).

In order to determine whether the vtRNAs do contribute to an increased splenomegaly during long term infection, 8 mice were infected with $4x10^5$ pfu of either MHV-68, MHV-76, intRNA(2), intRNA(9) and intRNA(9)Rev. The degree of splenomegaly was measured by whole spleen weight at 70 days and 120 days post-infection. In addition, the viral load was measured by infective centre assay at 120 days post-infection. At both time points, there was no significant increase in either splenomegaly in mice infected with any of the viruses ($p>0.05$, Mann Whitney test) (figure 5.19). It therefore appears that the insertion of the vtRNAs into the left-hand end of MHV-76 has no effect upon the ability of the virus to cause splenomegaly. At 120 days post-infection, no infective centres were detected within the spleens of any of the mice. It therefore appears that the levels of latent virus within the spleen are below the level of detection of this assay and whilst it does appear that insertion of the vtRNAs in to left-hand end of MHV-76 had no effect upon the levels of latent virus during long-term persistence, the fact that small differences might exist cannot be ruled out.

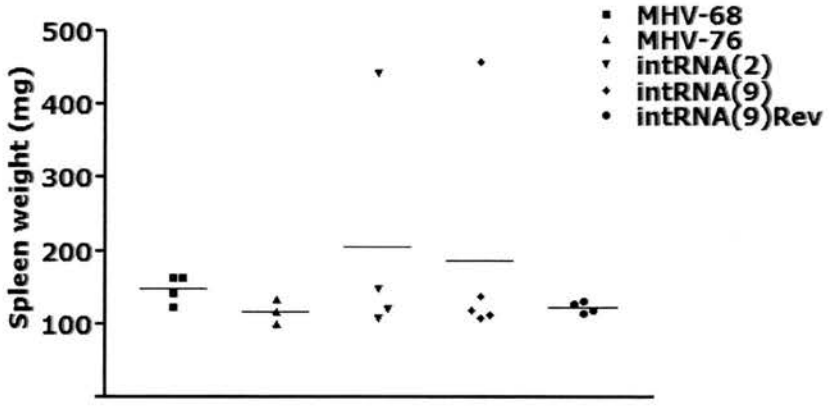

Figure 5.17 Long term experiment 1: Whole spleen weights of BALB/c mice infected intranasally with 4 x 10^5 pfu of either MHV-68, MHV-76, intRNA(2), intRNA(9) or intRNA(9)Rev, at 77 days post-infection. Data points represent the whole spleen weight from individual mice. The mean spleen weight per group is represented by a solid line.

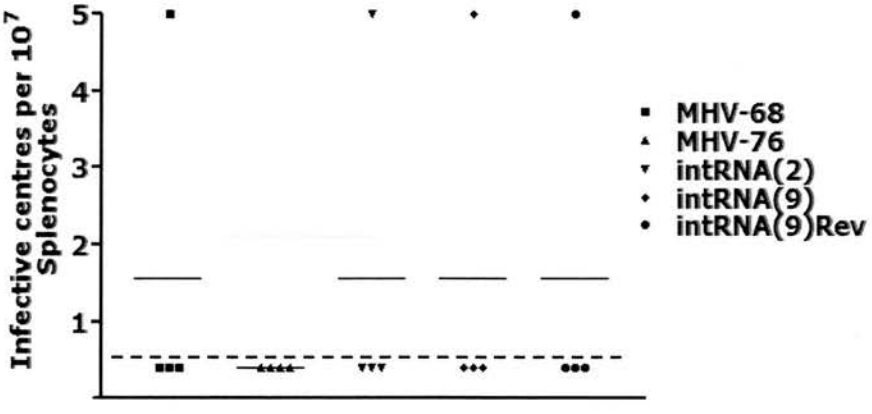

Figure 5.18 Long term experiment 1: Latent virus in the spleens of BALB/c mice infected intranasally with 4 x 10^5 pfu of either MHV-68, MHV-76, intRNA(2), intRNA(9) or intRNA(9)Rev, at 77 days post-infection as determined by infective centre assay. Data points represent the numbers of infective centres from individual mice. The number of infective centres per group is represented by a solid line.

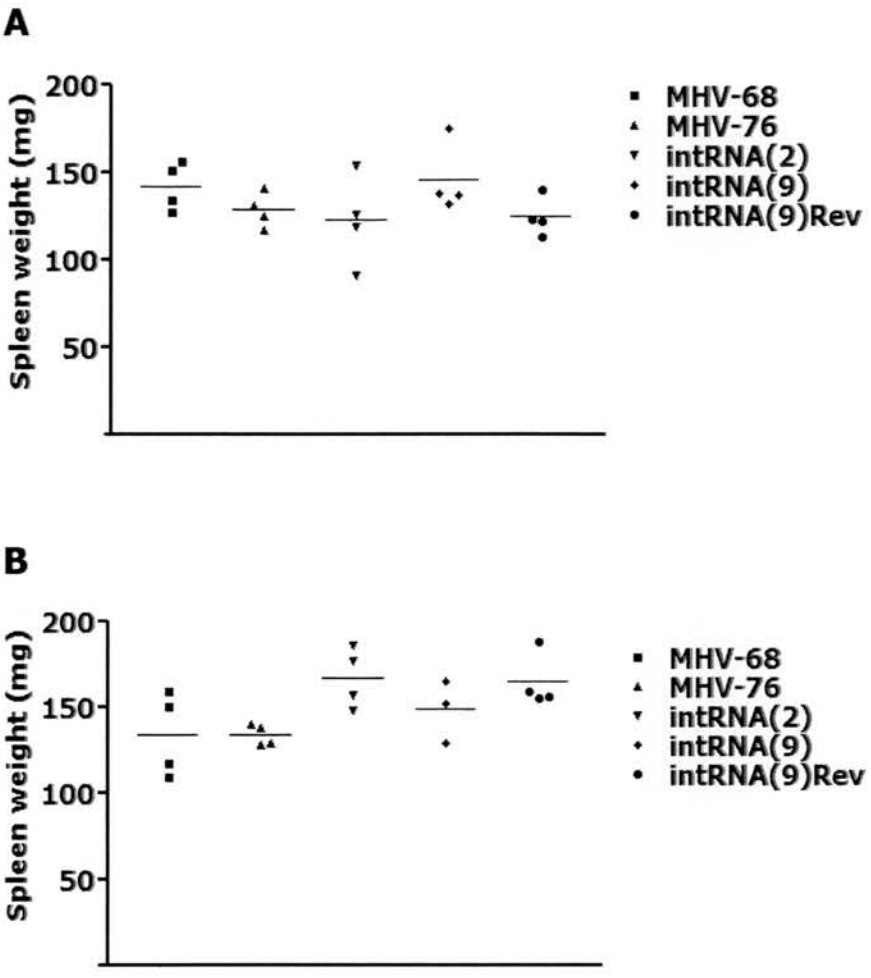

Figure 5.19 Long term experiment 2: Whole spleen weights of BALB/c mice infected intranasally with 4 x 10^5 pfu of either MHV-68, MHV-76, intRNA(2), intRNA(9) or intRNA(9)Rev, at 70 (A) and 120 (B) days post-infection. Data points represent the whole spleen weight from individual mice. The mean spleen weight per group is represented by a solid line.

5.9 Construction of a vtRNA expressing cell line

In order to investigate the function of the vtRNAs *in vitro* in the absence of any other viral gene expression, a cell line was constructed to stably express the vtRNA1-5. vtRNAs1-5 were amplified from the MHV-68 genome with PfuTurbo DNA polymerase (Stratagene, UK) using the tRNAforBamHI and tRNArev primers, which yielded a PCR product of 1.7kb containing vtRNAs1-5. The primers used generated upstream and downstream *Bam*HI restriction sites to allow cloning. Following gel purification and digestion with *Bam*HI, the insert was directionally cloned into pLXSN (see appendix 1 for plasmid map). Correct insertion of the vtRNAs was confirmed by restriction digest.

The resulting plasmid was transfected into the mouse epithelial C127 cell line, and cells containing the plasmid were selected for by addition of G418. Clonal cell populations were produced using a limiting dilution approach (see section 2.8.6). RNA was extracted from the clonal cell lines and the expression of the vtRNAs analysed by both PCR and Northern blotting. Although the expression of vtRNA1 could be detected in two clonal lines by PCR analysis, vtRNA expression could not be detected by Northern blotting (figure 5.20). Given that the expression level was so much lower than that following viral infection, it was decided that the cell lines could not be used to assay the function of the vtRNAs *in vitro*.

5.10 Discussion

The generation of mutant viruses by deletion of genes from MHV-68 has given insight into the function of a number of genes within viral pathogenesis, such as identifying a role for M11, ORF73 and K3 during the establishment of latency (de Lima *et al*, 2005; Fowler *et al*, 2003; Stevenson *et al*, 2002). In addition, the use of homologous recombination to insert genes into the left-hand end of MHV-76 has ascertained roles for two genes found within the left hand region of MHV-68 (Macrae *et al*, 2003; Townsley *et al*, 2004), along with characterizing genes from other gammaherpesviruses (Douglas *et al*, 2004). In this study, a similar approach was taken to try and establish a role for the vtRNAs within the pathogenesis of MHV-68, by insertion of vtRNAs1-5 into the left-hand end of MHV-76. The

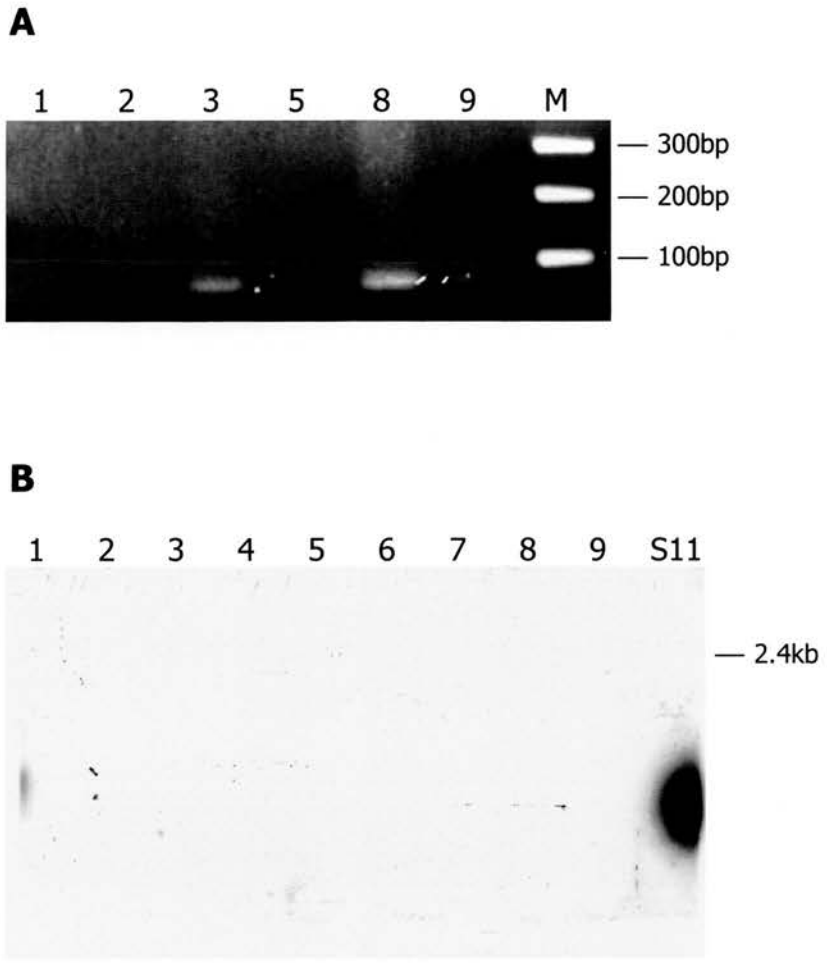

Figure 5.20 Expression of the vtRNAs from a stably transfected cell line. Clonal cell populations were produced by transfection of C127 cells with a plasmid containing the vtRNAs1-5 and the gentamycin resistance gene. Positive cells were selected for by growth in the presence of G418 and cloned from single cells. RNA was extracted from the different clonal lines and analyzed for the expression of the vtRNA by PCR for vtRNA 1 (A). The relative expression levels of the vtRNAs was analyzed by Northern blotting. Hybridization was carried out using a probe specific for vtRNAs 1-4 (EH1.4 nt 106-1517) (B).

vtRNAs were expressed from their natural promoters and no additional sequences were added to aid the purification of the viruses. Recombinant viruses have previously been purified by the insertion of selection markers, such as the LacZ or GFP under the control of foreign promoter elements (Clambey *et al*, 2000; Hoge *et al*, 2000) However, the insertion of such sequences, particularly into the left-hand end of the genome can result in an attenuation of the virus during latency. For example the insertion of LacZ under the expression of HCMV immediate early promoter and enhancer into the M1 locus results in a decreased ability of the virus to establish latency *in vivo* (Clambey *et al*, 2000). In addition, the insertion of GFP into the left-hand end of MHV-76 results in a decreased viral latent load within the spleens of infected mice (Brass, 2004). The reason for such attenuation is not clear, although it is possible that an immune response generated against foreign elements results in an increased clearance of the virus. Additionally, the insertion of foreign promoter elements may disturb chromatin remodelling occurring during the establishment of latency (reviewed in Efstathiou and Preston, 2005) therefore affecting the expression of latency associated genes.

Due to the fact that no selection markers were present within the recombinant viruses, a PCR approach taken to detect both recombinant and contaminating parental virus, which was much more time consuming than detection based upon the presence of selection markers. However, recombinant viruses have been successfully purified using this method in the past (Townsley *et al*, 2004) and this method was successfully employed in this study for the purification of intRNA(2) and intRNA(9)Rev. Thus the inability to purify a number of insertion viruses away from wild-type virus using this method was puzzling. The repeated selection of single plaques should result in the production of a purified viral stock. It is possible that using the limiting dilution approach, foci of infected cells may have gone unnoticed and therefore be harvested in addition to the observed plaque. However, overlaying with agarose would only have allowed cell to cell spread of the virus thus increasing the confidence of harvesting only a single clone of virus. Therefore the repeated combination of the two approaches should have eventually led to the purification of the viruses. However, one virus (intRNA5) could never be purified away from

parental MHV-76, whereas the WTTintRNA virus appeared to be lost following four rounds of purification.

There are two possible reasons for the inability to purify intRNA5 and WTTintRNA. The first being that insertion of the vtRNAs resulted in the production of viruses with decreased abilities to replicate. However, it is unlikely that the expression of the vtRNAs themselves resulted in a growth defect as MHV-68, which contains the vtRNAs, exhibits identical growth characteristics to MHV-76 *in vitro*, as do the intRNA viruses created in this study. It is possible that insertion of the vtRNAs resulted in deregulated expression of neighbouring genes causing a decreased growth rate. However, given that the neighbouring sequences include the terminal repeats, a residual M4 sequence that is not known to be expressed (Macrae *et al*, 2001) and ORF4, which has not been found to be required for viral replication *in vitro* (Kapadia *et al*, 2002), this is unlikely to be the case. Nevertheless, it is possible that the recombinant cassette inserted elsewhere in the genome resulting in the disruption of genes required for viral replication.

A second possibility as to why the intRNA5 and WTTintRNA viruses could not be purified away from MHV-76 is that the insert sequences are not maintained within the viral genome. It has been noted in the past that the left-hand terminus has a propensity to undergo recombinant events *in vitro*, as highlighted by the observation that inserted sequences are able to undergo duplication events within this region (Simas et al, 1998). This is possibly the mechanism by which M1 arose through a duplication event from M3, or vice versa, given that they are approximately 25% homologous (Virgin *et al*, 1997). The targeted knock out of the ORF74 in MHV-68 was previously found to result in integration of the cloning vector into the left-hand region of the genome (Wakeling, 2001), highlighting the presence of a possible recombination "hot-spot" in this area. In support of this, various deletion mutants of MHV-68 have been isolated which lack all or a portion of this left-hand sequence (Clambey *et al*, 2002; Macrae *et al*, 2001; Oda *et al*, 2005). The nature of this hot-spot is unknown, although there are a number of possible contributing factors, such as the close proximity to the terminal repeats or an origin of replication that has been

hypothesized to localise to this region (Bowden *et al*, 1997). It is also possible that the vtRNAs themselves create areas easily able to undergo recombination, as is the case for tRNAs found within pathogenicity islands of certain bacteria (reviewed in Hou, 1999). If this is the case it may also have resulted in the insertion of vtRNA sequences elsewhere within the genome disrupting the function of essential genes as described above.

Despite the problems encountered in the purification of the recombinant viruses, it was possible to generate vtRNA knock-in viruses that contained partial terminal repeat sequence at the left-hand end. If the partial terminal repeat sequences do have an effect upon the replication of the virus, this would be evident during *in vitro* replication. However, recombinant viruses have been produced previously using this approach, which were found not to be attenuated during replication (Townsley *et al*, 2004). Hence it was decided to go ahead and characterise the intRNA viruses. Southern analysis on the recombinant viruses demonstrated that their genomes possessed the desired genomic rearrangements clearly indicating that the sequences had been inserted correctly within the left-hand end and no additional insertion events had taken place. RT-PCR and Northern analysis demonstrated that all five vtRNAs were expressed during lytic infection with the intRNA viruses to the same levels as that seen following MHV-68 infection. The identical replication of the viruses to both MHV-68 and MHV-76 *in vitro* was not surprising given that MHV-76 displays identical replication kinetics to MHV-68 (Macrae *et al*, 2001).

In vivo analysis of the mutant viruses demonstrated no differences from parental MHV-76 during productive replication within the lungs. This is perhaps surprising given that MHV-76 is cleared more rapidly from the lungs than MHV-68, with an accompanying increase in inflammatory infiltrate (Macrae *et al*, 2001). This was initially hypothesised to be due to the presence of the M3 gene within MHV-68, which encodes a broad spectrum chemokine binding protein (Parry *et al*, 2000; van Berkel *et al*, 2000) and hence may block the inflammatory response resulting in increased persistence of the virus. However, disruption of the M3 gene from MHV-68 had no effect on the ability of the virus to replicate within the lung (Bridgeman *et*

al, 2001). Recombinant virus studies have been conducted in order to ascertain the function all four of the unique genes absent from MHV-76, but none have highlighted a role for a single gene in the persistence of the virus in the lung (Macrae *et al*, 2003; Simas *et al*, 1998; Townsley *et al*, 2004). It was therefore possible that the vtRNAs were involved in the increased persistence of MHV-68 within the lung, especially given their high level of expression during this period of infection (Bowden *et al*, 1997). However, if this is the case it could not be demonstrated by insertion of vtRNAs1-5 into MHV-76. Given that the increased persistence of MHV-68 within the lung has not been found to be due to the action of a single gene within the left-hand region, it appears that they act together, either as a cumulative effect or working in combination. Therefore perhaps a better approach to characterise the role of the vtRNAs would be to delete all eight from MHV-68. However, this is much more problematic due to the location of the vtRNAs. Multiple recombination events would be required to disrupt all eight vtRNAs, increasing the probability of unwanted recombination events and possible disruptions to the expression of the M1-M4 genes.

Insertion of the vtRNAs into the left-hand end of MHV-76 appeared to have no effect on either the establishment or reactivation from latency. This was also surprising given their high level of expression during the latent stage of infection (Bowden *et al*, 1997). In a similar manner to replication within the lungs, it appears that M1-4 genes do not function in isolation to mediate the increased pathogenicity associated with MHV-68. For instance, the insertion of M4 into the left-hand region results in the increased establishment of latency, but not to the same levels as MHV-68 (Townsley *et al*, 2004). Similarly, although deletion of M2 results in a decreased establishment of latency, this was still greater than that achieved by MHV-76 (Macrae *et al*, 2003). Interestingly, neither of these effects was associated with a change in splenomegaly, indicating that an increased establishment of latency is not directly associated with an increased splenomegaly. In fact, the production of recombinant viruses has failed to identify which of the genes within the left-hand region contribute to the increased splenomegaly seen following MHV-68 infection. It therefore appears that the genes within this region act in cooperation to mediate this

effect, either as a cumulative effect or by working together. Hence it is possible that the vtRNAs work in conjunction with the other genes found within the left-hand region to mediate their effects.

Given that the vtRNAs could not be detected by *in situ* hybridization within the spleens of mice infected with either intRNA viruses, it is possible that they were not expressed. However, PCR analysis revealed that in seven out of eight mice infected with the intRNA viruses, the genomes still contained vtRNA sequences, indicating that recombination events resulting in the absence of the vtRNAs from the genome had not taken place. It would have been useful to check for wild-type MHV-76 within these mice. However, the PCR used to detect MHV-76 is very insensitive, most likely due to the multiple primer binding sites present within the terminal repeats. Therefore it was not possible to determine whether a subset of viruses had undergone recombination. An alternative explanation is that the levels of vtRNA expression were below the limit of detection of the *in situ* hybridization. This could occur if the copy number of virus present per cell is less than MHV-68, which is likely given that the viral latent load is decreased.

Given that infection with the recombinant viruses failed to highlight a role for the vtRNAs within infection, alternative approaches need to be taken. As mentioned above, one such approach would be to knock all eight vtRNAs out of the genome of MHV-68. Another approach would be to infect wood-mice instead of BALB/c mice with the recombinant viruses. As wood-mice are the natural host of the virus (Blasdell *et al*, 2003) it is possible that the vtRNAs play a role within infection not evident within BALB/c mice, especially since experimental infection of wood-mice with MHV-68 results in differing pathologies to those seen in BALB/c mice, as demonstrated by a greater inflammatory response within the lung and an absence of splenomegaly (D. Hughes, personal communication). At least one left-hand gene (M3) has been found to play a role during infection in the lung of wood-mice, but not within BALB/c mice (Bridgeman *et al*, 2001; D. Hughes, personal communication), highlighting the need to also investigate the role of genes within their natural host.

An alternative approach to characterizing the role of the vtRNAs would be to investigate their function *in vitro*. This was attempted through construction of a stably transfected epithelial cell line in order to investigate any effects that the vtRNAs might have upon cell growth, transformation, apoptosis or protein synthesis. A similar approach has been taken to dissect possible functions of the EBERs of EBV (Laing *et al*, 2002). However, as was found for the EBERs, the stable transfection of the vtRNAs resulted in a very low level of expression. The reason for the low level of expression is not clear. It is perhaps a result of only a low copy number of the plasmid being maintained within transfected cells. It is also possible that vtRNA expression is enhanced by viral factors. Indeed, cellular tRNA genes have up and down-stream sequences which regulate their levels of expression, akin to those found in RNA polymerase II expressed genes (Sprague, 1995). In addition, certain viruses enhance RNA polymerase III mediated transcription and it is therefore possible that MHV-68 does this resulting in increased vtRNA expression within infection (Berger and Folk, 1985; Gaynor *et al*, 1985). The low level of expression of the EBERs during stable transfection was overcome by using an expression vector containing multiple copies of the EBERs. An analogous approach was attempted in this project, but unfortunately it was not possible to clone the concatemeric vtRNA sequences, perhaps as a result of their large degree of secondary structure.

Although infection of BALB/c mice with the intRNA viruses failed to ascertain the function of the vtRNAs within infection, it is unlikely that they play no role at all. Further investigations are required in order to determine exactly what role the vtRNAs do play. The recombinant viruses produced in this study will be excellent tools to characterize the role of the vtRNAs during lytic and latent infection based upon more specific assays that can be performed during both lytic and latent infection *in vitro*, in addition to during the course of viral pathogenesis *in vivo*.

Chapter 6 – Conclusions

As the function of the vtRNAs has not been previously characterised, a global approach was taken in this study to try and ascertain the role of the vtRNAs within infection. This was undertaken by examining their expression pattern and localization during infection, along with investigating their ability to interact with both viral and cellular proteins. In order to determine whether the vtRNAs play a key role in viral pathogenesis, recombinant MHV-76 viruses were produced by insertion of the vtRNAs into the left-hand end of the genome and the ability of the knock-in viruses to persist within the lung and to establish and reactivate from a latent infection was studied.

The presence of the vtRNAs immediately following *in vitro* infection was surprising. However, studies on purified virus stocks indicated that this was a result of their presence within the virus particle. Although both viral and cellular mRNA have previously been found to be packaged within herpesviruses (Bechtel *et al*, 2005; Greijer *et al*, 2000; Sciortino *et al*, 2001), this is the first study to demonstrate the preferential packaging of a non-coding RNA. A functional role for RNA incorporated within the virion still remains to be resolved. In particular whether it is related to a specific function of the packaged RNA or whether it simply occurs as a result of the random incorporation of cytoplasmic material into the maturing virion. The observation in HCMV that the level of each RNA packaged is in proportion to its relative expression within the cell supports the random incorporation model (Terhune *et al*, 2004). However, this does not appear to be the case for HSV-1 and KSHV, which both package mRNA present at low levels late within infection (Bechtel *et al*, 2005; Sciortino *et al*, 2001). In addition, the presence of proteins within both HSV-1 and HCMV virions capable of binding packaged RNA indicates that there is a specific mechanism in play (Sciortino *et al*, 2002; Terhune *et al*, 2004). In this study, it was confirmed that viral proteins are capable of specifically interacting with the vtRNAs, thus demonstrating a possible selective mechanism of incorporation. In addition, it can be argued that given the highly evolved nature of herpesviruses, it is unlikely that they perform useless functions, and hence would not package RNA unless it carried out a beneficial role within infection.

Determining the mechanism by which RNA is incorporated within the maturing virion may give an indication as to the function of packaged RNA. For instance, whether RNA is able to act as a scaffold during virion assembly, perhaps through mediating protein-protein interactions. tRNA molecules play a role in virion formation of a variety of viruses, such as retroviruses and bromoviruses (Choi *et al*, 2002; Muriaux *et al*, 2001; Wang and Aldovini, 2002). Given that the most abundant RNA species found to be present within the MHV-68 virion were the vtRNAs, along with perhaps cellular tRNAs, it is possible that they perform an analogous role within MHV-68 virion maturation. In order to address this issue it is necessary to identify proteins that mediate RNA incorporation and their location within the virion. The available data so far on incorporated RNA suggests that it is found within the viral tegument (Sciortino *et al*, 2002; Terhune *et al*, 2004) and the high level of vtRNAs present within the cytoplasm during lytic infection indicates their more likely incorporation during virus tegumentation. The presence of RNA within the virus tegument would allow its immediate release into the cytoplasm following infection of a new cell. In the case of packaged mRNA, this has been shown to be translated (Bechtel *et al*, 2005; Greijer *et al*, 2000; Sciortino *et al*, 2001), allowing the resulting proteins to function immediately upon infection. However, whether the vtRNAs carry out a role at very early time points cannot be addressed until their function within infection has been characterised.

Given that no role had previously been ascribed to the vtRNAs within infection, the obvious first step was to try and establish this through the construction of recombinant viruses. As the vtRNAs are found interspersed amongst other genes within the genome of MHV-68 (Bowden *et al*, 1997), it was decided to insert them into MHV-76. However this failed to demonstrate a key role for the vtRNAs within infection. Although past studies utilizing recombinant viruses have determined roles for key genes within both the lytic and latent stages of infection, the fact that the recombinant viruses displayed identical characteristics to MHV-76 *in vivo* does not necessarily mean that the vtRNAs do not carry out a role during viral pathogenesis. Given that they are found within a region of the genome associated with a high level

of recombination, if they were not beneficial to the virus then it is likely that they would have been lost during the period of viral evolution.

Studies on deletion mutants of HSV-1 have uncovered a role for the LATs during the latent stage of infection (reviewed by Kent *et al*, 2003). Given that they are the only species present to high levels within neurones it is perhaps not surprising that their absence results in attenuation of the virus during latent infection. In contrast, MHV-68 expresses a much larger array of genes during latency (Marques *et al*, 2003). Hence it may not be possible to determine the function of the vtRNAs through recombinant studies investigating changes in the level of viral load present within infected mice, as the presence or absence of latency associated genes may not have such a profound effect. Other genes expressed during latency include those found within the left-hand region of the genome. Experimental evidence suggests that the effects of these genes in isolation can not explain the attenuated phenotype of MHV-76 (Macrae *et al*, 2003; Simas *et al*, 1998; Townsley *et al*, 2004). Therefore it appears that they work in cooperation to mediate the increased pathogenicity associated with MHV-68. The left-hand region of the MHV-68 genome could be said to resemble pathogenicity islands found in certain strains of bacteria, such as *E. coli* and *Vibrio cholerae*, which are areas of the genome encoding virulence associated genes that often work together to mediate their effects and regulate gene expression (reviewed by Wain *et al*, 2001). A propensity of pathogenicity islands to undergo recombination facilitates their horizontal transfer between individual bacteria. A key feature of pathogenicity islands is their location downstream of tRNA genes, which have been hypothesized to mediate DNA recombination by an unknown mechanism (Hou, 1999). Past studies have highlighted the existence of a recombination "hot-spot" within the left-hand region of the MHV-68 genome (Simas *et al*, 1998; Wakeling, 2001). In addition, the inability to purify recombinant viruses consisting of the vtRNAs inserted into the genome of MHV-76 indicated either possible recombination events taking place resulting in the reversion of the viruses back to wild-type, or insertion of the vtRNAs elsewhere in the genome. Hence it is possible that the vtRNAs facilitate DNA recombination. The location of the vtRNAs within the left-hand region of the genome would enable the generation of genetic diversity

by allowing the incorporation of DNA within disrupting the function of genes essential for viral replication and the establishment of latency.

Although studies conducted on the intRNA viruses failed to highlight a key role for the vtRNAs during infection, the recombinant viruses produced in the course of this study will be useful tools for further investigating the function of the vtRNAs. It is possible that the vtRNAs play a more important role during infection of their natural host, the wood mouse. Although roles have been established for a number of genes during pathogenesis within BALB/c mice, given that the pathogenesis of the virus differs within its natural host, it is possible that genes display differing functions. This is highlighted by the role of the broad-spectrum chemokine binding protein M3, which appears to function in reducing the inflammatory response within the lungs of wood-mice (Hughes *et al*, 2005), but not in BALB/c mice (Bridgeman *et al*, 2001). It is therefore possible that the vtRNAs play a role within pathogenesis of their natural host not evident during infection of BALB/c mice.

The intRNA viruses can also be used for more targeted *in vitro* investigations into the functions of the vtRNAs. Such studies have characterized functions for the EBERs in the regulation of protein synthesis, resistance to apoptosis and cell transformation (Komano *et al*, 1999; Laing *et al*, 2002; Nanbo *et al*, 2002; Ruf *et al*, 2000). These investigations have relied upon the transient and stable transfection of the EBERs. However, their function in the context of viral infection has not been characterized due to the inability of EBV to undergo lytic infection *in vitro*. Given that MHV-68 is able to undergo productive infection within a variety of cell types *in vitro*, specific functions of the vtRNAs can be investigated in the context of viral replication. In addition MHV-68 is also able to establish a latent infection within the NS0 B-cell line (Sunil-Chandra *et al*, 1993), enabling the contribution of the vtRNAs during latent infection to be studied *in vitro*. Based upon the functions of both uncharged and other viral non-coding RNAs, perhaps the most obvious starting point would be to investigate their contribution to the regulation of protein synthesis.

Uncharged tRNAs play a role in the regulation of protein synthesis in both eukaryotic and prokaryotic cells during periods of amino acid starvation. In certain strains of Gram-negative bacteria, mRNA encoding genes involved in the regulation of aminoacyl-tRNA synthetase and amino acid biosynthesis have untranslated leader sequences (known as T boxes) to which uncharged tRNAs are capable of binding (Putzer *et al*, 2002). Direct tRNA binding results in the stabilization of an anti-termination element, thus allowing translation to proceed. It is not known whether the vtRNAs are able act in a similar way to regulate the expression of viral proteins. Therefore studies into the expression of viral proteins in the presence and absence of the vtRNAs would give an indication of whether they are able to function in this manner.

Within eukaryotic cells a different mechanism exists to stimulate the transcription of genes involved in amino acid biosynthesis, wherein uncharged tRNAs induce the phosphorylation of eIF2α via a protein kinase known as GCN2 (general control nonderepressible 2) (Wek *et al*, 1995). This results in a decrease in global protein synthesis, complemented by an increase in the transcription of genes related to amino acid biosynthesis. It is possible that MHV-68 has created a way to hijack an aspect of this pathway by the expression of uncharged tRNAs in order to alter protein expression within infected cells.

A common function of viral non-coding RNA is their ability to regulate protein synthesis. The LATs of HSV-1 appear to down-regulate the expression of lytic genes during the establishment of latency (Garber *et al*, 1997), whereas the HSURs of HVS are able to up-regulate the expression of host genes linked to T-cell activation (Cook *et al*, 2005). The EBERs of EBV are able to prevent dsRNA mediated down-regulation of protein synthesis, in a manner that was initially hypothesized to be due to the inhibition of PKR activation (Sharp *et al*, 1993). However, their ability to mediate this response within a PKR knock-out cell line indicates an alternative mechanism of action (Laing *et al*, 2002).

VAI of adenovirus acts in a variety of ways to prevent the down-regulation of protein synthesis as a result of virus infection. Firstly by preventing the activation of PKR and subsequent phosphorylation of eIF-2α (Clemens *et al*, 1994; Laing *et al*, 2002; Sharp *et al*, 1993), and secondly inhibiting the RNA silencing response (Lu and Cullen, 2004), an anti-viral mechanism known to operate within animal cells (Li *et al*, 2002). One way in which it has been shown to do this is through binding the nuclear export protein exportin-5; a protein involved in the export of pre-miRNAs from the nucleus (Lu and Cullen, 2004). Due to the large amounts of VAI present within infected cells, it out-competes pre-miRNAs for export from the nucleus and hence they can no longer interact with Dicer to mediate RNA silencing. The abundance of the vtRNAs within the cytoplasm along with their presence within the outer nuclear membrane fraction indicates their export from the nucleus. It is clear that at least one vtRNA is able to bind proteins found in the outer nuclear membrane fraction. Further work is required to identify any nuclear export proteins capable of binding the vtRNAs in order to characterise the mechanism by which they are transported across the nuclear membrane whether this occurs at the expense of cellular RNAs.

The vtRNAs are processed from a longer primary transcript, which also contains miRNA sequences (Bowden *et al*, 1997; Pfeffer *et al*, 2005). It has been suggested that the only role for the vtRNAs is to provide RNA polymerase III promoter elements required for the transcription of miRNAs (Pfeffer *et al*, 2005). Although this is a possibility, it is unlikely given that such high levels of vtRNAs are present within the cell and not subsequently degraded. Furthermore, the selective packaging of the vtRNAs into the virion indicates a specific role for the vtRNAs in either virion assembly or immediately upon infection of host cells. In addition, as mentioned previously, the tRNA structure is conserved between all eight tRNAs. As other miRNAs can be processed in the absence of tRNA elements (Bartel, 2004), it is likely that they would have diverged from the predicted cloverleaf structure if this was not necessary for their function. The role of the vtRNAs within miRNA processing can be addressed by mutating critical residues required for maintenance of the tRNA-like structure and determining whether the miRNAs are still processed.

Although miRNAs have been found to be expressed during latent infection, it is not clear whether they function as miRNAs to regulate protein synthesis. It should be noted that the intRNA viruses also contained miRNAs absent from MHV-76, and therefore no key role for the miRNAs within infection could be demonstrated in this study. Functions of miRNAs may involve the regulation of both viral and protein synthesis, either by the degradation or translational silencing of target mRNA, perhaps at the same time deviating from a cellular anti-viral response. Recent evidence has also uncovered a role for RNA in transcriptional silencing. siRNAs have been shown to be involved in the recruitment of histone methyltransferase to target genes, resulting in the formation of heterochromatin (Volpe *et al*, 2002). An additional mechanism has also been discovered within plants, in which siRNAs direct DNA methylation (Wassenegger *et al*, 1994). However, whether this occurs in other organisms is still a matter of debate (reviewed by Matzke and Birchler, 2005). Given that the transcription control of herpesvirus genes during latent infection has been related to chromatin remodelling (Kubat *et al*, 2004), it is possible that this is mediated by miRNAs.

It is therefore clear that more targeted studies are required to determine the function of both the vtRNAs and miRNAs of MHV-68. In order to uncover their mechanism of action, it is important to identify interacting proteins. It is evident from this study that vtRNAs are capable of interacting with both cellular and viral proteins. Perhaps a more focused approach should now be taken to determine whether the vtRNAs and miRNAs are capable of interacting with cellular proteins such as PKR, GCN2, exportin-5 and DICER, along with identifying the vtRNA-binding viral proteins. The continued investigations into the functions of the vtRNAs and miRNAs will not only give insight into the role of viral non-coding RNAs within infection, but also the versatility of RNA as a whole.

References

Adler H, Messerle M, Wagner M, Koszinowski UH (2000). Cloning and mutagenesis of the murine gammaherpesvirus 68 genome as an infectious bacterial artificial chromosome. *J Virol* **74:** 6964-74.

Ahmed M, Fraser NW (2001). Herpes simplex virus type 1 2-kilobase latency-associated transcript intron associates with ribosomal proteins and splicing factors. *J Virol* **75:** 12070-80.

Ahn JW, Powell KL, Kellam P, Alber DG (2002). Gammaherpesvirus lytic gene expression as characterized by DNA array. *J Virol* **76:** 6244-56.

Albrecht JC, Nicholas J, Biller D, Cameron KR, Biesinger B, Newman C, Wittmann S, Craxton MA, Coleman H, Fleckenstein B, et al. (1992). Primary structure of the herpesvirus saimiri genome. *J Virol* **66:** 5047-58.

Arnold GJ, Gross HJ (1987). Unrelated leader sequences can efficiently promote human tRNA gene transcription. *Gene* **51:** 237-46.

Arrand JR, Rymo L, Walsh JE, Bjorck E, Lindahl T, Griffin BE (1981). Molecular cloning of the complete Epstein-Barr virus genome as a set of overlapping restriction endonuclease fragments. *Nucleic Acids Res* **9:** 2999-3014.

Babcock GJ, Hochberg D, Thorley-Lawson AD (2000). The expression pattern of Epstein-Barr virus latent genes in vivo is dependent upon the differentiation stage of the infected B cell. *Immunity* **13:** 497-506.

Balciunas D, Ronne H (2000). Evidence of domain swapping within the jumonji family of transcription factors. *Trends in Biochemical Sciences* **25:** 274-276.

Ballestas ME, Chatis PA, Kaye KM (1999). Efficient persistence of extrachromosomal KSHV DNA mediated by latency-associated nuclear antigen. *Science* **284:** 641-4.

Baltimore D (1970). RNA-dependent DNA polymerase in virions of RNA tumour viruses. *Nature* **226:** 1209-11.

Banfield BW, Leduc Y, Esford L, Visalli RJ, Brandt CR, Tufaro F (1995). Evidence for an interaction of herpes simplex virus with chondroitin sulfate proteoglycans during infection. *Virology* **208:** 531-9.

Barends S, Bink HHJ, van den Worm SHE, Pleij CWA, Kraal B (2003). Entrapping Ribosomes for Viral Translation: tRNA Mimicry as a Molecular Trojan Horse. *Cell* **112:** 123-129.

Barends S, Rudinger-Thirion J, Florentz C, Giege R, Pleij CW, Kraal B (2004). tRNA-like structure regulates translation of Brome mosaic virus RNA. *J Virol* **78:** 4003-10.

Bartel DP (2004). MicroRNAs: Genomics, Biogenesis, Mechanism, and Function. *Cell* **116:** 281-297.

Batterson W, Roizman B (1983). Characterization of the herpes simplex virion-associated factor responsible for the induction of alpha genes. *J Virol* **46:** 371-7.

Bechtel J, Grundhoff A, Ganem D (2005). RNAs in the virion of Kaposi's sarcoma-associated herpesvirus. *J Virol* **79:** 10138-46.

Bennasser Y, Le SY, Yeung ML, Jeang KT (2004). HIV-1 encoded candidate micro-RNAs and their cellular targets. *Retrovirology* **1:** 43.

Beral V, Peterman TA, Berkelman RL, Jaffe HW (1990). Kaposi's sarcoma among persons with AIDS: a sexually transmitted infection? *The Lancet* **335:** 123-128.

Berger SL, Folk WR (1985). Differential activation of RNA polymerase III-transcribed genes by the polyomavirus enhancer and the adenovirus E1A gene products. *Nucleic Acids Res* **13:** 1413-28.

Bieleski L, Talbot SJ (2001). Kaposi's sarcoma-associated herpesvirus vCyclin open reading frame contains an internal ribosome entry site. *J Virol* **75:** 1864-9.

Biesinger B, Muller-Fleckenstein I, Simmer B, Lang G, Wittmann S, Platzer E, Desrosiers RC, Fleckenstein B (1992). Stable growth transformation of human T lymphocytes by herpesvirus saimiri. *Proc Natl Acad Sci U S A* **89:** 3116-9.

Biesinger B, Tsygankov AY, Fickenscher H, Emmrich F, Fleckenstein B, Bolen JB, Broker BM (1995). The product of the Herpesvirus saimiri open reading frame 1 (Tip) interacts with T cell-specific kinase p56(lck) in transformed cells. *Journal of Biological Chemistry* **270:** 4729-4734.

Blasdell K, McCracken C, Morris A, Nash AA, Begon M, Bennett M, Stewart JP (2003). The wood mouse is a natural host for Murid herpesvirus 4. *J Gen Virol* **84:** 111-3.

Blaskovic D, Stancekova M, Svobodova J, Mistrikova J (1980). Isolation of five strains of herpesviruses from two species of free living small rodents. *Acta Virol* **24:** 468.

Blaskovic D, Stanekova D, Rajcani J (1984). Experimental pathogenesis of murine herpesvirus in newborn mice. *Acta Virol* **28:** 225-31.

Block TM, Spivack JG, Steiner I, Deshmane S, McIntosh MT, Lirette RP, Fraser NW (1990). A herpes simplex virus type 1 latency-associated transcript mutant reactivates with normal kinetics from latent infection. *J Virol* **64:** 3417-26.

Bohenzky RA, Lagunoff M, Roizman B, Wagner EK, Silverstein S (1995). Two overlapping transcription units which extend across the L-S junction of herpes simplex virus type 1. *J Virol* **69:** 2889-97.

Boname JM, May JS, Stevenson PG (2005). Murine gammaherpesvirus 68 open reading frame 11 encodes a nonessential virion component. *J Virol* **79:** 3163-8.

Bortz E, Whitelegge JP, Jia Q, Zhou ZH, Stewart JP, Wu TT, Sun R (2003). Identification of proteins associated with murine gammaherpesvirus 68 virions. *J Virol* **77:** 13425-32.

Borza CM, Hutt-Fletcher LM (2002). Alternate replication in B cells and epithelial cells switches tropism of Epstein-Barr virus. *Nat Med* **8:** 594-9.

Boshoff C, Chang Y (2001). Kaposi's sarcoma-associated herpesvirus: a new DNA tumor virus. *Annu Rev Med* **52:** 453-70.

Boshoff C, Schulz TF, Kennedy MM, Graham AK, Fisher C, Thomas A, McGee JO, Weiss RA, O'Leary JJ (1995). Kaposi's sarcoma-associated herpesvirus infects endothelial and spindle cells. *Nat Med* **1:** 1274-8.

Boshoff C, Weiss RA (2001). Epidemiology and pathogenesis of Kaposi's sarcoma-associated herpesvirus. *Philos Trans R Soc Lond B Biol Sci* **356:** 517-34.

Bowden RJ, Simas JP, Davis AJ, Efstathiou S (1997). Murine gammaherpesvirus 68 encodes tRNA-like sequences which are expressed during latency. *J Gen Virol* **78 (Pt 7):** 1675-87.

Brass A (2004). vOx2-a potential immune regulatory protein involved in Kaposi's sarcoma-associated herpesvirus pathogenesis. PhD Thesis. University of Edinburgh.

Bresnahan WA, Shenk T (2000). A subset of viral transcripts packaged within human cytomegalovirus particles. *Science* **288:** 2373-6.

Bridgeman A, Stevenson PG, Simas JP, Efstathiou S (2001). A secreted chemokine binding protein encoded by murine gammaherpesvirus-68 is necessary for the establishment of a normal latent load. *J Exp Med* **194:** 301-12.

Bridgen A, Herring AJ, Inglis NF, Reid HW (1989). Preliminary characterization of the alcelaphine herpesvirus 1 genome. *J Gen Virol* **70 (Pt 5):** 1141-50.

Brooks L, Yao QY, Rickinson AB, Young LS (1992). Epstein-Barr virus latent gene transcription in nasopharyngeal carcinoma cells: coexpression of EBNA1, LMP1, and LMP2 transcripts. *J Virol* **66:** 2689-97.

Brown HJ, Song MJ, Deng H, Wu TT, Cheng G, Sun R (2003). NF-kappaB inhibits gammaherpesvirus lytic replication. *J Virol* **77:** 8532-40.

Burton EA, Hong CS, Glorioso JC (2003). The stable 2.0-kilobase intron of the herpes simplex virus type 1 latency-associated transcript does not function as an antisense repressor of ICP0 in nonneuronal cells. *J Virol* **77:** 3516-30.

Cai X, Lu S, Zhang Z, Gonzalez CM, Damania B, Cullen BR (2005). Kaposi's sarcoma-associated herpesvirus expresses an array of viral microRNAs in latently infected cells. *Proc Natl Acad Sci U S A* **102:** 5570-5.

Cantello J, Parcells M, Anderson A, Morgan R (1997). Marek's disease virus latency-associated transcripts belong to a family of spliced RNAs that are antisense to the ICP4 homolog gene. *J Virol* **71:** 1353-1361.

Cantello JL, Anderson AS, Morgan RW (1994). Identification of latency-associated transcripts that map antisense to the ICP4 homolog gene of Marek's disease virus. *J Virol* **68:** 6280-90.

Carroll PA, Brazeau E, Lagunoff M (2004). Kaposi's sarcoma-associated herpesvirus infection of blood endothelial cells induces lymphatic differentiation. *Virology* **328:** 7-18.

Cen S, Khorchid A, Javanbakht H, Gabor J, Stello T, Shiba K, Musier-Forsyth K, Kleiman L (2001). Incorporation of Lysyl-tRNA Synthetase into Human Immunodeficiency Virus Type 1. *J Virol* **75:** 5043-5048.

Cesarman E, Chang Y, Moore PS, Said JW, Knowles DM (1995). Kaposi's sarcoma-associated herpesvirus-like DNA sequences in AIDS-related body-cavity-based lymphomas. *N Engl J Med* **332:** 1186-91.

Chang Y, Cesarman E, Pessin MS, Lee F, Culpepper J, Knowles DM, Moore PS (1994). Identification of herpesvirus-like DNA sequences in AIDS-associated Kaposi's sarcoma. *Science* **266:** 1865-9.

Chang Y, Moore PS (2001). Kaposi's sacroma-associated herpesvirus. In: *Fields Virlogy*. Knipe DM, Howley P, (eds). Lippincott, Williams and Wilkins.

Choi J, Means RE, Damania B, Jung JU (2001). Molecular piracy of Kaposi's sarcoma associated herpesvirus. *Cytokine Growth Factor Rev* **12:** 245-57.

Choi JK, Ishido S, Jung JU (2000). The collagen repeat sequence is a determinant of the degree of herpesvirus saimiri STP transforming activity. *J Virol* **74:** 8102-10.

Choi YG, Dreher TW, Rao AL (2002). tRNA elements mediate the assembly of an icosahedral RNA virus. *Proc Natl Acad Sci U S A* **99:** 655-60.

Chou J, Kern ER, Whitley RJ, Roizman B (1990). Mapping of herpes simplex virus-1 neurovirulence to gamma 134.5, a gene nonessential for growth in culture. *Science* **250:** 1262-6.

Ciampor F, Stancekova M, Blaskovic D (1981). Electron microscopy of rabbit embryo fibroblasts infected with herpesvirus isolates from Clethrionomys glareolus and Apodemus flavicollis. *Acta Virol* **25:** 101-7.

Clambey ET, Virgin HWt, Speck SH (2000). Disruption of the murine gammaherpesvirus 68 M1 open reading frame leads to enhanced reactivation from latency. *J Virol* **74:** 1973-84.

Clambey ET, Virgin HWt, Speck SH (2002). Characterization of a spontaneous 9.5-kilobase-deletion mutant of murine gammaherpesvirus 68 reveals tissue-specific genetic requirements for latency. *J Virol* **76:** 6532-44.

Clarke PA, Schwemmle M, Schickinger J, Hilse K, Clemens MJ (1991). Binding of Epstein-Barr virus small RNA EBER-1 to the double-stranded RNA-activated protein kinase DAI. *Nucleic Acids Res* **19:** 243-8.

Clemens MJ, Laing KG, Jeffrey IW, Schofield A, Sharp TV, Elia A, Matys V, James MC, Tilleray VJ (1994). Regulation of the interferon-inducible eIF-2 alpha protein kinase by small RNAs. *Biochimie* **76:** 770-8.

Coffey AJ, Brooksbank RA, Brandau O, Oohashi T, Howell GR, Bye JM, Cahn AP, Durham J, Heath P, Wray P, Pavitt R, Wilkinson J, Leversha M, Huckle E, Shaw-Smith CJ, Dunham A, Rhodes S, Schuster V, Porta G, Yin L, Serafini P, Sylla B, Zollo M, Franco B, Bentley DR, et al. (1998). Host response to EBV infection in X-linked lymphoproliferative disease results from mutations in an SH2-domain encoding gene. *Nat Genet* **20:** 129-35.

Coleman HM, de Lima B, Morton V, Stevenson PG (2003). Murine gammaherpesvirus 68 lacking thymidine kinase shows severe attenuation of lytic cycle replication in vivo but still establishes latency. *J Virol* **77:** 2410-7.

Cook HL, Lytle JR, Mischo HE, Li MJ, Rossi JJ, Silva DP, Desrosiers RC, Steitz JA (2005). Small nuclear RNAs encoded by Herpesvirus saimiri upregulate the expression of genes linked to T cell activation in virally transformed T cells. *Curr Biol* **15:** 974-9.

Cook HL, Mischo HE, Steitz JA (2004). The Herpesvirus saimiri small nuclear RNAs recruit AU-rich element-binding proteins but do not alter host AU-rich element-containing mRNA levels in virally transformed T cells. *Mol Cell Biol* **24:** 4522-33.

Crawford DH (2001). Biology and disease associations of Epstein-Barr virus. *Philos Trans R Soc Lond B Biol Sci* **356:** 461-73.

Cuillel M, Herzog M, Hirth L (1979). Specificity of in vitro reconstitution of bromegrass mosaic virus. *Virology* **95:** 146-153.

Cullen BR (2004). Transcription and processing of human microRNA precursors. *Mol Cell* **16:** 861-5.

Dai W, Jia Q, Bortz E, Shah S, Atanasov I, Taylor K, Sun R, Hong Zhou Z (2005). Unique structures of gammaherpesvirus revealed by electron cryomicroscopy and cryomography. In: *International Herpesvirus Workshop*: Turku, Finland.

Damania B, Desrosiers RC (2001). Simian homologues of human herpesvirus 8. *Philos Trans R Soc Lond B Biol Sci* **356:** 535-43.

Dawson CW, Rickinson AB, Young LS (1990). Epstein-Barr virus latent membrane protein inhibits human epithelial cell differentiation. *Nature* **344:** 777-80.

De Carli M, Berthold S, Fickenscher H, Fleckenstein IM, D'Elios MM, Gao Q, Biagiotti R, Giudizi MG, Kalden JR, Fleckenstein B, et al. (1993). Immortalization with herpesvirus saimiri modulates the cytokine secretion profile of established Th1 and Th2 human T cell clones. *J Immunol* **151:** 5022-30.

de Lima BD, May JS, Marques S, Simas JP, Stevenson PG (2005). Murine gammaherpesvirus 68 bcl-2 homologue contributes to latency establishment in vivo. *J Gen Virol* **86:** 31-40.

de Lima BD, May JS, Stevenson PG (2004). Murine gammaherpesvirus 68 lacking gp150 shows defective virion release but establishes normal latency in vivo. *J Virol* **78:** 5103-12.

Desrosiers R, Sasseville V, Czajak S, Zhang X, Mansfield K, Kaur A, Johnson R, Lackner A, Jung J (1997). A herpesvirus of rhesus monkeys related to the human Kaposi's sarcoma- associated herpesvirus. *J Virol* **71:** 9764-9769.

Desrosiers RC, Bakker A, Kamine J, Falk LA, Hunt RD, King NW (1985). A region of the Herpesvirus saimiri genome required for oncogenicity. *Science* **228:** 184-7.

Dirheimer G, Keith G, Dumas P, Westhof E (1995). Primary, secondary and teriatry stuctures of tRNAs. In: *tRNA structure, biosynthesis and function.* Soll D, RajBhandary UL, (eds). ASM press, pp 93-126.

Dittmer D, Stoddart C, Renne R, Linquist-Stepps V, Moreno ME, Bare C, McCune JM, Ganem D (1999). Experimental transmission of Kaposi's sarcoma-associated herpesvirus (KSHV/HHV-8) to SCID-hu Thy/Liv mice. *J Exp Med* **190:** 1857-68.

Douglas J, Dutia B, Rhind S, Stewart JP, Talbot SJ (2004). Expression in a recombinant murid herpesvirus 4 reveals the in vivo transforming potential of the K1 open reading frame of Kaposi's sarcoma-associated herpesvirus. *J Virol* **78:** 8878-84.

Dreher TW (1999). Functions of the 3'-Untranslated Regions of Positive Strand Rna Viral Genomes. *Annu Rev Phytopathol* **37:** 151-174.

Drolet BS, Perng GC, Villosis RJ, Slanina SM, Nesburn AB, Wechsler SL (1999). Expression of the first 811 nucleotides of the herpes simplex virus type 1 latency-associated transcript (LAT) partially restores wild-type spontaneous reactivation to a LAT-null mutant. *Virology* **253:** 96-106.

Du M-Q, Liu H, Diss TC, Ye H, Hamoudi RA, Dupin N, Meignin V, Oksenhendler E, Boshoff C, Isaacson PG (2001). Kaposi sarcoma-associated herpesvirus infects

monotypic (IgM{lambda}) but polyclonal naive B cells in Castleman disease and associated lymphoproliferative disorders. *Blood* **97:** 2130-2136.

Duboise SM, Guo J, Czajak S, Desrosiers RC, Jung JU (1998). STP and Tip are essential for herpesvirus saimiri oncogenicity. *J Virol* **72:** 1308-13.

Dupre L, Andolfi G, Tangye SG, Clementi R, Locatelli F, Arico M, Aiuti A, Roncarolo M-G (2005). SAP controls the cytolytic activity of CD8+ T cells against EBV-infected cells. *Blood*: 2004-08-3269.

Ebrahimi B, Dutia BM, Roberts KL, Garcia-Ramirez JJ, Dickinson P, Stewart JP, Ghazal P, Roy DJ, Nash AA (2003). Transcriptome profile of murine gammaherpesvirus-68 lytic infection. *J Gen Virol* **84:** 99-109.

Efstathiou S, Ho YM, Hall S, Styles CJ, Scott SD, Gompels UA (1990). Murine herpesvirus 68 is genetically related to the gammaherpesviruses Epstein-Barr virus and herpesvirus saimiri. *J Gen Virol* **71 (Pt 6):** 1365-72.

Efstathiou S, Preston CM (2005). Towards an understanding of the molecular basis of herpes simplex virus latency. *Virus Research* **111:** 108-119.

Ehtisham S, Sunil-Chandra NP, Nash AA (1993). Pathogenesis of murine gammaherpesvirus infection in mice deficient in CD4 and CD8 T cells. *J Virol* **67:** 5247-52.

Elia A, Vyas J, Laing KG, Clemens MJ (2004). Ribosomal protein L22 inhibits regulation of cellular activities by the Epstein-Barr virus small RNA EBER-1. *Eur J Biochem* **271:** 1895-905.

Emery VC, Cope AV, Bowen EF, Gor D, Griffiths PD (1999). The dynamics of human cytomegalovirus replication in vivo. *J Exp Med* **190:** 177-82.

Emini EA, Luka J, Armstrong ME, Banker FS, Provost PJ, Pearson GR (1986). Establishment and characterization of a chronic infectious mononucleosislike syndrome in common marmosets. *J Med Virol* **18:** 369-79.

Ensoli B, Barillari G, Gallo RC (1992). Cytokines and growth factors in the pathogenesis of AIDS-associated Kaposi's sarcoma. *Immunol Rev* **127:** 147-55.

Ensoli B, Sgadari C, Barillari G, Sirianni MC, Sturzl M, Monini P (2001). Biology of Kaposi's sarcoma. *Eur J Cancer* **37:** 1251-69.

Ensoli B, Sturzl M, Monini P (2000). Cytokine-mediated growth promotion of Kaposi's sarcoma and primary effusion lymphoma. *Semin Cancer Biol* **10:** 367-81.

Ensser A, Pfinder A, Muller-Fleckenstein I, Fleckenstein B (1999). The URNA genes of herpesvirus saimiri (strain C488) are dispensable for transformation of human T cells in vitro. *J Virol* **73:** 10551-5.

Epstein MA, Achong BG, Barr YM (1964). Virus Particles in Cultured Lymphoblasts from Burkitt's Lymphoma. *Lancet* **15:** 702-3.

Epstein MA, Morgan AJ, Finerty S, Randle BJ, Kirkwood JK (1985). Protection of cottontop tamarins against Epstein-Barr virus-induced malignant lymphoma by a prototype subunit vaccine. *Nature* **318:** 287-9.

Farrell MJ, Dobson AT, Feldman LT (1991). Herpes simplex virus latency-associated transcript is a stable intron. *Proc Natl Acad Sci U S A* **88:** 790-4.

Fickenscher H, Fleckenstein B (2001). Herpesvirus saimiri. *Philos Trans R Soc Lond B Biol Sci* **356:** 545-67.

Flano E, Husain SM, Sample JT, Woodland DL, Blackman MA (2000). Latent murine gamma-herpesvirus infection is established in activated B cells, dendritic cells, and macrophages. *J Immunol* **165:** 1074-81.

Flano E, Kim IJ, Moore J, Woodland DL, Blackman MA (2003). Differential gamma-herpesvirus distribution in distinct anatomical locations and cell subsets during persistent infection in mice. *J Immunol* **170:** 3828-34.

Flano E, Kim IJ, Woodland DL, Blackman MA (2002). Gamma-herpesvirus latency is preferentially maintained in splenic germinal center and memory B cells. *J Exp Med* **196:** 1363-72.

Florentz C, Giege R (1995). tRNA-like structures in plat viral RNAs. In: *tRNA structure, biosynthesis and function*. Soll D, RajBhandary UL, (eds). ASM Press, pp 141-164.

Fowler P, Marques S, Simas JP, Efstathiou S (2003). ORF73 of murine herpesvirus-68 is critical for the establishment and maintenance of latency. *J Gen Virol* **84:** 3405-16.

Frank A, Andiman WA, Miller G (1976). Epstein-Barr virus and nonhuman primates: natural and experimental infection. *Adv Cancer Res* **23:** 171-201.

Friborg J, Jr., Kong W, Hottiger MO, Nabel GJ (1999). p53 inhibition by the LANA protein of KSHV protects against cell death. *Nature* **402:** 889-94.

Frolova-Jones EA, Ensser A, Stevenson AJ, Kinsey SE, Meredith DM (2000). Stable marker gene transfer into human bone marrow stromal cells and their progenitors using novel herpesvirus saimiri-based vectors. *J Hematother Stem Cell Res* **9:** 573-81.

Gangappa S, van Dyk LF, Jewett TJ, Speck SH, Virgin HWt (2002). Identification of the in vivo role of a viral bcl-2. *J Exp Med* **195:** 931-40.

Garber DA, Schaffer PA, Knipe DM (1997). A LAT-associated function reduces productive-cycle gene expression during acute infection of murine sensory neurons with herpes simplex virus type 1. *J Virol* **71:** 5885-93.

Gaynor RB, Feldman LT, Berk AJ (1985). Transcription of class III genes activated by viral immediate early proteins. *Science* **230:** 447-50.

Geck P, Medveczky MM, Chou CS, Brown A, Cus J, Medveczky PG (1994). Herpesvirus saimiri small RNA and interleukin-4 mRNA AUUUA repeats compete for sequence-specific factors including a novel 70K protein. *J Gen Virol* **75 (Pt 9):** 2293-301.

Geraghty RJ, Krummenacher C, Cohen GH, Eisenberg RJ, Spear PG (1998). Entry of alphaherpesviruses mediated by poliovirus receptor-related protein 1 and poliovirus receptor. *Science* **280:** 1618-20.

Ghadge GD, Swaminathan S, Katze MG, Thimmapaya B (1991). Binding of the adenovirus VAI RNA to the interferon-induced 68-kDa protein kinase correlates with function. *Proc Natl Acad Sci U S A* **88:** 7140-4.

Gibson W, Roizman B (1972). Proteins specified by herpes simplex virus. 8. Characterization and composition of multiple capsid forms of subtypes 1 and 2. *J Virol* **10:** 1044-52.

Giege R, Frugier M, Rudinger J (1998). tRNA mimics. *Current Opinion in Structural Biology* **8:** 286-293.

Gilligan K, Rajadurai P, Resnick L, Raab-Traub N (1990). Epstein-Barr virus small nuclear RNAs are not expressed in permissively infected cells in AIDS-associated leukoplakia. *Proc Natl Acad Sci U S A* **87:** 8790-4.

Glickman JN, Howe JG, Steitz JA (1988). Structural analyses of EBER1 and EBER2 ribonucleoprotein particles present in Epstein-Barr virus-infected cells. *J Virol* **62:** 902-11.

Goff SP (2001). Retroviridae: The retroviruses and their replication. In: *Fields viorlogy*. Knipe DM, Howley PM, (eds). Lippincott, Williams and Wilkins, pp 1871-1940.

Golembe TJ, Yong J, Battle DJ, Feng W, Wan L, Dreyfuss G (2005). Lymphotropic Herpesvirus saimiri Uses the SMN Complex To Assemble Sm Cores on Its Small RNAs. *Mol Cell Biol* **25:** 602-611.

Gotte M, Li X, Wainberg MA (1999). HIV-1 Reverse Transcription: A Brief Overview Focused on Structure-Function Relationships among Molecules Involved in Initiation of the Reaction. *Archives of Biochemistry and Biophysics* **365:** 199-210.

Granzow H, Klupp BG, Fuchs W, Veits J, Osterrieder N, Mettenleiter TC (2001). Egress of alphaherpesviruses: comparative ultrastructural study. *J Virol* **75:** 3675-84.

Greensill J, Sheldon JA, Murthy KK, Bessonette JS, Beer BE, Schulz TF (2000). A chimpanzee rhadinovirus sequence related to Kaposi's sarcoma-associated herpesvirus/human herpesvirus 8: increased detection after HIV-1 infection in the absence of disease. *Aids* **14:** F129-35.

Greenspan JS, Greenspan D, Lennette ET, Abrams DI, Conant MA, Petersen V, Freese UK (1985). Replication of Epstein-Barr virus within the epithelial cells of oral "hairy" leukoplakia, an AIDS-associated lesion. *N Engl J Med* **313:** 1564-71.

Gregory CD, Rowe M, Rickinson AB (1990). Different Epstein-Barr virus-B cell interactions in phenotypically distinct clones of a Burkitt's lymphoma cell line. *J Gen Virol* **71 (Pt 7):** 1481-95.

Greifenegger N, Jager M, Kunz-Schughart LA, Wolf H, Schwarzmann F (1998). Epstein-Barr virus small RNA (EBER) genes: differential regulation during lytic viral replication. *J Virol* **72:** 9323-8.

Greijer AE, Dekkers CAJ, Middeldorp JM (2000). Human Cytomegalovirus Virions Differentially Incorporate Viral and Host Cell RNA during the Assembly Process. *J Virol* **74:** 9078-9082.

Guasparri I, Keller SA, Cesarman E (2004). KSHV vFLIP Is Essential for the Survival of Infected Lymphoma Cells. *J Exp Med* **199:** 993-1003.

Gwizdek C, Ossareh-Nazari B, Brownawell AM, Evers S, Macara IG, Dargemont C (2004). Minihelix-containing RNAs mediate exportin-5-dependent nuclear export of the double-stranded RNA-binding protein ILF3. *J Biol Chem* **279:** 884-91.

Henderson G, Peng W, Jin L, Perng GC, Nesburn AB, Wechsler SL, Jones C (2002). Regulation of caspase 8- and caspase 9-induced apoptosis by the herpes simplex virus type 1 latency-associated transcript. *J Neurovirol* **8 Suppl 2:** 103-11.

Hengge UR, Ruzicka T, Tyring SK, Stuschke M, Roggendorf M, Schwartz RA, Seeber S (2002). Update on Kaposi's sarcoma and other HHV8 associated diseases. Part 1: epidemiology, environmental predispositions, clinical manifestations, and therapy. *The Lancet Infectious Diseases* **2:** 281-292.

Herskowitz J, Jacoby MA, Speck SH (2005). The murine gammaherpesvirus 68 M2 gene is required for efficient reactivation from latently infected B cells. *J Virol* **79:** 2261-73.

Hoge AT, Hendrickson SB, Burns WH (2000). Murine gammaherpesvirus 68 cyclin D homologue is required for efficient reactivation from latency. *J Virol* **74:** 7016-23.

Holley RW, Apgar J, Everett GA, Madison JT, Marquisee M, Merrill SH, Penswick JR, Zamir A (1965). Structure of a Ribonucleic Acid. *Science* **147:** 1462-5.

Honess RW, Roizman B (1974). Regulation of herpesvirus macromolecular synthesis. I. Cascade regulation of the synthesis of three groups of viral proteins. *J Virol* **14:** 8-19.

Hou YM (1993). The tertiary structure of tRNA and the development of the genetic code. *Trends Biochem Sci* **18:** 362-4.

Hou YM (1999). Transfer RNAs and pathogenicity islands. *Trends Biochem Sci* **24:** 295-8.

Huang YQ, Friedman-Kien AE, Li JJ, Nickoloff BJ (1993). Cultured Kaposi's sarcoma cell lines express factor XIIIa, CD14, and VCAM-1, but not factor VIII or ELAM-1. *Arch Dermatol* **129:** 1291-6.

Hughes DJ, Kipar A, Bennett M, Ebrahimi B, Stewart JP (2004). Murid gammaherpesvirus infection in its natural host. In: *29th International Herpesvirus Workshop*.

Husain SM, Usherwood EJ, Dyson H, Coleclough C, Coppola MA, Woodland DL, Blackman MA, Stewart JP, Sample JT (1999). Murine gammaherpesvirus M2 gene is latency-associated and its protein a target for CD8(+) T lymphocytes. *Proc Natl Acad Sci U S A* **96:** 7508-13.

Ishov AM, Maul GG (1996). The periphery of nuclear domain 10 (ND10) as site of DNA virus deposition. *J Cell Biol* **134:** 815-26.

Jacoby MA, Virgin HWt, Speck SH (2002). Disruption of the M2 gene of murine gammaherpesvirus 68 alters splenic latency following intranasal, but not intraperitoneal, inoculation. *J Virol* **76:** 1790-801.

Jia Q, Chernishof V, Bortz E, McHardy I, Wu TT, Liao HI, Sun R (2005a). Murine gammaherpesvirus 68 open reading frame 45 plays an essential role during the immediate-early phase of viral replication. *J Virol* **79:** 5129-41.

Jia Q, Chernishof V, Bortz E, Mchardy I, Wu T-T, Liao H-I, Sun R (2005b). Murine Gammaherpesvirus 68 Open Reading Frame 45 Plays an Essential Role during the Immediate-Early Phase of Viral Replication. *J Virol* **79:** 5129-5141.

Jiang M, Mak J, Ladha A, Cohen E, Klein M, Rovinski B, Kleiman L (1993). Identification of tRNAs incorporated into wild-type and mutant human immunodeficiency virus type 1. *J Virol* **67:** 3246-3253.

Jimenez-Garcia LF, Green SR, Mathews MB, Spector DL (1993). Organization of the double-stranded RNA-activated protein kinase DAI and virus-associated VA RNAI in adenovirus-2-infected HeLa cells. *J Cell Sci* **106 (Pt 1):** 11-22.

Johannessen I, Crawford DH (1999). In vivo models for Epstein-Barr virus (EBV)-associated B cell lymphoproliferative disease (BLPD). *Rev Med Virol* **9:** 263-77.

Jung JU, Trimble JJ, King NW, Biesinger B, Fleckenstein BW, Desrosiers RC (1991). Identification of transforming genes of subgroup A and C strains of Herpesvirus saimiri. *Proc Natl Acad Sci U S A* **88:** 7051-5.

Jussila L, Valtola R, Partanen TA, Salven P, Heikkila P, Matikainen MT, Renkonen R, Kaipainen A, Detmar M, Tschachler E, Alitalo R, Alitalo K (1998). Lymphatic endothelium and Kaposi's sarcoma spindle cells detected by antibodies against the vascular endothelial growth factor receptor-3. *Cancer Res* **58:** 1599-604.

Kang W, Mukerjee R, Fraser NW (2003). Establishment and maintenance of HSV latent infection is mediated through correct splicing of the LAT primary transcript. *Virology* **312:** 233-44.

Kapadia SB, Levine B, Speck SH, Virgin HWt (2002). Critical role of complement and viral evasion of complement in acute, persistent, and latent gamma-herpesvirus infection. *Immunity* **17:** 143-55.

Kaposi M (1872). Idiopathic multiple pigmented sarcoma of the skin. *Arch Dermatol Syphil* **4:** 265-73.

Kennedy G, Komano J, Sugden B (2003). Epstein-Barr virus provides a survival factor to Burkitt's lymphomas. *PNAS* **100:** 14269-14274.

Kent JR, Kang W, Miller CG, Fraser NW (2003). Herpes simplex virus latency-associated transcript gene function. *J Neurovirol* **9:** 285-90.

Kieff E, Rickinson AB (2001). Epstein Barr Virus and its Replication. In: *Fields Virology*. Knipe DM, Howley PM, (eds). Lippincott Williams and Wilkins, pp 2511-2574.

Kim IJ, Flano E, Woodland DL, Lund FE, Randall TD, Blackman MA (2003). Maintenance of long term gamma-herpesvirus B cell latency is dependent on CD40-mediated development of memory B cells. *J Immunol* **171:** 886-92.

Kitagawa N, Goto M, Kurozumi K, Maruo S, Fukayama M, Naoe T, Yasukawa M, Hino K, Suzuki T, Todo S, Takada K (2000). Epstein-Barr virus-encoded poly(A)(-) RNA supports Burkitt's lymphoma growth through interleukin-10 induction. *Embo J* **19:** 6742-50.

Knight JS, Cotter MA, 2nd, Robertson ES (2001). The latency-associated nuclear antigen of Kaposi's sarcoma-associated herpesvirus transactivates the telomerase reverse transcriptase promoter. *J Biol Chem* **276:** 22971-8.

Komano J, Maruo S, Kurozumi K, Oda T, Takada K (1999). Oncogenic role of Epstein-Barr virus-encoded RNAs in Burkitt's lymphoma cell line Akata. *J Virol* **73:** 9827-31.

Krause PR, Croen KD, Ostrove JM, Straus SE (1990). Structural and kinetic analyses of herpes simplex virus type 1 latency-associated transcripts in human trigeminal ganglia and in cell culture. *J Clin Invest* **86:** 235-41.

Krol MA, Olson NH, Tate J, Johnson JE, Baker TS, Ahlquist P (1999). RNA-controlled polymorphism in the in vivo assembly of 180-subunit and 120-subunit virions from a single capsid protein. *PNAS* **96:** 13650-13655.

Kubat NJ, Tran RK, McAnany P, Bloom DC (2004). Specific histone tail modification and not DNA methylation is a determinant of herpes simplex virus type 1 latent gene expression. *J Virol* **78:** 1139-49.

Kwek KY, Murphy S, Furger A, Thomas B, O'Gorman W, Kimura H, Proudfoot NJ, Akoulitchev A (2002). U1 snRNA associates with TFIIH and regulates transcriptional initiation. *Nature Structural Biology* **9:** 800-805.

Lagunoff M, Roizman B (1994). Expression of a herpes simplex virus 1 open reading frame antisense to the gamma(1)34.5 gene and transcribed by an RNA 3' coterminal with the unspliced latency-associated transcript. *J Virol* **68:** 6021-8.

Laing KG, Elia A, Jeffrey I, Matys V, Tilleray VJ, Souberbielle B, Clemens MJ (2002). In vivo effects of the Epstein-Barr virus small RNA EBER-1 on protein synthesis and cell growth regulation. *Virology* **297:** 253-69.

Lam N, Sugden B (2003). CD40 and its viral mimic, LMP1: similar means to different ends. *Cell Signal* **15:** 9-16.

Lan K, Kuppers DA, Verma SC, Robertson ES (2004). Kaposi's sarcoma-associated herpesvirus-encoded latency-associated nuclear antigen inhibits lytic replication by targeting Rta: a potential mechanism for virus-mediated control of latency. *J Virol* **78:** 6585-94.

Lee RC, Feinbaum RL, Ambros V (1993). The C. elegans heterochronic gene lin-4 encodes small RNAs with antisense complementarity to lin-14. *Cell* **75:** 843-854.

Lee SI, Murthy SC, Trimble JJ, Desrosiers RC, Steitz JA (1988). Four novel U RNAs are encoded by a herpesvirus. *Cell* **54:** 599-607.

Lee SI, Steitz JA (1990). Herpesvirus saimiri U RNAs are expressed and assembled into ribonucleoprotein particles in the absence of other viral genes. *J Virol* **64:** 3905-15.

Lee SP, Brooks JM, Al-Jarrah H, Thomas WA, Haigh TA, Taylor GS, Humme S, Schepers A, Hammerschmidt W, Yates JL, Rickinson AB, Blake NW (2004). CD8 T Cell Recognition of Endogenously Expressed Epstein-Barr Virus Nuclear Antigen 1. *J Exp Med* **199:** 1409-1420.

Leib DA, Bogard CL, Kosz-Vnenchak M, Hicks KA, Coen DM, Knipe DM, Schaffer PA (1989). A deletion mutant of the latency-associated transcript of herpes

simplex virus type 1 reactivates from the latent state with reduced frequency. *J Virol* **63:** 2893-900.

Lerner MR, Andrews NC, Miller G, Steitz JA (1981). Two small RNAs encoded by Epstein-Barr virus and complexed with protein are precipitated by antibodies from patients with systemic lupus erythematosus. *Proc Natl Acad Sci U S A* **78:** 805-9.

Li D, O'Sullivan G, Greenall L, Smith G, Jiang C, Ross N (1998). Further characterization of the latency-associated transcription unit of Marek's disease virus. *Arch Virol* **143:** 295-311.

Li H, Li WX, Ding SW (2002). Induction and suppression of RNA silencing by an animal virus. *Science* **296:** 1319-21.

Liao HJ, Kobayashi R, Mathews MB (1998). Activities of adenovirus virus-associated RNAs: purification and characterization of RNA binding proteins. *Proc Natl Acad Sci U S A* **95:** 8514-9.

Ling PD, Hsieh JJ, Ruf IK, Rawlins DR, Hayward SD (1994). EBNA-2 upregulation of Epstein-Barr virus latency promoters and the cellular CD23 promoter utilizes a common targeting intermediate, CBF1. *J Virol* **68:** 5375-83.

Lomonte P, Bublot M, van Santen V, Keil G, Pastoret PP, Thiry E (1996). Bovine herpesvirus 4: genomic organization and relationship with two other gammaherpesviruses, Epstein-Barr virus and herpesvirus saimiri. *Vet Microbiol* **53:** 79-89.

Lopes FB, Colaco S, May JS, Stevenson PG (2004). Characterization of murine gammaherpesvirus 68 glycoprotein B. *J Virol* **78:** 13370-5.

Lu S, Cullen BR (2004). Adenovirus VA1 noncoding RNA can inhibit small interfering RNA and MicroRNA biogenesis. *J Virol* **78:** 12868-76.

Lund E, Dahlberg JE (1998). Proofreading and aminoacylation of tRNAs before export from the nucleus. *Science* **282:** 2082-5.

Luppi M, Barozzi P, Schulz TF, Setti G, Staskus K, Trovato R, Narni F, Donelli A, Maiorana A, Marasca R, Sandrini S, Torelli G, Sheldon J (2000). Bone Marrow Failure Associated with Human Herpesvirus 8 Infection after Transplantation. *N Engl J Med* **343:** 1378-1385.

Ma Y, Mathews MB (1993). Comparative analysis of the structure and function of adenovirus virus-associated RNAs. *J Virol* **67:** 6605-17.

Macrae AI, Dutia BM, Milligan S, Brownstein DG, Allen DJ, Mistrikova J, Davison AJ, Nash AA, Stewart JP (2001). Analysis of a novel strain of murine gammaherpesvirus reveals a genomic locus important for acute pathogenesis. *J Virol* **75:** 5315-27.

Macrae AI, Usherwood EJ, Husain SM, Flano E, Kim IJ, Woodland DL, Nash AA, Blackman MA, Sample JT, Stewart JP (2003). Murid herpesvirus 4 strain 68 M2 protein is a B-cell-associated antigen important for latency but not lymphocytosis. *J Virol* **77:** 9700-9.

Mador N, Goldenberg D, Cohen O, Panet A, Steiner I (1998). Herpes simplex virus type 1 latency-associated transcripts suppress viral replication and reduce immediate-early gene mRNA levels in a neuronal cell line. *J Virol* **72:** 5067-75.

Magrath I (1990). The pathogenesis of Burkitt's lymphoma. *Adv Cancer Res* **55:** 133-270.

Mak J, Jiang M, Wainberg M, Hammarskjold M, Rekosh D, Kleiman L (1994). Role of Pr160gag-pol in mediating the selective incorporation of tRNA(Lys) into human immunodeficiency virus type 1 particles. *J Virol* **68:** 2065-2072.

Mansfield KG, Westmoreland SV, DeBakker CD, Czajak S, Lackner AA, Desrosiers RC (1999). Experimental infection of rhesus and pig-tailed macaques with macaque rhadinoviruses. *J Virol* **73:** 10320-8.

Marques S, Efstathiou S, Smith KG, Haury M, Simas JP (2003). Selective gene expression of latent murine gammaherpesvirus 68 in B lymphocytes. *J Virol* **77:** 7308-18.

Marquet R, Isel C, Ehresmann C, Ehresmann B (1995). tRNAs as primer of reverse transcriptases. *Biochimie* **77:** 113-24.

Martinez-Guzman D, Rickabaugh T, Wu TT, Brown H, Cole S, Song MJ, Tong L, Sun R (2003). Transcription program of murine gammaherpesvirus 68. *J Virol* **77:** 10488-503.

Matsuda D, Dreher TW (2004). The tRNA-like structure of Turnip yellow mosaic virus RNA is a 3'-translational enhancer. *Virology* **321:** 36-46.

Matsuda D, Yoshinari S, Dreher TW (2004). eEF1A binding to aminoacylated viral RNA represses minus strand synthesis by TYMV RNA-dependent RNA polymerase. *Virology* **321:** 47-56.

Matzke MA, Birchler JA (2005). RNAi-mediated pathways in the nucleus. *Nat Rev Genet* **6:** 24-35.

Maul GG, Ishov AM, Everett RD (1996). Nuclear domain 10 as preexisting potential replication start sites of herpes simplex virus type-1. *Virology* **217:** 67-75.

May JS, Coleman HM, Boname JM, Stevenson PG (2005a). Murine gammaherpesvirus-68 ORF28 encodes a non-essential virion glycoprotein. *J Gen Virol* **86:** 919-28.

May JS, Coleman HM, Smillie B, Efstathiou S, Stevenson PG (2004). Forced lytic replication impairs host colonization by a latency-deficient mutant of murine gammaherpesvirus-68. *J Gen Virol* **85:** 137-46.

May JS, Walker J, Colaco S, Stevenson PG (2005b). The murine gammaherpesvirus 68 ORF27 gene product contributes to intercellular viral spread. *J Virol* **79:** 5059-68.

McKie EA, Ubukata E, Hasegawa S, Zhang S, Nonoyama M, Tanaka A (1995). The transcripts from the sequences flanking the short component of Marek's disease virus during latent infection form a unique family of 3'-coterminal RNAs. *J Virol* **69:** 1310-4.

Medveczky P, Szomolanyi E, Desrosiers RC, Mulder C (1984). Classification of herpesvirus saimiri into three groups based on extreme variation in a DNA region required for oncogenicity. *J Virol* **52:** 938-44.

Medveczky PG, Medveczky MM (1989). Expression of interleukin 2 receptors in T cells transformed by strains of Herpesvirus saimiri representing three DNA subgroups. *Intervirology* **30:** 213-26.

Meinnel T, Mechulam Y, Blanquet S (1995). Aminoacyl-tRNA synthetases: Occurance, structure and function. In: *tRNA structure, biosynthesis and function.* Soll D, RajBhandary UL, (eds). ASM Press, pp 251-292.

Melendez LV, Daniel MD, Hunt RD, Garcia FG (1968). An apparently new herpesvirus from primary kidney cultures of the squirrel monkey (Saimiri sciureus). *Lab Anim Care* **18:** 374-81.

Mettenleiter TC (2002). Herpesvirus Assembly and Egress. *J Virol* **76:** 1537-1547.

Mittrucker HW, Muller-Fleckenstein I, Fleckenstein B, Fleischer B (1993). Herpes virus saimiri-transformed human T lymphocytes: normal functional phenotype and preserved T cell receptor signalling. *International Immunology* **5:** 985-990.

Mocarski ES, Courcelle CT (2001). Cytomegalovirus and their replication. In: *Fields Virology*. Knipe DM, Howley PM, (eds). Lippincott Willams and Wilkins, pp 2629–2673.

Moghaddam A, Koch J, Annis B, Wang F (1998). Infection of human B lymphocytes with lymphocryptoviruses related to Epstein-Barr virus. *J Virol* **72:** 3205-12.

Moghaddam A, Rosenzweig M, Lee-Parritz D, Annis B, Johnson RP, Wang F (1997). An animal model for acute and persistent Epstein-Barr virus infection. *Science* **276:** 2030-3.

Monstein HJ, Philipson L (1981). The conformation of adenovirus VAI-RNA in solution. *Nucleic Acids Res* **9:** 4239-50.

Montgomery RI, Warner MS, Lum BJ, Spear PG (1996). Herpes simplex virus-1 entry into cells mediated by a novel member of the TNF/NGF receptor family. *Cell* **87:** 427-36.

Moore PS, Chang Y (1998). Antiviral activity of tumor-suppressor pathways: clues from molecular piracy by KSHV. *Trends Genet* **14:** 144-50.

Moorman NJ, Lin CY, Speck SH (2004). Identification of candidate gammaherpesvirus 68 genes required for virus replication by signature-tagged transposon mutagenesis. *J Virol* **78:** 10282-90.

Moorman NJ, Willer DO, Speck SH (2003). The gammaherpesvirus 68 latency-associated nuclear antigen homolog is critical for the establishment of splenic latency. *J Virol* **77:** 10295-303.

Morgan RW, Xie JL, Cantello JL, Miles AM, Bernberg EL, Kent JR, Anderson AS (2001). Marek's disease virus latency. In: *Current Topics in Microbiology and Immunology*. Hirai K, (ed). Springer, pp 223-243.

Mourelatos Z, Dostie J, Paushkin S, Sharma A, Charroux B, Abel L, Rappsilber J, Mann M, Dreyfuss G (2002). miRNPs: a novel class of ribonucleoproteins containing numerous microRNAs. *Genes Dev* **16:** 720-728.

Mukherjee S, Trivedi P, Dorfman DM, Klein G, Townsend A (1998). Murine cytotoxic T lymphocytes recognize an epitope in an EBNA-1 fragment, but fail to lyse EBNA-1-expressing mouse cells. *J Exp Med* **187:** 445-50.

Muriaux D, Mirro J, Harvin D, Rein A (2001). RNA is a structural element in retrovirus particles. *Proc Natl Acad Sci U S A* **98:** 5246-51.

Murthy S, Kamine J, Desrosiers RC (1986). Viral-encoded small RNAs in herpes virus saimiri induced tumors. *Embo J* **5:** 1625-32.

Murthy SC, Trimble JJ, Desrosiers RC (1989). Deletion mutants of herpesvirus saimiri define an open reading frame necessary for transformation. *J Virol* **63:** 3307-14.

Myer V, Lee S, Steitz J (1992). Viral Small Nuclear Ribonucleoproteins Bind a Protein Implicated in Messenger RNA Destabilization. *PNAS* **89:** 1296-1300.

Nanbo A, Inoue K, Adachi-Takasawa K, Takada K (2002). Epstein-Barr virus RNA confers resistance to interferon-alpha-induced apoptosis in Burkitt's lymphoma. *Embo J* **21:** 954-65.

Nash AA, Dutia BM, Stewart JP, Davison AJ (2001). Natural history of murine gamma-herpesvirus infection. *Philos Trans R Soc Lond B Biol Sci* **356:** 569-79.

Neipel F, Fleckenstein B (1999). The role of HHV-8 in Kaposi's sarcoma. *Semin Cancer Biol* **9:** 151-64.

Nicholson LJ, Hopwood P, Johannessen I, Salisbury JR, Codd J, Thorley-Lawson D, Crawford DH (1997). Epstein-Barr virus latent membrane protein does not inhibit differentiation and induces tumorigenicity of human epithelial cells. *Oncogene* **15:** 275-83.

Nickoloff BJ, Griffiths CE (1989). The spindle-shaped cells in cutaneous Kaposi's sarcoma. Histologic simulators include factor XIIIa dermal dendrocytes. *Am J Pathol* **135:** 793-800.

Nicosia M, Zabolotny JM, Lirette RP, Fraser NW (1994). The HSV-1 2-kb latency-associated transcript is found in the cytoplasm comigrating with ribosomal subunits during productive infection. *Virology* **204:** 717-28.

Niedobitek G, Young LS (1994). Epstein-Barr virus persistence and virus-associated tumours. *Lancet* **343:** 333-5.

Nordengrahn A, Merza M, Ros C, Lindholmc A, Palfl V, Hannant D, Belak S (2002). Prevalence of equine herpesvirus types 2 and 5 in horse populations by using type-specific PCR assays. *Vet Res* **33:** 251-9.

Oda W, Mistrikova J, Stancekova M, Dutia BM, Nash AA, Takahata H, Jin Z, Oka T, Hayashi K (2005). Analysis of genomic homology of murine gammaherpesvirus (MHV)-72 to MHV-68 and impact of MHV-72 on the survival and tumorigenesis in the MHV-72-infected CB17 scid/scid and CB17+/+ mice. *Pathol Int* **55:** 558-68.

Oksenhendler E, Carcelain G, Aoki Y, Boulanger E, Maillard A, Clauvel J-P, Agbalika F (2000). High levels of human herpesvirus 8 viral load, human interleukin-6, interleukin-10, and C reactive protein correlate with exacerbation of multicentric Castleman disease in HIV-infected patients. *Blood* **96:** 2069-2073.

Omoto S, Fujii YR (2005). Regulation of human immunodeficiency virus 1 transcription by nef microRNA. *J Gen Virol* **86:** 751-755.

Parry CM, Simas JP, Smith VP, Stewart CA, Minson AC, Efstathiou S, Alcami A (2000). A broad spectrum secreted chemokine binding protein encoded by a herpesvirus. *J Exp Med* **191:** 573-8.

Peacock JW, Bost KL (2000). Infection of intestinal epithelial cells and development of systemic disease following gastric instillation of murine gammaherpesvirus-68. *J Gen Virol* **81:** 421-9.

Perng GC, Jones C, Ciacci-Zanella J, Stone M, Henderson G, Yukht A, Slanina SM, Hofman FM, Ghiasi H, Nesburn AB, Wechsler SL (2000). Virus-induced neuronal apoptosis blocked by the herpes simplex virus latency-associated transcript. *Science* **287:** 1500-3.

Pfeffer S, Sewer A, Lagos-Quintana M, Sheridan R, Sander C, Grasser FA, van Dyk LF, Ho CK, Shuman S, Chien M, Russo JJ, Ju J, Randall G, Lindenbach BD, Rice

CM, Simon V, Ho DD, Zavolan M, Tuschl T (2005a). Identification of microRNAs of the herpesvirus family. *Nat Methods* **2:** 269-276.

Pfeffer S, Sewer A, Lagos-Quintana M, Sheridan R, Sander C, Grasser FA, van Dyk LF, Ho CK, Shuman S, Chien M, Russo JJ, Ju J, Randall G, Lindenbach BD, Rice CM, Simon V, Ho DD, Zavolan M, Tuschl T (2005b). Identification of microRNAs of the herpesvirus family. *Nat Methods* **2:** 269-76.

Pfeffer S, Zavolan M, Grasser FA, Chien M, Russo JJ, Ju J, John B, Enright AJ, Marks D, Sander C, Tuschl T (2004). Identification of virus-encoded microRNAs. *Science* **304:** 734-6.

Pingel S, Hannig H, Matz-Rensing K, Kaup FJ, Hunsmann G, Bodemer W (1997). Detection of Epstein-Barr virus small RNAs EBER1 and EBER2 in lymphomas of SIV-infected rhesus monkeys by in situ hybridization. *Int J Cancer* **72:** 160-5.

Plancoulaine S, Abel L, van Beveren M, Tregouet D-A, Joubert M, Tortevoye P, de The G, Gessain A (2000). Human herpesvirus 8 transmission from mother to child and between siblings in an endemic population. *The Lancet* **356:** 1062-1065.

Putzer H, Condon C, Brechemier-Baey D, Brito R, Grunberg-Manago M (2002). Transfer RNA-mediated antitermination in vitro. *Nucleic Acids Res* **30:** 3026-33.

Quinlan MP, Chen LB, Knipe DM (1984). The intranuclear location of a herpes simplex virus DNA-binding protein is determined by the status of viral DNA replication. *Cell* **36:** 857-68.

Radkov SA, Kellam P, Boshoff C (2000). The latent nuclear antigen of Kaposi sarcoma-associated herpesvirus targets the retinoblastoma-E2F pathway and with the oncogene Hras transforms primary rat cells. *Nat Med* **6:** 1121-7.

Rajcani J, Blaskovic D, Svobodova J, Ciampor F, Huckova D, Stanekova D (1985). Pathogenesis of acute and persistent murine herpesvirus infection in mice. *Acta Virol* **29:** 51-60.

Rao AL, Dreher TW, Marsh LE, Hall TC (1989). Telomeric function of the tRNA-like structure of brome mosaic virus RNA. *Proc Natl Acad Sci U S A* **86:** 5335-9.

Reich PR, Forget BG, Weissman SM (1966). RNA of low molecular weight in KB cells infected with adenovirus type 2. *J Mol Biol* **17:** 428-39.

Reichman TW, Muniz LC, Mathews MB (2002). The RNA Binding Protein Nuclear Factor 90 Functions as Both a Positive and Negative Regulator of Gene Expression in Mammalian Cells. *Mol Cell Biol* **22:** 343-356.

Renne R, Barry C, Dittmer D, Compitello N, Brown PO, Ganem D (2001). Modulation of cellular and viral gene expression by the latency-associated nuclear antigen of Kaposi's sarcoma-associated herpesvirus. *J Virol* **75:** 458-68.

Renne R, Dittmer D, Kedes D, Schmidt K, Desrosiers RC, Luciw PA, Ganem D (2004). Experimental transmission of Kaposi's sarcoma-associated herpesvirus (KSHV/HHV-8) to SIV-positive and SIV-negative rhesus macaques. *J Med Primatol* **33:** 1-9.

Rickinson AB, Kieff E (2001). Epstein-Barr Virus. In: *Fields Virology*. Knipe DM, Howley PM, (eds). Lippincott Williams and Wilkins, pp 2575-2628.

Rietveld K, Pleij CW, Bosch L (1983). Three-dimensional models of the tRNA-like 3' termini of some plant viral RNAs. *Embo J* **2:** 1079-85.

Rivas C, Thlick AE, Parravicini C, Moore PS, Chang Y (2001). Kaposi's sarcoma-associated herpesvirus LANA2 is a B-cell-specific latent viral protein that inhibits p53. *J Virol* **75:** 429-38.

Rodriguez MS, Dargemont C, Stutz F (2004). Nuclear export of RNA. *Biol Cell* **96:** 639-55.

Roizman B, Knipe DM (2001). Herpes simplex viruses and their replication. In: *Fields Virology*. Knipe DM, Howley PM, (eds). Lippincott Williams and Wilkins, pp 2399-2460.

Roizman B, Pellet PE (2001). The family Herpesviridae: A brief introduction. In: *Fields Virology*. Knipe DM, Howley PM, (eds). Lippincott Williams and Wilkins, pp 2381-2398.

Rosbottom (2003). The molecular pathogenesis of ovine herpesvirus-2. University of Edinburgh.

Ruf IK, Rhyne PW, Yang C, Cleveland JL, Sample JT (2000). Epstein-Barr virus small RNAs potentiate tumorigenicity of Burkitt lymphoma cells independently of an effect on apoptosis. *J Virol* **74:** 10223-8.

Ruszczyk A, Cywinska A, Banbura MW (2004). Equine herpes virus 2 infection in horse populations in Poland. *Acta Virol* **48:** 189-92.

Sakisaka T, Taniguchi T, Nakanishi H, Takahashi K, Miyahara M, Ikeda W, Yokoyama S, Peng YF, Yamanishi K, Takai Y (2001). Requirement of interaction of nectin-1alpha/HveC with afadin for efficient cell-cell spread of herpes simplex virus type 1. *J Virol* **75:** 4734-43.

Salahuddin SZ, Nakamura S, Biberfeld P, Kaplan MH, Markham PD, Larsson L, Gallo RC (1988). Angiogenic properties of Kaposi's sarcoma-derived cells after long-term culture in vitro. *Science* **242:** 430-433.

Sarawar SR, Cardin RD, Brooks JW, Mehrpooya M, Hamilton-Easton AM, Mo XY, Doherty PC (1997). Gamma interferon is not essential for recovery from acute infection with murine gammaherpesvirus 68. *J Virol* **71:** 3916-21.

Sarawar SR, Lee BJ, Anderson M, Teng YC, Zuberi R, Von Gesjen S (2002). Chemokine induction and leukocyte trafficking to the lungs during murine gammaherpesvirus 68 (MHV-68) infection. *Virology* **293:** 54-62.

Sarid R, Flore O, Bohenzky RA, Chang Y, Moore PS (1998). Transcription mapping of the Kaposi's sarcoma-associated herpesvirus (human herpesvirus 8) genome in a body cavity-based lymphoma cell line (BC-1). *J Virol* **72:** 1005-12.

Schaefer BC, Strominger JL, Speck SH (1997). Host-cell-determined methylation of specific Epstein-Barr virus promoters regulates the choice between distinct viral latency programs. *Mol Cell Biol* **17:** 364-77.

Schwemmle M, Clemens MJ, Hilse K, Pfeifer K, Troster H, Muller WE, Bachmann M (1992). Localization of Epstein-Barr virus-encoded RNAs EBER-1 and EBER-2 in interphase and mitotic Burkitt lymphoma cells. *Proc Natl Acad Sci U S A* **89:** 10292-6.

Sciortino MT, Suzuki M, Taddeo B, Roizman B (2001). RNAs extracted from herpes simplex virus 1 virions: apparent selectivity of viral but not cellular RNAs packaged in virions. *J Virol* **75:** 8105-16.

Seto AG, Zaug AJ, Sobel SG, Wolin SL, Cech TR (1999). Saccharomyces cerevisiae telomerase is an Sm small nuclear ribonucleoprotein particle. *Nature* **401:** 177-180.

Sharp TV, Schwemmle M, Jeffrey I, Laing K, Mellor H, Proud CG, Hilse K, Clemens MJ (1993). Comparative analysis of the regulation of the interferon-inducible protein kinase PKR by Epstein-Barr virus RNAs EBER-1 and EBER-2 and adenovirus VAI RNA. *Nucleic Acids Res* **21:** 4483-90.

Shimizu N, Tanabe-Tochikura A, Kuroiwa Y, Takada K (1994). Isolation of Epstein-Barr virus (EBV)-negative cell clones from the EBV- positive Burkitt's lymphoma (BL) line Akata: malignant phenotypes of BL cells are dependent on EBV. *J Virol* **68:** 6069-6073.

Shope T, Dechairo D, Miller G (1973). Malignant lymphoma in cottontop marmosets after inoculation with Epstein-Barr virus. *Proc Natl Acad Sci U S A* **70:** 2487-91.

Shukla D, Liu J, Blaiklock P, Shworak NW, Bai X, Esko JD, Cohen GH, Eisenberg RJ, Rosenberg RD, Spear PG (1999). A novel role for 3-O-sulfated heparan sulfate in herpes simplex virus 1 entry. *Cell* **99:** 13-22.

Simas JP, Bowden RJ, Paige V, Efstathiou S (1998). Four tRNA-like sequences and a serpin homologue encoded by murine gammaherpesvirus 68 are dispensable for lytic replication in vitro and latency in vivo. *J Gen Virol* **79 (Pt 1):** 149-53.

Simas JP, Marques S, Bridgeman A, Efstathiou S, Adler H (2004). The M2 gene product of murine gammaherpesvirus 68 is required for efficient colonization of splenic follicles but is not necessary for expansion of latently infected germinal centre B cells. *J Gen Virol* **85:** 2789-97.

Simas JP, Swann D, Bowden R, Efstathiou S (1999). Analysis of murine gammaherpesvirus-68 transcription during lytic and latent infection. *J Gen Virol* **80 (Pt 1):** 75-82.

Simpson SA, Manchak MD, Hager EJ, Krummenacher C, Whitbeck JC, Levin MJ, Freed CR, Wilcox CL, Cohen GH, Eisenberg RJ, Pizer LI (2005). Nectin-1/HveC Mediates herpes simplex virus type 1 entry into primary human sensory neurons and fibroblasts. *J Neurovirol* **11:** 208-18.

Singh RN, Dreher TW (1998). Specific site selection in RNA resulting from a combination of nonspecific secondary structure and -CCR- boxes: initiation of minus strand synthesis by turnip yellow mosaic virus RNA-dependent RNA polymerase. *Rna* **4:** 1083-95.

Sixbey JW, Nedrud JG, Raab-Traub N, Hanes RA, Pagano JS (1984). Epstein-Barr virus replication in oropharyngeal epithelial cells. *N Engl J Med* **310:** 1225-30.

Skepper JN, Whiteley A, Browne H, Minson A (2001). Herpes simplex virus nucleocapsids mature to progeny virions by an envelopment --> deenvelopment --> reenvelopment pathway. *J Virol* **75:** 5697-702.

Soderlund H, Pettersson U, Vennstrom B, Philipson L, Mathews MB (1976). A new species of virus-coded low molecular weight RNA from cells infected with adenovirus type 2. *Cell* **7:** 585-93.

Song MJ, Hwang S, Wong WH, Wu TT, Lee S, Liao HI, Sun R (2005). Identification of viral genes essential for replication of murine gamma-herpesvirus 68 using signature-tagged mutagenesis. *Proc Natl Acad Sci U S A* **102:** 3805-10.

Spear PG (2004). Herpes simplex virus: receptors and ligands for cell entry. *Cell Microbiol* **6:** 401-10.

Spear PG, Longnecker R (2003). Herpesvirus Entry: an Update. *J Virol* **77:** 10179-10185.

Spivack JG, Fraser NW (1988). Expression of herpes simplex virus type 1 latency-associated transcripts in the trigeminal ganglia of mice during acute infection and reactivation of latent infection. *J Virol* **62:** 1479-85.

Spivack JG, Woods GM, Fraser NW (1991). Identification of a novel latency-specific splice donor signal within the herpes simplex virus type 1 2.0-kilobase latency-associated transcript (LAT): translation inhibition of LAT open reading frames by the intron within the 2.0-kilobase LAT. *J Virol* **65:** 6800-10.

Sprague KU (1995). Transcription of eukaryotic tRNA genes. In: *tRNA stucture, biosynthesis and function.* Soll D, RajBhandary UL, (eds). ASM press, pp 31-50.

Staudt LM (2000). The Molecular and Cellular Origins of Hodgkin's Disease. *J Exp Med* **191:** 207-212.

Steven N (1996). Infectious mononucleosis. *EBV Reports* **3:** 91-95.

Stevenson AJ, Frolova-Jones E, Hall KT, Kinsey SE, Markham AF, Whitehouse A, Meredith DM (2000). A herpesvirus saimiri-based gene therapy vector with potential for use in cancer immunotherapy. *Cancer Gene Ther* **7:** 1077-85.

Stevenson PG, May JS, Smith XG, Marques S, Adler H, Koszinowski UH, Simas JP, Efstathiou S (2002). K3-mediated evasion of CD8(+) T cells aids amplification of a latent gamma-herpesvirus. *Nat Immunol* **3:** 733-40.

Stewart JP, Janjua NJ, Pepper SD, Bennion G, Mackett M, Allen T, Nash AA, Arrand JR (1996). Identification and characterization of murine gammaherpesvirus 68 gp150: a virion membrane glycoprotein. *J Virol* **70:** 3528-35.

Stewart JP, Silvia OJ, Atkin IM, Hughes DJ, Ebrahimi B, Adler H (2004). In vivo function of a gammaherpesvirus virion glycoprotein: influence on B-cell infection and mononucleosis. *J Virol* **78:** 10449-59.

Stewart JP, Usherwood EJ, Ross A, Dyson H, Nash T (1998). Lung epithelial cells are a major site of murine gammaherpesvirus persistence. *J Exp Med* **187:** 1941-51.

Storz G (2002). An expanding universe of noncoding RNAs. *Science* **296:** 1260-3.

Sullivan CS, Grundhoff AT, Tevethia S, Pipas JM, Ganem D (2005). SV40-encoded microRNAs regulate viral gene expression and reduce susceptibility to cytotoxic T cells. *Nature* **435:** 682-6.

Sun R, Lin S-F, Gradoville L, Miller G (1996). Polyadenylylated nuclear RNA encoded by Kaposi sarcoma- associated herpesvirus. *PNAS* **93:** 11883-11888.

Sunil-Chandra NP, Efstathiou S, Arno J, Nash AA (1992a). Virological and pathological features of mice infected with murine gamma-herpesvirus 68. *J Gen Virol* **73 (Pt 9):** 2347-56.

Sunil-Chandra NP, Efstathiou S, Nash AA (1992b). Murine gammaherpesvirus 68 establishes a latent infection in mouse B lymphocytes in vivo. *J Gen Virol* **73 (Pt 12):** 3275-9.

Sunil-Chandra NP, Efstathiou S, Nash AA (1993). Interactions of murine gammaherpesvirus 68 with B and T cell lines. *Virology* **193:** 825-33.

Svobodova J, Blaskovic D, Mistrikova J (1982a). Growth characteristics of herpesviruses isolated from free living small rodents. *Acta Virol* **26:** 256-63.

Svobodova J, Stancekova M, Blaskovic D, Mistrikova J, Lesso J, Russ G, Masarova P (1982b). Antigenic relatedness of alphaherpesviruses isolated from free-living rodents. *Acta Virol* **26:** 438-43.

Talbot SJ, Weiss RA, Kellam P, Boshoff C (1999). Transcriptional analysis of human herpesvirus-8 open reading frames 71, 72, 73, K14, and 74 in a primary effusion lymphoma cell line. *Virology* **257:** 84-94.

Telford EA, Studdert MJ, Agius CT, Watson MS, Aird HC, Davison AJ (1993). Equine herpesviruses 2 and 5 are gamma-herpesviruses. *Virology* **195:** 492-9.

Tellam J, Connolly G, Green KJ, Miles JJ, Moss DJ, Burrows SR, Khanna R (2004). Endogenous Presentation of CD8+ T Cell Epitopes from Epstein-Barr Virus-encoded Nuclear Antigen 1. *J Exp Med* **199:** 1421-1431.

Terhune SS, Schroer J, Shenk T (2004). RNAs are packaged into human cytomegalovirus virions in proportion to their intracellular concentration. *J Virol* **78:** 10390-8.

Thimmappaya B, Weinberger C, Schneider RJ, Shenk T (1982). Adenovirus VAI RNA is required for efficient translation of viral mRNAs at late times after infection. *Cell* **31:** 543-51.

Thompson M, Haeusler RA, Good PD, Engelke DR (2003). Nucleolar clustering of dispersed tRNA genes. *Science* **302:** 1399-401.

Thompson MP, Kurzrock R (2004). Epstein-Barr Virus and Cancer. *Clin Cancer Res* **10:** 803-821.

Thompson RL, Sawtell NM (1997). The herpes simplex virus type 1 latency-associated transcript gene regulates the establishment of latency. *J Virol* **71:** 5432-40.

Thorley-Lawson DA (2001). Epstein-Barr virus: exploiting the immune system. *Nat Rev Immunol* **1:** 75-82.

Thorley-Lawson DA, Gross A (2004). Persistence of the Epstein-Barr Virus and the Origins of Associated Lymphomas. *N Engl J Med* **350:** 1328-1337.

Tierney RJ, Steven N, Young LS, Rickinson AB (1994). Epstein-Barr virus latency in blood mononuclear cells: analysis of viral gene transcription during primary infection and in the carrier state. *J Virol* **68:** 7374-85.

Toczyski DP, Steitz JA (1991). EAP, a highly conserved cellular protein associated with Epstein-Barr virus small RNAs (EBERs). *Embo J* **10:** 459-66.

Townsley AC, Dutia BM, Nash AA (2004). The m4 gene of murine gammaherpesvirus modulates productive and latent infection in vivo. *J Virol* **78:** 758-67.

Tripp RA, Hamilton-Easton AM, Cardin RD, Nguyen P, Behm FG, Woodland DL, Doherty PC, Blackman MA (1997). Pathogenesis of an infectious mononucleosis-like disease induced by a murine gamma-herpesvirus: role for a viral superantigen? *J Exp Med* **185:** 1641-50.

Tsygankov AY (2005). Cell transformation by Herpesvirus saimiri. *J Cell Physiol* **203:** 305-18.

Uchiumi T, Kominami R (1997). Binding of Mammalian Ribosomal Protein Complex P0·P1·P2 and Protein L12 to the GTPase-associated Domain of 28S Ribosomal RNA and Effect on the Accessibility to Anti-28 S RNA Autoantibody. *J Biol Chem* **272:** 3302-3308.

Usherwood EJ, Ross AJ, Allen DJ, Nash AA (1996a). Murine gammaherpesvirus-induced splenomegaly: a critical role for CD4 T cells. *J Gen Virol* **77 (Pt 4):** 627-30.

Usherwood EJ, Stewart JP, Robertson K, Allen DJ, Nash AA (1996b). Absence of splenic latency in murine gammaherpesvirus 68-infected B cell-deficient mice. *J Gen Virol* **77 (Pt 11):** 2819-25.

van Berkel V, Barrett J, Tiffany HL, Fremont DH, Murphy PM, McFadden G, Speck SH, Virgin HI (2000). Identification of a gammaherpesvirus selective chemokine binding protein that inhibits chemokine action. *J Virol* **74:** 6741-7.

van Berkel V, Levine B, Kapadia SB, Goldman JE, Speck SH, Virgin HWt (2002). Critical role for a high-affinity chemokine-binding protein in gamma-herpesvirus-induced lethal meningitis. *J Clin Invest* **109:** 905-14.

van Berkel V, Preiter K, Virgin HWt, Speck SH (1999). Identification and initial characterization of the murine gammaherpesvirus 68 gene M3, encoding an abundantly secreted protein. *J Virol* **73:** 4524-9.

van Dyk LF, Virgin HWt, Speck SH (2000). The murine gammaherpesvirus 68 v-cyclin is a critical regulator of reactivation from latency. *J Virol* **74:** 7451-61.

Verma SC, Robertson ES (2003). Molecular biology and pathogenesis of Kaposi sarcoma-associated herpesvirus. *FEMS Microbiol Lett* **222:** 155-63.

Virgin HWt, Latreille P, Wamsley P, Hallsworth K, Weck KE, Dal Canto AJ, Speck SH (1997). Complete sequence and genomic analysis of murine gammaherpesvirus 68. *J Virol* **71:** 5894-904.

Virgin HWt, Presti RM, Li XY, Liu C, Speck SH (1999). Three distinct regions of the murine gammaherpesvirus 68 genome are transcriptionally active in latently infected mice. *J Virol* **73:** 2321-32.

Volpe TA, Kidner C, Hall IM, Teng G, Grewal SI, Martienssen RA (2002). Regulation of heterochromatic silencing and histone H3 lysine-9 methylation by RNAi. *Science* **297:** 1833-7.

Wagner EK, Devi-Rao G, Feldman LT, Dobson AT, Zhang YF, Flanagan WM, Stevens JG (1988). Physical characterization of the herpes simplex virus latency-associated transcript in neurons. *J Virol* **62:** 1194-202.

Wain J, House D, Pickard D, Dougan G, Frankel G (2001). Acquisition of virulence-associated factors by the enteric pathogens Escherichia coli and Salmonella enterica. *Philos Trans R Soc Lond B Biol Sci* **356:** 1027-34.

Wakefield JK, Wolf AG, Morrow CD (1995). Human immunodeficiency virus type 1 can use different tRNAs as primers for reverse transcription but selectively maintains a primer binding site complementary to tRNA(3Lys). *J Virol* **69:** 6021-9.

Wakeling MN (2001). Characterisation of the Murine Gammaherpesvirus-68 G-protein-coupled Receptor. PhD Thesis. University of Edinburgh.

Wakeling MN, Roy DJ, Nash AA, Stewart JP (2001). Characterization of the murine gammaherpesvirus 68 ORF74 product: a novel oncogenic G protein-coupled receptor. *J Gen Virol* **82:** 1187-97.

Wang F, Rivailler P, Rao P, Cho Y (2001). Simian homologues of Epstein-Barr virus. *Philos Trans R Soc Lond B Biol Sci* **356:** 489-97.

Wang HD, Yuh CH, Dang CV, Johnson DL (1995). The hepatitis B virus X protein increases the cellular level of TATA-binding protein, which mediates transactivation of RNA polymerase III genes. *Mol Cell Biol* **15:** 6720-8.

Wang SW, Aldovini A (2002). RNA incorporation is critical for retroviral particle integrity after cell membrane assembly of Gag complexes. *J Virol* **76:** 11853-65.

Wang X, Kenyon WJ, Li Q, Mullberg J, Hutt-Fletcher LM (1998). Epstein-Barr Virus Uses Different Complexes of Glycoproteins gH and gL To Infect B Lymphocytes and Epithelial Cells. *J Virol* **72:** 5552-5558.

Wassenegger M, Heimes S, Riedel L, Sanger HL (1994). RNA-directed de novo methylation of genomic sequences in plants. *Cell* **76:** 567-76.

Weck KE, Kim SS, Virgin HI, Speck SH (1999). Macrophages are the major reservoir of latent murine gammaherpesvirus 68 in peritoneal cells. *J Virol* **73:** 3273-83.

Wedderburn N, Edwards JM, Desgranges C, Fontaine C, Cohen B, de The G (1984). Infectious mononucleosis-like response in common marmosets infected with Epstein-Barr virus. *J Infect Dis* **150:** 878-82.

Wek SA, Zhu S, Wek RC (1995). The histidyl-tRNA synthetase-related sequence in the eIF-2 alpha protein kinase GCN2 interacts with tRNA and is required for activation in response to starvation for different amino acids. *Mol Cell Biol* **15:** 4497-506.

Whitby D, Stossel A, Gamache C, Papin J, Bosch M, Smith A, Kedes DH, White G, Kennedy R, Dittmer DP (2003). Novel Kaposi's Sarcoma-Associated Herpesvirus Homolog in Baboons. *J Virol* **77:** 8159-8165.

Wightman B, Ha I, Ruvkun G (1993). Posttranscriptional regulation of the heterochronic gene lin-14 by lin-4 mediates temporal pattern formation in C. elegans. *Cell* **75:** 855-862.

Willer DO, Speck SH (2003). Long-term latent murine Gammaherpesvirus 68 infection is preferentially found within the surface immunoglobulin D-negative subset of splenic B cells in vivo. *J Virol* **77:** 8310-21.

Wolin SL, Cedervall T (2002). The La protein. *Annu Rev Biochem* **71:** 375-403.

Wu TT, Tong L, Rickabaugh T, Speck S, Sun R (2001). Function of Rta is essential for lytic replication of murine gammaherpesvirus 68. *J Virol* **75:** 9262-73.

Yang Z, Zhu Q, Luo K, Zhou Q (2001). The 7SK small nuclear RNA inhibits the CDK9/cyclin T1 kinase to control transcription. *Nature* **414:** 317-322.

Yao QY, Rickinson AB, Epstein MA (1985). A re-examination of the Epstein-Barr virus carrier state in healthy seropositive individuals. *Int J Cancer* **35:** 35-42.

Yeh L, Schaffer PA (1993). A novel class of transcripts expressed with late kinetics in the absence of ICP4 spans the junction between the long and short segments of the herpes simplex virus type 1 genome. *J Virol* **67:** 7373-82.

Yokogawa T, Watanabe Y, Kumazawa Y, Ueda T, Hirao I, Miura K, Watanabe K (1991). A novel cloverleaf structure found in mammalian mitochondrial tRNA(Ser) (UCN). *Nucleic Acids Res* **19:** 6101-5.

Young LS, Finerty S, Brooks L, Scullion F, Rickinson AB, Morgan AJ (1989). Epstein-Barr virus gene expression in malignant lymphomas induced by experimental virus infection of cottontop tamarins. *J Virol* **63:** 1967-74.

Young LS, Rickinson AB (2004). Epstein-Barr virus: 40 years on. *Nat Rev Cancer* **4:** 757-68.

Zech L, Haglund U, Nilsson K, Klein G (1976). Characteristic chromosomal abnormalities in biopsies and lymphoid-cell lines from patients with Burkitt and non-Burkitt lymphomas. *Int J Cancer* **17:** 47-56.

Zhou ZH, Chen DH, Jakana J, Rixon FJ, Chiu W (1999). Visualization of tegument-capsid interactions and DNA in intact herpes simplex virus type 1 virions. *J Virol* **73:** 3210-8.